CHEMICAL REVIEWS

pubs.acs.org/CR

Review

Nonspecific Binding—Fundamental Concepts and Consequences for Biosensing Applications

Andreas Frutiger, Alexander Tanno, Stephanie Hwu, Raphael F. Tiefenauer, János Vörös,* and Nako Nakatsuka*

Cite This: *Chem. Rev.* 2021, 121, 8095–8160

Read Online

ACCESS | Metrics & More | Article Recommendations

ABSTRACT: Nature achieves differentiation of specific and nonspecific binding in molecular interactions through precise control of biomolecules in space and time. Artificial systems such as biosensors that rely on distinguishing specific molecular binding events in a sea of nonspecific interactions have struggled to overcome this issue. Despite the numerous technological advancements in biosensor technologies, nonspecific binding has remained a critical bottleneck due to the lack of a fundamental understanding of the phenomenon. To date, the identity, cause, and influence of nonspecific binding remain topics of debate within the scientific community. In this review, we discuss the evolution of the concept of nonspecific binding over the past five decades based upon the thermodynamic, intermolecular, and structural perspectives to provide classification frameworks for biomolecular interactions. Further, we introduce various theoretical models that predict the expected behavior of biosensors in physiologically relevant environments to calculate the theoretical detection limit and to optimize sensor performance. We conclude by discussing existing practical approaches to tackle the nonspecific binding challenge *in vitro* for biosensing platforms and how we can both address and harness nonspecific interactions for *in vivo* systems.

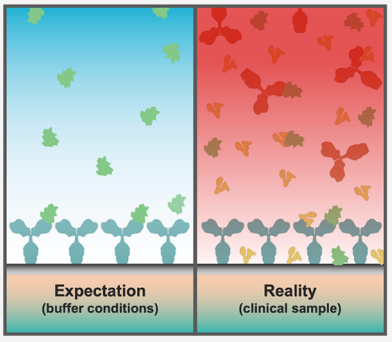

CONTENTS

Received: January 19, 2021
Published: June 9, 2021

https://doi.org/10.1021/acs.chemrev.1c00044
Chem. Rev. 2021, 121, 8095–8160

1. INTRODUCTION

1.1. Nonspecific Binding in Biology

The orchestrated interactions of macromolecules compose a fundamental element of all forms of life. Cellular and organism complexity arises from controlled biomolecular recognition. Considering that over 18,000 identified proteins operate with molecular-level control within the human body[1] and that the cytoplasm of a cell is a heavily crowded environment composed of over 30% proteins,[2,3] it is confounding that Nature has found ways to discriminate specific interactions, with desired biological effects, in the forest of much more abundant nonspecific interactions that have undesired or no specific biological effects.

Nature achieves this differentiation by two means: by controlling the local concentration of biomolecules in space and time through compartmentalization and coexpression and via the binding affinity of an interaction.[4,5] However, precise control of confined environments and interaction strengths only solves the problem for a limited number of proteins in the system, as nonspecific interactions in a biological system scale with the number of proteins (N) as a square law (N^2), whereas specific interactions are on the order of N.[6] For instance, there is usually one specific interaction partner per protein whereas each protein can interact with all others in a nonspecific way. Due to this unfavorable scaling, at a certain number of proteins, the specific interactions are overwhelmed by the nonspecific, which ultimately calls for compartmentalization of biological systems.

Thus, it is not a coincidence that organism complexity is not reflected in the size of the proteome but rather in the complexity of the gene regulatory network, the degree of compartmentalization, and the variety of different cell types.[6] All these measures

https://doi.org/10.1021/acs.chemrev.1c00044
Chem. Rev. 2021, 121, 8095−8160

lead to spatiotemporal control of protein expression, which in turn reduces the possibility of nonspecific interactions. Furthermore, the minimization of nonspecific interactions has implications in the evolution of the proteomes and, in particular, on the interface of highly expressed proteins.[7] Since there is a high chance of protein misinteractions for these highly expressed proteins, they are forced to evolve in a slow manner.[8]

Nonspecific interactions also fundamentally influence the way in which cells cope with misfolded proteins. Misfolded or denatured proteins usually expose hydrophobic regions that can lead to aggregation, which then causes the onset of diseases such as Alzheimer's or Parkinson's.[9] For example, the hydrophobic domain exposure of amyloid species correlates with their toxicity.[10] The initial nucleation is thought to be a nonspecific process, but the subsequent amyloid fibril formation is highly specific.[9,11]

A nonspecific effect of profound importance but largely neglected is molecular crowding, better known as the excluded volume effect. It is manifested by an omnipresent nonspecific steric repulsion due to the impenetrability of macromolecules and solvent molecules.[3] This steric exclusion is entirely nonspecific and has significant influence on protein aggregation in complex heterogeneous media and, thus, is an important phenomenon to consider to understand reaction rates and equilibria in crowded milieu.[11] Blood plasma is a crowded environment (80 g/L of proteins), and recently, it has been suggested that highly expressed plasma proteins such as albumin act as chaperones by binding to exposed hydrophobic domains of stressed client proteins.[3] This phenomenon leads to the formation of stable high-molecular-weight complexes, which reduces specific aggregation of the stressed proteins.[12]

Classical molecular chaperones that internalize proteins and assist folding within their cavity have an interior surface that can resist nonspecific binding (NSB) of all kinds of nonphysiological protein surfaces. Molecular chaperones create an environment with an increased hydrophobic effect, caused by charged amino acids such as lysine, glutamic acid, and aspartic acid, which strongly discourage hydrophobic interactions. This geometrically independent nonspecific hydrophobic effect assists protein folding.[13,14]

Similar to how Nature has harnessed NSB for fundamental biological mechanisms, there are research areas in biomedical engineering that utilize nonspecific interactions (Figure 1). For instance, most liquid chromatography methods (except affinity chromatography) separate different proteins by nonspecific effects such as hydrophobic interactions, electrostatic interactions, (ion exchange), and size (gel exclusion).[15,16] Further, the toxicity of nanomaterials in biological systems *in vivo* can be greatly reduced by NSB of serum proteins. For example, NSB to the high-energy surface of nanoparticles limits direct contact of their surface with cells,[17] and binding of blood proteins to carbon nanotubes was shown to reduce cytotoxicity.[18] Similarly, the nonspecific adsorption of proteins also determines the physiological response and the biocompatibility of a foreign material such as an implant introduced into the body.[19,20] Further, in protein crystallography, the protein interfaces that form contacts are artificially induced despite not being evolved for specific interactions.[21]

Conversely, NSB has hindered the implementation and dissemination of biological technologies in diverse medical fields. In the area of drug delivery, nonselective drugs can cause severe side effects by nonspecifically binding to unwanted targets.[22] Furthermore, many drugs are also bound nonspecifically in substantial fractions to plasma proteins. Approximately 10% of the 100 most prescribed drugs exhibit plasma protein binding of over 98%, which significantly limits their potency, resulting in higher dosages.[23] In the field of biosensing, NSB is the principal phenomenon responsible for hindering the translation of the most promising new techniques and many state-of-the-art sensing platforms, such as surface plasmon resonance (SPR) for clinical implementation. I SPR, the NSB of interfering molecules to the surface masks the signal from the analytes of interest that exist in significantly lower concentrations. The NSB effect is also extremely important in the fibrous encapsulation process that hinders progress for *in vivo* sensing approaches and controls the fate of implanted materials.[24] Similarly, the complement system can also be activated by NSB making it extremely difficult to prevent unwanted blood coagulation at the catheter and other blood-contacting-device surfaces.[25]

One of the main reasons why NSB has remained a critical issue despite technological advancements such as miniaturization, faster speed, lower detection limits, *etc.* is due to a lack of fundamental understanding of the phenomenon. To date, the identity, cause, and influence of NSB remain topics of debate within the scientific community.[26] In the literature, the terms "specific" and "nonspecific" binding are often used abundantly without explicit definitions. As the manner in which these terms apply is system-specific, it is often misconstrued. In a

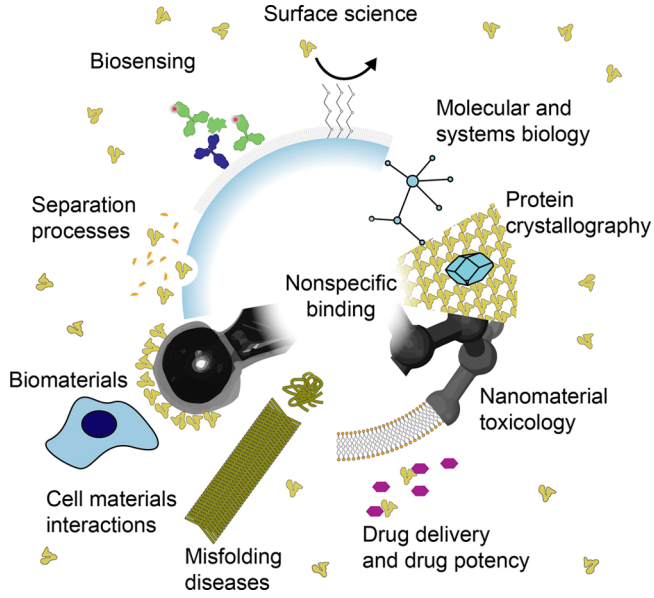

Figure 1. Fields of study in which nonspecific binding (NSB) has major implications. In surface science, the development of nonfouling coatings emerged with the goal of minimizing NSB. In separation processes, nonspecific interactions based on the size or charge are used to separate different biomolecules. For biosensing, NSB is the main limiting factor of state-of-the-art molecular diagnostic sensors. In systems biology, NSB shapes the form of protein interaction networks and in protein crystallography, nonspecific contacts between individual proteins are responsible for the formation of protein crystals. Regarding nanomaterial toxicology, NSB to nanomaterials can effectively reduce their toxicity and determines their biodistribution. Simultaneously, in drug delivery, NSB of drugs to plasma proteins reduces their effective concentration and opsonization (the NSB to drug carriers) affects their half-life in biological systems. In biomaterials research, NSB determines the cellular and physiological responses to foreign materials—*i.e.* implants. In medicine, NSB is important in the prevention and nucleation of protein misfolding diseases.

https://doi.org/10.1021/acs.chemrev.1c00044
Chem. Rev. 2021, 121, 8095−8160

provocative article, Ball et al. emphasized the difficulty of discriminating specific vs nonspecific interactions, stating that distinguishing these two interactions is as difficult as making the distinction between "interactions of physical" vs "interactions of chemical" nature.[27]

Thus, the subtlety of the concept coupled to the belief that nonfouling surfaces are sufficient to completely eliminate nonspecific adsorption of biomolecules to surfaces has hindered the development of devices that function in physiologically relevant, complex biological environments. Investigations into understanding the effects of NSB only began in the past decade. Henceforth, we provide an overview of the evolution of the understanding of NSB from the 1970s to today and attempt at providing unifying definitions and classifications of specific binding (SB), reversible vs irreversible NSB, multispecificity, and cross-reactivity.

1.2. Historical Perspective of Nonspecific Binding

The term "nonspecific binding" is nearly as old as the realization that protein−protein interactions are not only purification artifacts, which was a firm belief up to the 1970s.[28] Albano et al. first introduced the terms "nonspecific effects/factors" to describe the variation of insulin radioimmunoassay results in plasma samples.[29] Over the next few years, investigations into receptor−ligand interactions resulted in an observation that NSB manifested as a nonlinearity in Scatchard plots.[30−32] In these systems, there was only one ligand interacting with hormone receptors immobilized on a surface and the assay was often performed as a classical radioimmunoassay.[33] Therefore, NSB was defined as the composite binding of the ligand to all components of the surface with much lower affinity (≤100-fold) than the specific binders of interest.[32] The NSB effect was measured by competition experiments with an unlabeled ligand, which should only displace the high-affinity ligand from the binding site but not from the nonspecific sites. Hence, at that time, NSB was referred to as binding that is not displaceable and nonsaturable (non-Langmuir) and should increase linearly with the free analyte concentration.

Mendel et al. realized that this phenomenon of nonsaturability was due to the fact that nonspecific sites have considerably lower affinity and the analyte concentrations used in these experiments were too low.[34] In this regime, the Langmuir isotherm is essentially a linear function and NSB appears nonsaturable (see section 5). Despite these observations, the belief of the nonsaturability of NSB held until the end of the 1980s.[35] This misconception arose also partly due to the fact that researchers applied dynamic ranges of concentrations that were too low in their experiments, and thus, Scatchard plots were heavily misinterpreted.[36,37] The beginning of the 1990s sparked the cognizance that minimizing NSB by choosing the appropriate assay format (noncompetitive assays instead of competitive ones) had profound implications on immunoassay sensitivity.[38−40] This period also marked the launch of the first commercial SPR system which fueled the development of a variety of antifouling surfaces for biomolecular interaction analysis.[41,42] However, despite improvements to reduce surface biofouling, it is still and most likely always will remain impossible to eliminate NSB completely.[43]

Concurrently, the structural understanding of molecular recognition greatly accelerated. Van Oss emphasized that specific and nonspecific interactions were mediated by the same noncovalent forces and that their macroscopic manifestation must arise due to structural differences of the interacting interfaces.[44,45] In the mid-1990s, major advances in the understanding of protein−protein recognition sites and, through this, an improved knowledge of the structural basis of specific interactions were developed. For a review on the history of protein−protein interactions, see Kastritis et al.[28] Importantly, it was discovered that for specific protein complexes, the propensity to bind is driven by only a few amino acid residues called hotspots.[46] This finding implied that in biological systems, protein surfaces are designed such that only low-affinity NSB occurs and all high-affinity and specific interactions need to be evolved.[14,47]

High-affinity interactions can be suppressed effectively by a few negative design elements such as charge or steric complementarity mismatches at the interface.[2] While organizational patterns emerged when studying specific protein interaction interfaces,[28,48,49] knowledge on nonspecific interfaces was still lacking. Therefore, researchers began to search for model systems that would enable the quantitative comparison of nonspecific vs specific interfaces. Crystal contacts appeared to be a candidate system that elicited quantifiable differences.[21] However, only a significantly smaller buried surface area could be identified for crystal contacts compared to typical interfaces.[50,51] Further, the distinction between nonspecific interfaces and interfaces that emerge from interactions of flexible molecules that lack defined structures prior to binding (*i.e.*, disordered proteins) was even more challenging.[52−54]

Thus, a conceptual understanding of how these complex proteins achieved specificity only developed in the mid-2000s when the energy landscape theory, already popular in protein folding since the 1990s, was correlated to protein binding.[55] This powerful framework has the capacity to explain specificity conceptually in transient and flexible molecular recognition systems.[56,57] The existence of low-affinity SB in transient systems indicated that a simple affinity threshold cannot be used to distinguish SB vs NSB.[2] The observation of these transient and ultraweak interactions was only possible with the advent of the paramagnetic relaxation enhancement techniques,[58−60] while techniques for studying high-affinity specific molecular interactions such as isothermal titration calorimetry or SPR were already widespread.[28] These studies revealed that ultraweak association involves multiple interaction sites on one protein in stark contrast to the well-defined interaction sites of specific interactions.[60] Hence, multiple interaction sites could considerably increase the affinity of nonspecific interactions by rebinding to the other sites.[61]

Recently, based on new insight that nonspecific interactions with short surface-bound peptide sequences can be rather selective, it was even suggested that "SB" and "NSB" are misnomers and rather the terms "structured" and "unstructured" interactions should be used, respectively.[26] While we observe significant progress by overviewing the chronological advances in the general understanding of NSB, there is still an evident lack of understanding structure−affinity and structure−specificity relationships.

1.3. Defining Specific and Nonspecific Binding

Despite the progress in understanding the concept of NSB, there are still varying perspectives including different nomenclatures. For example, nonspecific,[27] unspecific,[62] undesired,[63] nonfunctional,[11] or unstructured[26] are all used in the literature. We suggest using "nonspecific binding" abbreviated as NSB, as it is by far the most commonly used term. While the definition "structured" and "unstructured" of Wang and Woodbury is

https://doi.org/10.1021/acs.chemrev.1c00044
Chem. Rev. 2021, 121, 8095−8160

appealing and in line with the architectural differences between the two phenomena that we cover later in section 4, the terms specific and nonspecific are too widespread to be forsaken.

Historically, the term NSB originated from the attempts to explain matrix effects in early radioimmunoassay experiments, often associated with the word undesired.[32] Hence, a practical definition of NSB would be to define it as binding to other biomolecules, particles, or surfaces that does not elicit the desired response of the biological or artificial system. However, this definition is too simplistic as NSB is on occasion, the desired outcome. For instance, in chromatography, NSB is used to separate proteins selectively.[15,16]

Furthermore, it is difficult to define the nature of the desired response, and the definition of binding itself is not straightforward. Biologically relevant binding spans affinities from fM (10^{-15}) to mM (10^{-3}). An example of low-affinity binding (mM) is the reversible cell−cell adhesion processes, which despite their multivalency (higher functional affinity) must still mediate fast adhesion turnover.[28] Very tight binding (fM) occurs with cell destruction proteins (proteases, RNases, DNases), which if not immediately neutralized, damages the cell irreversibly.[28] Schreiber et al. pointed out that a simple affinity threshold is therefore not sufficient for the definition of SB or NSB.[2] Rather, for biologically relevant binding, two proteins must be spatially and temporally colocalized at a concentration that promotes interactions. An inherent flaw in the concept of specificity is that it is a relative trait that is context dependent. For instance, in ligand−receptor interactions, specificity is the ability of a specific ligand to discriminate against different macromolecular receptors,[55] whereas in immunology, specificity measures the degree to which the immune system differentiates between different antigens.[64]

The term "specificity" originated from "species", a nebulous concept in itself as outlined by Van Regenmortel.[65] Further difficulties to define SB and NSB were pointed out in a discussion by Ball and Maechling.[27] From a purely practical perspective, specificity can be defined as preferential binding to one molecule over another, even if the concentrations are unfavorable. However, specificity implies at least the existence of some specific final state or a very confined subset of states when we assume that binding between two interaction partners is possible. For this reason, we propose to define SB and NSB conceptually on a simple molecular geometric level rather than on an application level.

Therefore, a *specific binder* represents a molecule that interacts with its partner via a defined end state with stereospecificity and shape complementarity. The final state should be thought of as a confined set in conformational space, rather than a single state. Alternatively, we define a *nonspecific binder* as a molecule with an ill-defined binding interface where two molecules can interact in multiple ways without stereospecificity and shape complementarity. We will develop a more general understanding of the features of SB and NSB after having discussed the thermodynamic and structural differences at the end of section 4. The suggested classification scheme is summarized in Table 1.

Specific binding can be further subdivided at the level of individual binders. A specific interaction can either be *desired* (*e.g.* most antigen−antibody interactions) or *undesired* (*e.g.* amyloid-beta oligomer formation). Other terms to describe these subtypes of SB are *functional* and *nonfunctional*, which we will use in favor of desired and undesired.[7,67]

In most cases, a binder does not only bind one partner but *multiple*—a phenomenon called *multispecificity* or *promiscu-*

Table 1. Proposed Discrimination of the Different Types of Specific and Nonspecific Binding Based on Structural and Thermodynamic Features

Overarching Features	Specific Binding (SB)					Nonspecific Binding (NSB)	
	Defined final binding interface and orientation, unique complex					Multiple binding interfaces and not well-defined orientation	
	One specific interaction per binder			Multiple specific interactions per binder (Multispecificity)			
	Transient functional SB	*Permanent functional SB*	*Nonfunctional SB*	*Functional selective binding*	*Cross-reactive binding*	Reversible NSB	Irreversible NSB
Description	*A specific interaction that mediates a biological function with low affinity*	*A specific interaction that mediates a biological function with high affinity*	*A specific interaction that is nonfunctional, undesired or disadvantageous for the organism.*	*Multiple specific interactions with different partners that all mediate a biological function*	*A nonfunctional specific interaction with at least one functional specific interaction*	*A nonspecific interaction that exhibits low-affinity and no denaturation of the macromolecules.*	*A nonspecific interaction with high-affinity and significant denaturation of the macromolecules*
Features	Low affinity (mM−μM)	High affinity (nM−fM)	No biological function	Single interface to bind multiple targets (promiscuity) or multiple interfaces that bind single target (moonlighting)[66]	Undesired Interface evolved to bind one interface but accidentally binds multiple targets	Low-affinity (mM) Binding is reversible and fast in terms of biologically relevant time scales	High-affinity (nM−fM) Binding is irreversible Biomolecules undergo structural changes and might lose their function upon binding
Examples	Electron transfer complexes, interactions involving disordered proteins	Antigen−antibod Protein−protein interactions	Amyloid formation and other fibrillar protein diseases	Hub proteins	Cross-reactive antibodies	Native protein interacting with a defect-free nonfouling surface. Interaction between native proteins without SB sites.	Protein interacting with a hydrophobic (high energy) artificial surface or defects in a protein-repellent surface. Aggregation of denatured protein chains.

https://doi.org/10.1021/acs.chemrev.1c00044
Chem. Rev. 2021, 121, 8095−8160

ity.[2,68] Proteins that can bind multiple partners in a specific way, called hub proteins, are highly important for cell biology.[69,70] We propose the name *selective binders* for proteins that bind multiple other partners with each interaction having one defined final state. Another form of multispecificity that is most often nonfunctional is termed *cross-reactive binders*, which is when a binder interacts specifically with another protein for which it was not evolved or designed for.

We suggest that NSB should be subdivided into *reversible* and *irreversible* NSB. Proteins reside in crowded environments and always collide and interact in a nonspecific reversible way with interactions of little biological relevance and no evolutionary selection for a defined binding interface.[71] While the interface of these interactions varies considerably, the binding energy is similar and is in the millimolar range.[60,72] The biological purpose of reversible NSB is to increase the time for molecules to probe each other. When proteins interact with high-energy surfaces, they often undergo conformational changes and bind nonspecifically in an "irreversible" way (*i.e.*, they cannot be rinsed off in practical time scales).[73,74] We therefore propose to distinguish between these two types of NSB, since they differ in affinity and affect applications in very different ways. It is important to stress again that reversible NSB can be somewhat selective and can also have a biological function.

With these definitions in mind, in the following section, we review and define terms related to the strength of interactions such as affinity, avidity, and attinebility and summarize concepts such as the intrinsic specificity ratio. We discuss the origin of NSB from the perspective of thermodynamics of intermolecular interactions. In section 3, we review the molecular recognition process, how it proceeds from an initial encounter complex to the final bound configuration, accompanied by a discussion on the forces that are involved in each step. Section 4 then provides a snapshot of the structure of the interface of different types of interactions, namely protein−protein interactions, antigen−antibody interactions, as well as crystal interfaces, which are the prototypes of nonspecific interactions. Furthermore, we will see how certain amino acid combinations are predestined for molecular recognition while others efficiently hydrate proteins and thus avoid nonspecific aggregation. Based on these discussions, we conclude this section by summarizing the features of SB and NSB from thermodynamic, intermolecular, and structural viewpoints.

The remaining sections focus on the practical issues of NSB. In addition to being the critical bottleneck for molecular biomarker-based diagnostics, NSB also influences the complex reactions of our body to various foreign biomaterials, such as opsonization of drug delivery particles, integration or fibrous encapsulation of artificial materials, or the coagulation of blood at the surfaces of blood-contacting devices. To understand the effect of NSB in such applications, we start by introducing the various models that are used to quantify the specific and nonspecific interactions of biomolecules at solid−liquid interfaces. These models are applicable to many fields that bring biological systems in direct physical contact with artificial technologies and tools. We discuss ways in which SB that drives analytical biosensing should be quantified, and we highlight the challenges that are imposed by NSB in developing sensors that operate in complex biological matrices. We conclude section 5 by exemplifying how biosensor geometries should be tailored and optimized to maximize the SB by hindering NSB.

In section 6, we summarize the existing knowledge on how to reduce the effect of NSB in biosensor experiments using various orthogonal approaches. We discuss the development of surface functionalization strategies to limit the amount of NSB to surfaces. However, fine-tuning the surface chemistry is often insufficient as optimized, nonfouling surfaces still exhibit significant reversible and irreversible protein adsorption when exposed to complex biological fluids—*i.e.* blood, cell lysates, or tissue extracts. Therefore, improved methods to reduce the influence of NSB are necessary such as choosing the appropriate assay format with optimized parameters.

In the latter half of section 6, we also investigate how optimizing the transducing element by applying self-referencing protocols can reduce the influence of NSB. We present the concept of a "spatial lock-in amplifier" that generalizes the expected effect of referencing on sensor performance. We conclude the section by highlighting novel techniques that can inherently decouple SB from NSB using optical, electronic, and stochastic platforms.

Finally, in section 7, we shift our focus to addressing NSB specifically for *in vivo* applications such as drug delivery systems and implantable biosensors. For these systems, the primary goal is not to minimize NSB but, rather, to promote the adsorption of the right immunological factors to elicit the desired physiological response. Thus, after a holistic investigation of NSB from chemical, physical, and theoretical perspectives, we conclude by discussing how we can harness NSB to advantage in a system-dependent manner.

2. THERMODYNAMICS OF SPECIFIC AND NONSPECIFIC INTERACTIONS

This section aims at investigating the thermodynamic differences between specific and nonspecific interactions. We will first summarize the definition of important terms that are related to the binding energy such as the dissociation constant, affinity, avidity, and attinebility and terms used to describe specificity and its quantification. In particular, we will motivate specificity using an energy landscape approach. Based on these insights, we define and summarize the thermodynamic signatures of SB and NSB.

2.1. Strength of Interactions

The overall interaction strength is the sum of all individual interactions, regardless of whether it is specific or nonspecific, between two binding partners. Unfortunately, this definition is also often called binding affinity because typical experiments (*e.g.*, the dose response curve in Figure 2) determine this parameter. Therefore, we will refer to this property as "apparent affinity" throughout this review. The binding affinity that describes an intermolecular interaction with a single binding site, can be quantified via the equilibrium dissociation constant (K_d), which is directly linked to the Gibb's free energy at standard conditions (ΔG°), which in turn is determined by the enthalpy and entropy changes of the interaction. Thus, binding affinity is governed by the laws of thermodynamics directly,[28] and assessing ΔG° is important because it determines the stability of the biomolecular complex. The relationship between the Gibbs free energy of dissociation ΔG_d° and the dissociation constant is

$$\Delta G_d^\circ = -RT \ln(K_d) \tag{1}$$

where R is the ideal gas constant and T is the temperature. The dissociation constant K_d is determined by the ratio of the association and dissociation rate constants, *i.e.* the off-rate, k_{off}, and the on-rate, k_{on}:

https://doi.org/10.1021/acs.chemrev.1c00044
Chem. Rev. 2021, 121, 8095−8160

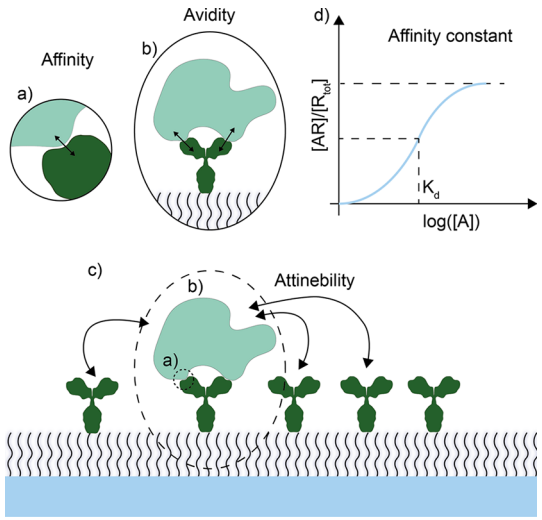

Figure 2. Illustration of the concepts of affinity, avidity, dissociation constant, and attinebility. (a) Affinity describes the interaction of a single interaction site. (b) Avidity is the functional affinity of multiple interaction sites acting together when the increased binding energy changes the kinetic constants. (c) The attinebility is a combined effect of increased local concentrations due to clustering of receptors at surfaces and a decreased dissociation rate (k_{off}) due to rebinding of the target. (d) While affinity, avidity, and attinebility are qualitative concepts, the dissociation constant K_d is the quantitative information obtained in an experiment and it typically exhibits contributions from all these effects. The [A] is the concentration of free analyte, [AR] is the concentration of the bound analyte, and [R_{tot}] is the concentration of the initially present receptors.

$$K_d = \frac{k_{off}}{k_{on}} \tag{2}$$

Notably, for most binding events, the association rates of biomolecules are often quite similar ($10^6 - 10^7$ M^{-1} s^{-1}), and changes in affinity constants are largely due to changes in off-rates.[75] Equilibrium association K_a [M^{-1}] and dissociation constants K_d [M] are related by $K_aK_d = 1$.

The K_a is what we typically measure in equilibrium binding experiments, because it connects to measurable concentrations via:

$$K_a = \frac{C_{RA}}{C_R C_A} \tag{3}$$

where K_a is the affinity constant and C_A, C_R, and C_{RA} are the concentrations of the free analyte, the receptor, and the receptor−analyte complex, respectively. Common methodologies for affinity determination include isothermal titration calorimetry (ITC),[27] fluorescence-based methods[28] as well as computational models.[76] Techniques such as surface plasmon resonance (SPR) enable determination of kinetic rate constants from which the binding affinity can be extracted.[77−79] The methodology that is best suited to measure a given interaction heavily depends on the binding affinity as thoroughly reviewed by Vuignier et al.[80] However, the K_d value can only be rigorously interpreted in ideal homogeneous solutions. There exists no straightforward thermodynamic theory that describes equilibrium in *heterogeneous* phase systems.[81] Furthermore, two macromolecules can interact via multiple different interaction sites all exhibiting different K_d values, making it difficult to state a simple mass action law.[82,83] Section 5 covers these issues in depth.

When performing an equilibrium binding experiment, it is often assumed that the measured K_d values can be translated to the binding affinity of molecular interactions in real biological systems, which then guides drug design or leads to discoveries of novel biomolecular interaction mechanisms. In the next section, we emphasize that affinity constants can be influenced significantly by the arrangement of the system and the biological environment.[84] In physiological environments, various intermolecular effects such as crowding[3] or clustering of receptors on biological membranes alter the thermodynamic activities of the interacting species and, in turn, change their effective concentrations (see section 3). This phenomenon also holds true for artificial systems, *i.e.* sensor surfaces[85] (see section 6). In particular, the thermodynamic activities of NSB may be altered in the aforementioned conditions, since a given molecule has numerous interaction partners in a complex environment and multiple binding interfaces of similar strength are often involved between interacting molecules.[60]

The intermolecular effects in complex systems cause the simple model applied for ligand−receptor interactions to break down, rendering the prediction of the concentration of complex formation not readily possible for given concentrations of the analyte and receptor. For such cases, more elaborate models can be found in the literature.[28,31,36] The accuracy of the measured affinity therefore strongly depends on the methodology and also the strength of the interaction investigated.[28,84] Nevertheless, although it is dubious as to what extent the experimentally measured vs the actual biological activity coincide, relative comparisons are possible provided that their immobilization densities are the same as widely applied in antibody characterization.[86] Later in section 6, we will discuss how to improve our measurements of affinity constants with different techniques by acknowledging and addressing the issues of NSB.

2.1.1. Concepts behind Binding Affinities. It is important to distinguish the quantitative dissociation constant K_d from qualitative concepts such as affinity, avidity, and attinebility.[85] These terms are schematically illustrated in Figure 2 and will be briefly summarized in this section.

2.1.2. Affinity and Monovalent Interactions. Affinity is commonly reported as the free energy difference between native binding (the complex with lowest energy) and the average of the unbound states of a *single interaction* or the *site binding constant*.[36,57,87] Hence, in antigen−antibody interactions, the affinity is the binding strength between the epitope and paratope.[88] This definition is not always strictly used. For instance, most immunologists refer to the affinity as the strength of binding between an antibody and its target antigen, which may have a lower dissociation constant (higher affinity) than the paratope−epitope interaction since the antibody can, in principle, bind the antigen at multiple locations or bind two receptors simultaneously on a cell surface.[81]

2.1.3. Avidity and Polyvalent Interactions. Avidity is the dissociation constant of a polyvalent interaction.[85] The dissociation constant of a binder can be increased by several orders of magnitude, when it binds the target with multiple binding sites simultaneously.[89] Prime examples are Immunoglobulin M antibodies, which have ten binding sites for an antigen and can increase their dissociation constant by 5−6 orders of magnitude.[89] These interactions are usually weak (mM) and exhibit poor specificity. It is only the polyvalent nature of the interaction that provides the required affinity and

https://doi.org/10.1021/acs.chemrev.1c00044
Chem. Rev. 2021, 121, 8095−8160

specificity for a selective biological interaction.[90,91] Other important examples include the entering of viruses into host cells[92] or the rolling of leukocytes on the blood vessel walls through selectin-mediated interactions.[93]

In a broader picture, avidity or more generally, multivalency is a fundamental chemical organization and action principle that is applied whenever a strong but reversible interaction is required. These interactions inspired from Nature have many important applications ranging from medicine, biochemistry, and supramolecular chemistry to material science. For more information, see two comprehensive reviews on this topic by Fasting et al.[85,92]

2.1.4. Attinebility and Effective Concentrations. Besides avidity, there is an additional effect on the dissociation constant that occurs when receptors are clustered on surfaces. Qualitatively, these phenomena can be explained by the rebinding of the antigen to proximal receptors after the unbinding event. The effect stems from the fact that the law of mass action would need to be expressed in terms of thermodynamic activities for a heterogeneous phase system. However, it is usually formulated in volume concentrations and assumes a homogeneous system. These assumptions are inaccurate if one of the interaction partners or the reaction product is confined in a two-dimensional (2-D) space, *e.g.*, on a surface, or on a particle. A rigorous statistical thermodynamic treatment is provided by Huskens et al.[94] To calculate the effective affinity of capture probes immobilized on 2-D surfaces, Sykes et al. derived the density-dependent cooperative binding model based on a statistical physics approach.[95] This model is based on the understanding that after binding the first target, a ligand can bind additional targets without further decrease in localization entropy.[61]

Experimentally, it was found that the apparent dissociation rate constant, k_{off}, is lowered significantly when additional receptors are in proximity to the antigen−antibody complex compared to isolated receptors.[96] This receptor density-dependent binding was also observed with clustered carbohydrates on surfaces.[90] Hwu et al. corroborated these findings where they observed the same effect when studying the mutual binding of two functionalized gold particles.[97,98] When altering the density of DNA on gold nanoparticles, the dissociation constant decreased and they termed the effect *attinebility* (creating the word from the Latin *attineo* meaning "to retain").

Similarly, Ozer et al. demonstrated that the *in vitro* aptamer selection procedure termed systematic evolution of ligands by exponential enrichment (SELEX) can generate nonspecific, low-affinity RNA aptamer ligands that can concurrently bind multiple targets to increase their effective binding affinity by two orders-of-magnitude.[61] This phenomenon based on the target concentration and surface density was termed "density-dependent cooperative binding". The study concluded that the NSB affinity is increased dramatically by cooperative binding due to the less stringent requirement for recognition at binding sites compared to SB. Affirmation of this effect has also been described by the immunosignaturing community, where the *immunosignaturing effect* describes the increased binding of off-targets at high immobilization densities compared to cognate epitopes that compete more favorably at low immobilization densities of peptides.[95]

2.2. Specificity of Interactions

So far, we have discussed the concepts related to the strength of interactions. Now we will discuss a few terms related to their specificity, which is a qualitative concept similar to the aforementioned affinity concepts. Specificity is commonly referred to as the binding of a molecular receptor to its binding partner, while not interacting with other biological compounds in the system. It is therefore a context-dependent property and is influenced by all interfaces and their relative spatial and temporal concentration in a system.[2,4] However, as we have seen in the definition section of the Introduction, there are different definitions of this term in various areas of research. Henceforth, we use the definition of specificity as "specific binding" discussed in the Introduction, where it represents the interaction between two biomolecules characterized by a well-defined end state with stereospecificity and shape complementarity.

Quantification of specificity is critical for the development of pharmaceuticals, since NSB of the high-affinity binders usually has severe side effects for the patient and also limits the bioavailability of the drug.[80] Until recently, the general belief was that high affinity and high specificity are always coupled.[99] However, it has come to light that high affinity cannot always guarantee high specificity.[100,101] Some works have even postulated that there are not necessarily direct correlations between affinity and specificity because, for instance, some low-affinity antibodies can show better discrimination among antigens than the high-affinity binders.[102] This hypothesis is in line with the observation that proteins in particular were evolved in order to optimize for functionality rather than affinity.[4]

One such example, where low-affinity binders exhibit high specificity, is provided by Chaires et al. where specific binding of a DNA aptamer to *L*-argininamide was obtained with a relatively large K_d value (low affinity) of 1.6×10^{-4} M.[103] Other examples of specific low-affinity binders are electron transfer complexes or proteins involved in signal transduction.[104] The specificity requirement for these biological messengers is not as stringent as for high-affinity binders such as inhibitors or antibodies, since their NSB is also of low energy and therefore transient. Recognition that affinity is not always linked to specificity is especially important in applications such as drug screening. Thus, it is important to develop more meaningful measures of specificity than affinity alone.[100]

2.2.1. Energy Landscape of Protein Folding. To quantify specificity rather than just affinity, we will first outline a concept that has attracted significant attention in the protein folding field and also holds great promise for providing novel insights into biomolecular interactions. Binding and folding are essentially the same processes with the only difference being the presence or absence of the chain connectivity, leading to two different terms, *intramolecular* and *intermolecular* recognition.[100,105] For this reason, the same statistical physics concepts used for protein folding can be used to describe biomolecular binding. In protein folding, the energy landscape is used to describe the folding process of a protein.[106] The energy landscape view of folding and binding has been extensively reviewed by Liu et al.[105] Briefly, the energy landscape is essentially a free energy vs entropy plot[107,108] or, more precisely, a map of all possible conformations based on their free energies.[109] The energy landscape has many dimensions but can be visualized by projection onto a few principal components (see Iida et al.[110] for details). It can be computed by sampling the conformational space by methods such as the generalized ensemble method or sampling by fast Fourier transform correlation and Monte Carlo minimization.[111]

Since proteins need to fold within biological time scales (Levithal's paradox)[112] into distinct shapes, the global minimum must be found rapidly and frustration in local minima should be

https://doi.org/10.1021/acs.chemrev.1c00044
Chem. Rev. 2021, 121, 8095−8160

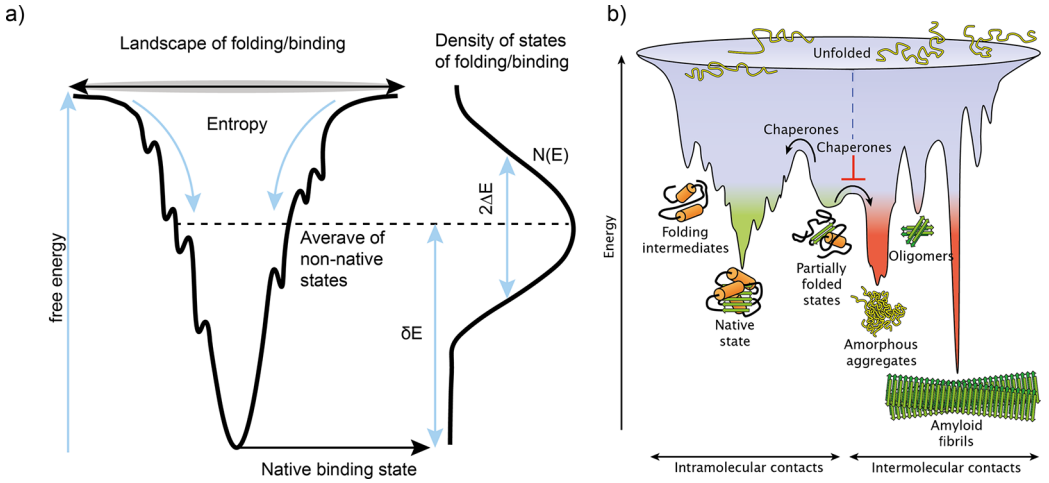

Figure 3. (a) Left: The funneled energy landscape theory in protein folding/binding. The extent of the funnel corresponds to the entropy/configurational space and the depth to the affinity (δE). Right: The corresponding density of states (N(E)) with dispersion (ΔE) (Reproduced with permission from ref 87. Copyright 2015 Zheng, Wang under Creative Commons Attribution license (CC BY) [https://www.plos.org/license]. (b) The energy landscape can conceptually describe different folding (intramolecular) and binding (intermolecular) states (each with a funnel leading to it). Here the example of the possible states of an amyloid peptide in both the intramolecular and intermolecular parts of the phase space is shown. Chaperones usually impede the exploration of the intermolecular part of the landscape (Reproduced with permission from ref 13. Copyright 2011 Nature).

avoided.[108] This constraint favored the evolution of protein chains that exhibit a funneled free energy landscape with sufficient overall slope (Figure 3a). The funneled shape implies that folding (as well as binding) is driven by the hydrophobic effect.[87,109] Qualitatively, the extent of the funnel is a measure for the entropy of the system (S), the depth is a measure of its affinity (δE), and the ruggedness of the funnel sidewalls (ΔE) is a measure for the chance of local trapping, while progressing toward the global minimum (see Figure 3a). Ruggedness of the landscape occurs if negative enthalpy cannot compensate for the loss in entropy, which leads to fluctuations in the free energy.[105] This ruggedness is an inherent property of frustrated systems such as glasses and is due to many competing interactions that cannot be satisfied at once.[105] The extent to which a system fits the folding funnel model can be assessed by the landscape topography ratio, Λ:

$$\Lambda = \frac{\delta E}{\Delta E\sqrt{2S}} \tag{4}$$

where δE is the free energy difference between the native binding and the average of the non-native binding states (the affinity), which *via* $\delta E = -RT\ln(K_d)$ is directly related to the affinity constant. The ΔE is the standard deviation in free energy of the non-native states, and S is the configurational entropy. For a detailed discussion on how to evaluate this quantity, see the following publications.[87,107,113]

The landscape topography ratio is a powerful concept since it was shown to be correlated monotonically with the thermodynamic stability against trapping and also with the folding kinetic rates, which enables quantitative links between the energy landscape and experimental folding measurements.[114] The landscape topography ratio represents the main properties of the ensemble of possible pathways a protein can take along an energy landscape and, by this, captures not only thermodynamic but also kinetic information on any process.[101]

2.2.2. Energy Landscapes from Folding to Binding. As mentioned above, the energy landscapes of folding are based on intramolecular interactions and it is straightforward to extend the concept to intermolecular interactions, which are the basis for molecular recognition. For instance, the binding funnel of a small ligand interacting with a protein is essentially an extension and deepening of a specific energy well located at the bottom of the protein folding funnel.[105] Protein−protein binding is then simply the combination of two folding energy landscapes with a binding energy landscape.[56] Figure 3b depicts how an energy landscape can conceptually describe different folding (intramolecular) and binding (intermolecular) states using amyloid-forming proteins as an example and how their aggregation is impeded by chaperone proteins.[13] In general, the binding landscape is simpler and its projection more interpretable than the folding landscape since binding is more conformationally restricted than folding.[111]

In terms of shape, binding landscapes are canyon-like and exhibit a smooth funnel. These canyons are due to the presence of "soft modes", principal motions of the protein encoded by its structure. It is interesting to note that most of the structural variations of proteins occur along these modes[115,116] and that all protein functions are mediated by their conformational distributions around the free energy minimum.[109] In addition to binding, the shape of the energy landscape can also be affected by changes in the physical environment such as pH, ionic concentration, presence of denaturant, pressure, and temperature.[105] The dynamic changes of energy landscapes and their interactions with the environment can capture the essence of molecular behavior in the system and have far-reaching implications in biology.[117]

2.2.3. Intrinsic Specificity Ratio as an Estimate of Specificity. Quantification of specificity according to the conventional definition implies finding the landscape topography ratio of the global landscape (Figure 4a).[101,113] However, assessing this quantity is impractical as it would involve studying the system under consideration in its entirety to construct the global energy landscape. Therefore, a quantity that correlates with specificity and can serve as its estimate is the only practical way.[55]

https://doi.org/10.1021/acs.chemrev.1c00044
Chem. Rev. 2021, 121, 8095−8160

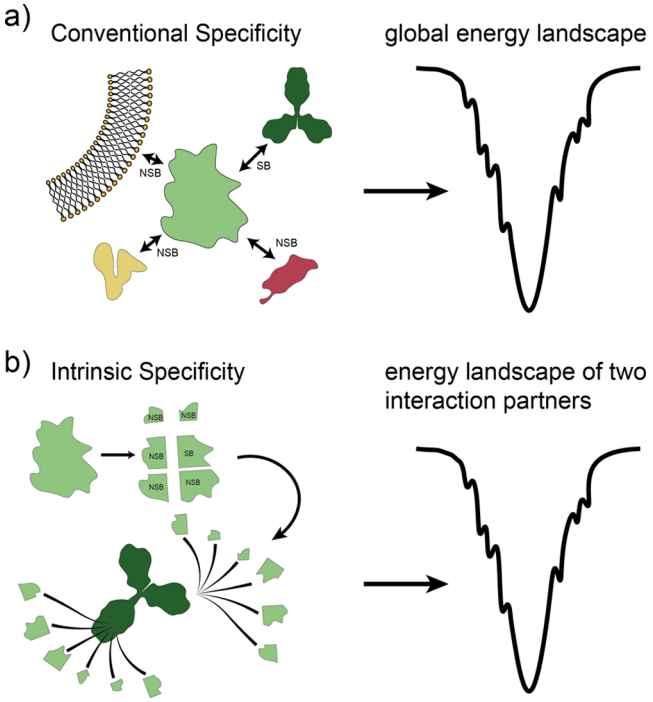

Figure 4. Illustration of the difference between conventional and intrinsic specificity. (a) Conventional specificity considers all interactions in a system and constructs the global energy landscape. (b) Intrinsic specificity investigates only the interaction between two partners, assuming that they are sufficiently large to be a good estimate of all the possible interfaces that are present in a system.

A quantity that estimates specificity can be derived if we recall that protein surfaces are large but finite.[118] In principle, if we consider a general protein surface of sufficient extent, we could link all proteins in a given system together into a "single large protein" and then assess the energy landscape of this protein interacting with a protein of interest.[87] The landscape topography ratio of this system can serve as an estimate of the global landscape topography ratio and, in turn, quantify the specificity. This topography ratio is termed the "intrinsic specificity ratio" when the energy landscape is simply stemming from the interaction between two proteins or a ligand with a protein of interest (Figure 4b).[55,100] When the protein−protein interaction studied is sufficiently general to represent the whole space of protein surfaces, specificity and intrinsic specificity are considered equivalent.[101]

Practical evidence that this approximation is somewhat justified stems from the same study where the authors showed that there is better correlation of experimental thermodynamic and kinetic specificity if, in addition to affinity, the intrinsic specificity ratio was included in the drug screening process. The intrinsic specificity ratio usually attains values between 1 and 6, with most of the values between 2 and 4.[55,56,101] However, there appears to be no distinct threshold for the intrinsic specificity ratio that discriminates specific and nonspecific interactions. Rather, there is a continuous transition between a value of 3−4,[55] which suggests that even if a single parameter is sufficient to describe the tendency, it is not enough to clearly discriminate all SB vs NSB.[107]

2.2.4. Qualitative Energy Landscapes of Specific vs Nonspecific Interactions. With the intrinsic specificity ratio in mind, we will now draw conceptual free energy landscapes of specific and nonspecific interactions, namely for the following four cases: transient and permanent functional SB and reversible and irreversible NSB (Figure 5; see Table 1 for definitions). The energy landscapes for these four cases differ mainly in the extent of the funnel and ruggedness of the topography, reflected in the values of the intrinsic specificity ratio.[101] In Figure 5, the histograms of the qualitative densities of the configurational states of the four interaction types are displayed and energy values were chosen according to the expected strength of the described interaction. The intrinsic specificity ratio was calculated from eq 4 whereas for simplicity, we assumed the entropy term S to be of order one, which is also the case in real systems.[100] The other two terms are directly accessible from the density of states. Also, the intrinsic specificity ratio of these qualitative landscapes attains larger values for the two specific interactions than for reversible or irreversible NSB.

2.3. Energy Landscapes of Nonspecific Binding

Due to many competing interactions that cannot be satisfied at once and interacting partners binding each other in many different configurations, NSB exhibits rough energy landscapes.[119] It is evident that under normal conditions, NSB within biological systems must be of low affinity and reversible; otherwise, proteins would just form undefined aggregates. Hence the ruggedness should be low enough such that the individual valleys can be overcome by thermal motion of the protein in reasonable biological time scales (ms), giving rise to a mM (11 k_BT) affinity, assuming that the k_{on} is in the range of 10^6 M^{-1} s^{-1} (k_{off} is then 10^3 s^{-1}).[75] This interaction energy is approximately what is found in the self-association rate of various proteins, with multiple possible interaction interfaces between binding partners.[60] Qualitatively, the same type of reversible NSB emerges when proteins interact with a defect-free nonfouling surface. The conceptual energy landscape of this reversible NSB is shown in Figure 5a.

Conversely, the interaction of biomolecules with hydrophobic surfaces or nonfouling surfaces with defects is typically of high affinity, leading to rugged energy landscapes with many deep minima (Figure 5b). These minima, which often go hand in hand with denaturation of the protein, are too deep (high energy barrier) to be overcome in meaningful time scales by the thermal energy of the protein (the thermal energy of a protein is debated but in the range of 17−34 k_BT),[117] hence why we proposed the term irreversible NSB for interactions with these types of energy landscapes in the Introduction.

2.4. Energy Landscapes of Specific Binding

We have seen before that the landscape of a specific interaction must be smooth and funneled to allow binding in biological time scales. The classical example of "permanent" (high-affinity) specific interactions that occur, for instance, between monoclonal antibodies and their targets or enzyme inhibitor complexes exhibits a deep funnel in an energy landscape of sufficient smoothness to avoid local trapping (Figure 5c).[28,55,100,119] We did not include nonfunctional, functional selective, and cross-reactive binding from Table 1 in the discussion, as nonfunctional SB is indistinguishable from functional SB in the energy landscape perspective. Further, functional selective (multispecific binding) and cross-reactive binding would simply exhibit multiple minima in the primary funnel.

In the special case of "transient functional SB" with millimolar affinities, a question that emerges is how Nature achieves functional specific interactions with millimolar affinity, if the average reversible nonspecific interactions are on the same order

https://doi.org/10.1021/acs.chemrev.1c00044
Chem. Rev. 2021, 121, 8095−8160

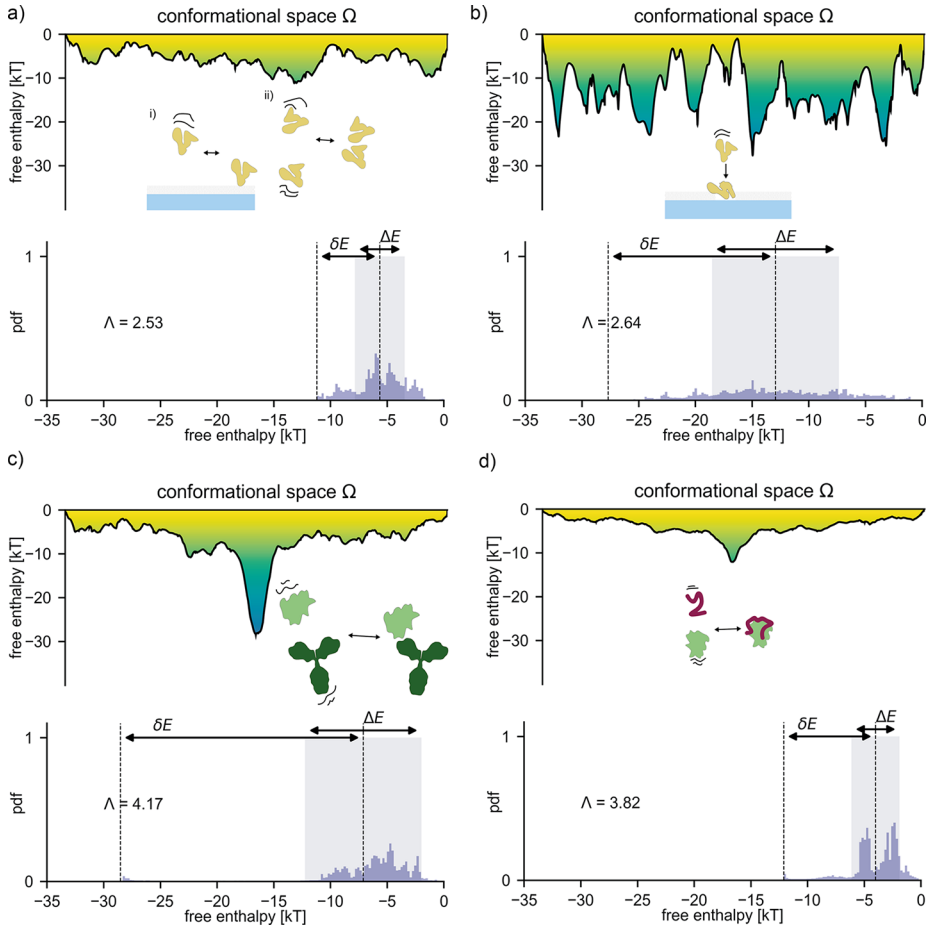

Figure 5. Qualitative intrinsic energy landscapes and the corresponding density of conformational states as they could be computed by rolling two interaction partners over each other and computing the energy of the states (see Figure 4b). It is important to stress that these conceptual landscapes do not represent the global landscapes of all proteins in the selected system but, rather, a landscape between two interaction partners. (a) Reversible nonspecific binding (NSB) as it could be computed from the surfaces of two proteins without specific interactions as well as from one protein with a defect-free nonfouling surface. (b) Irreversible NSB (frustrated system) as it occurs when proteins interact with high-energy surfaces as well as with defects of nonfouling surfaces. (c) Permanent specific binding (specific binding with high affinity) energy landscape that can be obtained, for instance, by rolling an antigen over the surface of an antibody and computing the respective energies. (d) Transient specific binding (specific binding with low affinity) with the prototype example where one of the partners is disordered upon binding. Lambda is the landscape topography ratio for the corresponding interaction, calculated from the probability density function (pdf). For ΔE and δE, see the discussion on the intrinsic specificity ratio in the text.

of magnitude.[4] First, most of these proteins have less stringent requirements on specificity as discussed above, and also, if electron transfer complexes are concerned, most of the nonspecific background binders do not exhibit the cofactors required for electron transfer.[120] Therefore, for these types of interactions, specificity arises mainly from the function and not the binding itself. Second, as long as the interactions are highly transient, the specific binder should still be able to access the binding site despite the noise of other reversible nonspecific interactions in meaningful time scales. It is important though, that if the binding partners actually meet, they can proceed quickly from the initial encounter complex to the specific bound state.[121]

Therefore, the capacity to achieve specificity in low-affinity interactions seems to arise from an easier kinetic accessibility of the specific state from different regions of the phase space.[122] Or in other words, for an arbitrary starting conformation, the interaction proceeds smoothly and quickly to the functional state. This phenomenon is common for a special type of interaction partner—an intrinsically disordered protein.[54] The disorder implies a smoothing of the energy landscape due to near perfect entropy−enthalpy compensation through conformational flexibility as shown in Figure 5d and therefore a fast progression to the final state.[56,57] This smoothing of the energy landscape is synonymous with a prolonged encounter state, which will be discussed in greater detail in sections 3 and 4. Interestingly, disordered proteins exhibit folding energy landscapes that are funneled yet are not steep enough to allow for folding. Only when encountering an interaction partner is the landscape rendered sufficiently steep to allow for the binding induced folding of the protein. Thus, for these types of proteins, binding is a prerequisite for folding.[123]

2.5. Enthalpy and Entropy Contributions to Biomolecular Interactions

We have discussed the energy landscape theory and attempted to draw conceptual free energy landscapes of specific and nonspecific interactions in the previous section. Here, we address the enthalpy and entropy contributions to biomolecular interactions. In particular, we will explore the thermodynamic tendencies of specific and nonspecific interactions. A great

https://doi.org/10.1021/acs.chemrev.1c00044
Chem. Rev. 2021, 121, 8095−8160

review on this topic has been published by Ball et al.,[27] and for a summary of thermodynamic terms, see the works by Liu et al.,[105] Chaires et al.,[103] and Perozzo et al.[82]

2.5.1. Binding Free Energy. The binding free energy can be subdivided into enthalpic and entropic parts, and the knowledge of both is of fundamental importance to unravel the different contributions of any interaction process occurring in the presence of a solvent.[27,88] This distinction allows one to discriminate the binding mode—*i.e.* binders that are excluded from the solvent into a hydrophobic pocket (entropic binders) compared to the ones that establish favorable interactions with the solvent (enthalpic binders).[124,125] In addition to enthalpy and entropy, a full thermodynamic characterization requires the change in heat capacity, ΔC_p to be assessed, which is directly linked to the amount of polar and nonpolar solvent accessible surfaces that are buried.[82]

Interestingly, it was also found in DNA−protein complexes that SB is accompanied by a large change in ΔC_p whereas a less dramatic change is observed for NSB.[126] This observation hints at more dehydration at interfaces in cases of SB. The correlation of ΔC_p and surface area burial provides a link between thermodynamic data and structural information on macromolecules.[82] Enthalpy, entropy, and heat capacity changes can readily be assessed by calorimetric measurements.[103,127] The free energy then reads

$$\Delta G_d = \Delta H_d^r - T\Delta S_d^r + \Delta C_p\left((T - T_r) - T\ln\left(\frac{T}{T_r}\right)\right) \quad (5)$$

where ΔH_d^r and ΔS_d^r are the enthalpy and entropy change, respectively, compared to an arbitrary reference temperature T_r.[103] The enthalpy, ΔH_d, and the entropy of dissociation, ΔS_d, can then be written as $\Delta H_d = \Delta H_d^r + \Delta C_p(T - T_r)$ and $\Delta S_d = \Delta S_d^r T\ln\left(\frac{T}{T_r}\right)$. However, it is more helpful for our discussion to break down ΔH_d and ΔS_d into more practical parts:

$$\Delta H_d = \Delta H_{ele} + \Delta H_{vdW} + \Delta H_{int} \quad (6)$$

$$\Delta S_d = \Delta S_{solv} + \Delta S_{conf} + \Delta S_{r/t} \quad (7)$$

The enthalpic part arises from bond formation and breaking and can be subdivided into contributions arising from electrostatic interactions (ΔH_{ele}), van der Waals interactions (ΔH_{vdw}), and internal contributions (ΔH_{int}) due to bond stretching, angle bending, bond torsions, *etc.*[128] Other decompositions of the binding enthalpy that also include protonation effects have been proposed.[82] More precisely, the enthalpic part reflects the loss of protein solvent hydrogen bonds and van der Waals interactions (desolvation enthalpy, which is always positive), formation of protein−protein bonds, salt bridges, and van der Waals contacts, and solvent reorganization near the protein surface.[82] We will discuss the molecular forces involved in detail in the next chapter. The ΔH_{ele} and ΔH_{vdw} both scale with the amount of surface buried, whereas the internal contributions ΔH_{int} cannot be easily described in terms of the change in accessible surface area.

The entropic part reflects the change in the degrees of freedom of the system and is composed of three individual parts: ΔS_{solv} is the solvent entropy, namely, the entropy gain due to surface burial and the accompanying solvent release (solvent molecules in solution have a higher entropy than the ones at the protein surface).[76,105] The entropy gain by the release of counterions is also included in this term. The conformational entropy difference caused by changes in the conformational freedom of the interacting molecules is depicted as ΔS_{conf}. Rotational and translational entropy is represented by $\Delta S_{r/t}$ and is lost upon complex formation. Estimates for these conformational and translational entropy changes are provided elsewhere.[129,130]

However, it is not possible to discriminate the individual contributions to enthalpy and entropy solely by calorimetric measurements. To distinguish each component fully, nuclear magnetic resonance (NMR) or circular dichroism experiments are needed to assess, for instance, the extent of conformational change vs the extent of desolvation.[27,60] We will now discuss how the contributions of these terms might differ in specific and nonspecific interactions to identify potential thermodynamic signatures of specificity.

2.5.2. Thermodynamic Considerations of Specific vs Nonspecific Interactions. All binding reactions exhibit an entropic penalty, in terms of lost rotational and translational degrees of freedom ($\Delta S_{r/t}$) on the order of 0−60 kJ/mol and conformational restriction (ΔS_{conf}) upon complex formation.[51,103,131] Although rigidification is a way to reduce ΔS_{conf} in the unbound state and thus have less entropy loss upon binding,[124] there still needs to be sufficient compensation by a favorable gain in solvation entropy (free water molecules that were in proximity to the protein surface and thus restricted) or a negative enthalpic contribution (formation of additional bonds).[103] Favorable enthalpy contributions arise from hydrogen-bonding and van der Waals interactions, and favorable entropic contributions arise primarily from hydrophobic interactions and desolvation, which implies the importance of desolvation of the binding interface for high-affinity binding.[103] Therefore, it is no coincidence that the buried surface area is the parameter that correlates most significantly with the binding affinity.[28]

However, the solvation entropy is a nonspecific force proportional to the hydrophobicity of the molecules, as it reflects a repulsion of the interaction partner from the solvent rather than an attraction toward the other interaction partner.[124] The same holds true for the nonspecific aggregation of oppositely charged polyelectrolytes at physiological conditions, which is mostly entropically driven through the release of their counterions (as restricted water molecules, the bound counterions gain entropy when released).[27,132]

While shape complementarity of two hydrophobic regions on two macromolecules may be used to achieve binding specificity, this framework is valid only to a certain extent, as too much exposed hydrophobic regions will cause aggregation and solubility issues.[124] Therefore, Nature seems to favor enthalpic over entropic interactions to increase the affinity while maintaining specificity.[133] This preference can be understood from the fact that a major part of the enthalpy is mediated through formation of additional favorable hydrogen bonds in the bound complex, which are stereospecific and thus imply selectivity (see section 3).

A high-affinity specific interaction should, therefore, exhibit a certain amount of favorable enthalpic contributions. Indeed, it was demonstrated that antibody specificity is enthalpically driven[134] and a considerable number of antigen−antibody interactions are mainly mediated by enthalpy.[135] Remarkably, there appears to be an optimal ratio of one-third enthalpic to two-thirds entropic contributions to the affinity constant for drugs that demonstrate high affinities and specificities.[103,124]

https://doi.org/10.1021/acs.chemrev.1c00044
Chem. Rev. 2021, 121, 8095−8160

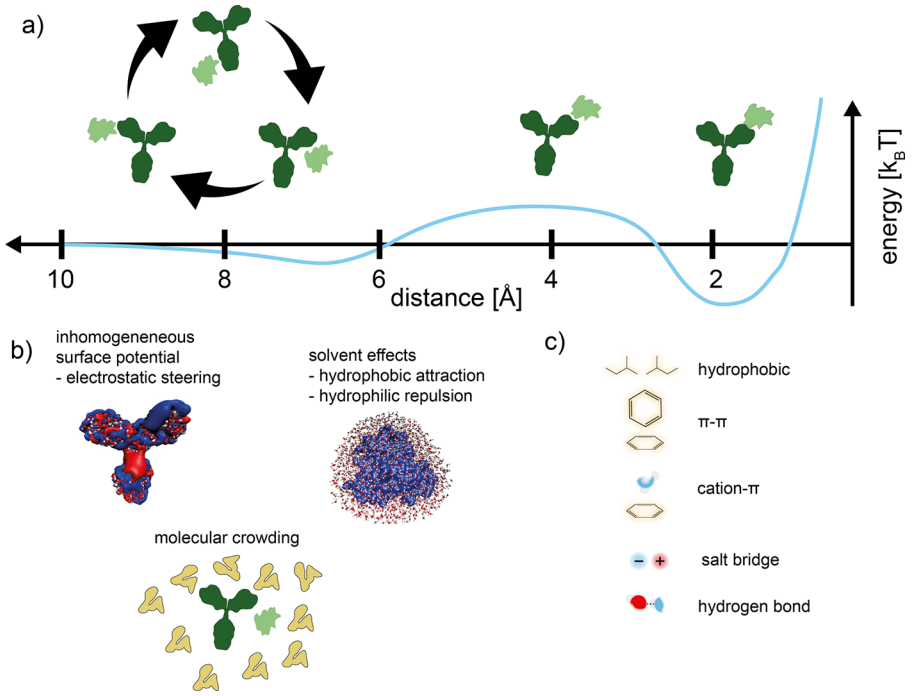

Figure 6. Molecular recognition process and the molecular forces involved. (a) The molecular recognition process commonly starts from a reversible nonspecific interaction complex and proceeds over a precursor state, where water is gradually expelled into the docked configuration. (b) The forces involved in the nonspecific encounter complex: an inhomogeneous surface potential, molecular crowding effects, as well as solvent effects. The nonspecific encounter complex is a requirement for fast specific binding but also leads to ubiquitous low-affinity nonspecific binding. Top left figure reproduced with permission from ref 153. Copyright 2012 Elsevier. Top right figure reproduced with permission from ref 154. Copyright 2009 JSTOR. (c) Forces involved in the docked configuration: hydrophobic, $\pi-\pi$, cation$-\pi$, salt bridges, and hydrogen bonds provide the necessary binding energy once the molecules are in close proximity to each other.

Yet, the difficulty in engineering enthalpically driven binding modes has challenged the field of medicinal chemistry.[124] The issue arises from the fact that increasing the binding enthalpy does not necessarily increase the binding affinity due to the enthalpy−entropy compensation mechanism.[136] Qualitatively speaking, tighter bonds (more negative enthalpy) will lead to a more rigid complex structure and hence a loss in configurational entropy yielding no change in the free energy. In recent years, enthalpy−entropy compensation was challenged to only be an artifact due to correlated experimental errors originating from the van't Hoff relationship as explained in depth by Olsson et al.[133] In ITC measurements, where ΔH and ΔG can be independently assessed, the effects of enthalpy−entropy compensation can be distinguished from other sources of correlation, and Olsson et al. confirmed a significant, widespread, and strong tendency toward enthalpy−entropy compensation in protein−ligand interactions. The enthalpy−entropy compensation phenomenon seems to be of fundamental importance for the specificity of an interaction, since it smoothens the energy landscape, resulting in a more funneled shape. When the enthalpy change cannot compensate for the entropy change, fluctuations occur, and the corresponding energy landscape is very rugged and binding specificity is lost.[105]

To conclude, we have asked the question whether there are fundamental differences in the thermodynamics of specific and nonspecific interactions. Apart from the tendency of SB to be enthalpically driven, exhibiting a more elaborate heat capacity change and a sufficient amount of enthalpy−entropy compensation to ensure a smooth energy landscape, the thermodynamic signature does not seem to be sufficient to firmly identify the specificity of an interaction. This finding is not surprising, as SB and NSB arise from the same fundamental intermolecular forces and, rather, the spatial arrangement of the recognition motif drives the extent of specificity. To this end, in the following section, we discuss the molecular recognition process and what intermolecular forces are involved in each step of the interaction in detail.

3. INTERMOLECULAR FORCES AND THE BIOMOLECULAR RECOGNITION PROCESS

With the thermodynamics discussion of the previous section in mind, we will now explore the interaction mechanisms between two biomolecules. In particular, we investigate the various forces and their strengths that act at different stages of the biomolecular recognition process. Concepts are discussed using the example of proteins but with some generality that applies to other biological macromolecules. We have seen that SB and NSB are manifested distinctively with regard to their biological outcome. However, as intermolecular interactions, both SB and NSB are mediated by the same noncovalent forces, although the relative strength and contribution of forces may differ.[44,45,137]

Generally speaking, the interaction energy between two molecules has four contributions:[138,139] first, an electrostatic component between permanent multipoles (monopoles, dipoles, and quadrupoles) that can be attractive or repulsive (Keesom interaction); second, an attractive inductive component that occurs when a permanent multipole causes an induced multipole in the interaction partner (Debye interaction); third, an attractive dispersive component that is due to interactions of fluctuating multipoles (London interaction); and finally, a repulsive component from the Pauli exclusion principle.[140]

https://doi.org/10.1021/acs.chemrev.1c00044
Chem. Rev. 2021, 121, 8095−8160

As these contributions can be attractive or repulsive and their strength depends heavily on the local environment, *i.e.* dielectric solution properties and the spatial separation of the interacting partners, specificity arises from the precise spatial arrangement of atoms within the configurational space of the two interacting molecules. For small-molecule interactions, it is especially convenient to discuss forces in units of k_BT, where k_B is the Boltzmann constant (J/K) and T the temperature (K), since the energy per degree of freedom of a molecule is 0.5 k_BT. At 25 °C, 1 k_BT equals 2.479 kJ/mol or 0.593 kcal/mol.[141] Attractive forces on the order of a few k_BT are within the range that can stabilize biomolecular structures, and only a few favorable interactions are required to achieve this.[142]

To get an idea of how energetics and affinity constants (K_d) are related, we recall that in order to achieve a millimolar affinity, only about −11 k_BT binding energy is required.[45] As a comparison, to achieve a strong interaction with nanomolar affinity, about −25 k_BT is necessary, and the average intrinsic energy fluctuation of a protein coupled with the local energy fluctuations in water is in the range of −17 to −34 k_BT.[117] Thus, interactions of nanomolar affinity and higher are easily reversible. Nooren and Thornton have published a review on the affinity constant ranges of biomolecular interactions,[4] and for an extensive book on forces in aqueous media and intermolecular interactions, see the work by van Oss.[143] Henceforth, we consider the chain of events that take place in a macromolecular biorecognition process and then summarize the forces that are acting in each of these processes.

3.1. Molecular Mechanism of Macromolecular Recognition

3.1.1. Molecular Recognition Process. The macromolecular recognition process can be subdivided into at least two phases—the formation of a nonspecific encounter complex and a docked configuration (Figure 6a). Furthermore, in the absence of long-range electrostatic forces, an intermediate precursor state mediated by water molecules can be identified in between the two aforementioned phases.[144,145] For any biomolecular interaction, irrespective of whether it is specific or not, a loosely bound nonspecific encounter complex always forms. This complex arises mainly due to the inhomogeneous charge and, to a lesser extent, the hydrophobic site distribution on protein molecules. The encounter complex was recently reviewed by Ubbink et al.[146] At this point, protein molecules mainly remain solvated and are essentially colloidal particles in an aqueous environment. The theory that describes the force fields that act between colloidal particles is the well-known DLVO theory.[147,148]

However, proteins exhibit a nonuniform charge distribution and an irregular molecular surface that complicates the calculation of the relevant forces, as dielectric permittivities and potentials depend on the local radius of curvature.[149] Furthermore, proteins are 1−2 orders of magnitude smaller than colloids, and therefore, hydrodynamic and solvation forces need to be included in the model. For this reason, an *extended DLVO theory* is necessary to describe the interaction of protein colloids in water.[149−151] Once the encounter complex has been formed, protein molecules are separated by their hydration shells, formed via electrostatic arrangements of water molecules. This transition state is called the precursor state, where conformational changes may occur, water is gradually expelled, and the interfaces align and approach each other in preparation to adopt the docked configuration.[151] The protein−protein interaction may involve a direct interaction via individual amino acid side-chains or an indirect connection via trapped water molecules at greater separation distances.[152]

3.1.2. Models for Molecular Recognition. There are three conceptual models for molecular recognition that have been proposed over the last 120 years, which have been reviewed extensively.[28,76,155] In particular, Du et al. discuss the thermodynamics and dominant forces in the different binding models in depth.[76] These models were primarily developed for protein−ligand binding but are conceptually valid for any biomolecular interaction. The models differ mainly by the amount of conformational change the interaction partners undergo and whether this change happens prior to or during the docking process.

The first is the lock-and-key model proposed by Fischer, who assumed the interaction partners to be completely rigid and to not undergo any conformational changes.[156] This model is still widely applicable in small ligand−protein interactions and for mature antibody−antigen interactions, which are often rigidified by internal salt bridges.[134] The lock-and-key theory can also explain the majority of interactions between protein domains.[157] The second induced-fit model comes into play if the interaction partners have noncomplementary surfaces and adjust their conformations significantly during the binding process to achieve complementarity.[158] The third conformational selection model is based on the fact that proteins exist as multiple conformational isomers, or conformers, with different arrangements of atoms around a single bond, prior to docking.

Differentiation between the induced-fit vs conformational selection models is often nontrivial as they essentially represent extreme cases of a continuum of binding modes.[157] To address this issue, Csermely et al. have proposed the use of the energy landscape perspective for visualization of binding models.[159] For example, the third conformational selection model can be viewed as multiple minima around the funnel in the folding energy landscape, and the interaction partner selects and increases the stability of one of these conformers.[159] The energy landscape representation is more versatile especially for explaining mixed or ambiguous binding modes.[66,119]

For example, in some interaction scenarios, protein motif flexibility plays a much more dominant role in binding that is not taken into consideration with the three aforementioned simplified models. In addition to the energy landscape perspective, there have been other proposed conceptual models such as extended conformational selection, mutually induced-fit, fly casting, or folding and binding.[160] For a more in-depth analysis on the differences in energy landscapes of specific vs nonspecific interactions, see our previous discussions in section 2.

In the following section, we will describe the molecular mechanisms of protein−protein interactions in chronology, starting with the nonspecific encounter complex, then the transition state, and finally ending with the specific docked configuration. We describe the relevant intermolecular forces involved in each recognition step and their strengths. We also discuss the different mechanisms by which the association rates of molecular recognition can be improved as well as the critical role of water in the recognition pathway.

3.2. Nonspecific Encounter Complex

3.2.1. Role of Nonspecific Encounter Complexes for Specific Binding. The nonspecific encounter complex is a necessity for SB because high-affinity specific binding often involves less than 1% of the total surface area of a protein.[149]

https://doi.org/10.1021/acs.chemrev.1c00044
Chem. Rev. 2021, 121, 8095−8160

Therefore, proteins need a way to reduce the dimensionality of the search space to improve the statistics of encountering the recognition motif.[59,111] Thus, a loosely attached nonspecific interaction complex that reduces translational degrees of freedom and allows the proteins to remain in closer proximity and sample considerably more surface area than in the case of an elastic collision is a necessary step for specific recognition.[104,119,146,161]

We can emphasize the necessity of nonspecificity of the encounter complex by using the energy landscape model. The nonspecific encounter complex can be perceived as a ring of states at the entrance of the binding funnel with the diameter directly proportional to the number of possible encounter states. If the encounter complex was too specific, the entrance of the funnel would be extremely small, making it impossible to enable binding in biological time scales. It appears that molecules are designed to probe each other constantly with low affinity to check for potential *specific* interactions. This hypothesis is supported by studies that suggest that half of biologically active molecules in the cell do not diffuse freely in the bulk medium despite their solubility but are transiently bound mostly nonspecifically to one another, to membranes, or to the cytoskeleton.[162]

3.2.2. Intermolecular Forces of Nonspecific Encounter Complexes. For molecular encounters for specific recognition, if pure diffusional association rates (k_{on}) are considered, an upper bound of ~1000 M^{-1} s^{-1} is calculated using the Einstein–Smoluchowski equation.[163,164] However, the requirement that the interaction partners must be properly aligned reduces the diffusional association rates to ~100 M^{-1} s^{-1} if no other attractive or repulsive forces are present.[165,166] These k_{on} values are significantly slower than what is usually observed in experiments ($\sim 10^4 - 10^8$ M^{-1} s^{-1} in the absence of conformational changes).[167] Notably, the alignment criterion for nonspecific interactions is less stringent due to the presence of multiple interfaces, and hence, their k_{on} rates may be considerably higher than for specific interactions.[60] Thus, binding rates can be enhanced through nonspecific encounter complexes, which aids in driving specific interactions. We will now discuss the intermolecular forces that are involved for rate enhancement (Figure 6b).

3.2.3. Electrostatic Steering. The mechanism of electrostatic steering is the primary driving force for rate enhancement beyond diffusional rates.[165,167,168] Electrostatic steering being the mechanism of action for rapidly associating complexes ($10^7 - 10^9$ M^{-1} s^{-1}) is evidenced by the fact that association rates can be reduced to diffusional rates by increasing the ionic strength while off-rates (k_{off}) remain largely unaffected.[169] A model based on the concept of a transition state for protein–protein association, which separates the bound and unbound protein state, has the capacity to predict association rates based on salt concentration in the diffusional regime ($10^4 - 10^9$ M^{-1} s^{-1}) with high accuracy.[164,170] Due to the relatively longer range (1–2 nm) of electrostatic forces, most of the affinity of the encounter complex and therefore reversible NSB is mediated through electrostatic interactions.[104,143]

3.2.4. Molecular Crowding Effects. In addition to electrostatic forces, crowding effects and the resulting nonspecific depletion interaction also have a fundamental implication on the association rates of proteins.[3] Molecules are impenetrable spheres, and as such, they exhibit nonspecific steric repulsion among each other. This repulsion leads to an excluded volume around each sphere that cannot be entered by other spheres. The available volume per macromolecule is therefore reduced and its effective concentration or thermodynamic activity can be much higher than its actual concentration. Let us assume that two big spheres form a complex; then the excluded volumes for the small spheres overlap partially and hence the available volume for all the small spheres in the solution increases. This condition leads to an attractive force between the big spheres, which is nonspecific in the sense that it can bring two spheres together but cannot orient them. Thermodynamically speaking, the configurational entropy of the small spheres has increased and the depletion interaction is therefore a purely entropic effect. Thus, biochemical reactions where a reduction of the excluded volume occurs are favored.[142]

For typical crowding conditions within cells, the strength of this force is roughly −0.5 to −1 k_BT (20–30% of the volume is assumed to be occupied by macromolecules). The entire process is summarized by Marenduzzo et al.[142] Besides the increased attraction of nearby molecules, crowding also slows down diffusion rates. On the one hand, this effect gives molecules in close proximity more time to sample their surface areas but, on the other hand, diminishes the likelihood that they actually meet. Generally speaking, crowding reduces the reaction rate of diffusion-limited processes and increases the rate of activity-limited processes. Therefore, no simple conclusions on the effect of the association rate can be drawn.

The optimal intracellular protein concentration that balances the effect of increased association and reduced diffusion was recently calculated by Wang et al. to be on the order of 1 mM, which is within the estimated range of the actual protein concentration.[171] The depletion interaction is proposed to have various biological effects from the assembly of cellular structures up to pathological fibril formation.[11,172]

3.2.5. Solvent Effects. The last force we will discuss involves interactions between the encounter complex and the solvent. The water molecules near the protein surface give rise to two forces: hydrophobic attraction and hydrophilic repulsion. These forces have been discussed extensively elsewhere,[151,173] and we will only provide a general description to lead into our discussion of the water-mediated transition state.

Hydrophobic attraction is the strongest noncovalent, nonelectrostatic binding force between macromolecules and is, thus, of fundamental importance in biology.[151,174] The hydrophobic effect is always attractive and purely due to the cohesion energy of water, which is 100 mJ/m^2, which corresponds to −10 k_BT per 40 $Å^2$ if the interface is fully dehydrated.[143,175] A phenomenological explanation for the effect is that water molecules near any surface irrespective of being hydrophobic or hydrophilic exhibit a diminished configurational freedom, which results in reduced entropy compared to bulk water molecules. If these molecules become expelled upon complex formation, a significant amount of entropy is gained. However, for any surface there is also an enthalpic component because the water molecules interact with the surface moieties. If this interaction is weak, as in the case of a hydrophobic surface, the entropic as well as the enthalpic changes are favorable. We note that the hydrophobic effect is mainly entropically driven but may also be enthalpically favored.[151]

In the case of hydrophilic surfaces, a compromising enthalpic contribution might completely offset the entropic gain.[124] The hydrophobic attraction can be increased by adding substances that polarize the water molecules, *i.e.* most salts, and thereby strengthen the internal hydrogen-bonding network of water, whereas chaotropic substances that disrupt the hydrogen-

https://doi.org/10.1021/acs.chemrev.1c00044
Chem. Rev. 2021, 121, 8095–8160

bonding network such as guanidine or ethanol lower this contribution. Similarly, when the electrostatic repulsion between molecules of the same kind decreases at a pH around their isoelectric point, hydrophobic interactions can take over and protein aggregation can occur.[41]

Thus far, we have mostly covered attractive forces. However, if there were only attractive forces, macromolecules would simply irreversibly aggregate, which is why a net repulsion of the protein surface is a necessary criterion for a thriving biological system.[174] Therefore, it comes as no surprise that the average protein surface was evolved to contain primarily nonsticky amino acid residues and that the stickiness of protein surfaces has a negative correlation with their abundance.[7] This nonstickiness is due to the large enthalpic dehydration penalty of polar and charged groups that opposes the favorable entropy of released water molecules.[124,144] This hydration layer that serves as a polar hydrated carpet that is approximately two layers of water (~5 Å) thick renders the average protein surface overall net repulsive.[14,154] However, within this carpet, there are many randomly arranged charged residues such as lysine and glutamic acid (zwitterionic properties), as well as a few small hydrophobic patches, and the random distribution can give rise to small attractive patches in an otherwise repulsive environment.[144]

The preferential selection of charged groups over polar residues due to higher hydration enthalpies that increase the hydrostatic repulsion field bestows nonsticky properties to surfaces and promotes reversible interactions.[176] While this nonspecific repulsion field may appear to have detrimental effects on association rates, the effect was found to be minor.[144] The repulsion also depends on the radius of curvature of the surfaces and can be more readily overcome at moieties with a small radius of curvature.[151] It is therefore no surprise that antigenic determinants tend to be located at protrusions of proteins[177,178] and that hydrophobic moieties are primarily hidden in cavities as in the case of the antigen-binding site of antibodies.[44,179]

3.2.6. The Nonspecific Encounter Complex Leads to Omnipresence of Low-Affinity Reversible Nonspecific Binding. For proteins to interact efficiently, they need to be able to sample surface areas sufficiently fast. The molecular proximity caused by the nonspecific encounter complex fulfills this purpose precisely, in that it allows the molecules to stick loosely together and sample each other's surface area. Unfortunately, this property also leads to ubiquitous low-affinity (mM K_d) and reversible interactions among many proteins. From a molecular standpoint, the nonspecific encounter complex and the low-affinity reversible NSB arise because the protein surface is a random carpet of charges and hydrophobic patches. The hydrophobic patches are always net attractive, and the electrostatic areas are attractive or repulsive depending on their relative sign. For an individual direct electrostatic bond without desolvation at the interface, the energy associated is approximately −2.5 to −10 kJ/mol (−1 to −4 k_BT).[141]

The strength of the hydrophobic interaction correlates with the size of the contactable surface area of water clusters, which is reported to be 40 Å^2.[141] The average area per amino acid residue, which drives electrostatic interactions, is on the same order of magnitude at 34 Å^2.[45,137] With the typical interface size of the encounter complex being in the range of 300−500 Å^2, approximately 7−12 hydrophobic or electrostatic interactions (each with a surface area of 40 Å^2) can occur.[144] Due to the random distribution of charges on the surface of proteins, there is a high probability that a small area on the surfaces of the two proteins interacts via reversible, low-affinity NSB. Or as the enthalpy funnel suggests, low affinity can be generated by essentially any combination of hydrophobic and polar/charged interactions.[124]

The necessity of nonspecific interactions to facilitate specific binding is not limited to protein−protein interactions. This phenomenon is also observed for protein−nucleic acid complexes that regulate biological processes such as transcription, translation, replication, activation, *etc.*[126] Interestingly, DNA-binding proteins have been shown to find their cognitive target sites at rates significantly faster than the expected three-dimensional (3D) diffusion rate governed by the Smoluchowski equation.[180] The unexpected fast kinetics of molecular recognition is driven by NSB of the protein to the DNA anywhere along the chain. Then, the protein translocates to the specific target site via one-dimensional (1-D) Brownian diffusion along the DNA.[181] This combined 1-D/3-D mechanism was termed "facilitated diffusion" where initial nonspecific interactions mediate the process of sequence-specific recognition of DNA and binding.[182] Thus, low-affinity reversible NSB is not only a requirement for fast specific binding, but it is also ubiquitous in any biological system.

3.3. Water-Mediated Precursor State

Water plays a critical role in molecular function and recognition; for a review on water-mediated interactions in cell biology, see the work by Ball.[183] In the early phases of the molecular recognition process, water mediates a precursor state of particular importance to steer the molecules to the binding sites—in the context of the energy landscape, water molecules effectively pull the proteins down the funnel. It was observed that the desolvation force and solvent-mediated interactions can guide the nonspecific encounter complex to the docked configuration and, by this mechanism, increase association rates to 10^7 M^{-1} s^{-1} without long-range electrostatic forces present.[144] However, these rates are still a hundred-fold slower than the upper bound of what can be achieved by electrostatic steering (*vide supra*). In other words, water molecules can guide a fully solvated protein to recognize another fully solvated protein. More specifically, it is proposed that the water in the interfacial gap forms an adhesive hydrogen-bond network between the interfaces that aligns hydrophilic residues over the distance of the hydration shells and, by gradual expulsion, navigates them to the docked stereospecific complex.[184,185]

This guidance is mediated by the strongly anisotropic binding properties of water in the interfacial gap that reduce dielectric shielding and result in a preferred directionality for electrostatic interactions along the direction perpendicular to the interface.[184] Water is therefore suggested to smoothen the binding funnel and to act as a molecular glue between the interaction partners. This mediation reduces the number of possible binding modes and eases the transition from the nonspecific encounter complex to the docked configuration.[185] However, compared to purely hydrophobic interfaces, which bind around 1000 times faster than hydrophilic ones, the trapped water still creates a barrier to rapid docking.[28] This effect seems to be even more pronounced for oppositely charged surfaces, where the last layer of water can get effectively trapped between the interfaces.[186] Most proteins therefore bind by a gradual expulsion of the solvent molecules overcoming the hydrostatic repulsion field in a stepwise manner while progressing to the docked state.[176,185]

https://doi.org/10.1021/acs.chemrev.1c00044
Chem. Rev. 2021, 121, 8095−8160

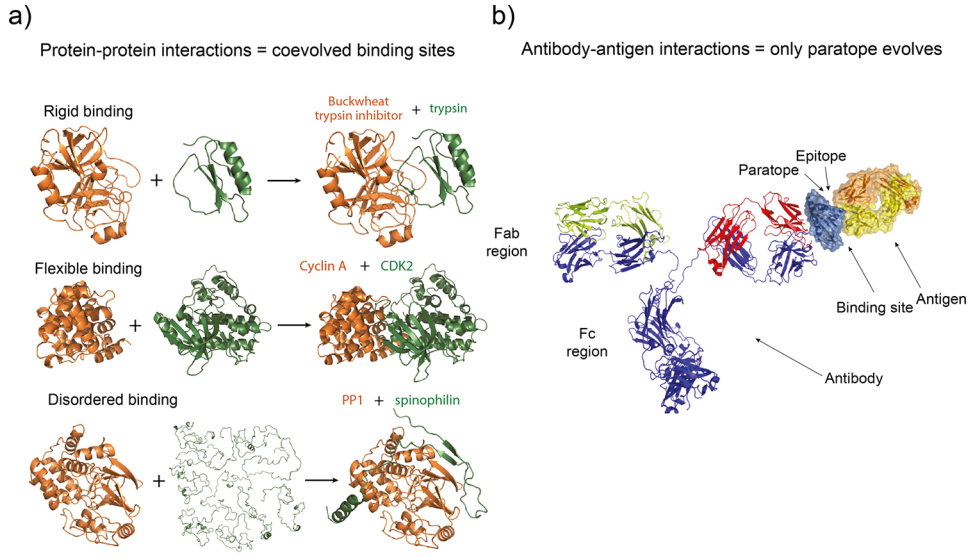

Figure 7. Features of protein−protein and antibody−antigen interaction sites. (a) Protein−protein interfaces always coevolve, where the interfaces of both partners evolve to mediate an interaction. This process supports many different binding modes such as rigid, flexible, and even binding of completely disordered proteins that only fold upon binding (Figure reproduced with permission from ref 201. Copyright 2014 Annual Reviews). In antibody−antigen interactions only one interface, namely the paratope, evolves in order to recognize a particular region (the epitope) on the antigen (Figure adapted with permission from ref 202. Copyright 2017 Jose L. Sanchez-Trincado et al.).

3.4. Stereospecific Complexes—Docked Configurations

The docked configuration is unique to specific interactions. In the docked configuration, water is usually completely expelled from parts of the interface and the functional moieties of the two interaction partners interact directly. At this point, short-range, noncovalent interactions such as hydrogen bonds,[187] salt bridges,[188] $\pi - \pi$ interactions,[140,189] and other interactions with aromatic rings form.[190,191] The forces involved in the docked configuration are shown in Figure 6c. The strength of these interactions mainly arises from enthalpic contributions and depends on the distance between the interaction partners as well as the geometric constraints especially in the case of hydrogen bonds.[192] Furthermore, their individual contributions are highly nonadditive.[193] In addition to these short-range intermolecular interactions, hydrophobic contacts also contribute to the binding energy via the entropic gain from expelled water molecules.

The energy of a hydrogen bond is −20 kJ/mol (−8 k_BT).[176] However, the strength of a hydrogen bond in proteins has been a highly debated question,[187] mainly because hydrogen bond strength is dependent on distance and angular orientation between residues and is not always favorable since there is competition with bulk water. For instance, there is virtually no net enthalpy gain when a hydrogen bond with bulk water is replaced with a hydrogen bond at the interaction interface. However, in this process, there is always the entropic gain of the water molecule (roughly −6 kJ/mol (−2.4 k_BT)) and there can also be a change in the number of hydrogen bonds (20 kJ/mol per bond).

This change in the number of hydrogen bonds is mostly because the initially bound water molecule could only participate in three or fewer hydrogen bonds compared to four in the bulk depending on the curvature of the interface, which explains the wide range of observed energies of hydrogen bond-mediating residues from −5 to −30 kJ/mol (−2 to-12.1 k_BT).[176,187,192,194] Alternatively, when buried hydrogen bond donors and acceptors cannot participate in hydrogen bonds (frustrated contacts), there is a significant energetic cost (up to 20 kJ/mol (8 k_BT) per bond).[176,195] Because of the strict requirements on complementarity and orientation, hydrogen bonds are thought to be by far the most important mediators of specificity.[192,196]

Salt bridges behave similarly to hydrogen bonds when it comes to specificity.[196] By analyzing over 200 salt bridges, Nussinov et al. determined the average energetic contribution of a salt bridge to be −15.4 ± 16.3 kJ/mol (+0.4 to −12.7 k_BT)[197] and found that >90% of the ion-pairs were stabilizing.[198] Besides hydrogen bonds and salt bridges, aromatic systems can mediate a variety of important interactions, with the strongest being the cation−π interaction, where a positively charged amino acid interacts with the aromatic π-system. The magnitude of this interaction has been reported in the range of −1.6 to −10 kJ/mol (−0.6 to −4 k_BT), which is approximately half the strength of a single hydrogen bond or salt bridge.[191] Direct interactions among π-systems ($\pi-\pi$) in the edge-to-face, parallel-displaced arrangements are slightly weaker and have been reported to be in the range of −2 to −3 kJ/mol (−1 k_BT).[191] Due to the release of solvent molecules, hydrophobic areas contribute roughly 0.1 kJ/mol per Å^2 or −3 to −4 kJ/mol (−1.2 to −1.6 k_BT) per water molecule contact (40 Å^2).[28,141,192]

The essence of this discussion is that the contribution of hydrogen bonds and salt bridges to the binding energy can vary substantially from highly favorable (less than −10 k_BT) to highly disadvantageous (>8 k_BT). Thus, these interactions are the main mediators of specificity in biological systems. Furthermore, to achieve nM affinity (−25 k_BT), only a few strong interactions are required. However, such high-affinity interactions can *only* be achieved if the environment of the residue that mediates the binding is excluded from the bulk water and the net count of interactions increases. In addition, the shape and charge complementarity of the remaining interface must not compromise the formation of the complex.

Thus, these high-affinity interactions must be carefully engineered in biological systems by the interplay of several amino acid residues. If such high-affinity interactions were

https://doi.org/10.1021/acs.chemrev.1c00044
Chem. Rev. 2021, 121, 8095−8160

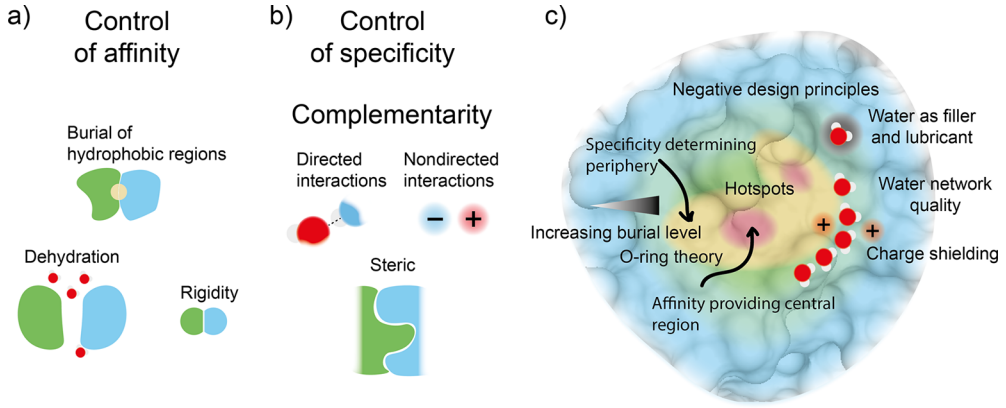

Figure 8. Structural features of affinity and specificity. (a) Structural control of the affinity of an interaction: the affinity of an interaction is controlled by the size of the buried hydrophobic surface area, the rigidity or conformational flexibility (reduction/increase of the entropy change upon binding) of the involved binding partners, as well as the extent of dehydration of the binding interface. (b) Structural control of the specificity of an interaction: specificity is mostly achieved by negative design principles. Thus, there is a large energetic penalty if complementarity is not fulfilled. There are three types of complementarity: shape (steric) complementarity, complementarity of directed interactions (hydrogen bonds), as well as complementarity of nondirected interactions (charges and hydrophobic regions). (c) Structural features of a binding interface: The specificity of a binding interface may be mediated through negative design elements in the periphery of the binding interface. Burial level increases from the periphery to the center. Some theories suggest that specific amino acids shield parts of the center of the binding interface from water molecules (O-ring theory). The affinity is usually provided by a few dehydrated amino acids in the center, so-called hotspots. Water molecules and their networks appear to be particularly important at binding interfaces and may act as a lubricant during the binding process and also as a filler that can offset unfavored contacts at the interface.

common between individual amino acids, the abundance of high-affinity interactions would heavily compromise the functionality of any biological system. For this reason, the next section is devoted to the architecture of the interface of biomolecular interactions to highlight the way Nature designed and assures the specificity of high-affinity interactions while restraining nonspecific interactions to low affinities.

4. ARCHITECTURE OF BIOMOLECULAR INTERACTION SITES

In an attempt to elucidate why proteins interact, Kastritis et al. reviewed the structural features of affinity in protein−protein interactions and concluded that current approaches are insufficient to predict binding affinities between proteins from the available structural information.[28] Predicting *specificity* from structural elements is expected to be even more challenging.[199] Therefore, the aim of this section is not to provide a structural explanation of specificity but, rather, to discuss the basic design principles likely to be associated with biomolecular interactions. We will also limit the discussion to protein−protein interactions and do not address other interactions such as protein−DNA or peptide−peptide interactions, although the concepts discussed also apply to these systems. Generally, Nature's principle for achieving highly specific interactions with minimal frustration involves the controlled arrangement of local attractive forces in an otherwise repulsive environment within a certain surface area of the protein.

Molecular recognition is mediated by carefully evolved recognition sites on the protein surface, called interfaces. However, recent evidence suggests that it is intrinsically challenging to control the behavior of the local attractive forces that are created at interfaces. In particular, interfaces where one of the binding partners is unstructured prior to recognition, (*e.g.* intrinsically disordered proteins that lack ordered 3-D structures) are more prone to inducing aggregation or nonspecific interactions than the rest of the protein surface.[105,200] Herein, we distinguish general protein−protein interactions that span a vast amount of different protein molecules from a particular subdivision, *i.e.* antigen−antibody interactions. The importance for specification arises from the difference in recognition mechanisms: in protein−protein interactions, *both* binding partners coevolve for optimal binding, whereas in antigen−antibody interactions, only the antibody evolves to recognize a specific surface area, *the epitope*, on the target antigen (Figure 7).

Furthermore, the binding affinity range varies significantly between the two: antigen−antibody interactions are usually limited within the micromolar to nanomolar range while general protein−protein interactions span ∼12 orders of affinity magnitude.[4,203] This expansive range of binding affinities for protein−protein interactions arises from the diverse ways in which proteins can interact. Protein−protein complexes that are *obligate*, where individual proteins cannot create stable structures alone but are stabilized by the constituent proteins within the complex, exhibit very strong, permanent interactions. Alternatively, *nonobligate* protein complexes are formed by proteins that can form well-folded structures alone without other associated proteins and have interactions that are either permanent or transient. However, as protein tertiary structures depend on numerous conditions such as pH, temperature, protein concentration, *etc.*, there exists no clear-cut division between obligate and nonobligate interactions; it is rather a continuum between the two. Differences between obligate vs nonobligate protein interactions are summarized by Ozbabacan et al.[204]

Due to the different characteristics of the interaction partners and the varying requirements for the interactions, the binding modes and the properties of the interfaces will also differ. For instance, flexible binding modes can result in larger interfaces, as the protein structures are more adaptable, in contrast to the limited interface of rigid constructs of a given size.[66] For this reason, complexes with interfaces larger than 1000 Å^2 are likely to undergo conformational changes upon binding.[4] The interface at which protein−protein interactions occur must be substantial in size to mediate biologically meaningful interactions with certain affinities and specificities. The standard size

https://doi.org/10.1021/acs.chemrev.1c00044
Chem. Rev. 2021, 121, 8095−8160

of these interfaces is in the range of 800 ± 200 Å^2, consisting of 24 amino acid residues,[51,167] which is sufficient for both stability and specificity.[205] The lower bound of biologically meaningful protein−protein interactions is estimated to be around 450 Å^2 (10 amino acids).[51]

With this introduction to binding interfaces, we will now address the structural features that give rise to the affinity and specificity of transient protein complexes and how specific and nonspecific interfaces differ. We further discuss how flexible or unstructured proteins can achieve specificity, which will lead to a discussion of how proteins mediate multispecificity. We conclude the section by investigating antigen−antibody interactions in detail and briefly address how the protein surface is tailored to resist nonspecific interactions, which sets the stage for the sections discussing biosensing.

4.1. Structural Features of Affinity

The first attempts to link binding affinity to structure were conducted by comparing various structural interface properties such as buried surface area, interfacial hydrogen bonds and salt bridges, buried water molecules, conservation of residues, planarity (shape and size of interface), hotspots, protein secondary structures, and conformational change, *etc.* by statistical means from known binding interfaces.[49,204−206] These indices work well when it comes to distinguishing homodimers consisting of two identical molecules from heterodimers that are composed of two different molecules.[204,207] However, they cannot discriminate transient interfaces from the rest of the protein surface reliably.[206] Nevertheless, for the subsequent discussions, it is useful to briefly review their most important interface properties (Figure 8a).

4.1.1. Buried Surface Area. For rigid complexes, the only parameter that correlates with binding affinity is the buried surface area.[28] However, this correlation does not hold for flexible complexes where there is not a single differentiating parameter between interfaces responsible for specific interactions vs the noninterfacing surface.[206] In such complexes, global surface properties play a role but the mechanisms by which they influence these protein interactions are still unclear.[28] A minimal model for binding affinity prediction based solely on the size of the interface and the magnitude of conformational change upon complex formation has been reported; however, this model lacks the accuracy and specificity needed to make useful biological predictions.[199] Thus, affinity predictions based on structural parameters appear to be inherently limited.

This limitation is linked to the conclusion of the previous section, that most of the binding strength of high-affinity complexes is provided by only a few amino acid residues.[53] However, this dependence on a few residues is contingent on the capacity of these specific residues to form strong bonds, which usually requires solvent expulsion from the recognition interface.[208] Yet, the interface is never completely dehydrated and the hydration of the interface is nonuniform, suggesting that the residues present at interfaces can be divided into affinity-providing and specificity-determining residues[69,185] (see Figure 8).

4.1.2. Hotspots. An amino acid residue that contributes significantly to the binding energy and is structurally conserved is referred to as a hotspot.[28,46,209,210] In the literature, there is some disagreement over the exact affinity threshold above which a residue should be called a hotspot. To address this controversy, distinction between "warm" and "hot" spots has emerged, with contributions to the free binding energy ranging from 8−16 kJ/mol (3.37−6.75 k_BT) or <16 kJ/mol (6.75 k_BT), respectively.[28,183] Hotspots have specific compositions and are enriched in amino acids that can form multiple interactions, such as tryptophan (21 %), arginine (13 %), and tyrosine (12 %), whereas they are depleted in uncharged amino acids such as leucine, valine, serine, and threonine.[211] These enriched amino acids are particularly suited for high-affinity interactions because they can participate in many intermolecular interactions upon desolvation and have long side-chains.[28]

4.1.3. Water Expulsion. Hotspots are primarily located in the center of an interface and in complementary surface pockets providing strong evidence for the need of dehydration to achieve high-affinity interactions (Figure 8c).[211,212] A well-established theory, the O-ring theory, postulates that residues around the hotspot effectively shield the high-affinity residues from the solvent.[212,213] Additionally, the dry-core-wet-rim theory proposed that atoms buried at similar levels within the protein are organized as rings and, in most cases, dehydration increases from rim to core.[214] In agreement with this theory, hotspot residues tend to be clustered in order to be shielded from the solvent.[47] These clusters are referred to as "hot regions"[215,216] and protein interfaces are built in a modular fashion in a sense that the contributions of isolated hot spots are usually additive.[217] However, while water expulsion is a necessary criterion for a hotspot, alternative factors such as a residue that can participate in many interactions and the complementarity of the van der Waals surface are also important.[212,218]

We have now covered, very briefly, how affinity is mediated at protein−protein interaction interfaces and stressed the importance of sufficient surface area burial, specific amino acid residues that compose the hotspots, and the expulsion of water. Now we move on to address the structural features of specificity.

4.2. Structural Features of Specificity

Proteins can only interact specifically if the recognition elements within the interface are complementary. Three complementarity criteria must be fulfilled in order to achieve a highly specific interaction: (1) ion complementarity, (2) hydrogen-bonding complementarity, and (3) steric (shape) complementarity as generalized by Kastritis et al. (Figure 8b).[28] These conditions can also be viewed as patterns of molecular recognition,[27] as complementarity between two binding sites can be achieved by not just a single arrangement of amino acids but by a large number of alternative combinations.[219] When one of the binding partners fails to meet at least one of the complementarity criteria, nonspecific interactions occur at the interface.

Thus, the complementarity requirements can also be viewed as *elements of negative design* that *decrease* the affinity if they are not fulfilled.[2,220] The complementarity of hydrogen bonds and electrostatic interactions is especially key because even though they usually do not contribute substantially to the binding affinity, if these negative design elements are frustrated, the desolvation penalty is substantial.[124,220] For instance, unfulfilling a hydrogen-bond or an electrostatic interaction costs a thermodynamic penalty of 2−25 kJ/mol (0.8−10.4 k_BT)[28,196] or 8−25 kJ/mol (3.3−10.4 k_BT), respectively.[28,173] Recalling that a reduction in free enthalpy by 10 k_BT decreases the binding affinity by roughly four orders of magnitude, a mere one to two frustrated hydrogen bonds in a desolvated area can completely disrupt a nanomolar interaction.

https://doi.org/10.1021/acs.chemrev.1c00044
Chem. Rev. 2021, 121, 8095−8160

4.2.1. Role of Buried Water Networks. The important role of buried water or water networks that are present at any protein−protein interface has been reviewed extensively by Ahmed et al.[183,221] The small size and capacity to form multiple hydrogen bonds renders interfacial water a highly versatile element in protein recognition. Interestingly, water seems to mediate contradictory roles in recognition. On the one hand, interfacial water promotes adaptability to molecular surfaces resulting in a high degree of promiscuous interactions. For example, there are proteins (*e.g.* OppA peptide-binding protein) that recognize a few amino acids independent of their sequence and modify the water content depending on the residue arrangement.[152]

On the other hand, interfacial water contributes to highly controlled binding and can mediate specificity and affinity by offsetting unfavorable contacts, providing numerous interfacial hydrogen bonds, dissipating charges, and improving interface complementarity (Figure 8c).[152,186,220,222] The aforementioned conditions contribute favorably to the binding enthalpy; thus, it has been suggested that the water network stability could be reflected in this thermodynamic parameter.[103,222] Thus, it is possible to hypothesize that the quality of the water network at the interface is directly related to the specificity of the interfacial interaction.[221] Surprisingly, the majority of water molecules at interfaces do not participate in hydrogen bonding; ∼70 % of all water molecules form hydrophobic bubbles. These bubbles may lubricate the interaction interface and facilitate configurational rearrangements of recognition elements for optimal binding.[183,221]

4.2.2. Specific vs Nonspecific Interfaces. The hydration characteristics of specific and nonspecific interfaces also contrast significantly, where specific interfaces appear to contain more hydrogen bonds per polar atom than nonspecific interfaces.[47,137,221] In addition, water-mediated interactions with protein backbone atoms are more pronounced in the case of specific interfaces.[221] In terms of chemical properties, it was found that examining the hydrophobicity of the protein surface does not seem to be sufficient to distinguish specific vs nonspecific interfaces.[137]

Although we are beginning to understand differences in the architecture of specific vs nonspecific interfaces, understanding the phenomenon of specificity for proteins with rigid 3-D structures remains elusive. There is, however, an entire class of proteins that lack defined 3-D conformations.[54] It is also worth mentioning that shape complementarity does not necessarily confer specificity.[223] Depending on the number and position of negative design elements within a binding site, the size of the required complementary contact area with attractive elements can be rather different; below a certain cutoff area the interaction simply stays repulsive, and the partners will not bind. To investigate how macromolecules lacking distinct structures can also achieve specificity, we now discuss the need for multispecificity.

4.2.3. Multispecificity. On average, a single protein is involved in approximately five specific intermolecular interactions in even simple organisms such as *Saccharomyces cerevisiae*.[70] While a majority of proteins interact with only a few other proteins, a small number of highly interconnected proteins, called "hubs", can have anywhere from five to over 100 interaction partners resulting in promiscuity (Figure 9a).[69,224] There is evidence that the importance in function of a hub is correlated to the number of interaction partners; thus, promiscuity is an essential feature for biology.[2,224] For reviews on protein promiscuity, see the work by Nobeli et al.[68] and Erijman et al.[225]

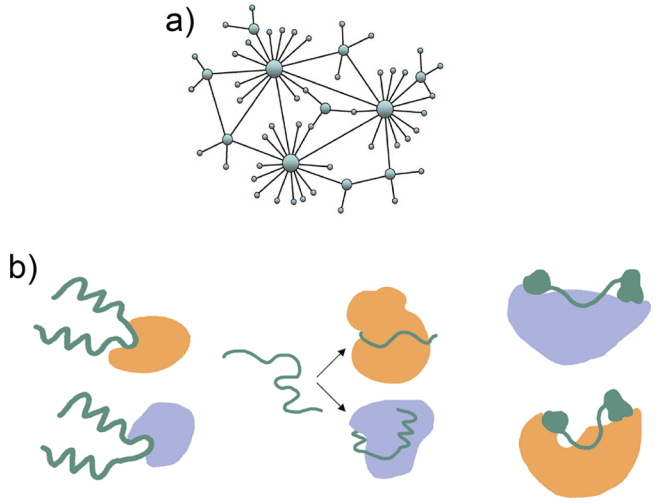

Figure 9. Protein hubs and multispecificity. (a) Protein interaction networks are built such that a few highly connected hub proteins integrate the signals from many partners. These hub proteins therefore need to be highly promiscuous (Figure reproduced with permission from ref 70. Copyright 2009 Elsevier). (b) Disordered proteins or segments are the main mechanism to achieve multispecificity. A disordered protein can bind to different partners via different orientations of the binding loops by folding into different structures, or disordered segments can link binding domains such that targets with different domain orientations can be bound (Figure reproduced with permission from ref 225. Copyright 2011 American Chemical Society).

Protein hubs can achieve many interactions while conserving specificity within limited surface areas due to the flexibility/plasticity of the protein, post-translational modifications, existence of several domains and multiple interaction sites, and solvent-mediated interactions.[68] Furthermore, an interface can mediate multispecificity via partial recognition of different proteins, but the most important parameter appears to be flexibility.[2] In the most extreme case, a *complete* disorder of the protein chain enables multispecificity in hubs known as intrinsically disordered proteins (Figure 9b).[54,226,227] For an in-depth review on intrinsically disordered proteins, see the work by Dunker et al.[54,226]

Disordered segments or disordered proteins are rich in charged amino acids, are deficient in hydrophobic residues, and exhibit a low degree of complexity. The extent of disorder can also be readily predicted from primary sequences with relatively good accuracy.[134,228] These disordered proteins bind through disorder-to-order transition mechanisms that allow adaptation to the interfaces of many different partners. The three complementarity criteria for specific interactions must hold true for flexible interactions as well; complementarity is created via conformational changes.[229] Not all segments of a disordered protein can mediate recognition, and the fragments that mediate recognition are called molecular recognition features (MoRF).[230] These structures are categorized into α-MoRF (α-helices), β-MoRF (β-sheets), ι-MoRF (irregular), and complex-MoRF (combination of the former three) based on the final structure these proteins adopt upon binding to a partner.[134]

The amino acid composition of intrinsically disordered proteins and their corresponding partners, as well as the physicochemical features of the interface, were assessed by the

https://doi.org/10.1021/acs.chemrev.1c00044
Chem. Rev. 2021, 121, 8095−8160

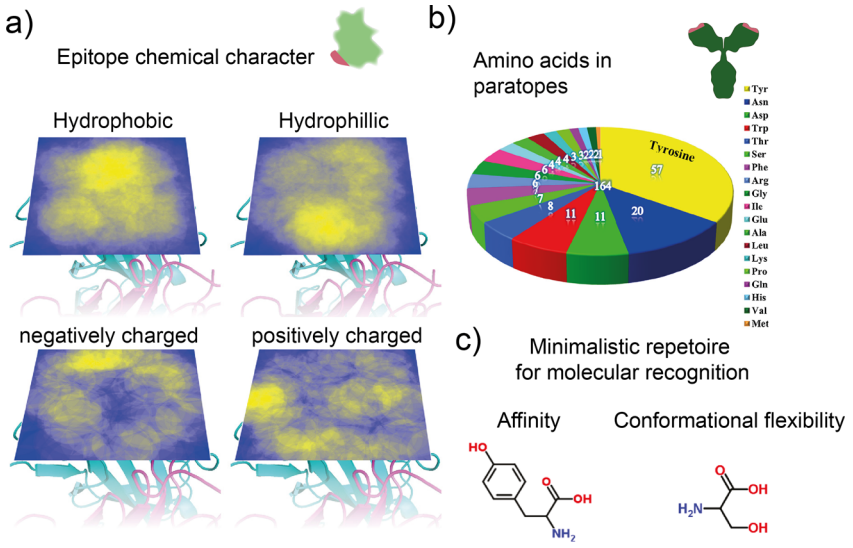

Figure 10. Architecture of antigen−antibody interaction interfaces. (a) Chemical character of the epitope. In general, the center of the epitope tends to be hydrophobic flanked by charged amino acids on the rim. Hydrophilic amino acids are usually dispersed in the entire plane (figure reproduced with permission from ref 179. Copyright 2013 Elsevier). (b) Amino acids that provide binding affinity in paratopes. Tyrosine is by far the most important amino acid for molecular recognition (Figure reproduced with permission from ref 234. Copyright 2016 Elsevier). (c) Minimalistic repertoire for molecular recognition. It is possible to evolve high-affinity specific antibodies with only tyrosine and glycine in the paratope.

following two publications.[230,231] Briefly, the MoRF regions contain higher local concentrations of large hydrophobic side-chains, especially aromatic residues, compared to the flanking disordered regions.[231] This difference is more pronounced for structure-forming MoRF (α, β) than for irregular MoRF, indicating the need of hydrophobicity to induce folding upon binding. Flexible regions also require fewer amino acids to form an interaction interface because there are no noncovalent interactions required to maintain the structure.[230]

To relate the structural properties of specific interactions back to the energy landscape, interactions involving a disordered partner smoothen the free energy landscape by their conformational entropy and enable low-affinity interactions to exhibit a funneled shape. In particular, the degree of conformational entropy allows the binding affinity to be fine-tuned while preserving the specificity. This regulation is especially important in signal transduction proteins.[232] The energy landscape of flexible recognition is discussed by Chu et al.[56] Furthermore, due to their highly dynamic nature, the flexible amino acid chains can prolong the lifetime of the nonspecific encounter complex and increase association rates, also known as the "fly-casting mechanism".[56,121]

To conclude, intrinsically disordered proteins provide a unique way to decouple specificity from affinity as well as serve as an efficient platform for multispecificity.[230] We are just beginning to understand their role and, in particular, how these proteins can achieve specificity. It is likely that kinetics in addition to thermodynamics and chaperone protein regulation plays a pivotal role in the control of their interactions.[231]

4.3. Specificity of Antigen−Antibody Interactions

After discussing the general structural features of specificity, we now narrow down the scope specifically to antigen−antibody interactions, to set the stage for later chapters that discuss protein-based biosensors. It is considerably simpler to gain an understanding of the structural principles of antigen−antibody interactions, since the antibody is a relatively rigid structure with a defined topology (Figure 7b). The surface of the antibody contacting the antigen is called the *paratope*, and the corresponding patch on the protein surface is the *epitope*. As mentioned previously, only the paratope evolves to achieve the binding affinity and specificity. Analogous to general protein−protein interactions, epitope−paratope pairs define complementary regions of shape, hydrogen bonds, and charge that can be obtained by various combinations of amino acids.[64,135]

Antibodies bind their target with six hypervariable antigen binding regions, termed complementary determining regions, with three regions situated in the light chain (L1−3) and the other three in the heavy chain (H1−3).[233] The heavy chain appears to be more critical for antigen recognition than the light chain and contributes more to the binding energy.[234] The antigen−antibody interface with 500−1000 Å^2 total surface area is smaller than the average protein−protein interface.[102,235] This interaction interface corresponds to roughly 5% of the surface area of the antibody molecule with ∼15−20 residues that are in contact with the epitope, whereas the variable region of antibodies is comprised of approximately 50 amino acids.[64,102,143,236]

The *functional epitope*, which provides most of the binding affinity, is much smaller and consists of only 3−5 amino acids on average.[102] These epitopes generally protrude from the protein structure and are more surface exposed than the rest of the antigen.[177−179] A table summarizing the most important structural properties of the epitope is provided by Kringelum et al.,[179] and for a review on this topic, see Rubinstein et al.[178]

In general, epitopes are characterized by hydrophobic amino acid residues in the center of the interface flanked by charged residues (Figure 10a). Hydrophilic amino acids are dispersed in the entire plane but with a preference to the periphery. Epitopes tend to be depleted of small hydrophobic amino acids (alanine, valine, leucine) while enriched by larger hydrophobic aromatic residues such as tyrosine.[179] The binding affinity seems to be provided by aromatic residues; half of the hotspots have been reported to consist of aromatic moieties.[209,237] Paratopes were found to be enriched in five residues that have hydrophobic (tryptophan, tyrosine), hydrophilic (asparagine), negatively

https://doi.org/10.1021/acs.chemrev.1c00044
Chem. Rev. 2021, 121, 8095−8160

charged (aspartate), positively charged (histidine), and aromatic characters (tryptophan, tyrosine, histidine) (Figure 10b).[179]

The enrichment of serine, glycine, and tyrosine have also been reported, particularly in the vicinity of the functional paratope.[209,238] Serine and glycine are believed to contribute little to the binding energy but provide the conformational flexibility that enables the rather bulky tyrosine residues to achieve optimal binding contacts with regard to shape and hydrogen-bonding complementarity.[238] Short-chain hydrophilic residues are particularly suited for this task because of the reduced side-chain conformational penalty at the interface. To support this hypothesis, minimalistic synthetic antibodies only composed of tyrosine and serine were able to recognize antigens with high affinity and specificity (Figure 10c).[209,238,239] In addition, the hydrophilicity of tyrosine and serine enables their exposure on surfaces without promoting nonspecific aggregation.[239]

Thus, in antibody complementarity determining regions, the combined spatial distribution of aromatic side-chains with short-chain hydrophilic residues enables recognition of common interface features, including backbone atoms, side-chain carbons, and surface-exposed hydrogen bond donors/acceptors, shared by all protein surfaces.[209] While the minimalistic repertoire of tyrosine, serine, and glycine is sufficient to achieve high affinity and specificity for most antigen−antibody interactions, some antigens also require other amino acids.[238] Hence, every amino acid has intrinsically different capabilities for molecular recognition. However, in addition to the amino acid composition of the paratope, the rigidity of the antibody molecule itself appears to contribute substantially to the specificity.[134,240]

4.4. The Protein Surface Is Designed to Resist Nonspecific Interactions

We have emphasized the importance of amino acid composition to achieve binding for antigen−antibody interactions. Here, we take a brief look at how Nature adapts the amino acid composition on the surface of proteins based on the biological environment. The average protein surface is a polar, zwitterionic carpet, but the exact composition depends on two factors: (1) the environment and (2) the relative abundance of the protein (Figure 11).[7,14,241]

First, proteins in more crowded environments, such as the cell cytoplasm, must be more resistant to nonspecific interactions than proteins secreted to extracellular space. Indeed, there are significant differences in their amino acid composition. For example, the surfaces of cytoplasmic proteins contain more charged amino acids, especially lysine and glutamic acid, compared to extracellular proteins that are composed of more polar residues (Figure 11b).[14] A more zwitterionic surface is more hydrated than polar surfaces, and therefore, the hydrostatic repulsion field is stronger.

Second, a highly abundant protein is more likely to interact with other proteins in a nonspecific manner, and thus, the evolutionary pressure to render the surface nonsticky or more hydrated is higher. Indeed, protein stickiness is inversely correlated with abundance (Figure 11c).[7] In biology, one of the harshest environments in terms of NSB is the interior surface of molecular chaperone proteins, which must resist thousands of different proteins and conformations.[14] These surfaces are even more enriched in glutamic acid and lysine with contents up to 70% in thermophilic *Escherichia coli*.[14] Thus, we can conclude that the even distribution of positively and negatively charged amino acid residues with high desolvation penalties, such as

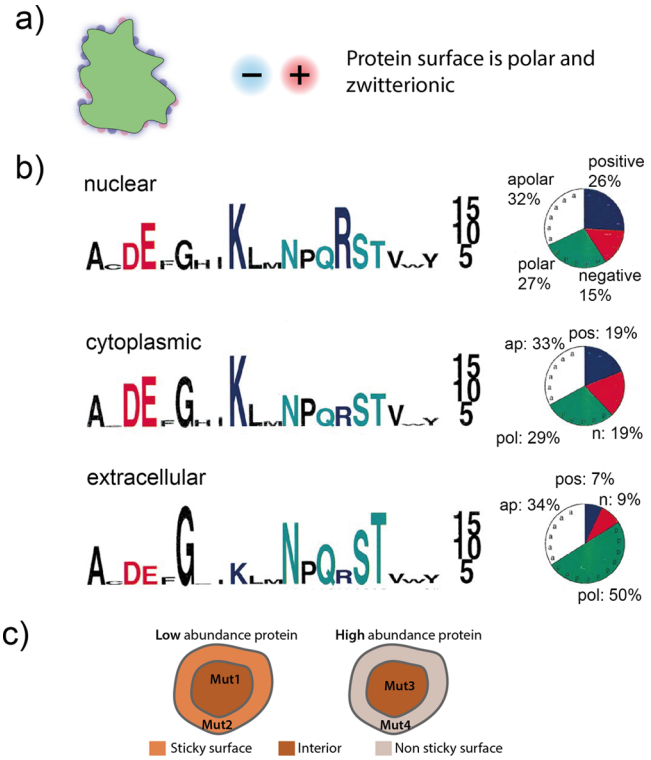

Figure 11. Protein surfaces are evolved to resist nonspecific binding. (a) Protein surfaces are highly zwitterionic and polar to create a strong hydrostatic repulsion field to limit the amount of nonspecific interactions. (b) Protein surface composition depends on the environment. The more crowded the environment (nucleus > cytoplasm > extracellular), the more zwitterionic the protein surface (Figure reproduced with permission from ref 241. Copyright 1998 Elsevier). Highly expressed proteins tend to have much less stickier surfaces than proteins with low expression levels.

glutamic acid and lysine, is Nature's preferred way to counteract nonspecific interactions.

4.5. Synopsis to Define Specific vs Nonspecific Binding

In the Introduction (section 1), we presented a classification framework of macromolecular interactions based on the number of binding partners, affinities, and interaction reversibility (see Table 1). Based on what we have covered in previous sections, we can integrate thermodynamic, intermolecular, and structural perspectives to define the features of SB and NSB concisely. To recap, in section 2, we outlined the *energy landscape theory*, which was originally developed for protein folding but in recent years also became a powerful way to explain protein interactions. We have seen that the energy landscape of NSB is rugged with many minima with similar depth and conformationally not well-defined end states. Alternatively, the energy landscape of SB is rather smooth and sufficiently steep to reach the ground state in relevant time scales. In the majority of cases, specific binders end up in a well-defined end state, irrespective of the binding mechanism (lock-and-key, induced-fit, or conformational selection), contrary to nonspecific binders.

In section 3, we discussed the distinction between SB and NSB in terms of *intermolecular forces*. It is important to stress again that SB and NSB are based on the same fundamental forces and their functional difference only arises from the relative contribution of the fundamental interaction forces. In particular, SB relies on short-range forces (van der Waals in general but, more specifically, hydrogen bonds and ionic interactions) while

https://doi.org/10.1021/acs.chemrev.1c00044
Chem. Rev. 2021, 121, 8095−8160

reversible NSB is composed of long-range, nondirected forces (electrostatic or hydrophobic). Irreversible NSB is mediated by exposure of hydrophobic protein motifs, which directly bind to the surface with high-affinity.

Finally, in this section, we stressed that the functional difference between SB and NSB primarily arises from the *architecture* of the involved interaction sites. The most evident structural difference between the two interactions is that SB has a clearly defined interface and orientation, whereas NSB has multiple interfaces and ill-defined orientations. Furthermore, SB is mediated by evolved binding sites that fulfill three complementarity criteria, while NSB interfaces do not undergo such evolutionary selection and violate at least one of the complementarity criteria.

By merging what we have learned from the energy landscape theory, intermolecular forces, and the architecture of biomolecular interactions, we can summarize SB vs NSB features in Table 2. With a clearer definition of these two phenomena in mind, in the following sections, we will discuss the challenges that reversible and irreversible NSB, as well as cross-reactive binding, impose on current state-of-the-art biosensors. We will also discuss existing practical methods to overcome NSB to enable the quantification of specific molecular recognition events.

Table 2. Synopsis of Specific and Nonspecific Binding Features upon Studying Thermodynamics, Intermolecular Interactions, and Structural Characteristics

Features	Specific Binding	Nonspecific Binding
Thermodynamics (energy landscape)	Funneled energy landscape with a defind final state	Rugged energy landscape with many local minima
Intermolecular forces	Short-range forces (van der Waals/acid−base interactions)	Long-range forces (electrostatic/hydrophobic)
Stuctural (interface architecture)	• Defined final interface and orientation • Evolved or designed binding sites • Specific interactions are higher in affinity than all other binders to interface	• Interface/orientation not well-defined • No evolved or designed binding sites • Can still be selective (interactions of some proteins are favored)

5. NONSPECIFIC BINDING AS A BOTTLENECK IN DIAGNOSTICALLY RELEVANT BIOSENSING

Current medical diagnostics are supported by two main technology pillars: *imaging modalities* (X-ray, MRI, ultrasound, PET-CT, *etc.*) that provide information about morphological changes that indicate a disease and *biosensors* that measure the changes in concentration of certain molecules called biomarkers that correlate with a disease. Sometimes the combination of these methods is needed, *e.g.* when tissue biopsies are specifically stained for certain molecules and imaged at the same time.

Genetic disease identification and tumor classification became straightforward due to the rapid progress of polymerase chain reaction (PCR)-based genetic tests and various sequencing technologies. These tools benefit from the high specificity of molecular tools that Nature has developed through millions of years of evolution. With these technological advancements, genetic tests are capable of detecting and identifying a single molecule, which means that they have essentially reached the ultimate sensitivity and, therefore, are typically not limited by NSB problems.

The rest of molecular diagnostics is based on biosensors that transduce a molecular recognition/binding event into a measurable signal. While enzymatic biosensors, such as the glucometers for diabetes management, use an enzyme to convert the analyte of interest (e.g., glucose) directly to a measurable electric current, most other sensors are based on a SB reaction between the analyte and a receptor. The thermodynamics and the details of this specific reaction are discussed in the previous sections. Here, we will focus on the critical role NSB plays in such immunoassay-based diagnostics. In the first part of this section, we will start by explaining why NSB is a current bottleneck in existing diagnostically relevant biosensors and how it influences their limit of detection (LOD) (section 5.1). We begin by describing how typical diagnostically relevant assays are performed (section 5.1.1). Then, we explain why NSB is critical for the correct assessment of the LOD, while also pointing out the dangers of blindly pushing for sensor sensitivity (section 5.1.2). Finally, we include a recipe for the correct assessment of the LOD for diagnostics (section 5.1.3.).

Most biosensing immunoassays take place on, or in the direct vicinity of, a man-made solid−liquid interface. Such artificial surfaces include polymer wells, glass slides, electrodes, or nanoparticles. Therefore, the quantification of binding events at such surfaces is of profound importance in all applications where an artificial surface is brought into direct physical contact with a biological system. For most applications, these surfaces are pretreated with polymers or small molecules to tailor the surface properties to elicit the desired biological response, *i.e.* the reduction of NSB. As both the SB and the NSB are governed by well-developed but often neglected kinetic models, the majority of this section will be dedicated to such theoretical models that enable the prediction and optimization of biosensor performance (section 5.2). This part of the section progresses from less complex toward more sophisticated models.

In particular, we discuss how to quantify the concentration of an analyte or the strength of an interaction mediated by specific interactions while avoiding influences of nonspecific interactions. The quantification of these adsorption types is essential to gain information on the theoretical limits of biosensors and how biosensor geometries can be optimized to maximize the LOD as well as the SB to NSB ratios for a given surface coating, receptor, or assay type. We will present existing models that describe such interactions based on the relevant physical parameters such as the association, dissociation, and equilibrium constants (k_{on}, k_{off}, and K_d).

We will first review the available models for specific and nonspecific interactions in biosensing (sections 5.2.1 and 5.2.2). We will then discuss which equilibrium models should be used for molecular interactions in biosensing and explain how to quantify NSB using the most basic kinetic (*i.e.*, the Langmuir) model (section 5.2.3). This section will also include an explanation on why and under what conditions sample dilution, a common experimental practice, is able to reduce the NSB problem using the double competitive model. To model an entire assay, we will also have to take some kinetic aspects into account, which will be discussed in section 5.3.1. Based on this toolbox, we will formulate a biosensing assay quantification model and discuss the implications of assay parameters on the biosensing LOD in section 5.4.

https://doi.org/10.1021/acs.chemrev.1c00044
Chem. Rev. 2021, 121, 8095−8160

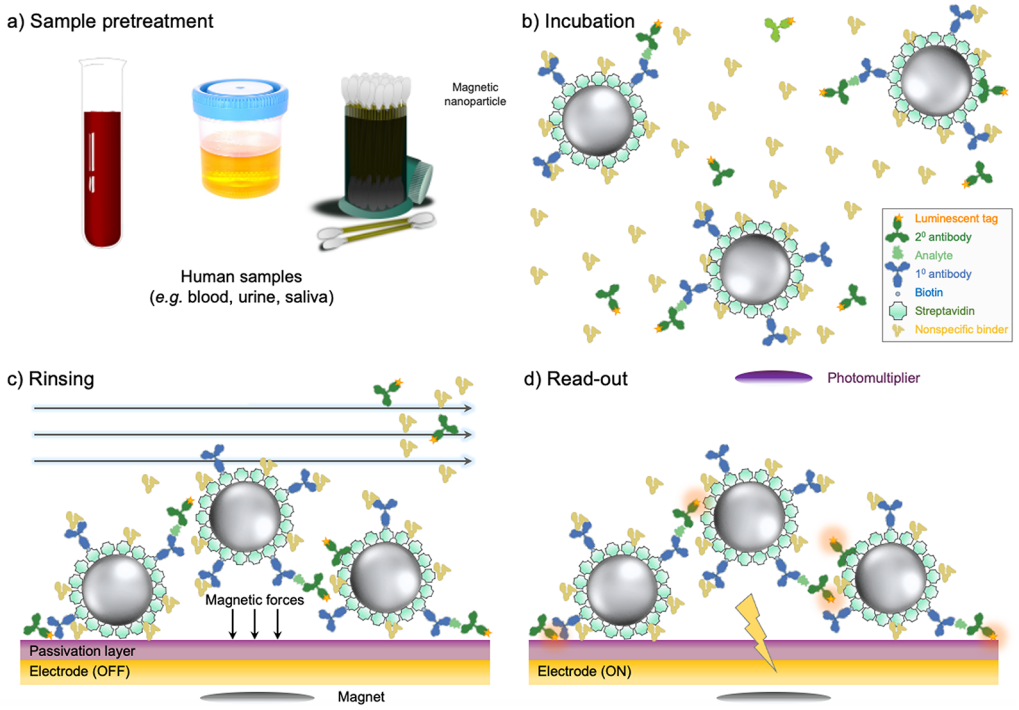

Figure 12. Steps of a modern immunoassay: (a) typical human samples need a brief pretreatment before the assay. (b) Next, the sample with the analyte is incubated with a pair of antibodies that target different epitopes: one is biotinylated, the other is labeled with a signal generating molecule. The formed sandwiches are then captured by streptavidin-coated magnetic particles. (c) A magnetic field brings the particles with the analyte molecules to the surface of the electrode, which is passivated against nonspecific binding, and the sample and unbound reagents are rinsed away. (d) Finally, the signal (in this case electrochemiluminescence) generated by the labels on the substrate-bound particles is read out.[245] The performance of this assay is limited by the NSB of the signal generating antibody primarily to the particles but also to the electrode.

5.1. Why Is Nonspecific Binding a Bottleneck in Diagnostics?

To understand this question, we first need to know how typical diagnostically relevant immunoassays are performed today, prior to analyzing the various noise sources and revealing the conditions when NSB is limiting sensor performance. Finally, we will provide a recipe for assessing the LOD of any diagnostically relevant biosensor correctly.

5.1.1. Typical Diagnostically Relevant Immunoassays.

First, a sample is collected from the patient. This sample can be whole blood (plasma, serum), urine, saliva, or other body fluids such as synovial, or cerebrospinal fluid, *etc.* Typically about 20–100 μL, but often several milliliters, are needed for the assays, which constitutes a serious problem for their use especially in neonatology. However, miniaturization approaches are being developed allowing for measurements that require as low as one microliter of sample.[242−244] After some necessary pretreatments (*e.g.*, centrifugation, sedimentation, or addition of anticoagulants, *etc.*) the sample is loaded into a fully automated laboratory analyzer that performs the assay (Figure 12).

The first step of a typical immunoassay is incubation of the sample with probes specific to the analyte of interest. Often, additional reagents have to be added to suppress unwanted binding of interfering compounds, which is also a type of NSB. Especially, human anti-mouse antibodies can cause problems by specifically blocking the primary antibodies that are used in the assays.[246] In addition, rheumatoid factors that bind to the fragment crystallization region of antibodies of other species can interfere with assay performance.[247] Details on these NSB-suppressing reagents are key to commercial success and therefore seldom found in the literature because of their extreme importance in achieving the required sensitivity. More information on this effect is presented later in section 5.3.

To shorten assay times, most modern setups already add the signal generating compounds during this first sample incubation step. Here, the choice of label is largely determined by the NSB properties of the signal generating molecules. This procedure is possible because the signal generating compounds are typically linked to receptors that recognize another epitope of the analyte than the capture probe (see Figure 12). Both probes are mostly antibodies, although recently other molecules such as aptamers,[248,249] SOMAmers,[250] or DARPins,[251] are emerging but often lag behind the performance of antibodies in terms of their NSB properties. While probes are also often optimized for low off-rates and low K_d values, the most important property of suitable probes is their minimal cross-reactivity (*i.e.*, low NSB). The most widely used signal generating compounds used to be enzyme-linked or fluorescent antibodies, but these labels are being replaced by particle systems and electrochemiluminescent ruthenium complexes,[252−254] which have clear advantages for high-end assays:

1. Assay times can be shortened using magnetic particles because particle-bound analytes and labels are brought in contact with the sensor using an external magnetic force, thereby overcoming diffusion limitations.

2. Particles (*e.g.*, magnetic,[255] metallic,[256,257] or liposomal[258]) can also contain many labels (enzymes,[259] fluorophores,[260] and electrochemiluminescent tags[261,262]), which means that in principle, a single particle could be detected via existing biosensor methodologies.

https://doi.org/10.1021/acs.chemrev.1c00044
Chem. Rev. 2021, 121, 8095−8160

3. It is also easier to separate specifically bound vs nonspecifically bound particles because larger magnetic or fluid-shear forces can be applied to test the strength of the biochemical bond that tethers these particles to the surface. Later in this and in the next section, we will see why this configuration contributes to the success of magnetic separation,[261] flow discrimination,[263] and lateral flow assays.[264]

4. Electrochemiluminescent labels tend to induce less NSB than fluorophores due to their small size and favorable solubility in water.

After the incubation step that can be as short as 9 min, the sample and the unbound signal generating compounds are washed away and an optional magnetic and/or fluidic force discrimination is applied to eliminate nonspecifically bound particles.[254,265] Finally, the signal is read out by the corresponding biosensor technology. At every step of this assay, NSB plays an important role and NSB-induced interferences must be eliminated for optimal performance.[266]

5.1.2. Contribution of Nonspecific Binding to the Limit of Detection. As we have seen in section 2, molecular interactions are determined by the Gibbs free energy of dissociation through eq 1, which directly leads to eq 3 that connects the proportion of captured analytes to the free analyte concentration and the equilibrium constant.

Alternatively, in section 3, we noted that already a few hydrogen bonds and/or salt bridges can lead to NSB with approximately millimolar equilibrium constants (see Figure 6). As all receptors and surfaces have chemical groups that engage in such bonds, any sensor surface, regardless of how well it is engineered, will have to deal with an inevitable NSB problem. Since the concentration of the most abundant proteins in human samples is in the millimolar range, this inevitable NSB is expected to account for at least a few percent receptor occupancy. Figure 13a shows the expected receptor occupancy (the % of receptors that capture an analyte) as a function of analyte concentration for a typical sandwich assay (enzyme-linked immunosorbent assay, ELISA).

It is interesting to note that the amount of captured analytes is not increasing if the affinity of the receptors is sufficiently good. Figure 13a shows no difference between receptors with nM and pM equilibrium constants because in both cases, nearly all analyte molecules are captured in equilibrium. Another important feature of such dose−response curves is the analyte concentration at which the receptor occupancy is 50%. This value is often within an order of magnitude on each side of the equilibrium constant (K_d) of the used receptors.

For the diagnostically relevant (typically fM−pM) concentrations, the receptor occupancy is very low and eq 3 reduces to a linear dependency of the receptor occupancy resulting in a dose−response curve similar to the one depicted in Figure 13b. In addition, at such low concentrations, equilibrium is seldom reached experimentally with such surface-based assays due to practical reasons. Therefore, diffusion also plays a key role in determining how many analyte molecules are captured and how fast. A key theoretical paper by Squires et al. constructively summarizes these effects.[267]

To calculate the LOD using such dose−response curves, the typical procedure is to find the concentration at which the signal equals the baseline, *i.e.* the signal at zero analyte concentration, (S_0) plus three times its standard deviation (σ_{S_0}):

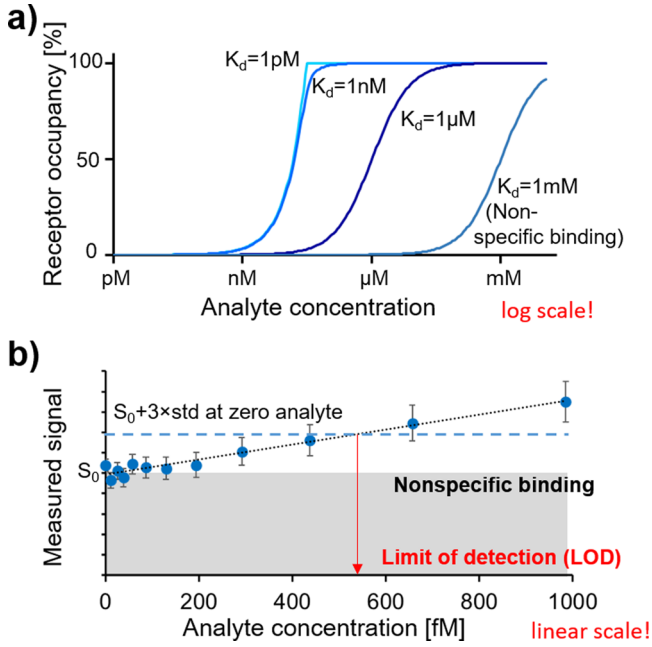

Figure 13. (a) Dose response curves of a typical enzyme-linked immunosorbent assay sandwich assay. The receptor occupancy saturates above the K_d value of the used receptors. The parameters of a 1536 well-plate were used for the calculations with 0.7 mm^2 surface area and 1 μL sample volume. (b) The measured signal of typical biosensors is directly proportional to the amount of captured analytes. Here, the diagnostically relevant, linear part of a typical dose−response curve is shown along with the inevitable nonspecific binding and the limit of detection (note the difference between the log and linear scale of the two curves).

$$\mathrm{LOD} = \frac{3\sigma_{S_0}}{dS/dc} \sim \frac{\sqrt{S_0}}{dS/dc} \sim \frac{\sqrt{\mathrm{NSB}}}{dS/dc} \tag{8}$$

This calculation is due to statistics, because for Gauss-distributed random variables, the chance to find a value within such bounds is 99.73%. Here, c denotes the analyte concentration and $\frac{dS}{dc}$, *i.e.* the slope of the dose−response curve, is the sensor's sensitivity.

Figure 13b and eq 8 also illustrate how the NSB plays a key role in determining the LOD. The standard deviation of the signal at zero analyte concentration is linearly proportional to the LOD. Most binding processes follow a Poisson distribution, where the standard deviation is proportional to the square root of the mean; therefore, the LOD is expected to be proportional to the square root of the measured signal at zero analyte concentration. As diagnostically relevant biosensors have lower instrumental noise than the measured NSB at zero analyte concentration, the NSB plays a significant role in determining the LOD.

One exception is the recently developed lateral flow assay (LFA) for the Covid-19 rapid test. Similar to most LFAs, this diagnostic test is based on the color change upon binding of gold nanoparticles to the test line. However, due to the highly scattering nature of the nitrocellulose substrate of the LFA, even in the absence of any gold particles, a large signal is obtained (*i.e.*, S_0 is large).[268] As a consequence, this sensor methodology is not limited by the NSB but rather by the number of gold particles that are required to obtain a measurable/visible change on the test line. At present, this threshold is between 1 and 10 million particles corresponding to a LOD on the order of 10,000

https://doi.org/10.1021/acs.chemrev.1c00044
Chem. Rev. 2021, 121, 8095−8160

viruses.[269,270] This constraint is the reason why such rapid tests miss many Covid-19 positive patients with low viral loads.

5.1.3. Recipe for Correctly Assessing the Diagnostically Relevant Limit of Detection. The concepts summarized in the previous section lead to a straightforward recipe for designing experiments to establish the LOD of a biosensor. Unfortunately, the vast majority of publications in the existing literature contain mistakes that could easily be avoided. Here, we list a few such examples without referring to specific publications:

(a) When the LOD is determined only in buffer, it is difficult to claim anything about diagnostic relevance because the effect of NSB is completely ignored.

(b) A common practice is to add the analyte of interest to a diagnostically relevant solution (*e.g.*, blood, plasma, or serum) but taking the sample from only a single patient. This protocol inevitably reduces the standard deviation of the signal at zero analyte concentration and leads to severe underestimation of the LOD. Multiple patient samples pooled together as one sample cause the same error.

(c) Another common mistake is when instead of determining the LOD, the authors report on the "improved" sensitivity of their methods by comparing the initial slopes of their dose response curves. Although a higher slope is expected to lead to lower LODs according to eq 8, often the effect is largely exaggerated because the "improved" sensitivity also effects the signal and its standard deviation at zero analyte concentration (see also Figure 23 in section 6).

(d) Many reports have tried to improve the performance of their sensor by referencing. This practice is so common that we dedicate a whole section to this topic in section 6. While referencing, when done correctly, can be highly beneficial, most often the noise at zero analyte concentration is not reduced but rather increased. This miscalculation arises from not properly accounting for error propagation when adding the individual errors of the two measurements.

Finally, here is a short description of the recipe that scientists (reviewers and editors) should follow when determining the LOD of a biosensor:

1. Obtain samples from at least three different patients (or biological replica) that definitively contain no analyte. For companies that plan to market a diagnostic assay, often hundreds of patients need to be tested because a small fraction of the population might exhibit different NSB than the majority.
2. Spike each patient sample with analyte concentrations in the vicinity of the expected LOD. For each patient/donor, a minimum of five evenly distributed data points should be collected above and below the LOD.
3. Obtain the dose−response curve for each patient. Ensure that the instrumental noise is smaller than the biological noise by measuring some of the samples multiple times.
4. Calculate the means and standard deviations at each measured concentration.
5. Calculate the slope and the standard deviation of the signal at zero concentration, which directly leads to the diagnostically relevant LOD.
6. If the standard deviation of the signal at zero concentration is substantially less than at any other analyte concentrations below the obtained LOD, then the LOD has to be recalculated using the largest standard deviation.

Following this protocol will guarantee that the experimental LOD is assessed correctly and practically. However, during the development of a new biosensor, such a protocol is often too cumbersome to apply at every step of the process. Therefore, in the following section, we will provide the theoretical models that help to enhance our understanding about the most important aspects of such assays and their expected performance. Being familiar with these models can shorten the biosensor development process and help to avoid common mistakes.

5.2. Models for Specific and Nonspecific Binding to Estimate the Limit of Detection

While SB can be considered as a chemical reaction, as we have seen in the previous sections, NSB is a more complex process. In modern diagnostic assays, *e.g.* the electrochemiluminescent assay depicted in Figure 12, the primary source of noise is the NSB of the labeled antibody to the detector's surface. Such NSB to surfaces is often referred to as adsorption and can exhibit diverse characteristics. To this end, a broad range of models are required to be adapted to the studied system: *e.g.* the adsorption of gas molecules to solid surfaces,[271] the adsorption of proteins at solid−liquid interfaces,[272,273] or the interaction of proteins with previously surface-adsorbed proteins.[274] Depending on the specific conditions, molecular adsorption to a surface can be reversible[272,274,275] or irreversible.[273]

Furthermore, based on the biosensing application, the end state of the binding process (equilibrium) or how this final state is reached (kinetics) is of interest. Kinetics can be dominated by the limited speed of the reaction (reaction limitation)[276] or by the finite diffusional transport (mass transport limitation)[276,277] or a combination thereof[275,278,279] (Figure 14). Different models

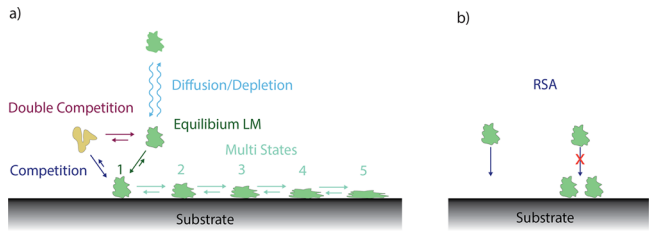

Figure 14. Illustration of equilibrium and nonequilibrium models for protein surface interaction. (a) Equilibrium models: Langmuir model (LM), optional with nonspecific competition, depletion, diffusion, and additional postadsorptive states. (b) Nonequilibrium model such as random sequential adsorption (RSA).

have been developed to describe these different scenarios quantitatively. Hence, it is of great importance to identify what type of adsorption process a system is dealing with prior to choosing and applying a model. Such a choice is in fact not trivial and is a common source of mistakes.[280]

One common source of error is the inaccurate understanding of the reversibility of the adsorption process.[280] The reversibility of a protein interaction on an artificial surface is often measured experimentally by the amount of desorption upon rinsing of a previously adsorbed molecule.[273,281−285] Hence, the term "irreversibility" will be used herein for situations where there are no observable desorption events within the time frame of the experiment, while exchange effects may still occur. Another important aspect of NSB quantification is the identification of the regime of the adsorption kinetics. Unfortunately, often it is

https://doi.org/10.1021/acs.chemrev.1c00044
Chem. Rev. 2021, 121, 8095−8160

not straightforward to determine whether an adsorption process is limited by the reaction kinetics or the diffusion kinetics. We will discuss this issue in section 5.3.1.

Once the actual NSB process is identified in terms of reversibility and kinetics, it is possible to choose a suitable model. On the basis of a few selected case studies, we will discuss the most important models and how they can be applied. Starting at minimal complexity, we will first discuss reversible and reaction limited adsorption processes without mass transport influences. We will successively increase the model complexity to address adsorption problems of different characteristics toward obtaining a quantitative description of more realistic experimental scenarios.

5.2.1. Models for Reversible Binding Processes. A successful strategy for modeling adsorption processes is to use a model that is analogous to the modeling of a reversible and kinetically limited chemical reaction[286] described by the law of mass action.[287] Three such models are outlined in the following section: the Langmuir model (LM), the competitive LM, and the Freundlich isotherm.

5.2.1.1. Langmuir Model (LM). Introduced more than a hundred years ago[288] and further developed soon thereafter[271] by Irving Langmuir, the Langmuir isotherm[289] grew to become a very commonly applied model for molecular adsorption to surfaces.[280] While studying the adsorption of gas molecules to a solid−gas interface, Langmuir proposed a mathematical model to quantify the experimental data. The model is based on the following six assumptions:[280]

1. All adsorption sites are homogeneous.
2. Each adsorption site can bind an individual solute molecule.
3. A dynamic reversible equilibrium is established in the time frame of the experiment.
4. A monolayer coverage is reached at saturation.
5. The heat of adsorption (and thus K_d) is independent of the coverage (no interaction in between solutes on the surface to alter their adsorption behavior).
6. The concentration of unbound molecules remains constant during the adsorption process.

Assumption 6, that the amount of unbound molecules is sufficiently large to be assumed constant during the adsorption process, is not usually included in the list.[280] Whether this assumption is inherent or not depends on the formulation of the Langmuir isotherm, but it is important to note that the original and most often applied version of the LM does include this assumption. Since the concentration of background molecules is in the millimolar range for most diagnostic samples, this condition is easily fulfilled for NSB. However, especially for diagnostically relevant biosensors with low analyte concentrations and low sample volumes, the depletion of analytes upon binding to the receptor can considerably alter the resulting dose−response curve. A formulation that does not include this assumption because it accounts for the change of the free binder concentration will be discussed in section 5.2.3.

Only if all these listed assumptions are fulfilled within the necessary accuracy, one can use the original LM to quantify an adsorption (NSB) process. Langmuir states that at equilibrium, the rate of adsorption equals the rate of desorption.[271,288]

$$A + R \rightleftharpoons RA \tag{9}$$

This relationship leads to the following condition at equilibrium (identical to eq 3):

$$K_a^A = \frac{C_{RA}}{C_R C_A} \tag{10}$$

where K_a^A is the affinity constant and C_A, C_R, and C_{RA} are the concentrations of the free analyte, the receptor, and the receptor−analyte complex, respectively. We will use K_d in the text and either K_a or K_d for the equations based on aesthetic reasons (see also section 2 for the thermodynamic origin of the definitions).

Subsequently, Langmuir derived an expression for the equilibrium surface coverage Θ_A, where the surface coverage is the amount of adsorbed molecules A normalized by the amount of receptors R (eq 12 and illustrated in Figure 15). In this particular case, it is the same value that we called "receptor occupancy" in Figure 13, and the two terms are often interchangeable in the nonspecific binding literature. The surface coverage only depends on the association constant K_a and the concentration of the free adsorbing molecules, C_A.

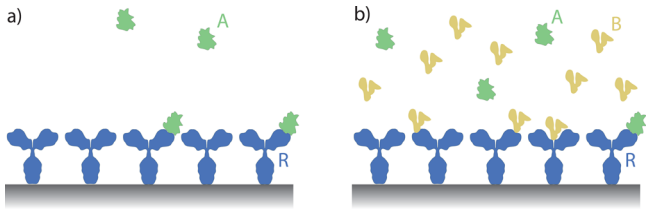

Figure 15. Langmuir (LM) and competitive Langmuir models (CLM). (a) Illustration of the adsorption equilibrium of an analyte (A) to surface bound receptors (R) according to the LM. (b) Illustration of the adsorption equilibrium of an analyte (A) to surface-bound receptors (R) in the presence of a competing molecule (B) according to the CLM.

$$\Theta_A = \frac{C_{RA}}{C_{R_{tot}}} \tag{11}$$

$$\Theta_A = \frac{K_a^A C_A}{1 + K_a^A C_A} \tag{12}$$

This formulation assumes a constant free molecule concentration C_A during the adsorption process. This assumption is valid for small surface-to-volume ratios or for assays with a continuous flow, replenishing the free molecules. In addition, this formulation assumes that the thermodynamic activity of the molecules in solution is equal to its concentration.[290,291] Especially for surface-bound reactions and reactions in nonideal mixtures, this assumption is not necessarily fulfilled. For the following discussions, we assume activity coefficients equal to one.

Langmuir's main attention was originally directed toward the equilibrium state of the adsorption.[271,288] However, some applications also demand the quantification of reaction kinetics and thus require an understanding of how the equilibrium is reached. In cases where the reaction rate dominates the kinetics, models such as the first and second order rate model are a common choice.[292] These models are analogous to chemical reaction kinetics and have been shown to be equivalent to kinetic models deduced from the LM.[293−295] More insight into the kinetic aspects of biosensing problems are shown in section 5.3.1. An extensive overview of reaction limited kinetic models used in the literature was published by Ho and co-workers.[292]

https://doi.org/10.1021/acs.chemrev.1c00044
Chem. Rev. 2021, 121, 8095−8160

5.2.1.2. Competitive Langmuir Model (CLM). Clinically relevant biosensing samples commonly consist not only of the analyte but also of a large amount of background molecules (B).[296] When such samples are incubated on a receptor surface, the background proteins will compete with the analyte for the receptor binding sites.[297] Which fraction of analyte and background proteins will bind to the receptors is dependent on the receptor specificity and the concentration of all molecules present.[297] The model applied in such cases is termed the CLM.[297−300] To calculate the fractional receptor occupancy in the presence of one background molecule B, the Langmuirian process represented by eq 9 with the equilibrium observation of eq 10 is still valid. In addition, we now have to introduce a second process via eq 13 with an equilibrium defined by eq 14:[297]

$$B + R \rightleftharpoons RB \tag{13}$$

$$K_a^B = \frac{C_{RB}}{C_R C_B} \tag{14}$$

The total amount of receptors, R_{tot}, is now the sum of the free receptors R and the receptors covered by molecule A and the receptors covered by molecule B:

$$C_{R_{tot}} = C_R + C_{AR} + C_{BR} \tag{15}$$

which results in a fractional receptor coverage of binder *A* for two modeled competing binders (*A* and *B*) as also illustrated in Figure 15b:

$$\Theta_A = \frac{K_a^A C_A}{1 + K_a^A C_A + K_a^B C_B} \tag{16}$$

Similarly, the fractional receptor coverage of binder B for two modeled competing binders (A and B) is the following:

$$\Theta_B = \frac{K_a^B C_B}{1 + K_a^A C_A + K_a^B C_B} \tag{17}$$

Since there is not only one but also many relevant nonspecific binders present as background proteins in complex biological samples, we might want to consider more than just one background protein. For *n* relevant molecules, the fractional receptor coverage of the binder *j* for *n* total modeled competing binders is[301]

$$\Theta_j = \frac{K_a^j C_j}{1 + \sum_{i=1}^{n} K_a^i C_i} \tag{18}$$

5.2.1.3. Non-Langmuirian, Cooperative Models. Various scientific applications deal with processes that are non-Langmuirian in the sense that at least one of the Langmuirian assumptions are violated. A large variety of non-Langmuirian models were designed for such cases.[302,303] One early example for such a model was the Hill equation describing cooperative adsorption effects.[304] Such cooperativity is present, if the Langmuirian assumption 5 is violated. Hence, the equilibrium fractional occupancy of receptors is no longer linearly dependent on the ligand concentration,[304] which also happens if binding of additional molecules changes the ligand's affinity.[305] The Hill equation is an equivalent formalism to the Langmuir−Freundlich isotherm:[306]

$$\Theta_A = \frac{K_a C_A{}^{\alpha}}{1 + K_a C_A{}^{\alpha}} \tag{19}$$

The exponent alpha is the Hill coefficient. A Hill coefficient smaller than one describes negative cooperativity, and one larger than one, positive cooperativity. If the Hill coefficient is equal to one, the observed process is a noncooperative Langmuirian process.[304] Further developments will not be discussed here but have been summarized comprehensively by many authors.[35,37,304,307−310]

An alternative empirical non-Langmuirian isotherm, often used to model adsorption of charged molecules to liquid−gas interfaces, is the Frumkin isotherm.[311] Such an adsorption process is dependent on the coverage due to interactions of the binders with previously immobilized molecules.[311−313] Hence, it is violating the fifth Langmuirian assumption. Further generalizations for the LM can be found elsewhere.[302,303]

After having introduced some relevant basic adsorption models, we will now discuss which one can be implemented to explain effects observed in biosensing assays. In particular, we will focus on how these models can be extended to answer relevant biosensing questions and problems related to SB and NSB. The aforementioned effect of cooperativity has been brought into context with a rather controversial effect sometimes observed in DNA biosensors.

Several groups have observed non-Langmuirian receptor density-dependent DNA−DNA interactions.[61,314] The observed effect is non-Langmuirian because the fractional occupancy of DNA was increased by increasing the receptor DNA density. Ozer et al. accounted for this effect by implementing a cooperative model, which combines the Langmuirian specific binding with a non-Langmuirian receptor density-dependent cooperative NSB.[61] We call this effect nonspecific avidity in addition to the specific avidity of the multivalent DNA.[85] Rajendran et al. suggested an alternative explanation. They proposed an effect called "attinebility", which describes the increased rebinding probability of an analyte if the neighboring receptor density is higher. This phenomenon results in a higher apparent affinity of the analyte, despite being bound to only one receptor at a time.[314] These examples demonstrate that the original Langmuirian isotherm sometimes is unable to model biosensing data correctly and that there is a need for better models. The following section will discuss a variety of Langmuir extensions that prove essential for many biosensing applications as well as a selection of useful, completely non-Langmuirian models.

5.2.2. Models Including Irreversibilities of the Adsorption Process. Up to this point, we discussed the quantification of reversible adsorption processes that establish an equilibrium of adsorption and desorption during the time course of the experiment. This reversibility is not inherent in all adsorption processes, as the nonspecifically bound proteins become part of the protein film coating the surface.[315−317] Hence, different adsorption models, such as the random sequential adsorption (RSA) model, were developed to address such scenarios.[315−317]

5.2.2.1. Random Sequential Adsorption (RSA). The underlying adsorption mechanism of the RSA is, to some extent, diametrically opposed to the process described by the LM. The LM describes an equilibrium of a completely reversible process, without steric hindrance.[288] Alternatively, the RSA was developed for a completely irreversible adsorption process "far from equilibrium".[315−317] Due to steric hindrance, and the inherent irreversibility and immobility, the surface is saturated at a characteristic coverage well below the optimal packing density (see Figure 14b).[317] Talbot et al. derived a selection of typical saturation coverages, dependent on the geometry of the

https://doi.org/10.1021/acs.chemrev.1c00044
Chem. Rev. 2021, 121, 8095−8160

problem.[318] The RSA is often successfully applied to model the adsorption of colloidal particles under the influence of gravity[319−321] or diffusional forces.[322] The model is sometimes used for protein adsorption to hydrophobic surfaces that can exhibit large irreversible binding.[323,324]

However, the NSB of proteins to sensor surfaces, *i.e.* protein adsorption, often includes a small lateral mobility on the surface after adsorption, called diffusion or crawling.[325] If the RSA is extended with such crawling, the resulting surface coverage varies from the original RSA model. For example, at low coverages, the radial distribution function is higher for the smallest distances, resulting in clustered adsorption of binders.[325] In applied studies, protein adsorption to a wide range of surfaces often shows partially reversible, as well as partially irreversible, effects where the proteins undergo structural changes during the adsorption process.[281,326] Therefore, neither of the two extreme cases, neither the LM nor the RSA, can explain adsorption phenomena generalized for a large set of surfaces.[319] In search of a more general model, various reports demonstrate an elegant way to account for such differences, by allowing the adsorbing molecules to undergo transitions and rearrangements from one adsorbed state to another with different properties.[327,328] Such models will be discussed in the following section.

5.2.2.2. Multistates Models. A powerful method to increase the flexibility of adsorption models is to chain multiple models where an adsorption process is often modeled as a series of subsequent states, typically with a decreasing likelihood of desorption for later states.[329] Such models are called multistate models. Previously, we discussed various models for different cases of biomolecular adsorption to a solid−liquid interface. Indeed, many different kinds of behavior have been studied and described in the literature: irreversible adsorption,[273] reversible adsorption,[272,274,275] conformational change upon adsorption correlating to a decrease in reversibility over time,[74,330−334] and also the opposite situation of initial irreversibility with a shift toward larger reversibility depending on the surface saturation.[335] This variety of protein adsorption properties to solid−liquid interfaces, especially in terms of reversibility, exemplifies the difficulty of developing a generalized model. However, multistate models can be adjusted to the properties of each individual problem and therefore extend the applicability to more simple models.[323,329]

Some of the suggested multistate models start with a reversible state that later progresses to an irreversible end state[336,337] and are thus probably more closely related to RSA than the LM. One possible source of confusion is the exact meaning of the term irreversible. Experimentally, irreversible adsorption often means that there will be no measurable desorption of directly bound molecules upon rinsing during the time frame of the experiment,[273,338−341] while exchange effects such as the Vroman-effect[342,343] are not necessarily prevented.[273,338−341] However, a completely irreversible state as used in the aforementioned models does not permit any exchange effects.[318] Hence, irreversibility in the sense of rinsing-irreversibility while allowing exchange effects demands for a model that keeps some reversibility in all states such as the models by Lundström, Wertz, or Szöllősi et al. Such models are also thermodynamically consistent with the expected complex energy landscape of the NSB process[329,341,344] (Figure 3) and are more related to the LM than to the RSA. A good overview of multistate models was published by Rabe et al. in 2011.[345]

After having summarized a basic toolbox for the quantification of adsorption processes and what situations they can be applied to, we will discuss in the next section what type of interactions and models are important for biosensing and how these basic models can further be tailored to specific sensing scenarios.

5.2.3. Equilibrium Models for Specific and Nonspecific Interactions in Biosensing. In a typical biosensing experiment, quantification of the specific binding of analytes to surface-immobilized receptors is of interest. Additionally, most sensors are precoated with a nonfouling layer to decrease possible interactions of the adsorbing molecule with the underlying surface.[346] As nonfouling layers that completely resist NSB do not exist, all biosensors have small exposed surface areas where nonspecific, irreversible protein−surface interactions may occur.[43] Modeling these surface defects is very challenging due to the large amount of unknown parameters such as the number and surface area of the defect sites. Most biosensing assays employ blocking steps to saturate such impurities wherever possible. However, nonspecific interactions are not limited to the underlying surface but also occur on the receptor surface. Additionally, if the nonspecific binder and the analyte interact with the same binding site, they will compete for that binding site (competitive binding).[347] Taking such interactions into account is of major importance for the optimization of biosensors with respect to the LOD and NSB, as we will show in the remainder of this section.

5.2.3.1. The Isotherm of Choice for Specific Interactions in Biosensing. We will focus on the modeling of specific and nonspecific protein−protein and nonspecific protein−surface interactions with the paratope of antibodies or antibody fragments as receptors immobilized at a solid−liquid interface. While we will only discuss the models with respect to protein−protein interactions in this section, the majority of the models can also be applied to DNA−DNA interactions. Many authors have discussed the model of choice for such protein receptor−ligand interactions at the solid−liquid interface.[348−353] These models have become especially critical for the measurement of K values since they are often performed using SPR. In such K value measurements, as well as in many other biosensors, it is pivotal to precoat the sensor surface with a nonfouling layer to avoid the influence of the underlying surface on the measured interaction.[354,355] In SPR, a common coating is the dextran matrix[353] but biosensors also often utilize self-assembled monolayers[356,357] or graft copolymers.[354−356] Without a suitable surface coating, the measured interactions can differ greatly from the true values.[277]

Many experimental parameters can influence the measurements, even with optimized surface functionalization.[277,358,359] However, many authors have reported that the apparent equilibrium interaction can be modeled well with the original LM, if the experimental procedure is carefully optimized.[277,348,351,352,360−362] Apart from the equilibrium values, the kinetic information is especially relevant for the measurement of on and off-rates for the K value determination.[362] The question, whether the LM is a good approximation for surface-bound receptor−ligand interactions can be answered by verifying whether the involved processes violate any of the Langmuirian assumptions. First, we direct our attention toward the adsorption sites. It is sometimes assumed that certain measured deviations from the Langmuir isotherm are caused by inhomogeneities of the adsorption site, due to steric hindrance.[358,363] However, these effects are dependent on the antibody immobilization architecture and are avoidable.[364]

https://doi.org/10.1021/acs.chemrev.1c00044
Chem. Rev. 2021, 121, 8095−8160

Thus, we can assume that the immobilized monoclonal antibodies will provide homogeneous adsorption sites in an optimized setup.

Accordingly, influences of previously adsorbed ligands to subsequent adsorption, such as surface exclusion effects, are only relevant for large analytes at high coverages, and they are receptor density-dependent. Hence, they are also avoidable by optimizing the receptor density.[364,365] In addition, the antibody−antigen interaction can be completely reversible, provided a proper surface treatment helps to avoid the influence of the underlying surface.[275,359,366] On the one hand, a multistate model, consisting of more than one compartment LM has been suggested for situations where irreversibilities cannot be avoided. On the other hand, one of the few critical sources of deviations from the equilibrium LM is whether the time frame of the experiment is sufficient to reach equilibrium. At ultralow concentrations, reaching equilibrium can take several hours or days.[267] Thus, the LM overestimates the adsorption amount for some sensors at ultralow concentrations, and the expected symmetry in the dose−response curve is lost.[367]

To compensate for this effect, the kinetics of the interaction process must be taken into account. Additionally, some effects are mainly observable in complex samples such as serum. These effects are either (undesired) specific cross reactivities[368] or effects caused by nonspecific binders, which are competing with the specific ligands for the receptor epitope.[297,347,368] Finally, one of the major effects to be considered in many biosensors is the depletion of analytes in small sample volumes at low concentrations.[293,368] This constraint in combination with a large protein background and the resulting nonspecific adsorption is the reason why small sensor surfaces in the range of hundreds of micrometers can sometimes perform better than sensors with larger surface areas.[368,369] This effect has not been given enough attention in the existing literature, which is why the depletion corrected Langmuir isotherm will be presented here in detail.

5.2.3.2. Depletion Corrected Langmuir Model (LMD) for Specific Adsorption. If an adsorption problem has a large surface-to-volume ratio and free analyte/binder amounts that are too small to be assumed to remain constant during the adsorption process, then depletion needs to be taken into account. The amount of free analytes/binders will be depleted during the adsorption process, which changes the free analyte/binder concentration.[293,370,371] In this case, the sixth and last Langmuirian assumption is violated. However, this situation is often still called Langmuirian[368] because the first five original assumptions still hold. For clarity, we call this model the depletion corrected Langmuirian isotherm. The differentiation of a case with depletion versus without depletion is an important characteristic of the LM, which will not only lead to different equilibrium values but will also define whether the adsorption follows first or second order kinetics (see section 5.3.1).[293]

Here, we will derive the LMD, as it is rarely reported in the literature despite its significant relevance for biosensors. Some quantitative reasoning on when which type of the LM should be used will follow at the end of this section. We start again with a simple version consisting of the two elements: receptors (R) and analytes (A) in solution. For the original LM, we assumed that the free analyte concentration, C_A, is large enough and assumed it would stay constant and that C_A thus represents the total amount of analyte, C_{tot}. However, now we have to take the adsorbed concentration of analytes, C_{RA}, into account. Hence, the equilibrium formulation of the original Langmuir problem (eq 12) still holds, but for the total concentration of analytes we now get

$$C_{A_{tot}} = C_{RA} + C_A \tag{20}$$

The same relation is applied to the receptors:

$$C_{R_{tot}} = C_{RA} + C_R \tag{21}$$

We now replace C_A and C_R in eqs 11 and 12 with eqs 20 and 21 and get a second order expression for C_{RA}:

$$C_{RA} = K_a(C_{A_{tot}} - C_{RA})(C_{R_{tot}} - C_{RA}) \tag{22}$$

$$\Theta_A = \frac{C_{RA}}{C_{R_{tot}}} \tag{23}$$

Solving for C_{RA} and dividing by $C_{R_{tot}}$ leads to expression 24 for the receptor coverage for the depletion corrected Langmuir isotherm:

$$\Theta_A = \left[C_{A_{tot}} + C_{R_{tot}} + K_d - \sqrt{(C_{A_{tot}} + C_{R_{tot}} + K_d)^2 - 4C_{A_{tot}}C_{R_{tot}}}\right]/2C_{R_{tot}} \tag{24}$$

Since the volume is no longer assumed infinite, we now have to be careful to do the calculation either in concentrations or amounts of ligands and receptors. Here, we formulated the expression in terms of concentrations, including the somewhat counterintuitive receptor concentration $C_{R_{tot}}$, dependent on the molar receptor density, r, the sensor surface area, A, and the volume, V:

$$C_{R_{tot}} = \frac{rA}{V} \tag{25}$$

The mentioned use of receptor concentration, rather than receptor amount, reflects the fact that in a real assay, the fractional receptor coverage depends on the volume, in the presence of relevant amounts of depletion. By increasing the volume at a constant concentration of ligands while keeping the sensor surface constant, we do increase the amount of binders, but we do not increase the amount of receptors (so the receptor concentration decreases); thus, the equilibrium value of the surface coverage will increase.

5.2.3.3. Competitive Langmuir Model with Depletion (CLMD). For measurements of small amounts of analytes in complex samples such as serum with a large amount of nonspecific binders, this effect is especially influential. The large amount of nonspecific binders experiences negligible depletion, while the analyte is depleted. If a high receptor surface coverage is used in a sensor, the analyte is depleted more than on a surface with lower coverage, while the nonspecific binders are not depleted in the same manner. For this reason, small sensor surfaces can have a better SB to NSB ratio and thus also a better LOD than larger surfaces, in complex samples.[368]

Alternatively, measurements of pure analytes in buffer are affected by this depletion effect only in terms of the accuracy of the fitting of the binding curve. In this case, however, the LOD does improve with larger sensor surfaces, because of the absence of nonspecific binders. This context exemplifies why biosensors optimized in buffers in the absence of nonspecific binders will perform poorly in complex samples. As the depletion modeled with the limited volume Langmuir isotherm is especially relevant

https://doi.org/10.1021/acs.chemrev.1c00044
Chem. Rev. 2021, 121, 8095−8160

for biosensing in a sample with a large protein background, it makes sense to combine it with the competitive Langmuir isotherm. Since the nonspecific competitor typically is present at a much larger concentration than the analyte, we can neglect the depletion of the competitor. The depletion LM for the analyte combined with one nondepleting competitor yields the following equation for the coverage with the CLMD (a formulation that we have not found in the literature):[372]

$$\Theta_A = \frac{C_{A_{tot}} + C_{R_{tot}} + K_d^A(1 + K_a^B C_{B_{tot}})}{2C_{R_{tot}}} - \frac{\sqrt{(C_{A_{tot}} + C_{R_{tot}} + K_d^A(1 + K_a^B C_{B_{tot}}))^2 - 4C_{A_{tot}}C_{R_{tot}}}}{2C_{R_{tot}}} \tag{26}$$

Also here, we can generalize the model for n nondepleting competitors:

$$\Theta_A = \frac{C_{A_{tot}} + C_{R_{tot}} + K_d^A\left(1 + \sum_{j=1}^{n} K_a^j C_{tot}^j\right)}{2C_{R_{tot}}} - \frac{\sqrt{\left(C_{A_{tot}} + C_{R_{tot}} + K_d^A\left(1 + \sum_{j=1}^{n} K_a^j C_{tot}^j\right)\right)^2 - 4C_{A_{tot}}C_{R_{tot}}}}{2C_{R_{tot}}} \tag{27}$$

Knowing these two versions of the LM, we also need a tool to decide which model should be used for which case. The following approximation can serve as such a tool. The fraction of depletion (D) can be quantified by the equilibrium concentration $C_{A_{eq}}$, relative to the initial concentration $C_{A_{tot}}$, where the equilibrium concentration is equal to the difference of the initial concentration at $t = 0$ ($C_{A_{tot}}$) and the concentration change due to adsorption C_{RA} to the receptor:

$$D = 1 - \frac{C_{A_{eq}}}{C_{A_{tot}}} \tag{28}$$

$$C_{A_{eq}} = C_{A_{tot}} - C_{RA} \tag{29}$$

Azizian et al. introduces the following expression for the adsorbed concentration equivalent with coverage θ (equivalent to our Θ_A as Azizian et al. do not consider competition) and a characteristic factor β:[293]

$$C_{RA} = \beta\theta \tag{30}$$

$$\beta = \frac{R_{tot}}{V} \tag{31}$$

$$C_{RA} = \frac{rA}{V}\theta \tag{32}$$

5.2.3.4. Double Competitive Model without Depletion (DCLM). The LM and the CLM were already introduced in this section. While the LM can only be used in model experiments with buffer, the CLM already tries to capture the effect of NSB to the sensor surface. Here, we introduce a further consequence of NSB, the competition for the binding sites by analytes in solution (see Figure 16). The well-established and accepted CLM describes the partial displacement of analytes from the receptors due to the interaction of the receptors with background molecules.[297−300] We call this type of competition

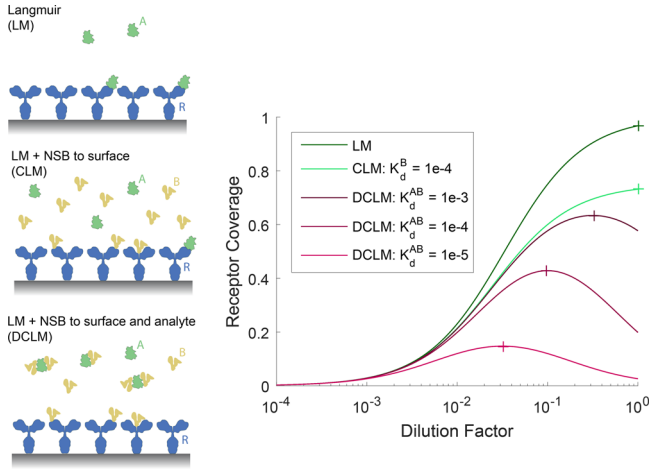

Figure 16. Illustrations for three isotherms: The original Langmuir model (LM), the competitive LM (CLM), and the double competitive LM (DCLM) according to eqs 12, 16, and 37, respectively. The plot on the right shows the predicted dependence of the receptor coverage (that defines the signal) on the dilution factor of the sample for the specified K_d^B and K_d^{AB} values. The DCLM predicts an optimal dilution ratio (+) for undepleted biosensors, which is often observed experimentally. The stronger the solution competition, the more we should dilute the sample for optimal performance. The other two models predict a monotonically decreasing coverage for more dilution (smaller dilution factor) indicating the importance of the correction.

"paratope competition". However, for clarity, we will use the less precise but more figurative term "surface competition" herein.

Since this interaction is a nonspecific protein−protein interaction of the background proteins with the paratope on the receptor, it is difficult to imagine why the background proteins in solution should not also nonspecifically interact with the epitope on the analyte. We call this additional type of interaction "epitope competition" or simply "solution competition". Solution competition can be incorporated into a simple mathematical description by including an additional Langmuirian interaction of the analytes with the background proteins in solution. In this section, we discuss the simple case of Langmuir interactions with infinite volume and thus no depletion due to interactions with the surface. A few authors have addressed the influence of this additional competition on the performance of biosensors.[368,373,374] However, to the best of our knowledge, there have been no attempts to incorporate this aspect into a mathematical model for biosensors. This solution competition also contributes to the so-called *matrix effect* in biosensing, which describes the interference of background molecules with the specific interactions in a biosensor.[374−376]

Equations 12 and 16 describe the fractional occupancy Θ_A of the receptors R by the analyte A according to the LM (eq 12) and the CLM (eq 16). In addition to these expressions, one may formulate the interaction of the background molecule, B, and the analyte, A, with the equilibrium constant K_a^{AB}:

$$K_a^{AB} = \frac{C_{AB}}{C_A C_B} \tag{33}$$

This interaction reduces the amount of free analyte C_A by the additional term C_{AB} according to eq 34.

$$C_A = C_{A_{tot}} - C_{RA} - C_{AB} \tag{34}$$

Due to the infinite volume and the absence of depletion on the surface, this equation simplifies to eq 35:

https://doi.org/10.1021/acs.chemrev.1c00044
Chem. Rev. 2021, 121, 8095−8160

$$C_A \gg C_R$$
$$C_A \approx C_{A_{tot}} - C_{AB} \quad (35)$$

Combined, these expressions lead to the additional equilibrium:

$$C_{AB} = \frac{C_A}{1 + K_a^{AB} C_B} \quad (36)$$

Including eqs 34 and 36 yields the new DCLM combining the surface and the solution competition:

$$\Theta_A = \frac{K_a^A C_{A_{tot}}}{K_a^A C_{A_{tot}} + (1 + K_a^B C_B)(1 + K_a^{AB} C_B)} \quad (37)$$

It is common practice in biosensing to dilute a sample prior to detection. The evident benefit of dilution renders this protocol to be a standard assay procedure. However, experimental dilution optimization is rarely published, since it is a well-known and accepted effect. Yet, the benefit of dilution can only be explained with the new DCLM. Figure 16 shows the receptor coverage, which is usually directly proportional to the sensor signal, as predicted by the LM, the CLM, and the DCLM. Only the double competition provides an explanation for the benefits of dilution in a quantitative manner, as it predicts an optimal surface occupancy for a diluted sample. For the tested surface and solution competition parameters in Figure 16, the optimal dilution ratio varies between 1:1 and 1:30.

Expression 37 represents the simple version of the double competitive Langmuir isotherm for the infinite volume situation without depletion. We expect that the depletion of the analyte will strongly affect the competition in solution. This situation, where the interplay of depletion and interactions of the analyte and background proteins in solution greatly influences the results obtained with biosensors, has stirred an ongoing discussion in the biosensing community[377,378] related to the free hormone measurements revolving around the free hormone hypothesis.[373,379]

When measuring hormone levels, the effect of hormones on biological systems, and the titrations of hormones, it has been observed that only a small proportion of the hormones added to a sample actually appears to produce an effect.[373,379] Furthermore, different biosensing methods can give rise to considerably different results.[378] We believe that the DCLM model can contribute to a better understanding of the mechanisms that underlie these observations.

5.3. Double Competitive Model with Depletion

The following set of equations is the basis for our Double Competitive Langmuirian model including depletion (DCLMD) of the analyte. In this model we include one background molecule, and we model all interactions as Langmuirian interactions.

$$C_A = C_{A_{tot}} - C_{AB} - C_{RA} \quad (38)$$
$$C_B = C_{B_{tot}} - C_{AB} - C_{RB} \quad (39)$$
$$C_R = C_{R_{tot}} - C_{RA} - C_{RB} \quad (40)$$
$$C_{AB} = K_a^{AB} C_A C_B \quad (41)$$
$$C_{RA} = K_a^A C_A C_R \quad (42)$$
$$C_{RB} = K_a^B C_B C_R \quad (43)$$

This system is solvable, but it is not conveniently solvable by hand. However, we can simplify the model slightly. Background molecules such as albumin that can nonspecifically interact with the analyte are present in serum at millimolar concentrations.The analyte and receptor concentration, however, are approximately 6 orders of magnitude lower.[296] For that reason, the background molecules will not deplete during any of the equilibrium reactions involved in this model. Equation 39 therefore simplifies to

$$C_B \gg C_A$$
$$C_B \gg C_R$$
$$\Rightarrow C_B \approx C_{B_{tot}} \quad (44)$$

Using this simplification (eq 44), the solution is nicely hand derivable:

$$C_A = \frac{-b \pm \sqrt{b^2 - 4ac}}{2a} \quad (45)$$
$$C_{RA} = \frac{K_a^A C_A C_{R_{tot}}}{1 + K_a^A C_A + K_a^B C_{B_{tot}}} \quad (46)$$
$$\Theta_A = \frac{C_{RA}}{C_{R_{tot}}} \quad (47)$$

With the parameters

$$a = K_a^A + K_a^{AB} K_a^A C_{B_{tot}} \quad (48)$$
$$b = 1 - K_a^A C_{A_{tot}} + K_a^B C_{B_{tot}} + K_a^{AB} C_{B_{tot}} + K_a^{AB} K_a^B C_{B_{tot}}^2 + K_a^A C_{R_{tot}} \quad (49)$$
$$c = -K_a^B C_{B_{tot}} C_{A_{tot}} - C_{A_{tot}} \quad (50)$$

5.3.1. Kinetic Models for Biosensing. In biosensing, the equilibrium models are often sufficient to quantify the relevant aspects of a given adsorption process, but in some cases, we are also interested in how the equilibrium is reached. For example, it may be the case that the incubation time is too short to reach equilibrium. Moreover, measurements of the adsorption and desorption rates may be of interest. For such kinetic models, there are two relevant regimes, the reaction- and diffusion-limited regimes. The dominant regime is dependent on the geometry,[267,380] flow conditions,[267,381] and receptor density.[359] Generally and qualitatively speaking, an adsorption process will be shifted toward mass transport limited kinetics, if the surface is flatter[380] and larger,[267,380] if the flow rate is lower,[267,381] and if the receptor density is higher.[359,382] Alternatively, a smaller[267,380] and more curved[380] surface with a higher flow[267,381] and lower receptor density[359,382] will shift the adsorption process kinetics toward the reaction-limited case.

A quantitative assessment of which regime is dominating can be obtained with the help of the Damköhler number,[380] which represents the ratio between the maximum reaction rate and the maximum diffusional mass transport rate.[380] Hence, the reaction kinetics limited adsorption models are a good approximation if the Damköhler number is much larger than one,[267,380] while for Damköhler numbers significantly below one, the system is transport limited.[267,380] In terms of modeling complexity, the

https://doi.org/10.1021/acs.chemrev.1c00044
Chem. Rev. 2021, 121, 8095−8160

most challenging situation is described by a Damköhler number on the order of one, where both regimes are accounted for by using a combined model.[267,380]

5.3.1.1. Reaction-Limited Kinetics. In section 5.2.3, we established that the equilibrium reaction of a receptor ligand interaction is well modeled by the Langmuir isotherm in many situations. Thus, we can also use the LM for reaction-limited kinetics. However, there are two different versions in use for the Langmuirian reaction kinetics, the first and the second order model.[293,294] Originally, these models were merely empirically derived while the justification for their use and the decision which of the two should be used was motivated experimentally.[294] It was not until 2004 that Azizian derived the Langmuirian kinetics analytically.[293] This analytical solution shows that the first order kinetics are a good approximation if there is no depletion, while one has to use the second order kinetics if a problem with relevant amounts of depletion is modeled.[293]

This analogy is evident by evaluating the first and second order kinetic models for times t toward infinity, which derive the original equilibrium model equations. Thus, evaluating the solutions of the first order (Azizian 2004, eq 14[293] repeated here as eq 51 with $\beta\Theta = 0$) and second order kinetic solution for times t toward infinity (Azizian 2004, eq 42[293] repeated here as eq 63), yields the original and the limited volume LM respectively. An interesting aspect of this comparison is that none of the inherent parameters of Azizian 2004, eq 42[293] (a, b, and f), are lost if the mentioned limit is calculated. Thus, remarkably, we can model the time-dependent Langmuirian kinetics using Azizian 2004, eq 42,[293] by estimating the parameters a, b, and f by fitting the equilibrium LM to equilibrium values, without actually observing any time-dependent behavior.[293] Such a model extension could potentially be used to improve the accuracy of nonequilibrated biosensing data and should thus be further studied in the future.

According to Azizian, the differential eq 51 for the general LM reads (Azizian 2004 eq 14):[293]

$$\frac{d\theta}{dt} = k_a(C_0 - \beta\theta)(1 - \theta) - k_d\theta \tag{51}$$

with parameter β (Azizian 2004, eqs 12 and 13):

$$\beta = \frac{m_c q_m}{M_w V} \tag{52}$$

$$\beta = \frac{C_0 - C_e}{\theta_e} \tag{53}$$

The first order differential eq 54 without depletion ($\beta\Theta = 0$) can then be written as (Azizian 2004, eq 19)

$$\frac{d\theta}{dt} = f - k_1\theta \tag{54}$$

$$f = k_a C_0; \quad k_1 = k_a C_0 + k_d \tag{55}$$

and the solution for the first order kinetics (Azizian 2004, eq 21)

$$\ln\left(1 - \frac{k_1}{f}\theta\right) = -k_1 t \tag{56}$$

with the parameters (Azizian 2004, eqs 17 and 18):

For the limited volume, the differential eq 57 for the coverage reads (Azizian 2004, eq 29)

$$\frac{d\theta}{dt} = a\theta^2 + b\theta + f \tag{57}$$

$$a = k_a\beta; \quad f = K_a C_0 \tag{58}$$

with the parameters (Azizian 2004, eqs 30−32):

Integration yields the result (Azizian 2004, eq 34):

$$\frac{1}{\sqrt{b^2 - 4af}}\left[\ln\frac{2a\theta + b - \sqrt{b^2 - 4af}}{2a\theta + b + \sqrt{b^2 - 4af}} - \ln\frac{b - \sqrt{b^2 - 4af}}{b + \sqrt{b^2 - 4af}}\right] = t \tag{59}$$

$$\ln\left(\frac{2a\theta + \gamma}{2a\theta + \xi}\right) - \tau = \lambda t \tag{60}$$

With Azizian 2004, eqs 35−38:

$$\lambda = \sqrt{b^2 - 4af}; \quad \gamma = b - \lambda; \quad \xi = b + \lambda; \quad \ln\frac{\gamma}{\xi} = \tau \tag{61}$$

Azizian 2004, eq 40:

$$\theta = \frac{\xi e^{\lambda t + \tau} - y}{2a(1 - e^{\lambda t + \tau})} \tag{62}$$

For t toward infinity, this equation simplifies to (Azizian 2004, eq 42):

$$\theta = \frac{\xi}{2a}$$

$$\xi = b + \sqrt{b^2 - 4af} \tag{63}$$

which is equivalent to eq 24 for the equilibrium adsorption with depletion but without competition.

5.3.1.2. Diffusion-Limited Kinetics. If an adsorption problem is not reaction, but diffusion limited, we have to build a different model for the quantification. A diffusion model that was adapted for a biosensor problem is represented by the following differential equation (with C_A, bulk concentration of an analyte A; C_S, concentration of A at the surface, which usually means within the diffusion boundary layer; C_{RA}, concentration of the analyte−receptor complex; and finally $C_{R_{tot}}$, the total receptor concentration):[275]

$$\frac{dC_S}{dt} = k_\tau(C_A - C_S) - k_a C_S(C_{R_{tot}} - C_{RA}) + k_d C_{RA}$$

$$\frac{dC_{RA}}{dt} = k_a C_S(C_{R_{tot}} - C_{RA}) - k_d C_{RA} \tag{64}$$

Solutions to these equations are not trivial. A solution for a flat sensor surface was reported in two papers by Stenberg et al. in 1988[276] and in 1986.[380] Also, the diffusion kinetics for different geometries have been studied comprehensively by various authors.[278,279,311,380,383,384] These solutions shall not be repeated here in further detail. However, we may conclude that diffusion-limited kinetics can be calculated for a variety of specific geometries.

5.3.1.3. Combined Kinetic Models. As mentioned earlier for the quantification of on and off-rates in K value measurements, it is of prime importance that the kinetics of a system are modeled correctly. Critical analysis of the data measured by SPR has revealed that the adsorption process on a flat solid−liquid interface can be influenced by both the reaction kinetics, but also by mass transport,[277,358,359,361,381,385] as well as a number of

https://doi.org/10.1021/acs.chemrev.1c00044
Chem. Rev. 2021, 121, 8095−8160

Table 3. K_d Values as Well as On- and Off-Rates for the Four Interactions of the Implemented Model

	K_d [M]	K_{on} [M^{-1} s^{-1}]	K_{off} [s^{-1}]
Specific binding (SB)	10^{-10}	10^{5}	10^{-5}
Reversible nonspecific binding (NSB_{rev})	10^{-3}	10^{3}	1
Irreversible strong nonspecific binding ($NSB_{irrev,strong}$)	10^{-12}	10^{4}	10^{-8}
Irreversible weak nonspecific binding ($NSB_{irrev,weak}$)	10^{-4}	10^{-2}	10^{-6}

additional effects. Such effects include matrix effects,[349] receptor heterogeneity,[358] flow rate,[385] and most importantly, receptor density (including surface exclusion).[277,358,359,362] However, by careful optimization of the assay parameters, it is possible to minimize mass transport and other influences.[277,351,362,386] The process can then, in certain cases, be accurately modeled by the original LM.[277,348,351,352,360−362]

If the diffusion influence is still too large, for example, in most diagnostically relevant assays that are typically mass transport limited,[267] a combination of the kinetic and the diffusion models has to be considered. Yet, to date, there has been no analytical solution to this particular problem. Instead of an analytical solution, approximations[311] or numerical computer models[279] have been developed in an attempt to solve the problem. An elegant and successful method is to numerically solve the differential eq 64 and fit the experimental real-time binding data with different concentrations globally with respect to the parameters that will be quantified.[275,387]

Also, numerical models including a continuous flow have been suggested.[279] Not directly relevant for the kinetic regime, but generally of great importance, is the influence of NSB on the measured sensor data.[277] The most common counter-strategy to deal with NSB is the use of a reference channel,[277] which will be discussed in more detail in section 6. An interesting additional insight in diffusion- vs reaction-controlled kinetics is the work of Stenberg et al. in 1986.[380] This work concludes that the kinetics of antibody interactions on a cell surface with a diameter on the order of 10 μm are not diffusion limited, while the regime switches if we look at adsorption phenomena on particles with a diameter on the order of 100 μm. Since the spherical diffusion problem is symmetric, this solution is a good approximation for small sensor surfaces with half the receptor density. This result leads to the hypothesis that SPR sensor surfaces would not be diffusion limited if one could decrease their typical minimal diameter (on the order of 100 μm) by 1 order of magnitude.

The models reviewed so far in this section can be used to model specific and nonspecific interactions in biosensing. In the following section, we will use this modeling toolbox to quantify the relevant interactions for a label-free and sandwich immunoassay. For further reading on the complex topic of mathematical modeling in biosensing, we recommend an extensive, recently published summary by Saftics et al. that also includes software packages for biosensor data evaluation.[388]

5.4. Application of Known Models to Estimate Theoretical Biosensing Limits

In this section, we use the models introduced in the first part of this section for the estimation of the SB to NSB ratio which determines the LOD of diagnostically relevant assays in complex samples. We also show how such models can be used to optimize sensor geometry and assay parameters. We use the CLMD (eq 26) for the SB. We will discuss the two most common assay types: a direct, label-free assay and a sandwich assay. For the rinsing step, we use the first order LM kinetics without readsorption (eq 56), assuming perfect continuous rinsing. For the NSB, we will use the LM as there is no need for the depletion correction (LMD) because the concentrations of nonspecific binders in a clinical blood plasma sample are typically high enough to neglect depletion.[296]

Apart from the depletion aspect, we have to assign reasonable binding parameters for the NSB, which is caused by a wide distribution of adsorption type parameters. Thus, to model the NSB in a realistic, yet efficient way, we chose to implement three different sets of NSB parameters, representing the essential and averaged groups of adsorption types. The reversible NSB is implemented with the original LM, using a low affinity (K_d = 10^{-3} M) and a high desorption rate (k_{off} = 1 s^{-1}). For the "irreversible" NSB we also use the reversible LM, but with very slow off-rates, because an irreversible model is thermodynamically inconsistent.[329] As mentioned before, irreversible in this context means that there is no desorption in the time course of the observed experiment.

Instead of using a multistate model, we approximate such binding by two decoupled original LM. One LM with a high affinity (K_d = 10^{-12} M) and a very low off-rate (k_{off} = 10^{-8} s^{-1}) represents adsorption to free surface defects. The other LM has an intermediate affinity (K_d = 10^{-4} M) and off-rate (k_{off} = 10^{-6} s^{-1}) but a very slow on-rate (k_{on} = 10^{-2} M^{-1} s^{-1}) (see Table 3). With this pragmatic but consistent model comprised of three separate, original LM models, we can cover all relevant NSB effects. However, the main difficulties are the two unknown parameters governing NSB, the variation of the free NSB concentration, and the unknown surface defect density and size. As a result, the NSB can vary considerably among applications. We used representative values reported by Rissin et al. to predict the NSB in a realistic manner.[389]

In summary, we use one set of parameters for the SB and three different sets of parameters for the NSB to include all relevant effects. The four interactions that were implemented in the model are visualized in Figure 17 with the adsorption parameters in Table 3.

With these parameters, we can investigate what happens at different stages of the assay systematically (Figures 18a−d). The first step is sample incubation (Figure 18a). The equilibrium

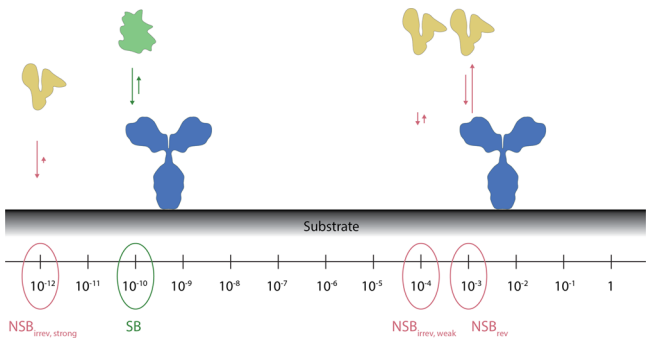

Figure 17. Implemented interactions and strengths (K_d values) for the biosensing model discussed here. The four interactions $NSB_{irrev,strong}$, SB, $NSB_{irrev,weak}$, and NSB_{rev} are arranged horizontally according to their affinity, with arrows indicating the used on- and off-rates.

https://doi.org/10.1021/acs.chemrev.1c00044
Chem. Rev. 2021, 121, 8095−8160

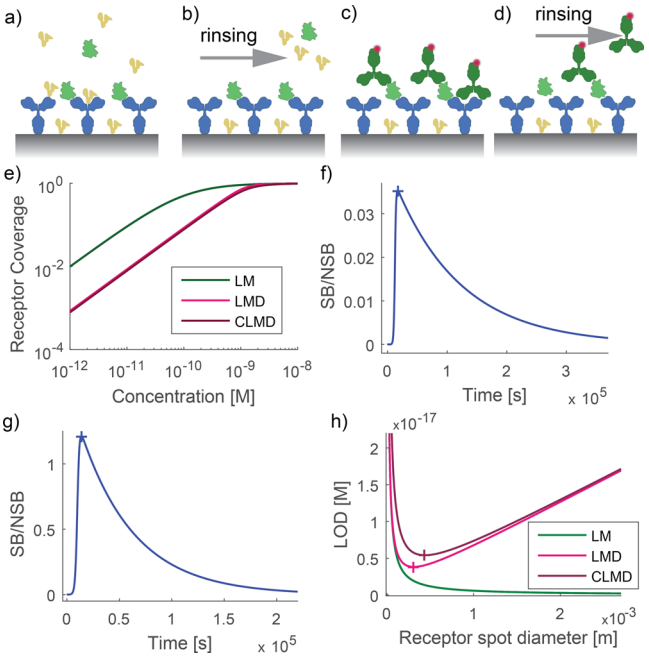

Figure 18. Optimization of biosensing assays using thermodynamic models. (a–d) Schematic drawings of assay steps: (a) Sample incubation depicting the green analyte binding specifically to the blue capture probes in the presence of yellow nonspecific binders (NSB). (b) During rinsing, the reversible NSB are washed away while irreversible NSB and specifically bound analytes are retained. (c) Incubation of the labeling receptor. (d) A second rinsing step washes away labeled NSB. (e) Receptor coverage depends on the equilibrium concentration (Langmuir Model, LM) and is influenced by depletion (depletion corrected Langmuir model, LMD) and NSB-induced competition (competitive Langmuir model with depletion, CLMD). (f) The ratio of specific binding (SB)/NSB molecules reaches a maximum during the first rinsing step. The plus marks the optimal rinsing time. (g) Sandwich labeling step that can also bind specifically or nonspecifically. The SB/NSB ratio of this label shows a similar maximum as in part f, but the signal is higher showing the advantage of sandwich assays. (h) The predicted limit of detection (LOD) of the modeled sandwich assay depends on the used spot size for three different adsorption models. Calculations were based on the dimensions of a 96-well plate.

state of the SB of the analyte to the receptor is calculated with three different models for comparison: the LM, LMD, and CLMD (Figure 18e). This figure depicts the expected dependency of the receptor coverage on the analyte concentration, which shows that while depletion has a dramatic effect, competition has little influence on the specific binding. Here, as discussed above, the NSB of the background molecule to the paratope on the receptor was calculated with the CLM without depletion, and two LMs were used for the NSB of background molecules to the sensor surface.

To implement the first rinsing step (Figure 18b), we used the first order LM kinetics, which describes the expected exponential desorption. Since the bulk of NSB molecules have fast off-rates while the SB analyte has slow off-rates, the SB/NSB ratio will improve at the start of the rinsing step rapidly (Figure 18f). The slower the dissociation of the SB analyte, the larger the maximum of SB/NSB at the optimal rinsing time, which is why most assays require capture probes with slow off-rates.[390] Models for direct binding (label-free) assays end here.

For sandwich assays, the next step is the incubation of the labeled antibody (LA) (Figure 18c). Here the concentration of the LA ($\sim$1 μM) is chosen such that the majority of the captured analytes will bind a LA within the relatively short (<1 h) incubation time. Since the concentration of the LA is large enough, we use the LM to model this interaction. The LA is interacting specifically with the remaining surface antigens and nonspecifically with the surface defects. The next stage is the second rinsing phase (Figure 18d), which is implemented in the same way as the first rinsing step and results in a similar curve.

However, for the sandwich assay, the absolute values of the SB/NSB ratio are orders of magnitude higher (Figure 18g). This variance is due to the large difference between the approximately millimolar concentration of the nonspecific binders and the approximately micromolar concentration of the LA. Moreover, while the concentration and type of nonspecific binders have a large sample-to-sample variation, in a sandwich assay, we can choose and precisely control the LA concentration, which results in minimal variations in NSB.

Finally, we estimate the resulting LOD as a function of the receptor surface size in Figure 18h according to eq 8, the definition of the LOD.[391] Here, we estimate the slope from the dependency of the SB on the analyte concentration using our models. Figure 18h shows that without depletion, the optimal surface area is as large as possible. However, when depletion is included, the optimal receptor spot diameter was calculated as $d_{opt} = 4.3 \times 10^{-4}$ m resulting in an optimal A_{opt} of 5.9×10^{-7} m^2 for the LMD with competition. The influence of the competition with the chosen parameters has a small influence by counteracting the depletion and, thus, creates a larger optimal surface area compared to the case without competition. These observations confirm the *ambient analyte assay theory* developed by Roger Ekins, who postulated the improved maximal LOD for assays with smaller receptor areas that minimize depletion.[40]

The models presented in this section can be used to study specific and nonspecific interactions quantitatively. The two main problems with NSB in biosensing are the large variation of background proteins in biological samples and the inhomogeneity of surface defects, which lead to differing amounts of nonspecific adsorption, which masks the specific signal. Therefore, the amount of nonspecific adsorption in a biosensor cannot be modeled nor compensated without knowing the exact amount and composition of the background proteins and the defect density. However, by modeling the typical amounts of nonspecific binders and defect densities, we can derive the ideal dimensions of a biosensor and hence minimize the influence of NSB. Figure 19 is an illustrative example for using the CLMD model to predict how the LOD depends on four additional important assay parameters: the affinity of the used receptor (K_d), the defect density (ρ_d), the assay volume (V), and the used label concentration (C_L).

An important observation of these graphs is the orientation of the groove formed by the LOD minima depending on the spot diameter and the four different y-axes. The minimal spot diameters are diagonal for the receptor affinity (Figure 19a) and the volume (Figure 19b). However, they are parallel to the y-axis for the defect density (Figure 19c) and the label concentration (Figure 19d). Hence, a change in defect densities or label concentrations does not require a change in flow cell dimensions, but the use of a different IgG with higher or lower binding affinity does. The label concentration variation induces minimal LOD changes with a shallow plateau, buried in between two steeper edges. The optimization of the label concentration therefore does not require outstanding accuracy, as long as the plateau region is found.

https://doi.org/10.1021/acs.chemrev.1c00044
Chem. Rev. 2021, 121, 8095–8160

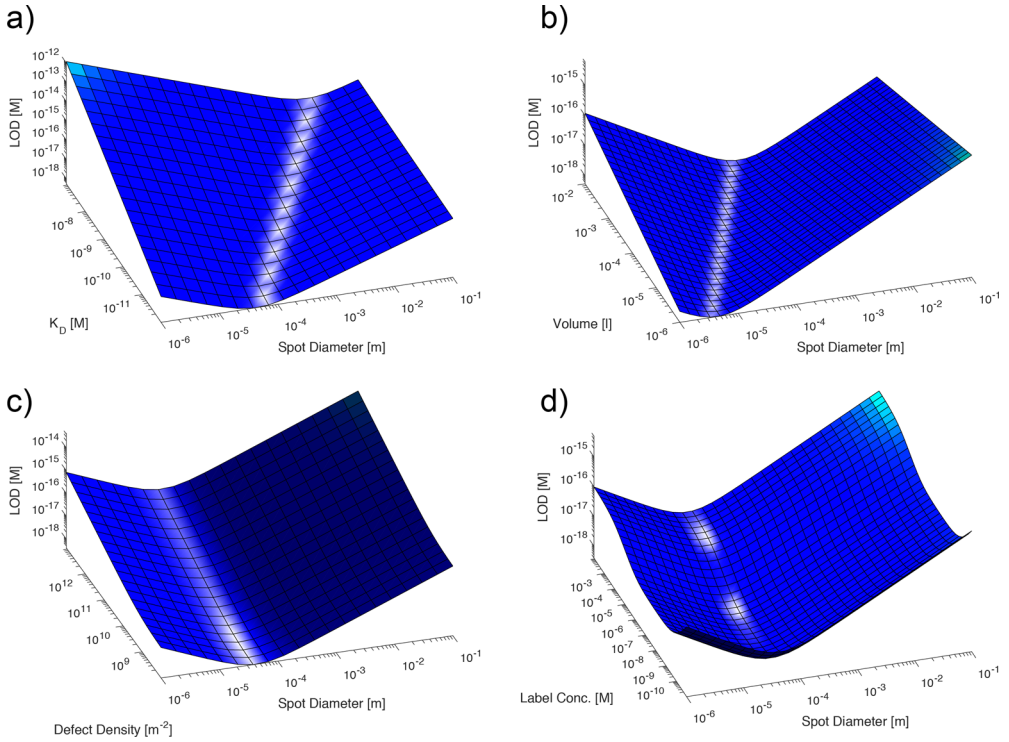

Figure 19. Dependency of the limit of detection (LOD) on various assay parameters as predicted using the competitive Langmuir model with depletion model. The three-dimensional surface plots depict the LOD vs spot diameter vs (a) receptor affinity (K_d), (b) assay volume, (c) surface defect density, and (d) concentration of the labeled antibody. The orientation of the groove clearly shows that the optimal detection spot diameter varies for parts a and b but not for parts c and d.

The parameters used for calculating the curves in this section are typical values corresponding to the dimensions of a 96-well ELISA plate or typical biosensing flow cells: the volume, V, is 100 μL, and the surface area, A, is 1.5×10^{-4} m^2. These graphs demonstrate how a biosensor may be optimized in order to reach an optimal assay LOD. The transducer was not included in these calculations. The models used for our quantification do not include any interactions that may occur in the solution; that is, we have ignored the solution competition described in the DCLM part of section 5.2.3.

In summary, this section began by introducing why NSB is currently a bottleneck in diagnostically relevant sensing, including a specific recipe for correct experimental assessment of the LOD of a sensor. Then we introduced the various theoretical models that describe the expected behavior of a sensor in the presence of nonspecific binders and showed how to use these models to optimize sensor performance. Finally, we concluded by providing examples of how the ratio of SB to NSB affects the theoretically expected LOD.

6. OVERCOMING NONSPECIFIC BINDING FOR BIOSENSORS

Biosensors are heterogeneous assays that are based on recognition elements integrated into an artificial sensor surface.[392] The biomolecular binding event is transduced into a measurable signal. In an ideal biosensor, every bioreceptor has one target that binds specifically and selectively. In the absence of the target molecule, the receptor should remain unoccupied. In reality, this scenario is not the case due to NSB as well as multiple binding sites (*e.g.*, multiple epitopes and paratopes) as discussed in previous sections. For DNA-hybridization-based sensing, target specificity is high due to the discrete nucleic acid building blocks, and any mismatched bases in the DNA sequence reduce the binding strength. Thus, it is possible to have one specific target fitting to one receptor. However, this target specificity is reduced in the case of proteins. Antibodies are susceptible to cross-reactivity, where many different molecules can bind to the same binding region on a receptor surface even though they should ideally be specific for a single target.[393,394]

Thus, antibody promiscuity can lead to one receptor having multiple strong affinity binders. For example, Hudson et al. demonstrated that antibodies found in healthy people react with roughly 28% of human proteins.[395] Further, Haab et al. investigated 115 antibody−antigen pairs and concluded that only 20% were specific.[396] Also, only 531 out of 22,000 antibodies from the Human Protein Atlas Project[397] bound to a single line in a serum Western blot.[398] Additionally, many peptides are found to bind weakly to almost any target protein.[399]

Critical challenges arise from targets with similar affinities (cross-reactivity to other strong binders) and from the expansive concentration range (~10^{12}) of proteins in blood,[399−401] which compensates for the affinity differences. If the affinity of the nonspecific binder is 10 times weaker but the binder is 10 times more abundant, the chance of binding is the same due to the thermodynamic equilibrium (see previous section). When the plasma proteins are highly abundant in comparison to the analyte of interest, NSB will contribute to a significant fraction of the capture antibody signals.[399,402,403] Protein avidity and rebinding (attinebility) further increase the noise in such systems.

Various approaches have been attempted to overcome these cross-reactivity issues in physiological environments where NSB

https://doi.org/10.1021/acs.chemrev.1c00044
Chem. Rev. 2021, 121, 8095−8160

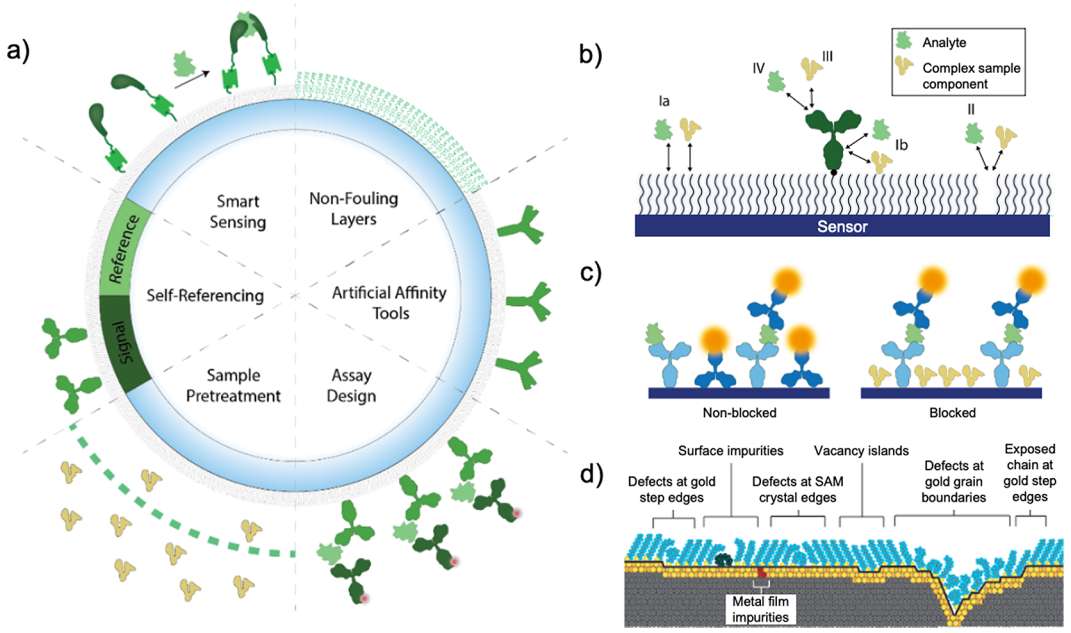

Figure 20. (a) Approaches to minimize nonspecific binding (NSB). (b) Different NSB possibilities on a sensor surface: direct binding (I) to the surface (Ia) or to the capture probe (Ib), binding to surface defects (II), and binding to the paratope of the capture probe by interferents (III). The specific binding is represented by IV. (c) Blocking can reduce NSB of the labeled component of a typical immunoassay by reducing type I and II interactions. (d) Different types of surface defects (II) that can induce NSB (Figure adapted with permission from ref 43. Copyright 2005 American Chemical Society).

effects are pronounced. In the first part of this section, we discuss common techniques that have been applied to biosensing platforms to minimize NSB. We then cover examples of artificial recognition elements that improve the selectivity by reducing the cross-reactivity that plagues antibody use. We also examine ways in which the sensor geometry can be optimized to render biosensors "self-referencing" as it is evidently impossible to completely eliminate NSB. Finally, we give examples of novel biosensing platforms that have been specifically designed to overcome the issues of NSB (see Figure 20a).

6.1. Approaches to Minimize Nonspecific Binding in Heterogeneous Assays

The minimization of NSB is an intrinsic challenge for all biosensors regardless of platform and design. There are several common strategies for preparing and/or handling biosensor platforms to reduce NSB. In this section, we will summarize the following approaches: (1) blocking agents, (2) surface chemistry, and (3) sample pretreatment.

6.1.1. Blocking Agents. Biosensors interact with the sample through a solid−liquid interface, which can be categorized into the receptor component and the surface component (Figure 20b). The receptor component addresses the interaction site, *e.g.* the epitope−paratope binding sites of an antibody−antigen complex, and the surface component addresses the surrounding areas, *i.e.* the nonbinding sites that neighbor the specific interaction sites. To improve assay performance, the receptor−target system should have maximal specificity, while the nonspecific background sites and the surface should be low-fouling, as NSB can occur in both areas. False positive signals can arise from NSB to a nonbinding-site region of the receptor or to the surface where the receptors are attached (Figure 20b). High NSB leads to a high background signal, which then decreases the LOD.

Particularly in immunoassays, blocking steps are commonly used on sensing surfaces to mask the remaining areas exposed for potential irreversible NSB (Figure 20c). The blocking step is achieved by incubation of surfaces functionalized with recognition elements responsible for sensing targets of interest, with protein solutions that cover remaining areas on the surface. Blocking agents have the common goal of improving assay sensitivities by reducing nonspecific background noise and maximizing the signal-to-noise ratio of the assay. Besides inhibiting NSB, the optimal blocking agent should have the following properties: exhibit minimal to no cross-reactivity with subsequent assay components, act as a stabilizer for biomolecules, exhibit low enzymatic activity, not affect the bond of the immobilized specific receptors, and display reproducible performance.[404]

Common blocking agents for immunoassays include bovine serum albumin, lactalbumin, nonfat dry milk, whole normal (nonimmune) serum, and gelatin.[405,406] Bovine serum albumin and nonfat dry milk are the most generally used and economical blocking agents. Normal serum is the gold standard of blocking agents but is costlier. The working principle is based on the fact that these proteins will bind more to the nonspecific epitopes compared to the secondary antibodies and thus "out-compete" the secondary antibodies and lower the background noise. However, it is important to note that there is no blocking agent that is optimal for all assays.[406]

Thus, blocking agents need to be optimized depending on the sample and assay type, antibody source, detection methods, and unexpected protein−protein interactions. Currently, blocking agents are often chosen for empirical and convenience reasons.[404,407] Many blocking agents still exhibit immunological features that lead to undesired cross-reactivity of antibodies, but the topic has been overlooked since the 1980s.[406,407] Therefore, there is still a need to understand the principles of efficient blocking agents and to develop new candidates to improve the blocking of nonspecific sites at the surface of immunoassays.

https://doi.org/10.1021/acs.chemrev.1c00044
Chem. Rev. 2021, 121, 8095−8160

6.1.2. Surface Engineering. As NSB to surfaces is unavoidable, besides blocking techniques, also the surface chemistry needs to be adapted to minimize NSB. The most common approach to reduce NSB on exposed surfaces is by coating with a nonfouling or low-fouling layer.[77,408,409] The principles for the design of nonfouling layers include flexibility, charge, minimal surface defects, and hydrophobicity. Surfaces that resist NSB are called "inert" surfaces, and the most widely adopted protein-repellent surface to date is composed of oligo- or polyethylene glycol (OEG or PEG).[42,43,354] Ethylene glycols covalently immobilized on sensing surfaces provide effective nonfouling coatings by repelling nonspecific proteins due to their high conformational entropy and high exclusion volume.[410,411] Vaisocherova et al. reviewed the recent advances in the development of antifouling polymers and their applications in optical biosensing.[412]

Surface defects can also introduce opportunities for NSB. Love et al. reviewed the surface defects in self-assembled monolayers (SAMs), which are among the best-defined and understood surface coatings and, as such, serve as a good example on what type of defects occur in functionalized surfaces (Figure 20d).[43] There are both extrinsic and intrinsic causes of defects. Extrinsic defects are caused by any variation in the surface of the substrate (cleanliness, intergrain boundaries, faceting, occlusions, twins density of atomic steps, or impurities) and impact the structure of the SAM. Mismatches between the SAM and the substrate can lead to single-atom vacancies, which could grow into large vacancy islands.[413]

The preparation method and purity of the adsorbate solution further complicate the kinetics of formation and the final structure of the SAM.[357] Intrinsic defects are due to the dynamic nature of the SAM itself, which arises from thermodynamic constraints to its stability and intrinsic structural dynamics. The intrinsic dynamics of the organic component of the SAM leads to further defects due to complex phase transitions such as tilt-order phase transitions.[414] Although PEG-like coatings of neutral hydrophilic molecules still dominate the area of nonfouling surfaces, new approaches have emerged based on zwitterionic polymer brushes.[415] These methods are based on the same design principles that Nature uses to reduce NSB as described in sections 3 and 4.

Despite progress, to date, no perfect nonfouling layer exists. Nonfouling coatings help to improve the detection limit, but even the most successful nonfouling coatings cannot decrease the NSB enough to achieve the necessary sensitivity for clinically relevant assays in most applications.

6.1.3. Sample Treatment. In biological samples such as serum or plasma, the concentration of protein or peptide biomarkers is often very low; that is, biomarkers are typically low-abundance proteins (LAPs). The detection of LAPs is hindered by other proteins present at relatively high concentrations: the high-abundance proteins (HAPs).[405,416] Removal of such interfering compounds by pretreating the sample can increase the ratio of the interesting LAPs to the interfering HAPs. For example, mass spectrometry is a highly specific technique with essentially single molecule sensitivity, but in complex solutions, it can only be used after a pretreatment of the sample that removes the majority of the biological matrix proteins.[417,418]

Despite the evident importance of understanding the effect of sample pretreatment in terms of reducing NSB, limited research has been conducted in this area and current knowledge is largely empirical. Here, we will focus only on the most common sample pretreatment methods that are described in the literature and how these techniques play a role in reducing NSB as well as their advantages and disadvantages (Figure 21).

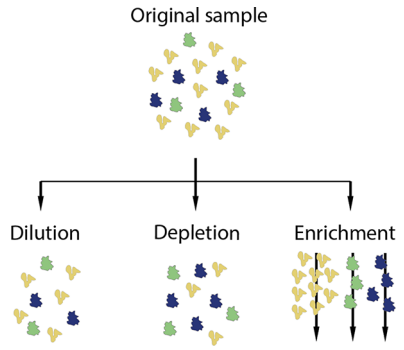

Figure 21. Three main pretreatment methods that help to reduce unwanted nonspecific binding (NSB): dilution lowers the concentration of NSB molecules to significantly below their K_d, but it also reduces the binding of the analyte of interest. Depletion reduces the concentration of highly abundant proteins thereby reducing their NSB without affecting the concentration of low abundant proteins. Enrichment creates fractions of the sample where certain proteins of interest are collected specifically.

A first common practice, especially among enzyme-linked immunosorbent assay (ELISA)-users, involves dilution of a complex sample to achieve better performance.[419] Such a dilution step only has an effect on the first "capture" step of the assay. Although this method works in practice, this concept is not at all intuitive because the amount of captured specific binders is also expected to be reduced, similarly to the NSB (see section 5). Consequently, this step should manifest as a monotonic decrease of the amount of captured analyte molecules as a function of dilution.

In 2003, Pieper et al. introduced the targeted depletion of abundant plasma proteins with antibody columns.[420] Since then, affinity depletion of abundant proteins from human plasma and serum has become a routine sample pretreatment strategy in proteomics and is used prior to protein identification and quantification. These columns remove nontarget proteins through nonspecific association and have been described as the most specific method for removal of HAPs.[416,421] Polaskova et al. compared the performance of commercially available depletion products based on three criteria: efficiency of HAP depletion, nonspecific removal of the undesired proteins, and the total number of protein spots detected after depletion.[422] All of these commercially available depletion products share the same final goal: to efficiently separate HAPs from LAPs. Depletion is often combined with enrichment methods, where the proteins of interest are enriched within their respective fractions.

There are two categories of current commercial depletion columns: albumin/IgG removal and dynamic range reduction. Since albumin is the most abundant plasma protein and represents 60−70% of all protein mass in serum and IgG is the second most abundant protein (10−20%), these two components effectively mask the presence of many LAPs. Therefore, to enrich LAPs, these proteins must be removed prior to downstream separation or analysis. Commercial kits such as the Aurum Affi-Gel Blue kit can be used for the removal of both albumin and IgG.[423] The second category of depletion columns aim at dynamic range reduction of the protein concentration.

https://doi.org/10.1021/acs.chemrev.1c00044
Chem. Rev. 2021, 121, 8095−8160

Commercial products, such as the ProteoMiner protein enrichment kit, can be used for enriching medium- and low-abundance proteins and for decreasing the amount of HAPs.[424]

The main drawback of HAP depletion is that it dilutes the sample, and many diagnostically relevant proteins may be unintentionally removed during depletion. This outcome is commonly known as the "sponge effect", where small proteins and peptides may bind to large proteins that normally serve as their carriers either specifically or nonspecifically.[422,425,426] Therefore, sensitivity is not necessarily increased by applying more than one depletion step.[417,427−429] To date, there is no quantitative data on how much of the nontargeted proteins are nonspecifically bound to the specifically depleted proteins and how much of the nontargeted proteins are nonspecifically bound to the depletion matrices.

6.2. Selectivity of Molecular Recognition Elements

Nearly every diagnostically relevant biosensing approach relies on some form of receptor molecule that specifically and selectively recognizes a biomarker of interest. Therefore, in addition to reducing the NSB to the biosensor platform using the methods mentioned in the previous sections, also the inherent and unavoidable NSB to the recognition elements has to be considered. Traditionally, the receptors that are used in such sensors are natural antibodies that are optimized through evolution to selectively bind a target molecule *in vivo*. However, the past decades have seen the emergence of new artificial receptors that have the advantage of tunable affinities as opposed to biological receptors that are challenging to modify without altering binding behavior (see Figure 22).

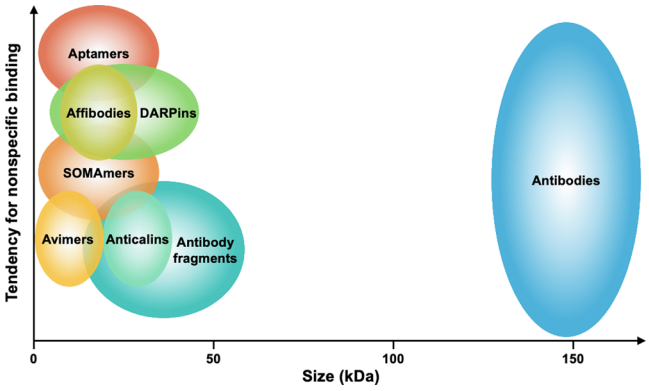

Figure 22. Recognition elements that are used in biosensing arranged according to their size and tendency for nonspecific binding.

As outlined in section 2, the affinity of receptors depends on the on and off-rates of the target (eq 2). The k_{on} parameter is typically in the same range for all antibodies.[430] By increasing the binding strength of the receptor−target complex, k_{off} rates can be changed dramatically, thus changing the affinity. The specificity is improved only when the ratio of specific affinity vs nonspecific affinity is increased. From our discussion on the nature of NSB in sections 2−4, it is evident that the larger a molecule and the more sticky groups it has on its surface, the higher the expected NSB. Therefore, artificial receptors should reduce the size and number of structural elements that provide the molecular stability and shape, in favor of moieties that participate in SB.

Such artificial affinity tools including antibody fragments, engineered binding proteins, molecular imprinted polymers, and aptamers have been nicely reviewed by Ruigrok et al.[431] Aptamers, which are short (typically ca. 80 bases or less) single-stranded oligonucleotides,[432] have gained substantial attention due to the *in vitro* selection procedure termed the systematic evolution of ligands by exponential enrichment (SELEX) by which they are isolated for specific targets of interest.[433,434] A large starting library of 10^{-14} to 10^{-15} synthetic oligonucleotides are used for selection.[61,435] This initial pool is $>10^4$ times larger than standard peptide, protein, or antibody combinatorial molecular libraries.[436] During subsequent selection rounds with increasing stringency, target-binding molecules are separated from low-affinity or nonbinding molecules. An effective selection procedure that, for example, incorporates counter-selection of nonspecific molecules is essential for identifying high-affinity and selective binding partners.[437,438]

However, aptamers are inherently prone to NSB due to the high amount of negative charges on the oligonucleotide backbone as well as the large variety of RNA/DNA-binding proteins that are present in blood, particularly in the immune system. To address this issue, SOMAmers (slow off-rate modified aptamers) were developed, which are specifically designed not only to increase the k_{on} and in turn the affinity but also to have a very slow dissociation rate with their cognate analytes (half-lives of 30 min to several hours) but fast k_{off} rates for most other nonspecific proteins in plasma or serum.[401,435,439] This difference in k_{off} allows selective disruption of nonspecific interactions by rinsing. Chemical modifications (*e.g.*, the substitution of every tyrosine with 5-benzyl-dUMP)[401] of the oligonucleotide building blocks helps to further expand the repertoire of targets to which SOMAmers can bind.[440]

In addition to oligonucleotide-based artificial receptors, protein engineering has advanced the development of antibody surrogates with high ligand affinity in the form of engineered proteins including designed ankyrin repeat proteins (DARPins),[441] avimers,[442] affimers,[443] affibodies,[444] anticalins,[445] adnectins,[446] *etc.* These protein-based recognition elements are derived from proteins that typically possess endogenous affinity for a target of interest and are composed of a single structural domain or repeated polypeptide units.[447] Thus, compared to antibodies, these engineered receptors are smaller in size (typically up to 100 amino acid residues) with increased stability.[448] The development of *in vitro* technologies such as phage display and ribosome display has enabled the selection of specific protein-based binders in a more rapid and high-throughput manner compared to antibody production.[449] For a review that covers the emergence of diverse nonimmunoglobulin scaffolds and their basic characteristics, see the work by Škrlec et al.[450]

While recent years have brought significant progress in the field of artificial receptors, it is still often observed that antibodies raised against an analyte of interest in animals surpass their artificial competitors in terms of their assay performance. This phenomenon is likely due to the fact that immunization optimizes not only for SB but also for NSB through glycosylation and other post-translational protein modification routes to avoid unwanted side effects for the host.[451] In recombinant receptors, serious effort is needed to provide the human-like glycosylation pattern that is required when using such molecules in humans or with human samples.[452] This glycosylation concept of Nature is mimicked in recent publications where artificial receptors have been modified with passivating groups (PEG, lipids, or glycans) to improve their NSB properties.[453,454]

https://doi.org/10.1021/acs.chemrev.1c00044
Chem. Rev. 2021, 121, 8095−8160

6.3. Discriminating Specific from Nonspecific Binding

As already stated in section 5, NSB is currently the limiting factor in improving the LOD of diagnostically relevant biosensors. In this section, we provide further explanations on how discriminating by time, force, or location—under certain special circumstances—could help to reduce this NSB problem.

Before we start discussing the solutions, Figure 23 needs to be understood. It is a general figure that describes the basis of any sensing experiment and depicts the probability distribution of the signal at different concentrations of the analyte. We always show pairs of curves, a curve at zero analyte concentration and a curve at the LOD, that correspond to situations with different types of referencing. The red curve shows the expected probability distribution of an unreferenced sensor centered around the signal at zero analyte concentration (S_0), which is nonzero because of the NSB. Here, the normal distribution is due to the inevitable patient-to-patient variations in NSB. The more biomarkers are present, the more this distribution will shift toward higher signals. The LOD is defined by the biomarker concentration at which the signal distribution will only have a marginal (0.27%) overlap with the distribution corresponding to the zero analyte concentration. As such, the LOD is directly related to the width of the curves and how much the peak-position shifts with concentration (dS/dc). The width of the curve is due to NSB, while the sensitivity of the biosensor defines (dS/dc).

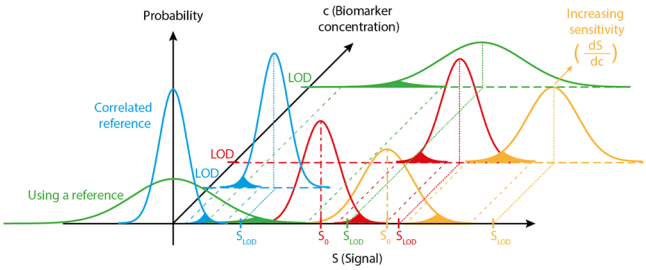

Figure 23. Nonspecific binding (NSB) determines the limit of detection (LOD) in most diagnostically relevant sensing experiments. The figure depicts the probability of obtaining a certain sensor response (signal) at the biomarker concentration that corresponds to the LOD and in the absence of the analyte. Gaussian distributions illustrate how the overlapping portions of the probability distributions determine the LOD. The red curve depicts a typical sensor response with the expected NSB. Orange illustrates what happens if we simply make the sensor more sensitive. The green curve shows that a single reference channel is not improving the LOD unless the signals in the sample and reference channels are correlated (blue curves).

Interestingly, a more sensitive biosensor typically does not lead to a lower LOD because the enhanced sensitivity also leads to broader probability distributions (see orange curves). However, a reduction in NSB would result in a narrower probability distribution, which directly lowers the LOD as the two curves can be closer to having the same overlapping areas. This effect is used for the majority of referencing approaches. For example, by rinsing, it is possible to reduce NSB as the nonspecifically bound molecules are removed faster than the specifically bound ones (see section 6.3.1). Similarly, by applying external forces, we can reduce the amount of nonspecifically bound, signal-generating assay components, thereby narrowing the probability distribution curves (see section 6.3.2).

Referencing (discrimination by space) is widely used in biosensing to reduce instrumental offsets and the NSB problem. However, this process has to be conducted cautiously, because referencing involves multiple measurements, which can worsen the LOD. For example, the green curve in Figure 23 depicts a situation where a reference channel is used to determine the NSB, which is then subtracted from the signal. This form of referencing is normally done such that the sensor in the reference channel is functionalized with a receptor that does not bind the biomarker and the resulting differential signal is expected to be zero. However, it is often ignored that the corresponding probability distribution has twice the variance due to the error propagation when using two independent measurements to calculate the signal, which leads to a worse (*i.e.*, higher) LOD.

Here, it is critical that this argument only holds for "independent" measurements, when the NSB in the reference channel is *not* correlated to the NSB in the sample channel. However, the immune system of a patient is designed to respond disparately to individual molecules, which manifests as varied NSB signatures on different receptors when exposed to a sample from the same patient. Therefore, the biochemical difference between the receptors in the reference and sample channel needs to be minimized, preferably only altering the epitope region of the receptor. Similar chemical signatures between the sample and reference channels lead to correlated NSB that results in a probability distribution with reduced width and consequently an improved (*i.e.*, lower) LOD (see blue curve in Figure 23).

6.3.1. Discrimination by Time-Differences in Off-Rates. When optimizing the ratio of SB over NSB, as mentioned in section 5 and in the sections above, the surface functionalization should be as nonfouling as possible to reduce NSB to the underlying surface. Additionally, NSB to the receptors has to be minimized by using highly specific receptors. However, NSB occurs despite our best efforts to optimize these two parameters, which has two critical effects on the sensor response: (i) NSB blocks a substantial fraction of the receptors thereby reducing the amount of captured analytes; (ii) NSB induces a signal offset in the sensor that worsens the achievable LOD.

An effective tool that circumvents NSB is rinsing (Figure 20).[455] During rinsing, fast-desorbing nonspecifically bound molecules are discriminated via their off-rates from the stably captured, specifically bound analytes of interest. Thus, it makes sense to select receptors not only for their specificity but also for slow off-rates. Apart from the kinetic properties (slow off-rates) of the receptor, we can also now comprehend why it is useful to perform sandwich assays. A simple theoretical model was derived by Ozer et al. demonstrating that washing only reduces the fraction of target-bound ligand that is retained but does not alter the shape of the binding curve.[61] A more comprehensive model was presented in section 5.4 where Figure 18 nicely illustrated how rinsing can improve the SB to NSB at various steps of the assay process. Here, we summarize the most important messages of that section for cases when diagnostically relevant, low-abundance analytes need to be detected in a complex sample:

1. During the association phase, the receptors will always interact with more NSB proteins than specific analytes (see low SB/NSB ratios in Figure 18b).

https://doi.org/10.1021/acs.chemrev.1c00044
Chem. Rev. 2021, 121, 8095−8160

2. The optimal rinsing time depends on the concentrations of the analyte and the interfering molecules but also on the off-rates of the SB and NSB. Rinsing times are typically on the order of several hours.
3. Sandwich assays are 2−3 orders of magnitude more sensitive than alternative assay formats because only the NSB of the labeled antibody, which is present at concentrations significantly lower than the interferents, determines the extent of NSB. In addition, the SB of the labeled antibody can be optimized for low off-rates (Figure 18c).

While rinsing is widely used because it is a simple procedure while effectively reducing the NSB problem, it has two major drawbacks:

1. Rinsing is time-consuming due to the off-rates of nonspecifically bound molecules, which are slower than what is expected based on their binding energy. This phenomenon is mostly due to nonequilibrium effects related to the presence of the sensor surface. As many receptors and the sensor surface itself can interact with nonspecifically bound molecules, multivalent interactions, attinebility, and rebinding are all expected to influence the experimentally observed desorption kinetics.
2. A substantial portion of nonspecifically bound molecules have similar off-rates as the analyte (or the labeled receptor) itself. For these molecules, rinsing has little to no effect.

Finally, it is worth mentioning that rinsing can be improved by applying external forces between the binding partners using shear or magnetic forces. Such force-discrimination assays will be discussed in detail in the next section.

6.3.2. Discrimination by Force—Differences in Affinity. Based on our theoretical discussions in section 2, another possibility emerges to distinguish SB and NSB. As affinity is directly related to the actual strength of an interaction, we expect large differences in the binding force between SB and NSB (Figure 3). In 1994, the first publications appeared demonstrating that SB can be discriminated from NSB using atomic force microscopy (AFM) that enables direct measurements of the forces between molecules.[456−458] These early studies used the streptavidin−biotin model system, but soon the measurements could be extended to include all kinds of molecular interactions, facilitating exploration of the energy landscape between the binding partners (sections 2 and 3).[459] Such single-molecule force spectroscopy assays involve one of the binding partners to be anchored to an actuator and the other to a force sensor. The molecules are brought into contact to enable binding, and then when bound molecules are separating, the force is recorded as a function of the separation distance of the actuator and force sensor until the bond ruptures.[458,460]

By force unbinding, force discriminating assays can resolve specific vs nonspecific interactions, different binding modes, and even energetically equivalent interactions.[456,459−461] Examples include antibody−antigen interactions,[460] single-nucleotide polymorphism detection,[462] and eliminating cross-reactions on protein microarrays.[463] In conventional single-molecule force spectroscopy, inter- or intramolecular forces are measured with AFM cantilevers[464] or beads in optical or magnetic traps.[465] One of the unique properties of such force assays is the flexibility to choose the kinetics of the experiment according to assay parameters because the binding partners are forced apart. Besides single molecule studies, multiplexed force-based sandwich assays have been conducted to enhance the specificity of the assay. In the work by Blank et al., the secondary antibodies were connected to a soft stamp via a molecular force sensor and pulling forces were directly applied on all spots of the array.[463]

Practically more applicable, magnetic particle-based force discrimination assays were invented by Thomas E. Rohr in Abbott Laboratories in the early 1990s.[466] This generic concept was extended a few years later by Gil Lee and colleagues from the Naval Research Laboratory to cover all types of sandwich assays and include the important force-dependent lifetime of a bond concept and a superconducting quantum interference device (SQUID) with a magnetometer-based read-out.[457,467−469] The assay was refined by introducing fluid-force discrimination[263,470] that enabled application of forces two orders of magnitude higher and also in the preferential tangential (vs vertical) direction.[471] Interesting further enhancement was achieved when large magnetic beads were rolling over smaller, surface-bound magnetic beads in a microfluidic channel.[472]

Besides magnetic forces, electric forces have also been used for reducing NSB. An interesting implementation uses asymmetric electrodes in combination with an alternating electrical field to generate a surface flow of ions for "molecular nanoshearing".[473] Later, this concept was extended to enhance the diffusion and reduce the NSB of Raman labels in a sandwich assay.[474] Overall, force discrimination is currently the most promising method to improve specificity in demanding assays especially in complex biological solutions where NSB limits the performance.

6.3.3. Discrimination by Space—Differently Functionalized Areas to Filter Out Nonspecific Binding. The most common approach to deal with NSB in biosensing is "referencing". What is generally meant by this term is a differential measurement where two or more data points are acquired to separate the nonspecific from the specific signals. Although seemingly logical, most often this approach is not able to deal with NSB problems as we have already hinted on when describing Figure 23 above. Here, we will further explain how we can attempt to discriminate specific and NSB signals using reference channels and spots, *i.e.* discrimination by space. Why can we simply not eliminate NSB by subtracting the signal of a reference channel?

$$S_{Analyte} = S_{Sample} - S_{Reference} \tag{65}$$

This question is easiest to explain by a practical diagnostic scenario. Let us say we are interested in measuring the concentration of a protein biomarker in blood using a sensor modality that enables us to precisely quantify the amount of bound proteins on our sensors. Such integrative sensors include most label-free sensing modalities. As most proteins are sticky and we only want to measure our biomarker, we functionalize our sensor with some kind of receptor molecule that captures our analyte of interest specifically. Since we have no access to the blood of the same patient without the disease marker, we implement a reference channel where the sensor is functionalized with a "dummy" receptor that does not capture our analyte of interest.

As such, we can now measure the signal in a sample channel consisting of $S_{Sample} = S_{Analyte} + S_{NSB}$ and in the reference channel as $S_{Reference} = S_{NSB}$. Subtracting $S_{Reference}$ from S_{Sample} leads to eq 65 seemingly explaining how referencing is able to eliminate the NSB problem. Unfortunately, in most applications, this is only an illusion because the NSB in the sample and reference channels is different:

https://doi.org/10.1021/acs.chemrev.1c00044
Chem. Rev. 2021, 121, 8095−8160

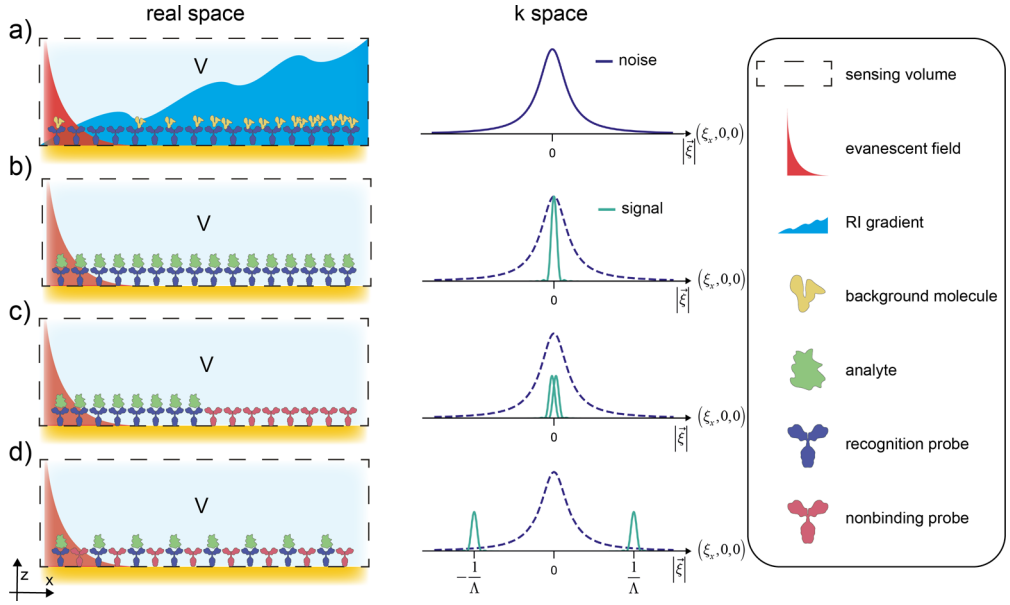

Figure 24. Illustration of how the distribution of sample and reference regions can be considered as a spatial affinity lock-in amplifier. (a) The correlation of environmental influences, including refractive index gradients or nonspecific binding-related noise, scales inversely with distance; therefore, it is distributed as $1/\xi$ (ξ is the spatial frequency) in Fourier space. (b) A typical unreferenced biosensor obtains the signal by averaging over the entire sensor area. Therefore, the signal is represented as a single peak centered around zero in k space. (c) Introducing a single reference channel with nonbinding probes does not improve the signal-to-noise situation significantly, but (d) coherently arranged many reference channels or areas can move the signal to the low-noise regions in Fourier space (to $1/\Lambda$ where Λ represents the periodicity of the coherent pattern). Figure reproduced with permission from ref 493 Copyright 2021 MDPI.

$$S_{Sample} - S_{Reference} = S_{Analyte} + S_{NSB(sample)} - S_{NSB(reference)} \quad (66)$$

Furthermore, diagnostic markers are often of low abundance; therefore, as we saw in the previous section, kinetics and diffusion laws will limit the amount of analytes that will be captured by our receptor covered surface. For most applications, these factors result in only a small fraction of the receptors ($\ll$1%) capturing an analyte. At the same time, the sample (blood) contains a very high concentration of various proteins, some of which will bind nonspecifically to the sensor covering typically over 20% of its surface. Thus, in a typical diagnostic experiment, $S_{Analyte} \ll S_{NSB}$. If the NSB in the reference and sample channels would be correlated, this relationship would not necessarily be a problem, but as we saw in the first few sections, NSB is a complex process that is governed by small molecular details.

As such, the NSB in the reference and sample channels is expected to be distinctly different. Consequently, the error of such differential measurements will be dominated by the noise of the NSB-related signals, and due to error propagation, this value will be larger than the error of the nonreferenced measurement. See, for example, the study by Homola et al. for an experimental example.[475] This is, hence, why in the past, especially in label-free biosensors, reference channels were mostly implemented to reduce other noise sources than NSB.

For example, such parallelization through multichannel systems diminishes synchronization issues (*e.g.*, Biacore 1000).[476] The use of a single probe/detector setup for all channels further reduces the differences in the instrument noise between the channels. An early commercial SPR instrument (Biacore 2000) simultaneously probed four channels through a 4-parted flow cell.[77,477] Nenninger et al. used symmetrical channels in which one spectrometer reads out the signal to decrease instrument noise.[478] Zhang and co-workers followed that trend by using the same laser source, optics, and photodetector—thereby eliminating errors due to thermal drift, mechanical noise, and laser fluctuations.[479] These authors used a quadrant cell photodetector, which simultaneously measured the SPR dips from the sample and reference spots. The reduction of the detector size and the averaging of the detector regions/flow cells enabled them to significantly reduce the detector noise.

In addition to the aforementioned contributions of instrument noise, also surface noise (*e.g.*, due to temperature and analyte concentration gradients) is a critical limitation to current label-free measurements. The signal and reference channels have to be virtually equal and should show the same degree of NSB to the surface.[275,478] However, the surface noise is not constant across all sensing areas.[478] The macroscopic distance between the spots (typically a few millimeters) results not only in essential differences and gradients in physical parameters during the measurements (temperature, pressure)[480,481] but also in concentration gradients and different distributions of surface defects (the latter contributes to the different NSB to the sensor surface). Therefore, a reduction in distance between signal and reference channel reduces environmental noise.[478,482]

The miniaturization and integration of reference and signal channels in adjacent flow cells were proposed to minimize the surface noise.[478,479,482] Multiple miniaturized signal and reference channels are used to further reduce those differences and enable averaging, which further improves the signal-to-noise ratio. Boecker et al. used numerous miniaturized referencing spots placed between miniaturized sensing spots instead of a single macroscopic referencing spot.[483] This arrangement led to an improved gradient compensation in the surface noise because the differences were reduced to the level of two miniaturized (200 μm) sensing and referencing spots, while the total surface

https://doi.org/10.1021/acs.chemrev.1c00044
Chem. Rev. 2021, 121, 8095−8160

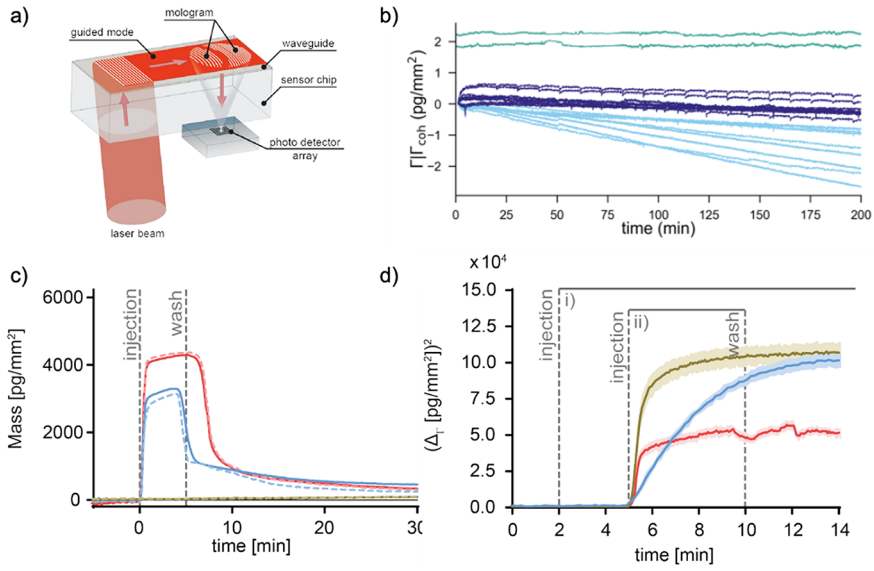

Figure 25. Coherent referencing is able to drastically reduce noise and nonspecific binding (NSB) effects in biosensors. (a) The concept of focal mology. Laser light coupled into a planar waveguide is diffracted on a coherent arrangement of biomolecules into a focal point on a photodetector array. This arrangement is ideal to implement the spatial lock-in amplifier concept. (b) Comparison of the baseline noise and drift of focal mology (green) and Biacore 8K (blue). Note that while the Biacore is stabilized to 0.01 °C, no temperature stabilization is used in the mology measurements (the dark blue curves show Biacore measurements with a reference channel). (c) Refractometric sensors, such as optical waveguide lightmode spectroscopy shown here, are highly subject to NSB from horse serum (blue) or human whole blood (red) compared to the baseline in PBS (gray). (d) The in-built coherent referencing of focal mology makes it not sensitive to NSB upon addition of serum (first injection) while specific binding of streptavidin (gray and red) or neutravidin (blue) remains clearly detectable (second injection). Parts a, c, and d reproduced with permission from ref 501. Copyright 2017 Nature. Figure b reproduced with permission from ref 500. Copyright 2021 MDPI.

area of these spots remained macroscopic. The splitting factor of the spots reduced the noise linearly.[483]

As SPR is the gold standard for label-free optical biosensors, most existing literature on referencing focuses on this technology. However, self-referencing is also used in other optical biosensors, *e.g.* photonic crystals,[484] whispering gallery modes,[485] interferometry,[486] waveguide gratings,[487] and ring resonators.[488] An overview on optical biosensors for unlabeled targets can be found here.[489] State-of-the-art commercial label-free biosensors, such as the Biacore-8000 or the Creoptix WAVEdelta, use any combination of four parallel channels for referencing.[477,490−492] Referencing is also routinely practiced in assays using labels. For example, Affymetrix uses 40 different reference spots to ensure specificity of their single nucleotide polymorphism chip,[417] and also ELISA plates include negative control wells and standards.

Recently, we have introduced the spatial affinity lock-in concept that explains how one can separate noise from signal with the help of reference areas cleverly distributed in space (see Figure 24).

It is well-known that temporal noise is distributed according to $1/f$ in the frequency domain, and thus, this noise can be filtered out using lock-in amplifiers.[494−498] Since the fluctuations of environmental parameters, such as temperature and refractive index in space, are connected to the temporal fluctuations of the same parameters via the convection−diffusion equations, we expect a similar $1/\xi$ behavior in space. Also, fluctuations related to the binding and dissociation of molecules (adsorption−desorption noise), *e.g.* due to specific or NSB, are connected in time and space.[499] (see Figure 24a). Most biosensors integrate within a certain time and also over a certain area of the sensor, which manifests as a peak-shaped signal distribution around the origin of Fourier space (see Figure 24b). It is common to sacrifice part of the available sensor surface for reference channels or areas that are often functionalized with nonbinding probes with the hope that we can subtract the NSB contributions as described above. Such a sensing arrangement simply distributes the signal into two smaller peaks still placed close to the origin in k space which means that the signal-to-noise ratio is not expected to improve significantly (Figure 24c).

However, distributing sensing and reference areas in a coherent arrangement results in a shift of the signal peaks in k space to locations that represent the periodicity of the original pattern, Λ (*i.e.*, centered at $\pm 1/\Lambda$ in the Fourier space), which enables a significant improvement of the signal-to-noise. Theoretically, the miniaturization and integration can be pushed until half the molecule size is investigated. However, the smaller feature size comes at the price of a more sophisticated fabrication, surface functionalization, and depending on the implementation, also the readout. This spatial lock-in amplifying concept is a unifying theory that is applicable to all sensors that employ referencing in space.[493]

6.4. Intrinsic Biosensor Design to Overcome Nonspecific Binding

In this section, we discuss biosensors that suffer less from NSB by their intrinsic design. These sensors are designed to be exposed to both specific and nonspecific interactions while measuring the ability to discriminate the two phenomena. We discuss three major classes of sensors: diffractometric techniques, molecular sensors, and stochastic sensors. For each class of sensors, we will first describe their fundamental sensing principles and then discuss their capacity to discriminate SB and NSB.

6.4.1. Inherent Self-Referencing: Diffractometric Techniques. In the previous section, we explained the concept of the spatial lock-in amplifier, *i.e.* how coherently placed

https://doi.org/10.1021/acs.chemrev.1c00044
Chem. Rev. 2021, 121, 8095−8160

reference and sensing areas can shift the expected signal distribution toward the lower noise regions of the Fourier space. Here, we briefly introduce diffractometric sensors that are ideal to read out a locked-in binding signal at a high spatial frequency with almost no measurment effort. For a more detailed explanation, the reader should refer to Frutiger et al.[500]

In the time domain, a carrier frequency is used to "lock" the signal to the low-noise regions of the Fourier space and mix it with a reference signal. This shifts one of the signal lobes to direct current (DC). The signal is locked to DC, and a low-pass filter can be used instead of a sophisticated tracking bandpass filter.[495] This method allows the detection of signals that are orders of magnitude smaller than the environmental noise background. Many scientific instruments but also our telecommunication devices are based on this effect.

How can we create something analogous in space? Diffraction of coherent light at coherently placed (submicron scale) reference and sensing regions of a biosensor is a phenomenon that enables a simple read out of a locked-in binding signal of high spatial frequency. Such coherently diffracted light creates specific high-intensity areas in real space—similarly to the well-known spots that appear on the screen during X-ray crystallography. In other words, the coherent light performs a Fourier transformation of the refractive index distribution on the substrate, and the binding signal is acquired in Fourier space.

By placing our detectors at locations that correspond to the periodicity of the coherent biochemical features on our sensor surface, we can create a sensor transfer function that only measures the signal carrying part of the Fourier space while rejecting almost all environmental noise.[493] This setup leads to an extremely simple measurement and a high spatial lock-in frequency. In contrast, if a spatial lock-in is implemented by a referenced SPR sensor, the measurement setup is substantially more sophisticated and the lock-in frequency is orders of magnitude lower.[493,500]

Recently, this concept was realized with optical waveguides (see Figure 25a). Focal molography uses a coherent bioaffinity pattern (termed mologram) as sensing and reference regions.[501] The mologram is designed as a Fresnel lens; that is, coherent light that is scattered on molecules that specifically bind to either the sensing or the reference lines interferes constructively at a diffraction limited focus spot. Light scattered from molecules that randomly bind to the surface, *e.g.* due to NSB, on the other hand, interferes destructively; therefore, its contribution to the intensity at the focus is negligible.

This technique has several advantages:

1. Noise due to environmental fluctuations is highly reduced, which renders the usual sophisticated temperature stabilization for label-free sensors obsolete. Figure 25b illustrates that even in the absence of temperature stabilization, the diffractometric sensor has a more stable baseline than the state-of-the-art Biacore 8K instrument.

2. Similarly, the system also becomes insensitive to bulk refractive index changes.

3. Most importantly, molography is also insensitive to NSB. Refractometric tools, such as optical waveguide lightmode spectroscopy (OWLS), exhibit a large signal response upon addition of complex solutions (*e.g.*, horse serum or human blood) due to the high amount of NSB proteins that takes hours to rinse away (see Figure 25c). In comparison, molography shows minimal response to such NSB, while preserving the ability to measure the specific analytes spiked into the samples (Figure 25d).

Here, we summarized how diffractometric sensors are highly suitable to cope with the NSB problem. We used focal molography as an example, because it is the most advanced and most recent sensor in this category, but a few related techniques using the same principles also have similar capabilities but are not as sensitive.[502,503]

6.4.2. Molecular Switch Sensors. In some sensing approaches, a difference between two states of a specific molecule generates the response. These biomolecular switches are recognition elements composed of proteins or nucleic acids that reversibly undergo conformational changes upon contact with the target analyte. The biomolecule changes its conformation only upon a specific interaction (*e.g.*, opening of an ion channel or the activation of enzyme), even when the target interaction is low in affinity. Through these unique conformational rearrangements with high selectivity against nonspecific interferents, switch sensors differentiate SB from NSB and render the output signal minimally sensitive to the presence of nonspecific molecules in complex environments.[504]

The first system that falls into this category was an ionic channel switch sensor, which was later commercialized under the name AMBRI biosensors.[505−507] Strictly speaking, AMBRI biosensors were not based on conformational changes of receptors but rather on a configuration change of a complex system. The working principle of this sensor includes a gold electrode to which a lipid membrane with ion channels (gramicidin) and an anchored antibody are tethered. This structure forms an ionic reservoir between the membrane and the gold electrode.

In the absence of a target, even in the presence of NSB, the anchored (lower) part and the freely diffusing (upper) part of gramicidin can meet, thereby forming an ion-channel in the membrane through which ion-current can flow. This ion current is switched off when the mobile part of the channel in the outer half of the membrane comes into contact with the analyte, because the formed sandwich is now anchored to the substrate (Figure 26a). This technique is minimally susceptible to NSB, because NSB only blocks some of the binding sites but it does not trigger a reduction in the ionic current.

Similarly, a biomolecule switch sensor to detect Ca^{2+} in living cells was developed.[508] This switch sensor (Figure 26b) is a genetically encoded, calcium-sensitive switch that fuses calmodulin, a calcium-binding protein, with two fluorescent proteins. When Ca^{2+} binds to calmodulin, the specific interaction brings the two fluorescent molecules close together, and the emitted wavelength of the fluorescence is shifted due to fluorescence resonance energy transfer.

As an example of DNA-based switch sensing, DNA aptamers with methylene blue, a redox dye, tethered to the 3′ terminus were functionalized to gold electrodes through thiol groups at the 5′ end.[509] Upon specific target recognition, these aptamers would rearrange into a configuration that brings the methylene blue closer to the electrode surface, thereby increasing the efficiency of electron transfer.[504] This switch sensor was used to detect cocaine molecules at micromolar concentrations, and electronic signal transduction necessitated specific conformational rearrangement of the aptamer backbone upon binding cocaine[509] (see Figure 26c).

Although switch sensors are less susceptible to NSB due to the intrinsic properties of the recognition elements themselves, re-engineering biomolecular switches to bind new clinically

https://doi.org/10.1021/acs.chemrev.1c00044
Chem. Rev. 2021, 121, 8095−8160

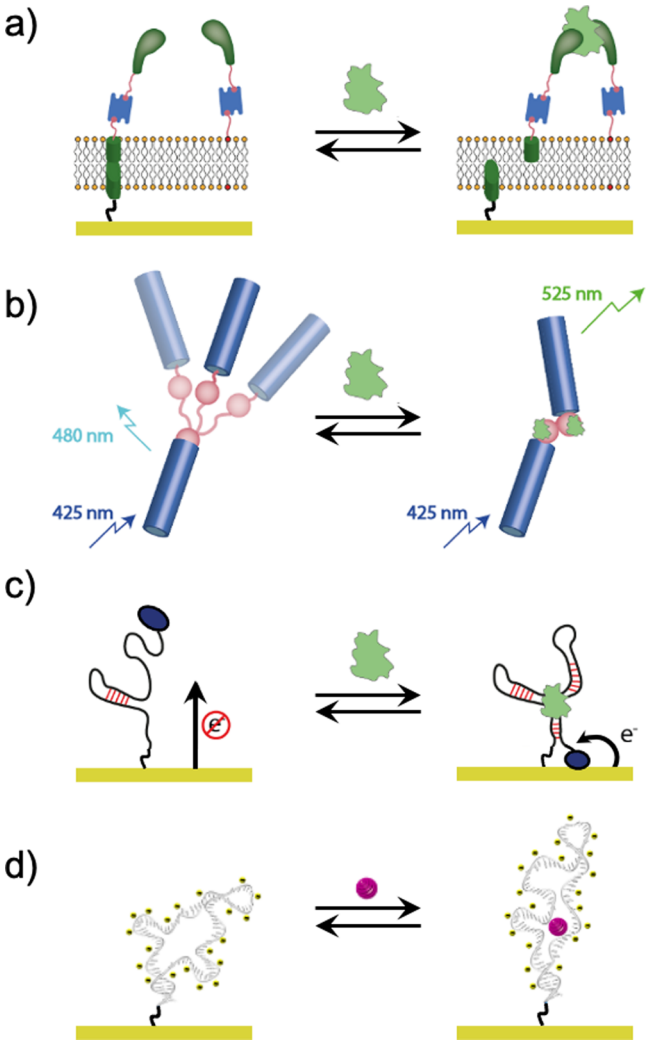

Figure 26. Molecular switch sensors: (a) ion-channel-based switch sensing: The binding of an analyte fixes the mobile part of gramicidin in the upper leaflet of the membrane to a position that prevents the formation of the ion-channel. The corresponding current drop is then proportional to the concentration of the analyte. (b) Calmodulin-based Förster resonance energy transfer (FRET) switch sensor: binding of Ca^{2+} triggers a conformational change in calmodulin that brings the two fluorescent peptides closer to each other resulting in a FRET signal. (c) DNA aptamer-based switch sensor: a redox reporter is attached to the end of a DNA aptamer. Binding of the analyte induces a conformation change that brings the reporter close to the surface of an electrode, thereby increasing the efficiency of electron transfer. (d) Aptamers that undergo conformational rearrangement can also be used to gate a field-effect transistor directly taking advantage of the analyte-induced rearrangement of the highly charged DNA backbone.

relevant targets remains challenging. To address this issue, four different strategies for re-engineering biomolecular switches have been proposed.[504] The first approach is to integrate naturally occurring biomolecular switches that bind the clinical target of interest and can readily be converted into a sensor.[510−514] The second technique is to link the recognition element to a naturally occurring effector molecule that selectively binds to specific proteins to regulate their biological activity.[515−517] The third option uses the analyte to stabilize the alternative, nonbinding conformation of the recognition instead of the switch turning "on" when interacting with the clinical target.[518−521] The fourth method fabricates the switch component such that the switch−target complex is destabilized such that it only folds upon binding.[509,522]

Due to their enhanced capacity to cope with NSB, switch-based biosensors can be implemented in complex environments. For example, aptamer-based switch sensors were used to detect cocaine in blood serum, saliva, and other complex samples.[522] However, although the signal generating molecule is robust against NSB, the commonly used electrochemical detection mechanism is not. Therefore, although small-molecule drugs such as doxorubicin and kanamycin were monitored in live, moving rats using miniaturized, aptamer-functionalized switch sensors, this platform required a continuous diffusion filter with laminar flow to keep blood from mixing with administered buffer.[523] The buffer was necessary to protect the electrode surface from nonspecific adsorption of blood components, and the filter bypassed the issue of long-term fouling that is often observed in whole blood or in any implantable biosensor. The challenges of such implantable biosensors will be addressed in greater detail in section 7.

Switch-based sensors are rapid and label-free and when combined with electrochemical methods, can be used to detect small-molecule targets that are conventionally more difficult to detect in comparison to larger biomolecules.[522] The sensor can respond to its target in seconds and can be easily regenerated. A sensing mechanism reliant on a specific target-induced conformational change of receptors, rather than less specific binding mechanisms such as adsorbed mass or charge, results in minimal interference from nonspecific contaminants. However, the electrochemical detection mechanism relies on distinct conformational changes that move the redox dye in close proximity to the electrode surface for electron transfer to occur. This requirement has limited the number of targets that can be sensed. This issue can be resolved by taking advantage of the negatively charged phosphodiester aptamer backbone that rearranges at the surface of highly sensitive electronic platforms.

Recently, Nakatsuka et al. reported on sensing small-molecule neurotransmitters such as dopamine and serotonin in complex environments using aptamer-based field-effect transistor biosensors.[524] Field-effect transistors are highly sensitive and label-free electronic platforms where receptors are functionalized to semiconducting channels and, upon target capture, gate the underlying channel transconductance due to changes in the electric field at the surface (Figure 26d).[525] Conventionally, the use of biomolecular receptor-coupled field-effect transistors for small-molecule detection has been hindered due to the "Debye-length limitation" in high ionic strength physiological conditions. High ion concentrations effectively screen semiconductor surfaces and reduce the Debye length to <1 nm, which prevents target-associated changes in local electric fields from being detected.

However, by harnessing the conformational rearrangement of negatively charged aptamer−oligonucleotide backbones upon target capture, ion redistribution occurs in compact regions close to transistor surfaces.[524,526] This mechanism has double benefits: it enables sensitive detection of small molecules even in Debye-limited systems, and this unique short-range sensitivity of aptamer conformational change-based detection also largely reduces sensor susceptibility to NSB, because NSB typically takes place on top of the receptor layer outside the zone of sensitivity.

Mechanistic studies of aptamer-functionalized-field-effect transistor systems suggested that aptamer backbone rearrangement is key for target detection.[524,527] In addition to sensing

https://doi.org/10.1021/acs.chemrev.1c00044
Chem. Rev. 2021, 121, 8095−8160

small-molecule neurotransmitters that have a single positive charge at physiological pH, the specific and selective detection of electroneutral targets such as glucose (neutral) and sphingosine-1-phosphate, a zwitterionic signaling lipid, further implicated target-induced rearrangement of aptamer backbone charge. Aptamer conformational change being a key contributor to electronic charge rearrangement at the surface of semiconductors suggests that any target of interest, regardless of size or charge, can potentially be detected.

Furthermore, the advantage of this system is the ability to limit NSB by designing the aptamers to have high selectivity in the solution-phase selection procedure.[437,528] Counter-selection, whereby nonspecific targets present in high concentrations in the biological system in which sensing will be conducted are exposed to aptamer candidates, significantly improves the selectivity of isolated aptamers.[529] Self-referencing is also possible by designing "scrambled" DNA sequences that retain the same number of each nucleotide base as the specific aptamer that binds to targets of interest, but by altering the order, the recognition property of the oligonucleotide is significantly hindered.[530] Multiplexing substrates with specific aptamers and scrambled DNA sequences will enable differentiation and quantification of NSB from the SB.

Another new possibility with such conformation-changing aptamers is to include them into nanometer-sized artificial pores as "gate-keepers" of ionic flux. Here, the charge rearrangement induced by the conformational change results in a measurable change in the pore's electrical conductance, but the typically large NSB molecules are excluded from the sensitive region, enabling quantification of small-molecule targets with high specificity and selectivity in complex media.[531,532]

6.4.3. Stochastic Sensors. Stochastic sensing is an analytical technique that relies on single-molecule detection.[533] It is a label-free approach that does not require receptors to be immobilized on a surface and commonly involves a nanoscale recognition element that interacts with the environment. This recognition element is often an artificial solid-state nanopore[534] or a biomolecular protein pore such as alpha hemolysin (aHL)[535] (Figure 27a). This nanopore is used to connect two membrane-separated solution volumes, and an ionic current is applied through this pore at a fixed applied potential. Stochastic sensors use such nanopores to detect the modulation of ionic current when a target analyte passes through the pore. The term "stochastic sensing" stems from the fact that the occurrence of binding events and their duration follow a Poissonian distribution, which is inherently linked to their kinetic properties.[536−538]

This sensing principle was first proposed in the mid-1990s.[540] Since then, nanopores have been used to sequence DNA,[541] to study covalent and noncovalent interactions,[542] to investigate biomolecular folding and unfolding,[543,544] and in various other applications.[545] Molecules of interest are characterized with four key readout variables—event residence time, event frequency, event amplitudes, and event area.[538,546] The residence time, which represents how long a particular pore is blocked by biomolecules, correlates with the off-rate (k_{off}) of the interaction, and it can therefore be used to differentiate between specific and reversible NSB.[547] Therefore, stochastic sensing only works if the k_{off} values of specific and nonspecific interactions are sufficiently different. As discussed in section 5, typical k_{off} values of natural antibodies are on the order of 10^{-6} – 10^{-5} s^{-1},[435] and typical on-rates (k_{on}) are on the order of 10^6 – 10^7 M^{-1} s^{-1};[75] hence, the affinity change ($K_d = k_{off}/k_{on}$) is highly dependent on the molecule's off-rate.

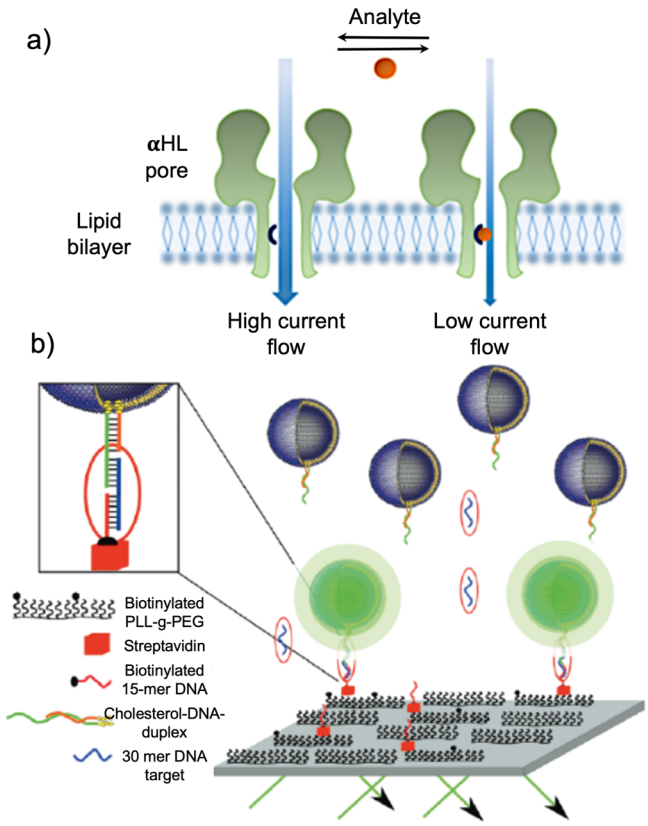

Figure 27. Stochastic sensors: (a) ion-channels, such as alpha hemolysin, can be used to record translocation of single molecules, which manifest as peaks in the corresponding ionic current measurement. The shape of the peak provides information about the type of molecule, which can be used to distinguish specific molecules. (b) Fluorescent vesicles or gold particles can be used as reporters to detect the binding of individual molecules. The statistics of binding features, such as residence time, provide information about the specificity of the interaction (Figure reproduced with permission from ref 539. Copyright 2007 American Chemical Society).

To differentiate between two distinct molecules, stochastic sensors need to be able to monitor single binding events and to acquire the necessary statistics. The fundamental sensing principle to differentiate specific and nonspecific interactions is based on the difference in the analytes' dissociation constants, which is reflected by the modulation of current through the sensing pore. Thus, low reversible NSB with low affinity does not stay in the pore for long, so it can be distinguished from the signal of specific interactions. However, if there is a high concentration of irreversible NSB in the medium, stochastic sensors will have difficulties extracting information from the readout signal. Thus, stochastic sensing typically requires a system with a low concentration of nonspecific binders. In addition, irreversible NSB manifests as clogging of the pore, a phenomenon that often causes problems when using nanopores in complex solutions.

Due to similarities in the detection mechanism, stochastic sensing is often compared with the multianalyte detection of the olfactory system.[548] The mammalian olfactory system uses a few hundred cross-reactive receptors that bind a different set of analytes. The receptors differ in their affinities for multiple analytes, and they are connected to "sensors", *i.e.* olfactory cells,

https://doi.org/10.1021/acs.chemrev.1c00044
Chem. Rev. 2021, 121, 8095−8160

that are sensitive to the binding of single analyte molecules. Millions of such cells for each receptor type perform parallel, continuous, single-molecule measurements, and the resulting expansive data enables mammals to identify millions of individual odors. In the context of stochastic sensing, we are not even close to this sophistication. At most, a few thousand pores can be recorded simultaneously,[549−551] and analytes are identified by their current signatures. Nevertheless, this idea of distinguishing signals from cross-reactive receptors could provide a powerful technology for analyte detection.

We mentioned that the sensing element of a stochastic sensor can either be a solid-state nanopore or a protein pore. Here, we will address the most common protein pores used in stochastic sensing—aHL. The aHL consists of a 14-stranded transmembrane beta-barrel and a bigger cap region that is positioned outside of the membrane.[548,552] These pores can detect a variety of analytes,[553] depending on the binding site that is placed within the lumen of the aHL pore. The reason why aHL is a popular nanopore is because it has a robust structure, which implies low background current fluctuations that facilitate the detection of analyte-induced blockades.[535] Furthermore, specificity can be engineered into the aHL pore since the channel walls of the protein can be designed for optimal binding by genetic and chemical means.[554] For example, the insertion of histidines by amino acid replacement or substitution allows aHL to detect metal ions,[533] while single-stranded DNA and proteins can be detected after immobilization of the corresponding bioreceptors on engineered nanochannels, including also genetically encoded sensor elements.[555]

Large proteins cannot be immobilized within the nanopore, so protein detection with stochastic sensors requires a system that is capable of detecting binding events outside of the pore. De la Escosura-Muñiz et al.[556] published a detailed review on strategies to make such modifications, such as using polymers bound within the pore but with a free ligand able to recognize proteins outside the pore[557] or using aptamers as bioreceptors.[552]

Stochastic sensors can be highly sensitive and reversible and provide real-time monitoring of analytes. Further, these sensors can quantify several analytes on a single sensing element simultaneously, except when the analytes are of low affinity and in the presence of cross reactive interference, which makes the readout pattern more complex. Moreover, high quantities of data need to be acquired to differentiate specific and nonspecific events. If the analyte is present in low concentrations, the time needed for the receptor in the pore to pick up a signal is long due to diffusion limitation. However, by combining the electrical sensing modality of nanopores with fluorescence-based optical read-outs, target detection with improved sensitivity and selectivity in human serum and urine has been achieved, demonstrating the potential of stochastic sensors for detection in complex environments.[558]

Despite the aforementioned drawbacks, stochastic sensors are already on the market with several applications. Companies such as Oxford Nanopore Technologies offer commercially available stochastic sensing elements. This low-cost device is by far the most portable DNA sequencer available and is capable of producing real-time data.[551,559] Life Technologies Corp uses single pore-based fluorescent labeling technology for DNA sequencing. Although the majority of nanopore sensing is performed with pores of natural origin, still several examples exist that demonstrate the practicality of solid-state nanopores. Recently for example, Rozesky et al. demonstrated fast and sensitive quantification of the SARS-CoV-2 RNA in a background of other human nucleotides using such nanopores.[560] Similarly, we were able to implement a scanning nanopore to analyze the content of live cells.[561]

Not all stochastic sensing is conducted on the same size scale as nanopores. For example, Höök and colleagues use fluorescent liposomes to detect DNA at a single-molecule level (Figure 27b).[562,563] Total internal reflection excitation is used where the evanescent wave penetrates only a few hundred nanometers into the liquid phase and efficiently removes background noise from out-of-focus fluorescent molecules. By tracking the fluorescent signal, each biomolecule binding event can be monitored.

Another popular stochastic sensor methodology is Digital ELISA that uses capture antibody-coated magnetic microspheres to harvest the analyte molecules from a sample.[370] A high number of beads compared to the number of target molecules is used to ensure that each bead binds zero or one analyte molecule (Poisson statistics) and to ensure that every analyte molecule encounters a bead within just a few minutes. Thereby, the problem of long binding times of analyte molecules from dilute solutions to a capture surface is avoided and the binding efficiency is drastically increased.

After washing, the beads are incubated with a biotinylated detection antibody and subsequently with enzyme-labeled streptavidin. Finally, the beads are loaded into microwells where the size of the wells ensures that just a single microsphere ends up in each well prior to being sealed with substrate molecules. The enzyme transforms substrates into fluorescence products, thus generating high local concentrations (since the product cannot diffuse away because the wells are sealed) that can easily be detected.[389] Counting the ratio of fluorescent wells to unlabeled wells then provides the concentration of analyte in the original sample.

Backgrounds in digital ELISA arise from NSB of detection antibody and enzyme conjugates to the capture bead surface. However, due to the high label sensitivity, much lower concentrations of labeling reagents are required to detect binding events as compared with conventional assays. In summary, by isolating and detecting single immuno-complexes in arrays of femtoliter-volume wells, digital ELISA enables clinically important proteins in serum to be measured at subfemtomolar concentrations.[564]

In this section, we have summarized the existing practical approaches to deal with the NSB problem in biosensors. After explaining why, at present, NSB is a critical bottleneck in limiting the LOD of diagnostically relevant biosensors, we systematically presented methods to address this issue. First, we showed how extensive rinsing can be used to discriminate SB from NSB (*i.e.*, discrimination by time), then we showed methods that discriminate the differences in affinity by measuring the forces between the binding partners. Next, we outlined a new theory about how referencing can be considered as a spatial lock-in amplifier. Finally, we presented existing biosensors that can inherently cope with the NSB problem. While the concepts discussed here are all related to *in vitro* methods, in the next section we will discuss how to address NSB *in vivo*.

7. ADDRESSING NONSPECIFIC BINDING *IN VIVO*

As discussed in previous sections, typical biological environments are crowded with macromolecules, where NSB not only is inevitable but also plays a major role in defining various interactions in the human body. In this section, the consequences of NSB for two main applications are discussed:

https://doi.org/10.1021/acs.chemrev.1c00044
Chem. Rev. 2021, 121, 8095−8160

drug delivery and implanted devices, where understanding and tailoring NSB are critical for the intended function. While excellent recent reviews exist both on drug delivery[565−567] and on biomaterials,[568,569] here we will only focus on the role of NSB in defining the fate of these materials *in vivo*.

7.1. Drug Delivery Using Nanocarriers

In the past decades, the development of nanomaterials for efficiently transporting and releasing drug molecules in diseased tissues has offered a wide range of applications in biotechnology and nanomedicine.[570] These nanoparticles deliver drugs to the target site in a controlled manner. Therefore, the drug dosage can be reduced, and the systemic side effects can be mitigated. For drug delivery systems to be applied in a clinical setting, several challenges need to be addressed such as cross-reactivity, large-scale manufacturing, biocompatibility, and overall cost-effectiveness.[162] In this section, the biological challenge of translating nanomedicine clinically will be discussed, with a specific focus on the implication of NSB in drug delivery platforms.

7.1.1. Nonspecific Binding Affects Bioavailability and Circulation of Drug-Loaded Nanoparticles. Many drug delivery platforms are based on the encapsulation of drugs in liposomes or polymeric micelles. Liposomes are considered the most promising nanoparticles in terms of applications,[571−573] and an excellent review on the history and current state of liposomal drug delivery systems is discussed by Allen and Cullis.[574] Regardless of the design of the drug delivery platforms, all drug-loaded particles are subjected to NSB. In principle, NSB affects drug delivery systems in two scenarios:

1. All drug molecules bind nonspecifically to serum proteins, reducing the ability of the drug to bind to the specific target of interest.
2. Proteins adsorb onto drug-loaded nanocarriers, thereby triggering the immune system to clear the particles from the bloodstream (opsonization).[575]

The first setting, where NSB compromises the bioavailability of the drug, is prominent—out of the 100 most prescribed drugs, 10% are found to exhibit plasma protein binding of more than 98%.[23] However, this NSB does not seem to have an effect on the success of these drug candidates.[23] The second scenario, where the immune system clears out the drug-loaded particles due to NSB, is particularly important because the particles need to have a longer circulation half-life to achieve their desired function.[576]

7.1.2. Protein Corona Formation on Nanoparticles from Nonspecific Binding. When a liposome or a nanoparticle is exposed to body fluids such as blood, lymph, or cerebrospinal fluids, proteins adsorb nonspecifically and form a "protein corona" around the nanoparticle. The protein corona has a thickness of 50−80 nm depending on the particle composition and the nature of the physiological environment.[573,577−579] The protein corona is composed of an inner shell of tightly bound proteins ("hard" corona) that is about 5−20 nm and an outer shell of more loosely bound proteins ("soft" corona).[578] Since proteins bind to the particle at various association and dissociation rates, the protein corona is a dynamic system instead of a stable "shell".[580−582] The architecture of the protein corona, especially the composition of the inner shell, is important because it determines the physiological response of the drug-loaded particle (*i.e.* how fast the drug carrier is recognized by the immune system). Monopoli et al. proposed that it is often this protein corona that interacts with biological systems, and therefore, the corona becomes an important element of the biological identity of the nanoparticle.[17]

It is often believed intuitively that the lower the amount of proteins adsorbed nonspecifically on the drug nanocarrier, the longer the circulation time of the drug delivery particle.[575] However, it is not the total amount of proteins adsorbed that regulates the clearance rate of the drug carriers but, rather, the accessible immunological features determined by the balance of opsonins and dysopsonins.[573,579,582,583] For this reason, it is important to understand the composition and architecture of the protein corona, how it affects the clearance of the drug-loaded particles, and how the NSB can be altered to elicit the desired physiological response.[584] A few studies have examined the structure of the protein corona using transmission electron microscopy (TEM)[585] and stochastic optical reconstruction microscopy.[586] Recently, Zhang et al. provided a detailed analysis of the function and structure of the protein corona on nanomaterials, which offers the possibility to control the nanomaterial's interaction with the biological system.[587] In the following section, the effect of NSB on the clearance rate is discussed.

7.1.3. Nonspecific Binding Influences the Clearance Rate of Drug Delivery Nanocarriers. Identifying all proteins that attach to a nanoparticle and quantifying their amount is challenging. The tightly bound proteins in the inner shell could be stained by immunochemical means,[588] but there is no tool that is able to characterize the protein content of the outer shell. Since assessing the entire protein corona and mapping the binding sites is not feasible to date, it is useful to look at how drug particle characteristics influence clearance and how these nanocarriers are recognized both specifically and nonspecifically. The clearance rate of a liposome is influenced by its synthetic identity, namely its size, surface charge, lipid composition (hydrophobicity and fluidity), and in the case of stealth liposomes, the properties and density of the grafted polymers.[573,575,589,590]

Lipids can be recognized specifically by antiphospholipid and anticholesterol antibodies.[575] These antibodies mark liposomes directly via their Fc region (IgG) for macrophage uptake or launch the complement cascade via the classical pathway (IgM), which indirectly attracts macrophages (C3b, iC3b) or assembles the membrane attack complex (MAC).[575,589,591] Even against stealth liposomes, the body is able to raise PEG-IgM antibodies that upon second exposure of PEGylated liposomes, lead to an accelerated blood clearance effect.[592,593] Furthermore, macrophages may also specifically detect drug particles in a serum-independent manner through scavenger and toll-like receptors.[578]

Antibodies and other opsonins also adsorb nonspecifically to any drug carrier surface with a certain affinity.[589] Even the best "stealth" liposomes exhibit a protein corona,[594,595] and while these opsonins show a roughly 10-fold reduced potency in activating the immune system, opsonization of the particles still occurs.[575] As the structural arrangement of biomolecules upon adsorption is important, an opsonin might even act as a dysopsonin when its epitope is not exposed.[17,585,596] Caracciolo et al. have shown that enrichment with opsonins does not correlate with increased macrophage uptake and hypothesized that human serum albumin and apolipoproteins may create a barrier that impedes interaction with immune cells.[573]

Size, surface charge, and hydrophobicity/hydrophilicity influence protein binding in a nonspecific way. Larger liposomes

https://doi.org/10.1021/acs.chemrev.1c00044
Chem. Rev. 2021, 121, 8095−8160

are cleared more rapidly than smaller ones[597] because their larger surface enables adsorption of the highly active complement proteins that require a certain surface area to assemble.[591] It is also observed that negatively charged liposomes are cleared faster than neutral or positive ones, likely due to the reduced NSB of the most abundant protein, albumin, that has a slightly negative charge.[591,597,598]

Complement proteins were found to be activated by both positive or negatively charged biomolecules, whereas neutral liposomes were poor activators of the complement (for details, see the following reviews).[575,591] On the one hand, hydrophobic surfaces are high-energy surfaces that are immediately covered by large amounts of proteins accompanied by conformational changes. These conformational changes then trigger an immune response.[578] On the other hand, hydrophilic surfaces cause significantly less protein denaturation and hence opsonin association, which is most strikingly reflected in the success of hydrophilic PEGylated stealth liposomes with long-circulation times.[572,589] The underlying reasons for the aforementioned effects are still debated.

7.1.4. Necessity of Serum Exposition for Stealth Properties. An interesting comparison is whether exposure to blood components enhances the uptake of particles by macrophages compared to nonserum exposed particles. Depending on the particle characteristics, serum exposure has been shown to either reduce or increase the rate of clearance of particles by macrophages.[575,579] Notably, serum exposure enhanced the uptake of negatively charged and neutral liposomes by macrophages but inhibited uptake for positively charged liposomes.[591] It was also observed that neutral and positively charged liposomes acquire a net negative charge in plasma.[582] In this review, it was hypothesized that a high-molecular-weight protein (>200 kDa) bound to positively charged liposomes and acted as a dysopsonin. However, to date, this protein has not been identified.

The uptake of liposomes containing phosphatidylserine was also reported to be reduced by serum exposure.[583] Phosphatidylserine is a strong opsonin and the "eat-me" signal of apoptotic cells; hence, these liposomes should be readily phagocytosed. Johnstone et al. hypothesized that bound serum proteins could mediate a nonspecific surface-shielding property that reduces charge-mediated interactions. Furthermore, this work demonstrated that stealth liposomes covalently modified with PEG exhibit reduced uptake when exposed to serum.[583] This finding was investigated in detail by Schöttler et al., who showed that protein adsorption is necessary for the stealth effect of PEGylated and poly(ethyl ethylene phosphate) (PEEP)-ylated drug nanocarriers.[579]

Clusterin (Apolipoprotein J) was identified as the main player of the dysopsonic activity of serum. The chemical structure of the stealth polymer was shown to influence the amount and type of adsorbed plasma proteins and thus the biological fate of the nanocarrier.[579] Another study investigated how the protein corona profile changes as a function of PEG grafting density for gold nanoparticles.[599] Four clusters of proteins were identified: cluster A binds to low PEG density nanoparticles, B to low–intermediate, C to intermediate–high, and cluster D to high PEG densities.[599] Further evidence of the importance of the protein corona for the stealth effect comes from studies that showed a reduced hepatic disposition of PEG liposomes modified with rat serum albumin[600] or that low-molecular-weight PEGs can be mixed with albumin but not fibrinogen, suggesting an interaction between albumin and PEG.[575,601] All these findings as a whole suggest the emergence of a stealth effect from the protein corona formed in serum for various forms of nanoparticles.[573]

7.1.5. Novel Ways to Shape the Protein Corona and to Modulate Clearance. Stealth liposomes and PEGylated drug nanocarriers in particular have revolutionized medical treatment strategies.[574] Despite the advantages of these systems that facilitate *in vivo* drug delivery, there is still room for improvement such as shaping the protein corona via clever materials engineering, especially since PEG initiates complement activation.[572,602] Examples include zwitterionic lipid polymers that are more hydrated and more similar to the average protein surface (section 4) and show reduced complement activation compared to PEG.[572,603]

Alternative options include biodegradable polyamino acids, which were the only polymer class where the accelerated blood clearance effect was not observed.[602] Other studies endeavored to mimic proteins expressed natively *in vivo* by attaching self-peptides (hCD47) to polystyrene nanobeads[604] or applying a biomimetic protein coating based on erythrocyte[605] or leucocyte[606] membranes to inhibit phagocytosis actively. In addition to the motivation of increasing the circulation time of nanocarriers, an innovative concept is to shape and optimize the protein corona for active targeting of a certain tissue, which may transform the issue of protein adsorption into an opportunity.[573]

Nonspecific interactions of plasma proteins with drug carriers and nanoparticles give rise to a protein corona that determines the biological recognition and clearance of the carrier. As a matter of fact, NSB to a material that is deployed *in vivo* can never be fully suppressed and even stealth drug carriers appear to obtain much of their camouflage from an adsorbed protein layer. It is therefore of fundamental importance to establish ways to predict the composition and architecture of the protein corona for a given nanoparticle material and to shape this adsorbed layer to elicit the desired physiological response.

7.2. Implications of Nonspecific Binding for Implantable Biosensors

As seen in sections 5 and 6, protein adsorption to the sensing surface is critical in determining the performance of a biosensor. In this section, the role of protein adsorption in determining the fate of biomedical implants is discussed.

7.2.1. Race for the Surface—The Challenges of Implantable Biomaterials. Implantable biomaterials are often used to substitute or provide support for a particular biological function in a patient. Upon insertion of a biomaterial into a patient's body, a biological response in the form of molecular interactions is initiated immediately. Proteins interact with the surface of the biomaterial via high-affinity NSB, and there are two models that describe this phenomenon: the Vroman effect and the "race for the surface".

The Vroman effect was demonstrated by Leo Vroman and Ann Adams in the 1960s, when they found out that exposure to blood plasma triggers a complex series of adsorption and displacement processes.[342] The most abundant proteins will form the first layer and will be displaced subsequently by less abundant proteins that have a higher affinity to the surface.[333,607] Vroman and Adams called this replacement, or "turning over" of proteins that were adsorbed in the first place by late-arrivers, as the Vroman effect.[342,608,609] "The race for the surface" is a concept introduced by Anthony Gristina in the 1980s,[610] suggesting that both host tissue and bacterial adhesion compete

https://doi.org/10.1021/acs.chemrev.1c00044
Chem. Rev. 2021, 121, 8095−8160

for the implant surface. Depending on who wins this race, tissue integration or bacterial infection will occur.

As bacteria outflanking the host cells results in serious consequences for the patient, enabling the host tissue to win this race is the aim of implant designers. Microbial infection is a challenge not only limited to passive implants such as joint prosthesis or bone fixation devices, but also for the development of continuous *in vivo* biosensors. With proper surface engineering, the fate of the implant can be altered, hence why engineering biomaterial surface properties has long been the biggest challenge to achieve a successful, long-term *in vivo* sensor.[611]

A problem in engineering the surface of implants arises from the fact that eukaryotic and prokaryotic cells share many adhesive mechanisms. Ideally, inherent cellular properties facilitate host cell adhesion and avoid foreign responses, but they may also favor the recruitment of microorganisms to the surface. One such example is the recognition of the extracellular matrix protein fibronectin, which can be found in both prokaryotic and eukaryotic cells.[63,612] A host cell, *i.e.* a fibroblast, adsorbs to implant surfaces by an integrin receptor-binding motif, which can also be recognized by bacteria having the same fibronectin-binding proteins.[613] Therefore, surface modification strategies must reliably attract host cells while disadvantaging microbes from winning the "race" (Figure 28).[614,615]

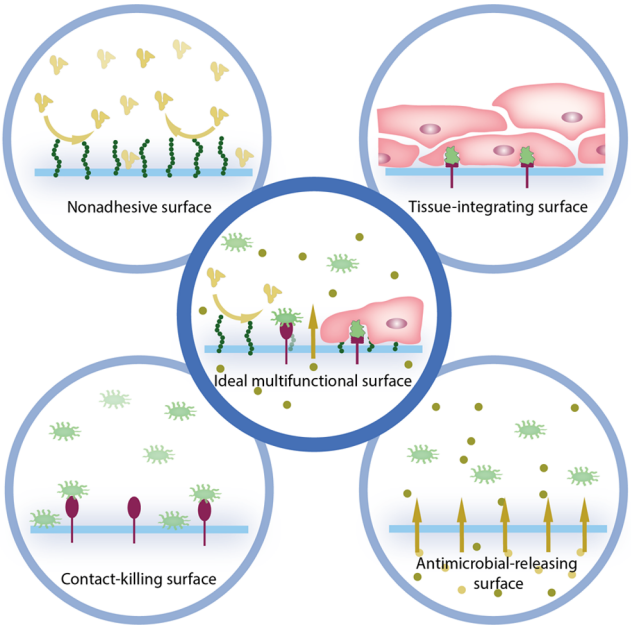

Figure 28. Surface engineering strategies for biomaterials.

There are several common single-step surface strategies including (1) nonadhesive surfaces,[616,617] (2) tissue-integrating surfaces,[618,619] (3) contact-killing surfaces,[620,621] and (4) antimicrobial-releasing surfaces[622] (Figure 28). These modifications are targeted either to eliminate NSB of proteins and the contact of microbes or to promote the attachment of target cells and thereby tissue integration of the biomaterial. However, none of these single modifications are sufficient to ensure a successful implant. The ideal surface modification would be a multifunctional coating. In contrast to single surface modifications, which do not offer sufficient relief to the problem of nonspecific interactions between the implant surface and proteins, a multifunctional coating combines established single-step surface modification strategies.

However, multifunctional coatings are still in their preliminary stage of development, as it is only recently that it has been recognized that single-step surface modification strategies are insufficient.[623] Thus, the effort to harness different surface modification strategies to "unbalance" or "shape" the race between the host cells and microbes is still one of the unsolved challenges in biomaterials research.[624] In the following section, we will focus on some of the challenges that are encountered after implantation.

7.2.2. Foreign Body Response to *In Vivo* Biosensors. Implantable biosensors, or *in vivo* biosensors, are able to provide continuous information on the levels of a target analyte without any need for intervention from either the patient or clinician. Therefore, implantable biosensors are promising devices for monitoring diverse diseases.[625] The standard working mechanism of *in vivo* biosensors involves the diffusion of the analyte through a blood capillary and the surrounding tissue and eventually to the sensor surface where the detection element is located.[623] Throughout its journey, the analyte must neither be consumed nor be blocked by nearby cells or tissues.

Unfortunately, *in vivo* biosensors typically lose functionality over time, mainly due to an effect called the foreign body response (FBR), caused by nonspecific protein adsorption and subsequent cell-attachment that occurs locally around the biosensor.[625] One of the main research efforts of modern implant design is to make use of the body's immune response to improve implanted sensor integration, while simultaneously avoiding chronic inflammation and FBR, which inhibit the intended function of the sensor (Figure 29).[19]

Controlling these immune responses requires an in-depth understanding of the immunological processes that take place at the interface between the implanted biomaterial and the host tissue. Franz et al. provided a detailed description of how the host's immune system responds to implants.[20] The degree of the

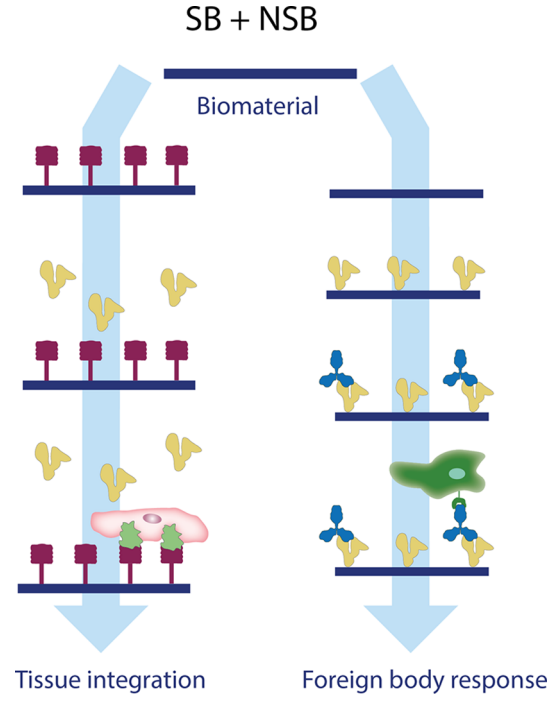

Figure 29. Importance of specific binding (SB) for tissue integration and the issues arising from nonspecific binding (NSB) that causes immune responses.

https://doi.org/10.1021/acs.chemrev.1c00044
Chem. Rev. 2021, 121, 8095−8160

FBR depends on the surface properties of the device; and the extent of nonspecific protein absorption can be used to evaluate the degree of biocompatibility of the implanted biosensor.[626]

7.2.3. The First Implantable Glucose Biosensor. With more than 420 million diabetic patients worldwide, the glucose sensor is one of the most widely used biosensors. Clark and Lyons first proposed the concept of enzyme-based electrodes for glucose detection in 1962,[627] and ever since, this platform has stimulated ongoing development of the glucose sensor.[628] However, despite billions of investments and significant progress, reliable, long-term implantable glucose sensors are still forthcoming.[628−630] The lack of implantable glucose sensors necessitates diabetic patients to prick their fingers to measure their glucose level in blood in a discrete manner, which leads to missing potential critical events such as hyperglycemia. Therefore, a solution to continuously measure glucose in a feedback loop (comparable to the artificial pancreas system) is indispensable.[631,632] However, solid devices have to be replaced regularly,[633] and the current best solutions based on hydrogel coatings also fail after a few months *in vivo*.[634−636]

The first implantable long-term glucose sensor available on the market carries the trade name Eversense (Senseonics, Maryland, USA).[637] This system extends the possible average continuous glucose monitor wear time from 7−14 days to up to 180 days. In contrast with the traditional glucose sensors that rely on electrochemical enzyme-based sensors, Eversense is based on a fluorophore-linked glucose-sensitive hydrogel. The fluorescent signal is both excited and recorded at the site of the implant, and the glucose concentration is conveyed by a wireless signal.[638] To increase the sensor's *in vivo* stability and functional lifetime, a layer of platinum is deposited onto the sensor to prevent signal loss due to *in vivo* oxidation that is generally caused by the FBR. For a biocompatible sensor−tissue interface, the hydrogel is covered by a glucose-permeable membrane.[638]

The introduction of the first implantable glucose sensor has brought excitement to the biosensing field. Nevertheless, due to the nonspecific protein adsorption onto the sensor surface, the *in vivo* lifespan of the implantable glucose sensor is limited. Permanent implanted biosensors for continuous monitoring can only become a reality when it is possible to exert precise control of protein adsorption to shape the physiological response of the human body.

8. CONCLUSIONS

The main purpose of this review article was to systematically explain why NSB is an inevitable phenomenon that always takes place in complex biological environments. We began by looking at how Nature harnesses NSB and also listed important biomedical application fields, which are based on such nonspecific interactions (Figure 1). We then provided a brief historical overview on how the concept of NSB evolved in the scientific literature and outlined the difficulties in clearly distinguishing SB and NSB. We also provided a detailed classification scheme that enables researchers to separate these interactions and provided a summary table based on structural and thermodynamic features (Table 1). We also provided the following practical definitions:

- *Specific binding* is when molecules interact with each other via a defined end state with stereospecificity and shape complementarity. The final state should be thought of as a confined set in conformational space rather than a single state.
- *Nonspecific binding*, on the other hand, is when two molecules have an ill-defined binding interface where they can interact in multiple ways without stereospecificity and shape complementarity.

In section 2, we presented the underlying thermodynamic considerations using an energy landscape approach. We revisited important concepts such as affinity, avidity, and attinebility as well as monovalency and polyvalency that all influence the strength of interactions. Here, we also provided characteristic qualitative energy landscape examples corresponding to reversible and irreversible NSB and to permanent and transient SB (Figure 5). Finally, we outlined the differences between SB vs NSB in terms of entropy and enthalpy contributions.

An alternative perspective was presented in section 3, where we reviewed how intermolecular forces and the biomolecular recognition process contribute to binding specificity/nonspecificity. We pointed out that the biomolecular recognition always starts with a reversible nonspecific interaction complex, where an inhomogeneous surface potential, molecular crowding, and solvent effects dominate the forces. While this nonspecific interaction complex is a requirement for fast specific binding, it is also the source of omnipresent low-affinity NSB (Figure 6). Here, we also reviewed the important role of water in defining both the precursor state and also the strength of the final docked state, as well as the intermolecular forces that mediate specificity in the docked configuration.

After covering the intermolecular forces that define the strength and specificity of molecular interactions, we reviewed the structural features of binding sites to provide another viewing angle on NSB (section 4). We discussed which molecular features of the architecture of the interaction site contribute to the affinity and what is required for specificity. The most important features, *i.e.* the buried surface area, the hot spots, the role of water, and the negative design principles, were specifically explained. In this section, we dedicated special attention to the specificity of antibody−antigen interactions and to the NSB properties of evolutionary optimized proteins, because these are highly important for biosensing applications. Finally, we presented a synopsis of features that enable distinguishing specific and nonspecific interactions based on thermodynamics, intermolecular forces, and the architecture of the interaction sites in Table 2.

While the first four sections introduced NSB from diverse angles, section 5 presented why NSB is currently a bottleneck in diagnostically relevant biosensing. By introducing a typical diagnostic assay, we explained at which step NSB is critical. We outlined how NSB at zero analyte concentration contributes to the LOD calculation and provided a list of typical mistakes that are committed by sensor developers in the scientific literature. Furthermore, we gave a detailed recipe to correctly assess the LOD of novel biosensors to aid the work of scientists, reviewers, and editors. We also reviewed the existing models that allow estimations of SB and NSB in a biosensing experiment. Further, we presented extensions of these basic models that are especially important when working with real samples. Finally, we also showed how such models can be used to optimize sensing performance, thereby shortening development time and reducing the chance of engaging in "dead-end" research activities.

Section 6 was dedicated to approaches that help to reduce NSB. The use of blocking agents, proper surface engineering, and sample pretreatment were summarized, because these are

https://doi.org/10.1021/acs.chemrev.1c00044
Chem. Rev. 2021, 121, 8095−8160

typical ways of dealing with NSB in heterogeneous assays that comprise most existing biosensor methodologies. A section was dedicated to the choice of molecular recognition elements, which is also critical as specific receptors have different tendencies toward inducing NSB when working with real samples. Then, we explained how SB can be separated from NSB by three techniques: first, by rinsing, which is based on differences in kinetic "off" rates; second, by force, which is based on differences in binding affinities; third, by space, using differently functionalized reference areas on a sensor surface.

In this section, we also presented the few promising methodologies that have the chance to overcome NSB limitations. Diffractometric techniques are ideally suited to take advantage of the spatial lock-in amplifier concept that allows reduction of NSB-induced noise that occurs at low spatial frequencies, by performing the measurement at a well-defined (high) spatial frequency using optical diffraction. Molecular switch sensors are designed such that only NSB to the sensing molecule itself disturbs the measurement, and often NSB to the receptor itself can also be minimized. Stochastic sensing approaches are also promising to separate SB and NSB because they provide additional information about the nature of the binding due to the single molecule sensitivity of these methods.

The last section presented the implications of NSB *in vivo*, because anything that is introduced into the human body will be subject to the NSB of proteins and other macromolecules. Here, we recited the most important consequences of NSB in drug delivery, where opsonization, *i.e.* the formation of a protein corona around nanocarriers, determines the fate of the particles. We also presented how NSB is critical for implantable biosensors finishing with the promising example of long-term glucose monitoring devices.

Nonspecific binding is a complex phenomenon that is omnipresent in Nature which, if properly understood, can be dealt with using Nature's tricks and our human intellect. This review about NSB fills a gap in the literature by systematically collecting existing knowledge about NSB and synthesizing important messages about its proper definition. The consequences of NSB in various applications were highlighted with special focus on diagnostically relevant biosensing.

AUTHOR INFORMATION

Corresponding Authors

János Vörös − *Laboratory of Biosensors and Bioelectronics, Institute for Biomedical Engineering, ETH Zürich, Zürich CH-8092, Switzerland;* orcid.org/0000-0001-6054-6230; Email: janos.voros@biomed.ee.ethz.ch

Nako Nakatsuka − *Laboratory of Biosensors and Bioelectronics, Institute for Biomedical Engineering, ETH Zürich, Zürich CH-8092, Switzerland;* orcid.org/0000-0001-8248-5248; Email: nakatsuka@biomed.ee.ethz.ch

Authors

Andreas Frutiger − *Laboratory of Biosensors and Bioelectronics, Institute for Biomedical Engineering, ETH Zürich, Zürich CH-8092, Switzerland*

Alexander Tanno − *Laboratory of Biosensors and Bioelectronics, Institute for Biomedical Engineering, ETH Zürich, Zürich CH-8092, Switzerland*

Stephanie Hwu − *Laboratory of Biosensors and Bioelectronics, Institute for Biomedical Engineering, ETH Zürich, Zürich CH-8092, Switzerland*

Raphael F. Tiefenauer − *Laboratory of Biosensors and Bioelectronics, Institute for Biomedical Engineering, ETH Zürich, Zürich CH-8092, Switzerland*

Complete contact information is available at: https://pubs.acs.org/10.1021/acs.chemrev.1c00044

Author Contributions

A.F., A.T., and S.H. contributed equally to this work.

Notes

The authors declare no competing financial interest.

Biographies

Andreas Frutiger has a Ph.D. in Biosensing from ETH Zürich. During the past 6 years he extensively investigated a novel label-free biosensing technology—focal molography. Since August 2020, he has been founder and head of R&D of lino Biotech AG, a Roche/ETH Zürich spinoff that commercializes focal molography. He is interested in the areas of biosensing and optics and loves to engage in interdisciplinary projects where biology, chemistry, and physics meet.

Alexander Tanno completed his M.Sc. degree in Biomedical Engineering at ETH Zürich in the field of polyelectrolyte multilayers. He dedicated his Ph.D. studies in Prof. Vörös' lab at ETH Zürich to investigating electrochemical readout technologies for point-of-need biosensing. He extensively studied mathematical modeling of specific and nonspecific interactions including the novel approach for considering double competition in biosensing. Alex is now tackling the entrepreneurial goal of bringing home-based biosensing to patients in need.

Stephanie Hwu received her M.Sc. in Applied Physics from the University of Geneva, where she developed novel experimental schemes to access and control molecular dynamics and studied the detection of multiple harmonic generation from nanoparticles. She then joined the Laboratory of Biosensors and Bioelectronics at ETH Zurich (Department for Information Technology and Electrical Engineering) and earned her Ph.D. in Biomedical Engineering in 2019. Her research focused on the design and development of nanoparticle-based biosensors for early disease diagnostics.

Raphael F. Tiefenauer received his M.Sc. in Nanosciences from the University of Basel focusing on developing neurological probes for brain−machine interfaces. He then joined the Laboratory of Biosensors and Bioelectronics at ETH Zurich and earned his Ph.D. in Biomedical Engineering in 2018. His research focused on the design and development of novel biosensing techniques with plasmonic nanostructures.

János Vörös has a Ph.D. in Biophysics from the Eötvös Loránd University in Budapest. In 1998 he came to ETH Zurich, where he is now a Professor in the Institute for Biomedical Engineering of the University and ETH Zurich (Department for Information Technology and Electrical Engineering) heading the Laboratory for Biosensors and Bioelectronics since 2006. He is interested in research in the areas of biosensors, bioelectronics, and bottom-up neuroscience.

Nako Nakatsuka received her Ph.D. in Chemistry from the University of California, Los Angeles. Her dissertation focused on integrating conformationally changing DNA aptamers on electronic biosensors for small-molecule biosensing in complex environments. She is currently a senior scientist at the Laboratory of Biosensors and Bioelectronics in the Department for Information Technology and Electrical Engineering at the ETH Zurich. Her research focuses on chemical biosensing in clinically relevant matrices by understanding the fundamental mechanisms of aptamer−target interactions.

https://doi.org/10.1021/acs.chemrev.1c00044
Chem. Rev. 2021, 121, 8095−8160

ACKNOWLEDGMENTS

This project received funding from the European Union's Horizon 2020 research and innovation programme under grant agreement number GrapheneCore3 881603 (N.N.) and was supported by the ETH Zurich. We also acknowledge Christof Fattinger for helpful discussions.

REFERENCES

(1) Wilhelm, M.; et al. Mass-spectrometry-based draft of the human proteome. *Nature* **2014**, *509*, 582−587.
(2) Schreiber, G.; Keating, A. E. Protein binding specificity versus promiscuity. *Curr. Opin. Struct. Biol.* **2011**, *21*, 50−61.
(3) Ellis, R. J. Macromolecular crowding: obvious but underappreciated. *Trends Biochem. Sci.* **2001**, *26*, 597−604.
(4) Nooren, I. M. A.; Thornton, J. M. Diversity of protein-protein interactions. *EMBO J.* **2003**, *22*, 3486−3492.
(5) Stein, A.; Pache, R. A.; Bernadó, P.; Pons, M.; Aloy, P. Dynamic interactions of proteins in complex networks: a more structured view. *FEBS J.* **2009**, *276*, 5390−5405.
(6) Johnson, M. E.; Hummer, G. Nonspecific binding limits the number of proteins in a cell and shapes their interaction networks. *Proc. Natl. Acad. Sci. U. S. A.* **2011**, *108*, 603−608.
(7) Levy, E. D.; De, S.; Teichmann, S. A. Cellular crowding imposes global constraints on the chemistry and evolution of proteomes. *Proc. Natl. Acad. Sci. U. S. A.* **2012**, *109*, 20461−20466.
(8) Yang, J.-R.; Liao, B.-Y.; Zhuang, S.-M.; Zhang, J. Protein misinteraction avoidance causes highly expressed proteins to evolve slowly. *Proc. Natl. Acad. Sci. U. S. A.* **2012**, *109*, E831−40.
(9) Sarić, A.; Chebaro, Y. C.; Knowles, T. P. J.; Frenkel, D. Crucial role of nonspecific interactions in amyloid nucleation. *Proc. Natl. Acad. Sci. U. S. A.* **2014**, *111*, 17869−17874.
(10) Bolognesi, B.; Kumita, J. R.; Barros, T. P.; Esbjorner, E. K.; Luheshi, L. M.; Crowther, D. C.; Wilson, M. R.; Dobson, C. M.; Favrin, G.; Yerbury, J. J. ANS binding reveals common features of cytotoxic amyloid species. *ACS Chem. Biol.* **2010**, *5*, 735−740.
(11) Ellis, R. J.; Minton, A. P. Protein aggregation in crowded environments. *Biol. Chem.* **2006**, *387*, 485−497.
(12) Finn, T. E.; Nunez, A. C.; Sunde, M.; Easterbrook-Smith, S. B. Serum albumin prevents protein aggregation and amyloid formation and retains chaperone-like activity in the presence of physiological ligands. *J. Biol. Chem.* **2012**, *287*, 21530−21540.
(13) Hartl, F. U.; Bracher, A.; Hayer-Hartl, M. Molecular chaperones in protein folding and proteostasis. *Nature* **2011**, *475*, 324−332.
(14) White, A. D.; Huang, W.; Jiang, S. Role of nonspecific interactions in molecular chaperones through model-based bioinformatics. *Biophys. J.* **2012**, *103*, 2484−2491.
(15) Carta, G.; Jungbauer, A. *Protein Chromatography: Process Development and Scale-Up*; John Wiley & Sons, 2010.
(16) Charcosset, C. Review: Purification of proteins by membrane chromatography. *J. Chem. Technol. Biotechnol.* **1998**, *71*, 95−110.
(17) Monopoli, M. P.; Åberg, C.; Salvati, A.; Dawson, K. A. Biomolecular coronas provide the biological identity of nanosized materials. *Nat. Nanotechnol.* **2012**, *7*, 779−786.
(18) Ge, C.; Du, J.; Zhao, L.; Wang, L.; Liu, Y.; Li, D.; Yang, Y.; Zhou, R.; Zhao, Y.; Chai, Z.; Chen, C. Binding of blood proteins to carbon nanotubes reduces cytotoxicity. *Proc. Natl. Acad. Sci. U. S. A.* **2011**, *108*, 16968−16973.
(19) Williams, D. F. On the mechanisms of biocompatibility. *Biomaterials* **2008**, *29*, 2941−2953.
(20) Franz, S.; Rammelt, S.; Scharnweber, D.; Simon, J. C. Immune responses to implants − A review of the implications for the design of immunomodulatory biomaterials. *Biomaterials* **2011**, *32*, 6692−6709.
(21) Bahadur, R. P.; Chakrabarti, P.; Rodier, F.; Janin, J. A dissection of specific and non-specific protein-protein interfaces. *J. Mol. Biol.* **2004**, *336*, 943−955.
(22) Wolfe, M. M.; Lichtenstein, D. R.; Singh, G. Gastrointestinal toxicity of nonsteroidal antiinflammatory drugs. *N. Engl. J. Med.* **1999**, *340*, 1888−1899.
(23) Smith, D. A.; Di, L.; Kerns, E. H. The effect of plasma protein binding on in vivo efficacy: misconceptions in drug discovery. *Nat. Rev. Drug Discovery* **2010**, *9*, 929−939.
(24) Anderson, J. M. Biological Responses to Materials. *Annu. Rev. Mater. Res.* **2001**, *31*, 81−110.
(25) Sotiri, I.; Robichaud, M.; Lee, D.; Braune, S.; Gorbet, M.; Ratner, B. D.; Brash, J. L.; Latour, R. A.; Reviakine, I. BloodSurf 2017: News from the blood-biomaterial frontier. *Acta Biomater.* **2019**, *87*, 55−60.
(26) Wang, W.; Woodbury, N. W. Unstructured interactions between peptides and proteins: exploring the role of sequence motifs in affinity and specificity. *Acta Biomater.* **2015**, *11*, 88−95.
(27) Ball, V.; Maechling, C. Isothermal microcalorimetry to investigate non specific interactions in biophysical chemistry. *Int. J. Mol. Sci.* **2009**, *10*, 3283−3315.
(28) Kastritis, P. L.; Bonvin, A. M. J. J. On the binding affinity of macromolecular interactions: daring to ask why proteins interact. *J. R. Soc., Interface* **2013**, *10*, 20120835.
(29) Albano, J. D.; Ekins, R. P.; Maritz, G.; Turner, R. C. A sensitive, precise radioimmunoassay of serum insulin relying on charcoal separation of bound and free hormone moieties. *Eur. J. Endocrinol.* **1972**, *70*, 487−509.
(30) Scatchard, G. The attractions of proteins for small molecules and ions. *Ann. N. Y. Acad. Sci.* **1949**, *51*, 660−672.
(31) Feldman, H. A. Mathematical theory of complex ligand-binding systems of equilibrium: some methods for parameter fitting. *Anal. Biochem.* **1972**, *48*, 317−338.
(32) Chamness, G. C.; McGuire, W. L. Scatchard plots: common errors in correction and interpretation. *Steroids* **1975**, *26*, 538−542.
(33) Yalow, R. S.; Berson, S. A. Assay of plasma insulin in human subjects by immunological methods. *Nature* **1959**, *184* (Suppl 21), 1648−1649.
(34) Mendel, C. M.; Mendel, D. B. Non-specific' binding. The problem, and a solution. *Biochem. J.* **1985**, *228*, 269−272.
(35) van Zoelen, E. J. Receptor-ligand interaction: a new method for determining binding parameters without a priori assumptions on non-specific binding. *Biochem. J.* **1989**, *262*, 549−556.
(36) Klotz, I. M. Ligand-receptor interactions: what we can and cannot learn from binding measurements. *Trends Pharmacol. Sci.* **1983**, *4*, 253−255.
(37) Klotz, I. M. Numbers of receptor sites from Scatchard graphs: facts and fantasies. *Science* **1982**, *217*, 1247−1249.
(38) Jackson, T. M.; Ekins, R. P. Theoretical limitations on immunoassay sensitivity. Current practice and potential advantages of fluorescent Eu3+ chelates as non-radioisotopic tracers. *J. Immunol. Methods* **1986**, *87*, 13−20.
(39) Ekins, R. P. Multi-analyte immunoassay. *J. Pharm. Biomed. Anal.* **1989**, *7*, 155−168.
(40) Ekins, R. P.; Chu, F. W. Multianalyte microspot immunoassay - microanalytical "compact disk" of the future. *Clin. Chem.* **1991**, *37*, 1955−1967.
(41) Gedig, E. T. *Handbook of Surface Plasmon Resonance*; 2017; pp 171−254.
(42) Blaszykowski, C.; Sheikh, S.; Thompson, M. A survey of state-of-the-art surface chemistries to minimize fouling from human and animal biofluids. *Biomater. Sci.* **2015**, *3*, 1335−1370.
(43) Love, J. C.; Estroff, L. A.; Kriebel, J. K.; Nuzzo, R. G.; Whitesides, G. M. Self-assembled monolayers of thiolates on metals as a form of nanotechnology. *Chem. Rev.* **2005**, *105*, 1103−1169.
(44) Van Oss, C. J. Aspecific and specific intermolecular interactions in aqueous media. *J. Mol. Recognit.* **1990**, *3*, 128−136.
(45) Van Oss, C. J. Hydrophobic, hydrophilic and other interactions in epitope-paratope binding. *Mol. Immunol.* **1995**, *32*, 199−211.
(46) Clackson, T.; Wells, J. A. A hot spot of binding energy in a hormone-receptor interface. *Science* **1995**, *267*, 383−386.
(47) Janin, J.; Bahadur, R. P.; Chakrabarti, P. Protein-protein interaction and quaternary structure. *Q. Rev. Biophys.* **2008**, *41*, 133−180.
(48) Jones, S.; Thornton, J. M. Analysis of protein-protein interaction sites using surface patches. *J. Mol. Biol.* **1997**, *272*, 121−132.

https://doi.org/10.1021/acs.chemrev.1c00044
Chem. Rev. 2021, 121, 8095−8160

(49) Keskin, O.; Gursoy, A.; Ma, B.; Nussinov, R. Principles of protein-protein interactions: what are the preferred ways for proteins to interact? *Chem. Rev.* **2008**, *108*, 1225−1244.
(50) Rodier, F.; Bahadur, R. P.; Chakrabarti, P.; Janin, J. Hydration of protein-protein interfaces. *Proteins: Struct., Funct., Genet.* **2005**, *60*, 36−45.
(51) Janin, J.; Rodier, F.; Chakrabarti, P.; Bahadur, R. P. Macromolecular recognition in the Protein Data Bank. *Acta Crystallogr., Sect. D: Biol. Crystallogr.* **2007**, *63*, 1−8.
(52) Wright, P. E.; Dyson, H. J. Intrinsically unstructured proteins: reassessing the protein structure-function paradigm. *J. Mol. Biol.* **1999**, *293*, 321−331.
(53) Wright, P. E.; Dyson, H. J. Intrinsically disordered proteins in cellular signalling and regulation. *Nat. Rev. Mol. Cell Biol.* **2015**, *16*, 18−29.
(54) Dunker, A. K.; Oldfield, C. J.; Meng, J.; Romero, P.; Yang, J. Y.; Chen, J. W.; Vacic, V.; Obradovic, Z.; Uversky, V. N. The unfoldomics decade: an update on intrinsically disordered proteins. *BMC Genomics* **2008**, *9* (Suppl 2), S1.
(55) Wang, J.; Zheng, X.; Yang, Y.; Drueckhammer, D.; Yang, W.; Verkhivker, G.; Wang, E. Quantifying intrinsic specificity: a potential complement to affinity in drug screening. *Phys. Rev. Lett.* **2007**, *99*, 198101.
(56) Chu, X.; Gan, L.; Wang, E.; Wang, J. Quantifying the topography of the intrinsic energy landscape of flexible biomolecular recognition. *Proc. Natl. Acad. Sci. U. S. A.* **2013**, *110*, E2342−51.
(57) Chu, X.; Wang, J. Specificity and affinity quantification of flexible recognition from underlying energy landscape topography. *PLoS Comput. Biol.* **2014**, *10*, No. e1003782.
(58) Clore, G. M.; Iwahara, J. Theory, practice, and applications of paramagnetic relaxation Enhancement for the Characterization of Transient Low-Population States of Biological Macromolecules and Their Complexes. *Chem. Rev.* **2009**, *109*, 4108−4139.
(59) Tang, C.; Iwahara, J.; Marius Clore, G. Visualization of transient encounter complexes in protein−protein association. *Nature* **2006**, *444*, 383−386.
(60) Johansson, H.; Jensen, M. R.; Gesmar, H.; Meier, S.; Vinther, J. M.; Keeler, C.; Hodsdon, M. E.; Led, J. J. Specific and nonspecific interactions in ultraweak protein-protein associations revealed by solvent paramagnetic relaxation enhancements. *J. Am. Chem. Soc.* **2014**, *136*, 10277−10286.
(61) Ozer, A.; White, B. S.; Lis, J. T.; Shalloway, D. Density-dependent cooperative non-specific binding in solid-phase SELEX affinity selection. *Nucleic Acids Res.* **2013**, *41*, 7167−7175.
(62) Miles, D. W.; Mogensen, C. E.; Gundersen, H. J. Radioimmunoassay for urinary albumin using a single antibody. *Scand. J. Clin. Lab. Invest.* **1970**, *26*, 5−11.
(63) Johansson, S.; Svineng, G.; Wennerberg, K.; Armulik, A.; Lohikangas, L. Fibronectin-integrin interactions. *Front. Biosci., Landmark Ed.* **1997**, *2*, d126−46.
(64) Frank, S. A. *Immunology and Evolution of Infectious Disease*; Princeton University Press, 2002; Vol. *300*.
(65) Van Regenmortel, M. H.; Altschuh, D.; Chatellier, J.; Christensen, L.; Rauffer-Bruyère, N.; Richalet-Secordel, P.; Witz, J.; Zeder-Lutz, G. Measurement of antigen-antibody interactions with biosensors. *J. Mol. Recognit.* **1998**, *11*, 163−167.
(66) Levy, Y.; Cho, S. S.; Onuchic, J. N.; Wolynes, P. G. A survey of flexible protein binding mechanisms and their transition states using native topology based energy landscapes. *J. Mol. Biol.* **2005**, *346*, 1121−1145.
(67) Landry, C. R.; Levy, E. D.; Abd Rabbo, D.; Tarassov, K.; Michnick, S. W. Extracting insight from noisy cellular networks. *Cell* **2013**, *155*, 983−989.
(68) Nobeli, I.; Favia, A. D.; Thornton, J. M. Protein promiscuity and its implications for biotechnology. *Nat. Biotechnol.* **2009**, *27*, 157−167.
(69) Patil, A.; Kinoshita, K.; Nakamura, H. Hub promiscuity in protein-protein interaction networks. *Int. J. Mol. Sci.* **2010**, *11*, 1930−1943.
(70) Tsai, C.-J.; Ma, B.; Nussinov, R. Protein-protein interaction networks: how can a hub protein bind so many different partners? *Trends Biochem. Sci.* **2009**, *34*, 594−600.
(71) Marsh, J. A.; Teichmann, S. A. Structure, dynamics, assembly, and evolution of protein complexes. *Annu. Rev. Biochem.* **2015**, *84*, 551−575.
(72) Levi, V.; González Flecha, F. L. Reversible fast-dimerization of bovine serum albumin detected by fluorescence resonance energy transfer. *Biochim. Biophys. Acta, Proteins Proteomics* **2002**, *1599*, 141−148.
(73) Roach, P.; Farrar, D.; Perry, C. C. Interpretation of protein adsorption: surface-induced conformational changes. *J. Am. Chem. Soc.* **2005**, *127*, 8168−8173.
(74) Ball, A.; Jones, R. A. L. Conformational changes in adsorbed proteins. *Langmuir* **1995**, *11*, 3542−3548.
(75) Pollard, T. D. A guide to simple and informative binding assays. *Mol. Biol. Cell* **2010**, *21*, 4061−4067.
(76) Du, X.; Li, Y.; Xia, Y.-L.; Ai, S.-M.; Liang, J.; Sang, P.; Ji, X.-L.; Liu, S.-Q. Insights into protein-ligand interactions: mechanisms, models, and methods. *Int. J. Mol. Sci.* **2016**, *17*, 144.
(77) Fägerstam, L. G.; Frostell-Karlsson, A.; Karlsson, R.; Persson, B.; Rönnberg, I. Biospecific interaction analysis using surface plasmon resonance detection applied to kinetic, binding site and concentration analysis. *J. Chromatogr.* **1992**, *597*, 397−410.
(78) Malmqvist, M. Biospecific interaction analysis using biosensor technology. *Nature* **1993**, *361*, 186−187.
(79) Schasfoort, R. B. M. *Handbook of Surface Plasmon Resonance*, 2nd ed.; Royal Society of Chemistry, 2017.
(80) Vuignier, K.; Schappler, J.; Veuthey, J.-L.; Carrupt, P.-A.; Martel, S. Drug-protein binding: a critical review of analytical tools. *Anal. Bioanal. Chem.* **2010**, *398*, 53−66.
(81) Goldblatt, D. *eLS*; John Wiley & Sons, Ltd, 2001.
(82) Perozzo, R.; Folkers, G.; Scapozza, L. Thermodynamics of protein-ligand interactions: history, presence, and future aspects. *J. Recept. Signal Transduction Res.* **2004**, *24*, 1−52.
(83) Klotz, I. M.; Hunston, D. L. Protein interactions with small molecules. Relationships between stoichiometric binding constants, site binding constants, and empirical binding parameters. *J. Biol. Chem.* **1975**, *250*, 3001−3009.
(84) Santiesteban, O. J.; Kaittanis, C.; Perez, J. M. Assessment of molecular interactions through magnetic relaxation. *Angew. Chem., Int. Ed.* **2012**, *51*, 6728−6732.
(85) Mammen, M.; Choi, S.-K.; Whitesides, G. M. Polyvalent interactions in biological systems: implications for design and use of multivalent ligands and inhibitors. *Angew. Chem., Int. Ed.* **1998**, *37*, 2754−2794.
(86) Wagner, K. *Handbook of Surface Plasmon Resonance*; 2017; pp 295−327.
(87) Zheng, X.; Wang, J. The universal statistical distributions of the affinity, equilibrium constants, kinetics and specificity in biomolecular recognition. *PLoS Comput. Biol.* **2015**, *11*, No. e1004212.
(88) Osajima, T.; Suzuki, M.; Neya, S.; Hoshino, T. Computational and statistical study on the molecular interaction between antigen and antibody. *J. Mol. Graphics Modell.* **2014**, *53*, 128−139.
(89) Hornick, C. L.; Karush, F. Antibody affinity—III the role of multivalence. *Immunochemistry* **1972**, *9*, 325−340.
(90) Horan, N.; Yan, L.; Isobe, H.; Whitesides, G. M.; Kahne, D. Nonstatistical binding of a protein to clustered carbohydrates. *Proc. Natl. Acad. Sci. U. S. A.* **1999**, *96*, 11782−11786.
(91) Dubacheva, G. V.; Curk, T.; Mognetti, B. M.; Auzély-Velty, R.; Frenkel, D.; Richter, R. P. Superselective targeting using multivalent polymers. *J. Am. Chem. Soc.* **2014**, *136*, 1722−1725.
(92) Fasting, C.; Schalley, C. A.; Weber, M.; Seitz, O.; Hecht, S.; Koksch, B.; Dernedde, J.; Graf, C.; Knapp, E.-W.; Haag, R. Multivalency as a chemical organization and action principle. *Angew. Chem., Int. Ed.* **2012**, *51*, 10472−10498.
(93) McEver, R. P.; Zhu, C. Rolling cell adhesion. *Annu. Rev. Cell Dev. Biol.* **2010**, *26*, 363−396.

https://doi.org/10.1021/acs.chemrev.1c00044
Chem. Rev. 2021, 121, 8095−8160

(94) Huskens, J.; Mulder, A.; Auletta, T.; Nijhuis, C. A.; Ludden, M. J. W.; Reinhoudt, D. N. A model for describing the thermodynamics of multivalent host-guest interactions at interfaces. *J. Am. Chem. Soc.* **2004**, *126*, 6784−6797.
(95) Sykes, K. F.; Legutki, J. B.; Stafford, P. Immunosignaturing: a critical review. *Trends Biotechnol.* **2013**, *31*, 45−51.
(96) Sobek, J.; Rehrauer, H.; Schauer, S.; Fischer, D.; Patrignani, A.; Landgraf, S.; Korlach, J.; Schlapbach, R. Single-molecule DNA hybridisation studied by using a modified DNA sequencer: a comparison with surface plasmon resonance data. *Methods Appl. Fluoresc.* **2016**, *4*, 015002.
(97) Hwu, S.; Blickenstorfer, Y.; Ihle, S. J.; Forró, C.; Garzuel, M.; Schmidheini, L.; Demkó, L.; Vörös, J. Theoretical and experimental investigation of ligand-induced particle-particle interactions. *J. Phys. Chem. C* **2020**, *124*, 1566−1574.
(98) Hwu, S.; Garzuel, M.; Forró, C.; Ihle, S. J.; Reichmuth, A. M.; Kurdzesau, F.; Vörös, J. An analytical method to control the surface density and stability of DNA-gold nanoparticles for an optimized biosensor. *Colloids Surf., B* **2020**, *187*, 110650.
(99) Eaton, B. E.; Gold, L.; Zichi, D. A. Let's get specific: the relationship between specificity and affinity. *Chem. Biol.* **1995**, *2*, 633−638.
(100) Wang, J.; Verkhivker, G. M. Energy landscape theory, funnels, specificity, and optimal criterion of biomolecular binding. *Phys. Rev. Lett.* **2003**, *90*, 188101.
(101) Yan, Z.; Guo, L.; Hu, L.; Wang, J. Specificity and affinity quantification of protein-protein interactions. *Bioinformatics* **2013**, *29*, 1127−1133.
(102) Van Regenmortel, M. H. From absolute to exquisite specificity. Reflections on the fuzzy nature of species, specificity and antigenic sites. *J. Immunol. Methods* **1998**, *216*, 37−48.
(103) Chaires, J. B. Calorimetry and thermodynamics in drug design. *Annu. Rev. Biophys.* **2008**, *37*, 135−151.
(104) Bashir, Q.; Scanu, S.; Ubbink, M. Dynamics in electron transfer protein complexes. *FEBS J.* **2011**, *278*, 1391−1400.
(105) Liu, S.-Q.; Tan, D.-Y.; Zhang, K.-Q.; Ji, X.-L.; Tao, Y.; Fu, Y.-X. *Protein folding, binding and energy landscape: A synthesis*; INTECH Open Access Publisher, 2012.
(106) Frauenfelder, H.; Sligar, S. G.; Wolynes, P. G. The energy landscapes and motions of proteins. *Science* **1991**, *254*, 1598−1603.
(107) Janin, J. Quantifying biological specificity: The statistical mechanics of molecular recognition. *Proteins: Struct., Funct., Genet.* **1996**, *25*, 438−445.
(108) Wolynes, P. G.; Onuchic, J. N.; Thirumalai, D. Navigating the folding routes. *Science* **1995**, *267*, 1619−1620.
(109) Nussinov, R.; Tsai, C.-J. Free energy diagrams for protein function. *Chem. Biol.* **2014**, *21*, 311−318.
(110) Iida, S.; Nakamura, H.; Higo, J. Enhanced conformational sampling to visualize a free-energy landscape of protein complex formation. *Biochem. J.* **2016**, *473*, 1651
(111) Kozakov, D.; Li, K.; Hall, D. R.; Beglov, D.; Zheng, J.; Vakili, P.; Schueler-Furman, O.; Paschalidis, I. C.; Clore, G. M.; Vajda, S. Encounter complexes and dimensionality reduction in protein-protein association. *eLife* **2014**, *3*, No. e01370.
(112) Karplus, M. The Levinthal paradox: yesterday and today. *Folding Des.* **1997**, *2*, S69−75.
(113) Yan, Z.; Wang, J. Specificity quantification of biomolecular recognition and its implication for drug discovery. *Sci. Rep.* **2012**, *2*, 309.
(114) Wang, J.; Oliveira, R. J.; Chu, X.; Whitford, P. C.; Chahine, J.; Han, W.; Wang, E.; Onuchic, J. N.; Leite, V. B. P. Topography of funneled landscapes determines the thermodynamics and kinetics of protein folding. *Proc. Natl. Acad. Sci. U. S. A.* **2012**, *109*, 15763−15768.
(115) Haliloglu, T.; Bahar, I. Adaptability of protein structures to enable functional interactions and evolutionary implications. *Curr. Opin. Struct. Biol.* **2015**, *35*, 17−23.
(116) Sankar, K.; Liu, J.; Wang, Y.; Jernigan, R. L. Distributions of experimental protein structures on coarse-grained free energy landscapes. *J. Chem. Phys.* **2015**, *143*, 243153.
(117) Wei, G.; Xi, W.; Nussinov, R.; Ma, B. Protein ensembles: how does Nature harness thermodynamic fluctuations for life? The diverse functional roles of conformational ensembles in the cell. *Chem. Rev.* **2016**, *116*, 6516−6551.
(118) Koonin, E. V.; Wolf, Y. I.; Karev, G. P. The structure of the protein universe and genome evolution. *Nature* **2002**, *420*, 218−223.
(119) Tsai, C. J.; Kumar, S.; Ma, B.; Nussinov, R. Folding funnels, binding funnels, and protein function. *Protein Sci.* **1999**, *8*, 1181−1190.
(120) Prudêncio, M.; Ubbink, M. Transient complexes of redox proteins: structural and dynamic details from NMR studies. *J. Mol. Recognit.* **2004**, *17*, 524−539.
(121) Shoemaker, B. A.; Portman, J. J.; Wolynes, P. G. Speeding molecular recognition by using the folding funnel: the fly-casting mechanism. *Proc. Natl. Acad. Sci. U. S. A.* **2000**, *97*, 8868−8873.
(122) Espinoza-Fonseca, L. M. Reconciling binding mechanisms of intrinsically disordered proteins. *Biochem. Biophys. Res. Commun.* **2009**, *382*, 479−482.
(123) Chong, S.-H.; Ham, S. Folding free energy landscape of ordered and intrinsically disordered proteins. *Sci. Rep.* **2019**, *9*, 1−9.
(124) Ruben, A. J.; Kiso, Y.; Freire, E. Overcoming roadblocks in lead optimization: a thermodynamic perspective. *Chem. Biol. Drug Des.* **2006**, *67*, 2−4.
(125) Freire, E. Do enthalpy and entropy distinguish first in class from best in class? *Drug Discovery Today* **2008**, *13*, 869−874.
(126) Kalodimos, C. G.; Biris, N.; Bonvin, A. M. J. J.; Levandoski, M. M.; Guennuegues, M.; Boelens, R.; Kaptein, R. Structure and flexibility adaptation in nonspecific and specific protein-DNA complexes. *Science* **2004**, *305*, 386−389.
(127) Velazquez-Campoy, A.; Leavitt, S. A.; Freire, E. Characterization of protein-protein interactions by isothermal titration calorimetry. *Methods Mol. Biol.* **2004**, *261*, 35−54.
(128) Gilson, M. K.; Zhou, H.-X. Calculation of protein-ligand binding affinities. *Annu. Rev. Biophys. Biomol. Struct.* **2007**, *36*, 21−42.
(129) Amzel, L. M. Loss of translational entropy in binding, folding, and catalysis. *Proteins: Struct., Funct., Genet.* **1997**, *28*, 144−149.
(130) Amzel, L. M. Calculation of entropy changes in biological processes: folding, binding, and oligomerization. *Methods Enzymol.* **2000**, *323*, 167−177.
(131) Finkelstein, A. V.; Janin, J. The price of lost freedom: entropy of bimolecular complex formation. *Protein Eng., Des. Sel.* **1989**, *3*, 1−3.
(132) Fu, J.; Schlenoff, J. B. Driving forces for oppositely charged polyion association in aqueous solutions: enthalpic, entropic, but not electrostatic. *J. Am. Chem. Soc.* **2016**, *138*, 980−990.
(133) Olsson, T. S. G.; Williams, M. A.; Pitt, W. R.; Ladbury, J. E. The thermodynamics of protein-ligand interaction and solvation: insights for ligand design. *J. Mol. Biol.* **2008**, *384*, 1002−1017.
(134) Mohan, S.; Kourentzi, K.; Schick, K. A.; Uehara, C.; Lipschultz, C. A.; Acchione, M.; Desantis, M. E.; Smith-Gill, S. J.; Willson, R. C. Association energetics of cross-reactive and specific antibodies. *Biochemistry* **2009**, *48*, 1390−1398.
(135) Kumagai, I.; Tsumoto, K. *eLS*; John Wiley & Sons, Ltd, 2001.
(136) Ladbury, J. E.; Klebe, G.; Freire, E. Adding calorimetric data to decision making in lead discovery: a hot tip. *Nat. Rev. Drug Discovery* **2010**, *9*, 23−27.
(137) Prasad Bahadur, R.; Chakrabarti, P.; Rodier, F.; Janin, J. A dissection of specific and non-specific protein−protein interfaces. *J. Mol. Biol.* **2004**, *336*, 943−955.
(138) Rigby, M. *The Forces between molecules*; Oxford science publications; Clarendon Press, 1986.
(139) Wang, C.; Guan, L.; Danovich, D.; Shaik, S.; Mo, Y. The origins of the directionality of noncovalent intermolecular interactions. *J. Comput. Chem.* **2016**, *37*, 34−45.
(140) Hunter, C. A.; Sanders, J. K. M. The nature of pi-pi interactions. *J. Am. Chem. Soc.* **1990**, *112*, 5525−5534.
(141) van Oss, C. J. Kinetics and energetics of specific intermolecular interactions. *J. Mol. Recognit.* **1997**, *10*, 203−216.
(142) Marenduzzo, D.; Finan, K.; Cook, P. R. The depletion attraction: an underappreciated force driving cellular organization. *J. Cell Biol.* **2006**, *175*, 681−686.

https://doi.org/10.1021/acs.chemrev.1c00044
Chem. Rev. 2021, 121, 8095−8160

(143) van Oss, C. J. *Interfacial Forces in Aqueous Media*, 2nd ed.; Taylor & Francis, 2006.
(144) Camacho, C. J.; Kimura, S. R.; DeLisi, C.; Vajda, S. Kinetics of desolvation-mediated protein-protein binding. *Biophys. J.* **2000**, *78*, 1094−1105.
(145) Laue, T. M.; Shire, S. J. The molecular interaction process. *J. Pharm. Sci.* **2020**, *109*, 154−160.
(146) Ubbink, M. The courtship of proteins: understanding the encounter complex. *FEBS Lett.* **2009**, *583*, 1060−1066.
(147) Derjaguin, B. V.; Landau, L. Theory of the stability of strongly charged lyophobic sols and of the adhesion of strongly charged particles in solutions of electrolytes. *Acta Phys. Chim. URSS* **1941**, *14*, 633−662.
(148) Verway, E.; Overbeek, J. *Theory of stability of lyophobic colloids*; Amsterdam-New York, 1948.
(149) Leckband, D.; Sivasankar, S. Forces controlling protein interactions: theory and experiment. *Colloids Surf., B* **1999**, *14*, 83−97.
(150) Grasso, D.; Subramaniam, K.; Butkus, M.; Strevett, K.; Bergendahl, J. A review of non-DLVO interactions in environmental colloidal systems. *Rev. Environ. Sci. Bio/Technol.* **2002**, *1*, 17−38.
(151) van Oss, C. J. Long-range and short-range mechanisms of hydrophobic attraction and hydrophilic repulsion in specific and aspecific interactions. *J. Mol. Recognit.* **2003**, *16*, 177−190.
(152) Zafra-Ruano, A.; Luque, I. Interfacial water molecules in SH3 interactions: Getting the full picture on polyproline recognition by protein-protein interaction domains. *FEBS Lett.* **2012**, *586*, 2619−2630.
(153) Arzenšek, D.; Kuzman, D.; Podgornik, R. Colloidal interactions between monoclonal antibodies in aqueous solutions. *J. Colloid Interface Sci.* **2012**, *384*, 207−216.
(154) Frauenfelder, H.; Chen, G.; Berendzen, J.; Fenimore, P. W.; Jansson, H.; McMahon, B. H.; Stroe, I. R.; Swenson, J.; Young, R. D. A unified model of protein dynamics. *Proc. Natl. Acad. Sci. U. S. A.* **2009**, *106*, 5129−5134.
(155) Vogt, A. D.; Pozzi, N.; Chen, Z.; Di Cera, E. Essential role of conformational selection in ligand binding. *Biophys. Chem.* **2014**, *186*, 13−21.
(156) Fischer, E. Einfluss der configuration auf die wirkung der enzyme. *Ber. Dtsch. Chem. Ges.* **1894**, *27*, 2985−2993.
(157) Stein, A.; Rueda, M.; Panjkovich, A.; Orozco, M.; Aloy, P. A systematic study of the energetics involved in structural changes upon association and connectivity in protein interaction networks. *Structure* **2011**, *19*, 881−889.
(158) Koshland, D. E. Application of a theory of enzyme specificity to protein synthesis. *Proc. Natl. Acad. Sci. U. S. A.* **1958**, *44*, 98−104.
(159) Csermely, P.; Palotai, R.; Nussinov, R. Induced fit, conformational selection and independent dynamic segments: an extended view of binding events. *Trends Biochem. Sci.* **2010**, *35*, 539−546.
(160) Wang, Q.; Zhang, P.; Hoffman, L.; Tripathi, S.; Homouz, D.; Liu, Y.; Waxham, M. N.; Cheung, M. S. Protein recognition and selection through conformational and mutually induced fit. *Proc. Natl. Acad. Sci. U. S. A.* **2013**, *110*, 20545−20550.
(161) Blundell, T. L.; Fernández-Recio, J. Cell biology: brief encounters bolster contacts. *Nature* **2006**, *444*, 279−280.
(162) Hassan, S. A.; Steinbach, P. J. Water-exclusion and liquid-structure forces in implicit solvation. *J. Phys. Chem. B* **2011**, *115*, 14668−14682.
(163) Janin, J. The kinetics of protein-protein recognition. *Proteins: Struct., Funct., Genet.* **1997**, *28*, 153−161.
(164) Schreiber, G.; Shaul, Y.; Gottschalk, K. E. Electrostatic design of protein-protein association rates. *Methods Mol. Biol.* **2006**, *340*, 235−249.
(165) Schlosshauer, M.; Baker, D. Realistic protein-protein association rates from a simple diffusional model neglecting long-range interactions, free energy barriers, and landscape ruggedness. *Protein Sci.* **2004**, *13*, 1660−1669.
(166) Berg, O. G. Orientation constraints in diffusion-limited macromolecular association. The role of surface diffusion as a rate-enhancing mechanism. *Biophys. J.* **1985**, *47*, 1−14.
(167) Janin, J.; Sternberg, M. J. E. Protein flexibility, not disorder, is intrinsic to molecular recognition. *F1000 Biol. Rep.* **2013**, *5*, 2.
(168) Schreiber, G.; Fersht, A. R. Rapid, electrostatically assisted association of proteins. *Nat. Struct. Biol.* **1996**, *3*, 427−431.
(169) Zhou, H. X. Disparate ionic-strength dependencies of on and off rates in protein-protein association. *Biopolymers* **2001**, *59*, 427−433.
(170) Alsallaq, R.; Zhou, H.-X. Electrostatic rate enhancement and transient complex of protein-protein association. *Proteins: Struct., Funct., Genet.* **2008**, *71*, 320−335.
(171) Wang, W.; Xu, W.-X.; Levy, Y.; Trizac, E.; Wolynes, P. G. Confinement effects on the kinetics and thermodynamics of protein dimerization. *Proc. Natl. Acad. Sci. U. S. A.* **2009**, *106*, 5517−5522.
(172) de Nooijer, S.; Wellink, J.; Mulder, B.; Bisseling, T. Non-specific interactions are sufficient to explain the position of heterochromatic chromocenters and nucleoli in interphase nuclei. *Nucleic Acids Res.* **2009**, *37*, 3558−3568.
(173) Lazaridis, T. *eLS*; John Wiley & Sons, Ltd, 2001.
(174) Chothia, C.; Janin, J. Principles of protein-protein recognition. *Nature* **1975**, *256*, 705−708.
(175) Van Oss, C. J. *The Properties of Water and Their Role in Colloidal and Biological Systems*; Academic Press, 2008.
(176) Lim, V. I.; Curran, J. F.; Garber, M. B. Hydration shells of molecules in molecular association: A mechanism for biomolecular recognition. *J. Theor. Biol.* **2012**, *301*, 42−48.
(177) Thornton, J. M.; Edwards, M. S.; Taylor, W. R.; Barlow, D. J. Location of 'continuous' antigenic determinants in the protruding regions of proteins. *EMBO J.* **1986**, *5*, 409−413.
(178) Rubinstein, N. D.; Mayrose, I.; Halperin, D.; Yekutieli, D.; Gershoni, J. M.; Pupko, T. Computational characterization of B-cell epitopes. *Mol. Immunol.* **2008**, *45*, 3477−3489.
(179) Kringelum, J. V.; Nielsen, M.; Padkjær, S. B.; Lund, O. Structural analysis of B-cell epitopes in antibody:protein complexes. *Mol. Immunol.* **2013**, *53*, 24−34.
(180) Ando, T.; Skolnick, J. Sliding of proteins non-specifically bound to DNA: Brownian dynamics studies with coarse-grained protein and DNA models. *PLoS Comput. Biol.* **2014**, *10*, No. e1003990.
(181) Sheinman, M.; Bénichou, O.; Kafri, Y.; Voituriez, R. Classes of fast and specific search mechanisms for proteins on DNA. *Rep. Prog. Phys.* **2012**, *75*, 026601.
(182) Berg, O. G.; Winter, R. B.; Von Hippel, P. H. Diffusion-driven mechanisms of protein translocation on nucleic acids. 1. Models and theory. *Biochemistry* **1981**, *20*, 6929−6948.
(183) Ball, P. Water as an active constituent in cell biology. *Chem. Rev.* **2008**, *108*, 74−108.
(184) Ahmad, M.; Gu, W.; Geyer, T.; Helms, V. Adhesive water networks facilitate binding of protein interfaces. *Nat. Commun.* **2011**, *2*, 261.
(185) Levy, Y.; Onuchic, J. N. Water mediation in protein folding and molecular recognition. *Annu. Rev. Biophys. Biomol. Struct.* **2006**, *35*, 389−415.
(186) Marcovitz, A.; Naftaly, A.; Levy, Y. Water organization between oppositely charged surfaces: Implications for protein sliding along DNA. *J. Chem. Phys.* **2015**, *142*, 085102.
(187) Hubbard, R. E.; Kamran Haider, M. *eLS*; John Wiley & Sons, Ltd, 2001.
(188) Xu, D.; Tsai, C. J.; Nussinov, R. Hydrogen bonds and salt bridges across protein-protein interfaces. *Protein Eng., Des. Sel.* **1997**, *10*, 999−1012.
(189) Hunter, C. A.; Lawson, K. R.; Perkins, J.; Urch, C. J. Aromatic interactions. *J. Chem. Soc. Perkin Trans. 0* **2001**, *2*, 651−669.
(190) Dalkas, G. A.; Teheux, F.; Kwasigroch, J. M.; Rooman, M. Cation-π, amino-π, π-π, and H-bond interactions stabilize antigen-antibody interfaces. *Proteins: Struct., Funct., Genet.* **2014**, *82*, 1734−1746.
(191) Meyer, E. A.; Castellano, R. K.; Diederich, F. Interactions with aromatic rings in chemical and biological recognition. *Angew. Chem., Int. Ed.* **2003**, *42*, 1210−1250.
(192) Bissantz, C.; Kuhn, B.; Stahl, M. A medicinal chemist's guide to molecular interactions. *J. Med. Chem.* **2010**, *53*, 5061−5084.

https://doi.org/10.1021/acs.chemrev.1c00044
Chem. Rev. 2021, 121, 8095−8160

(193) Mahadevi, A. S.; Sastry, G. N. Cooperativity in noncovalent interactions. *Chem. Rev.* **2016**, *116*, 2775−2825.
(194) Bronowska, A. K. In *Thermodynamics - Interaction Studies - Solids, Liquids and Gases*; Moreno Pirajn, J. C., Ed.; InTech, 2011.
(195) Barratt, E.; Bronowska, A.; Vondrásek, J.; Cerný, J.; Bingham, R.; Phillips, S.; Homans, S. W. Thermodynamic penalty arising from burial of a ligand polar group within a hydrophobic pocket of a protein receptor. *J. Mol. Biol.* **2006**, *362*, 994−1003.
(196) Fersht, A. R.; Shi, J. P.; Knill-Jones, J.; Lowe, D. M.; Wilkinson, A. J.; Blow, D. M.; Brick, P.; Carter, P.; Waye, M. M.; Winter, G. Hydrogen bonding and biological specificity analysed by protein engineering. *Nature* **1985**, *314*, 235−238.
(197) Kumar, S.; Nussinov, R. Salt bridge stability in monomeric proteins. *J. Mol. Biol.* **1999**, *293*, 1241−1255.
(198) Kumar, S.; Nussinov, R. Relationship between ion pair geometries and electrostatic strengths in proteins. *Biophys. J.* **2002**, *83*, 1595−1612.
(199) Janin, J. A minimal model of protein−protein binding affinities. *Protein Sci.* **2014**, *23*, 1813−1817.
(200) Pechmann, S.; Levy, E. D.; Tartaglia, G. G.; Vendruscolo, M. Physicochemical principles that regulate the competition between functional and dysfunctional association of proteins. *Proc. Natl. Acad. Sci. U. S. A.* **2009**, *106*, 10159−10164.
(201) Marsh, J. A.; Teichmann, S. A. Structure, dynamics, assembly, and evolution of protein complexes. *Annu. Rev. Biochem.* **2015**, *84*, 551−575.
(202) Sanchez-Trincado, J. L.; Gomez-Perosanz, M.; Reche, P. A. Fundamentals and methods for T- and B-cell epitope prediction. *J. Immunol. Res.* **2017**, *2017*, 2680160.
(203) Foote, J.; Eisen, H. N. Kinetic and affinity limits on antibodies produced during immune responses. *Proc. Natl. Acad. Sci. U. S. A.* **1995**, *92*, 1254−1256.
(204) Ozbabacan, S.; Engin, H. B.; Gursoy, A. Transient protein−protein interactions. *Protein Eng., Des. Sel.* **2011**, *24*, 635.
(205) Lo Conte, L.; Chothia, C.; Janin, J. The atomic structure of protein-protein recognition sites. *J. Mol. Biol.* **1999**, *285*, 2177−2198.
(206) Jones, S.; Thornton, J. M. Principles of protein-protein interactions. *Proc. Natl. Acad. Sci. U. S. A.* **1996**, *93*, 13−20.
(207) De, S.; Krishnadev, O.; Srinivasan, N.; Rekha, N. Interaction preferences across protein-protein interfaces of obligatory and non-obligatory components are different. *BMC Struct. Biol.* **2005**, *5*, 15.
(208) Reichmann, D.; Rahat, O.; Cohen, M.; Neuvirth, H.; Schreiber, G. The molecular architecture of protein-protein binding sites. *Curr. Opin. Struct. Biol.* **2007**, *17*, 67−76.
(209) Peng, H.-P.; Lee, K. H.; Jian, J.-W.; Yang, A.-S. Origins of specificity and affinity in antibody-protein interactions. *Proc. Natl. Acad. Sci. U. S. A.* **2014**, *111*, E2656−E2665.
(210) Li, X.; Keskin, O.; Ma, B.; Nussinov, R.; Liang, J. Protein-protein interactions: hot spots and structurally conserved residues often locate in complemented pockets that pre-organized in the unbound states: implications for docking. *J. Mol. Biol.* **2004**, *344*, 781−795.
(211) Moreira, I. S.; Fernandes, P. A.; Ramos, M. J. Hot spots—A review of the protein−protein interface determinant amino-acid residues. *Proteins: Struct., Funct., Genet.* **2007**, *68*, 803−812.
(212) Bogan, A. A.; Thorn, K. S. Anatomy of hot spots in protein interfaces. *J. Mol. Biol.* **1998**, *280*, 1−9.
(213) Ramos, R. M.; Fernandes, L. F.; Moreira, I. S. Extending the applicability of the O-ring theory to protein−DNA complexes. *Comput. Biol. Chem.* **2013**, *44*, 31−39.
(214) Li, Z.; He, Y.; Wong, L.; Li, J. Progressive dry-core-wet-rim hydration trend in a nested-ring topology of protein binding interfaces. *BMC Bioinf.* **2012**, *13*, 51.
(215) Keskin, O.; Ma, B.; Rogale, K.; Gunasekaran, K.; Nussinov, R. Protein-protein interactions: organization, cooperativity and mapping in a bottom-up Systems Biology approach. *Phys. Biol.* **2005**, *2*, S24−35.
(216) Keskin, O.; Ma, B.; Nussinov, R. Hot regions in protein−protein interactions: the organization and contribution of structurally conserved hot spot residues. *J. Mol. Biol.* **2005**, *345*, 1281−1294.
(217) Reichmann, D.; Rahat, O.; Albeck, S.; Meged, R.; Dym, O.; Schreiber, G. The modular architecture of protein-protein binding interfaces. *Proc. Natl. Acad. Sci. U. S. A.* **2005**, *102*, 57−62.
(218) Moreira, I. S.; Martins, J. M.; Ramos, R. M.; Fernandes, P. A.; Ramos, M. J. Understanding the importance of the aromatic amino-acid residues as hot-spots. *Biochim. Biophys. Acta, Proteins Proteomics* **2013**, *1834*, 404−414.
(219) Van Regenmortel, M. H. V. What is a B-cell epitope? *Methods Mol. Biol.* **2009**, *524*, 3−20.
(220) Meenan, N. A. G.; Sharma, A.; Fleishman, S. J.; Macdonald, C. J.; Morel, B.; Boetzel, R.; Moore, G. R.; Baker, D.; Kleanthous, C. The structural and energetic basis for high selectivity in a high-affinity protein-protein interaction. *Proc. Natl. Acad. Sci. U. S. A.* **2010**, *107*, 10080−10085.
(221) Ahmed, M. H.; Habtemariam, M.; Safo, M. K.; Scarsdale, J. N.; Spyrakis, F.; Cozzini, P.; Mozzarelli, A.; Kellogg, G. E. Unintended consequences? Water molecules at biological and crystallographic protein−protein interfaces. *Comput. Biol. Chem.* **2013**, *47*, 126−141.
(222) Ladbury, J. E. Just add water! The effect of water on the specificity of protein-ligand binding sites and its potential application to drug design. *Chem. Biol.* **1996**, *3*, 973−980.
(223) Li, Y.; Zhang, X.; Cao, D. The role of shape complementarity in the protein-protein interactions. *Sci. Rep.* **2013**, *3*, 1−7.
(224) Aragues, R.; Sali, A.; Bonet, J.; Marti-Renom, M. A.; Oliva, B. Characterization of protein hubs by inferring interacting motifs from protein interactions. *PLoS Comput. Biol.* **2007**, *3*, 1761−1771.
(225) Erijman, A.; Aizner, Y.; Shifman, J. M. Multispecific recognition: mechanism, evolution, and design. *Biochemistry* **2011**, *50*, 602−611.
(226) van der Lee, R.; et al. Classification of intrinsically disordered regions and proteins. *Chem. Rev.* **2014**, *114*, 6589−6631.
(227) Oldfield, C. J.; Dunker, A. K. Intrinsically disordered proteins and intrinsically disordered protein regions. *Annu. Rev. Biochem.* **2014**, *83*, 553−584.
(228) Vuzman, D.; Levy, Y. Intrinsically disordered regions as affinity tuners in protein−DNA interactions. *Mol. BioSyst.* **2012**, *8*, 47−57.
(229) Demchenko, A. P. Recognition between flexible protein molecules: induced and assisted folding. *J. Mol. Recognit.* **2001**, *14*, 42−61.
(230) Vacic, V.; Oldfield, C. J.; Mohan, A.; Radivojac, P.; Cortese, M. S.; Uversky, V. N.; Dunker, A. K. Characterization of molecular recognition features, MoRFs, and their binding partners. *J. Proteome Res.* **2007**, *6*, 2351−2366.
(231) Yan, J.; Dunker, A. K.; Uversky, V. N.; Kurgan, L. Molecular recognition features (MoRFs) in three domains of life. *Mol. BioSyst.* **2016**, *12*, 697−710.
(232) Jane Dyson, H.; Wright, P. E. Intrinsically unstructured proteins and their functions. *Nat. Rev. Mol. Cell Biol.* **2005**, *6*, 197−208.
(233) Sela-Culang, I.; Kunik, V.; Ofran, Y. The structural basis of antibody-antigen recognition. *Immune system modeling*; 2015.
(234) Osajima, T.; Hoshino, T. Roles of the respective loops at complementarity determining region on the antigen-antibody recognition. *Comput. Biol. Chem.* **2016**, *64*, 368−383.
(235) Nielsen, M.; Marcatili, P. Prediction of antibody epitopes. *Methods Mol. Biol.* **2015**, *1348*, 23−32.
(236) Griffiths, G.; Lucocq, J. M. Antibodies for immunolabeling by light and electron microscopy: not for the faint hearted. *Histochem. Cell Biol.* **2014**, *142*, 347−360.
(237) Koide, S.; Sidhu, S. S. The importance of being tyrosine: lessons in molecular recognition from minimalist synthetic binding proteins. *ACS Chem. Biol.* **2009**, *4*, 325−334.
(238) Birtalan, S.; Fisher, R. D.; Sidhu, S. S. The functional capacity of the natural amino acids for molecular recognition. *Mol. BioSyst.* **2010**, *6*, 1186−1194.
(239) Fellouse, F. A.; Li, B.; Compaan, D. M.; Peden, A. A.; Hymowitz, S. G.; Sidhu, S. S. Molecular recognition by a binary code. *J. Mol. Biol.* **2005**, *348*, 1153−1162.
(240) Wedemayer, G. J.; Patten, P. A.; Wang, L. H.; Schultz, P. G.; Stevens, R. C. Structural insights into the evolution of an antibody combining site. *Science* **1997**, *276*, 1665−1669.

https://doi.org/10.1021/acs.chemrev.1c00044
Chem. Rev. 2021, 121, 8095−8160

(241) Andrade, M. A.; O'Donoghue, S. I.; Rost, B. Adaptation of protein surfaces to subcellular location. *J. Mol. Biol.* **1998**, *276*, 517−525.
(242) de Lange, V.; Habegger, M.; Schmidt, M.; Vörös, J. Improving FoRe: a new inlet design for filtering samples through individual microarray spots. *ACS Sens* **2017**, *2*, 339−345.
(243) Gervais, L.; Hitzbleck, M.; Delamarche, E. Capillary-driven multiparametric microfluidic chips for one-step immunoassays. *Biosens. Bioelectron.* **2011**, *27*, 64−70.
(244) Gervais, L.; de Rooij, N.; Delamarche, E. Microfluidic chips for point-of-care immunodiagnostics. *Adv. Mater.* **2011**, *23*, H151−76.
(245) Sapin, R.; Le Galudec, V.; Gasser, F.; Pinget, M.; Grucker, D. Elecsys insulin assay: free insulin determination and the absence of cross-reactivity with insulin lispro. *Clin. Chem.* **2001**, *47*, 602−605.
(246) Madry, N.; Auerbach, B.; Schelp, C. Measures to overcome HAMA interferences in immunoassays. *Anticancer research* **1997**, *17*, 2883−2886.
(247) Holm, B. E.; Sandhu, N.; Tronstrøm, J.; Lydolph, M.; Trier, N. H.; Houen, G. Species cross-reactivity of rheumatoid factors and implications for immunoassays. *Scand. J. Clin. Lab. Invest.* **2015**, *75*, 51−63.
(248) Tombelli, S.; Minunni, M.; Mascini, M. Analytical applications of aptamers. *Biosens. Bioelectron.* **2005**, *20*, 2424−2434.
(249) Keefe, A. D.; Pai, S.; Ellington, A. Aptamers as therapeutics. *Nat. Rev. Drug Discovery* **2010**, *9*, 537−550.
(250) Rohloff, J. C.; Gelinas, A. D.; Jarvis, T. C.; Ochsner, U. A.; Schneider, D. J.; Gold, L.; Janjic, N. Nucleic acid ligands with protein-like side chains: modified aptamers and their use as diagnostic and therapeutic agents. *Mol. Ther.–Nucleic Acids* **2014**, *3*, No. e201.
(251) Stumpp, M. T.; Dawson, K. M.; Binz, H. K. Beyond antibodies: the DARPin® drug platform. *BioDrugs* **2020**, *34*, 1−11.
(252) Miao, W. Electrogenerated chemiluminescence and its biorelated applications. *Chem. Rev.* **2008**, *108*, 2506−2553.
(253) Blackburn, G. F.; Shah, H. P.; Kenten, J. H.; Leland, J.; Kamin, R. A.; Link, J.; Peterman, J.; Powell, M. J.; Shah, A.; Talley, D. B. Electrochemiluminescence detection for development of immunoassays and DNA probe assays for clinical diagnostics. *Clin. Chem.* **1991**, *37*, 1534−1539.
(254) Hu, L.; Xu, G. Applications and trends in electrochemiluminescence. *Chem. Soc. Rev.* **2010**, *39*, 3275−3304.
(255) Van Reenen, A.; de Jong, A. M.; den Toonder, J. M.; Prins, M. W. Integrated lab-on-chip biosensing systems based on magnetic particle actuation−a comprehensive review. *Lab Chip* **2014**, *14*, 1966−1986.
(256) Zeng, S.; Yong, K.-T.; Roy, I.; Dinh, X.-Q.; Yu, X.; Luan, F. A review on functionalized gold nanoparticles for biosensing applications. *Plasmonics* **2011**, *6*, 491.
(257) Stark, W. J.; Stoessel, P. R.; Wohlleben, W.; Hafner, A. Industrial applications of nanoparticles. *Chem. Soc. Rev.* **2015**, *44*, 5793−5805.
(258) Bally, M.; Vörös, J. Nanoscale labels: nanoparticles and liposomes in the development of high-performance biosensors. *Nanomedicine* **2009**, *4*, 447−467.
(259) Sakamoto, S.; Putalun, W.; Vimolmangkang, S.; Phoolcharoen, W.; Shoyama, Y.; Tanaka, H.; Morimoto, S. Enzyme-linked immunosorbent assay for the quantitative/qualitative analysis of plant secondary metabolites. *Journal of natural medicines* **2018**, *72*, 32−42.
(260) Wolfbeis, O. S. An overview of nanoparticles commonly used in fluorescent bioimaging. *Chem. Soc. Rev.* **2015**, *44*, 4743−4768.
(261) Hu, L.; Xu, G. Applications and trends in electrochemiluminescence. *Chem. Soc. Rev.* **2010**, *39*, 3275−3304.
(262) Gross, E. M.; Maddipati, S. S.; Snyder, S. M. A review of electrogenerated chemiluminescent biosensors for assays in biological matrices. *Bioanalysis* **2016**, *8*, 2071−2089.
(263) Mulvaney, S. P.; Cole, C. L.; Kniller, M. D.; Malito, M.; Tamanaha, C. R.; Rife, J. C.; Stanton, M. W.; Whitman, L. J. Rapid, femtomolar bioassays in complex matrices combining microfluidics and magnetoelectronics. *Biosens. Bioelectron.* **2007**, *23*, 191−200.
(264) Mark, D.; Haeberle, S.; Roth, G.; von Stetten, F.; Zengerle, R. Microfluidic lab-on-a-chip platforms: requirements, characteristics and applications. *Chem. Soc. Rev.* **2010**, *39*, 1153−1182.
(265) Soares, R.; Martins, V. C.; Macedo, R.; Cardoso, F. A.; Martins, S. A.; Caetano, D. M.; Fonseca, P. H.; Silvério, V.; Cardoso, S.; Freitas, P. P. Go with the flow: advances and trends in magnetic flow cytometry. *Anal. Bioanal. Chem.* **2019**, *411*, 1839−1862.
(266) Favresse, J.; Burlacu, M.-C.; Maiter, D.; Gruson, D. Interferences with thyroid function immunoassays: clinical implications and detection algorithm. *Endocr. Rev.* **2018**, *39*, 830−850.
(267) Squires, T. M.; Messinger, R. J.; Manalis, S. R. Making it stick: convection, reaction and diffusion in surface-based biosensors. *Nat. Biotechnol.* **2008**, *26*, 417−426.
(268) Park, J. An optimized colorimetric readout method for lateral flow immunoassays. *Sensors* **2018**, *18*, 4084.
(269) Khlebtsov, B. N.; Tumskiy, R. S.; Burov, A. M.; Pylaev, T. E.; Khlebtsov, N. G. Quantifying the numbers of gold nanoparticles in the test zone of lateral flow immunoassay strips. *ACS Applied Nano Materials* **2019**, *2*, 5020−5028.
(270) Grant, B. D.; Anderson, C. E.; Williford, J. R.; Alonzo, L. F.; Glukhova, V. A.; Boyle, D. S.; Weigl, B. H.; Nichols, K. P. SARS-CoV-2 coronavirus nucleocapsid antigen-detecting half-strip lateral flow assay toward the development of point of care tests using commercially available reagents. *Anal. Chem.* **2020**, *92*, 11305−11309.
(271) Langmuir, I. The Adsorption of gases on plane surfaces of glass, mica and platinum. *J. Am. Chem. Soc.* **1918**, *40*, 1361−1403.
(272) Macritchie, F. The adsorption of proteins at the solid/liquid interface. *J. Colloid Interface Sci.* **1972**, *38*, 484−488.
(273) Penners, G.; Priel, Z.; Silberberg, A. Irreversible adsorption of triple-helical soluble collagen monomers from solution to glass and other surfaces. *J. Colloid Interface Sci.* **1981**, *80*, 437−444.
(274) van der Merwe, P. A.; Barclay, A. N. Analysis of cell-adhesion molecule interactions using surface plasmon resonance. *Curr. Opin. Immunol.* **1996**, *8*, 257−261.
(275) Karlsson, R.; Fält, A. Experimental design for kinetic analysis of protein-protein interactions with surface plasmon resonance biosensors. *J. Immunol. Methods* **1997**, *200*, 121−133.
(276) Stenberg, M.; Nygren, H. Kinetics of antigen-antibody reactions at solid-liquid interfaces. *J. Immunol. Methods* **1988**, *113*, 3−15.
(277) Myszka, D. G. Kinetic analysis of macromolecular interactions using surface plasmon resonance biosensors. *Curr. Opin. Biotechnol.* **1997**, *8*, 50−57.
(278) Schuck, P. Kinetics of ligand binding to receptor immobilized in a polymer matrix, as detected with an evanescent wave biosensor. I. A computer simulation of the influence of mass transport. *Biophys. J.* **1996**, *70*, 1230−1249.
(279) Glaser, R. W. Antigen-antibody binding and mass transport by convection and diffusion to a surface: a two-dimensional computer model of binding and dissociation kinetics. *Anal. Biochem.* **1993**, *213*, 152−161.
(280) Latour, R. A. The Langmuir isotherm: a commonly applied but misleading approach for the analysis of protein adsorption behavior. *J. Biomed. Mater. Res., Part A* **2015**, *103*, 949−958.
(281) Soderquist, M. E.; Walton, A. G. Structural changes in proteins adsorbed on polymer surfaces. *J. Colloid Interface Sci.* **1980**, *75*, 386−397.
(282) Kurrat, R.; Ramsden, J. J.; Prenosil, J. E. Kinetic model for serum albumin adsorption: experimental verification. *J. Chem. Soc., Faraday Trans.* **1994**, *90*, 587−590.
(283) Ramsden, J. J.; Roush, D. J.; Gill, D. S.; Kurrat, R.; Willson, R. C. Protein adsorption kinetics drastically altered by repositioning a single charge. *J. Am. Chem. Soc.* **1995**, *117*, 8511−8516.
(284) Kurrat, R.; Prenosil, J. E.; Ramsden, J. J. Kinetics of human and bovine serum albumin adsorption at silica-titania surfaces. *J. Colloid Interface Sci.* **1997**, *185*, 1−8.
(285) Billsten, P.; Wahlgren, M.; Arnebrant, T.; McGuire, J.; Elwing, H. Structural changes of T4 lysozyme upon adsorption to silica nanoparticles measured by circular dichroism. *J. Colloid Interface Sci.* **1995**, *175*, 77−82.

https://doi.org/10.1021/acs.chemrev.1c00044
Chem. Rev. 2021, 121, 8095−8160

(286) Hitchcock, D. I. Protein films on collodion membranes. *J. Gen. Physiol.* **1925**, *8*, 61−74.
(287) Guldberg, C. M. *Untersuchungen über die chemischen affinitäten. Abhandlungen aus den jahren 1864, 1867, 1879*; W. Engelmann: Leipzig, 1899.
(288) Langmuir, I. The constitution and fundamental properties of solids and liquids. Part I. Solids. *J. Am. Chem. Soc.* **1916**, *38*, 2221−2295.
(289) Bradley, R. S. XXIII. Linear adsorption. The London, Edinburgh, and Dublin. *Philosophical Magazine and Journal of Science* **1929**, *8*, 202−204.
(290) Goutelle, S.; Maurin, M.; Rougier, F.; Barbaut, X.; Bourguignon, L.; Ducher, M.; Maire, P. The Hill equation: a review of its capabilities in pharmacological modelling. *Fundam. Clin. Pharmacol.* **2008**, *22*, 633−648.
(291) Gilson, M. K.; Given, J. A.; Bush, B. L.; McCammon, J. A. The statistical-thermodynamic basis for computation of binding affinities: a critical review. *Biophys. J.* **1997**, *72*, 1047−1069.
(292) Ho, Y. S.; McKay, G. Pseudo-second order model for sorption processes. *Process Biochem.* **1999**, *34*, 451−465.
(293) Azizian, S. Kinetic models of sorption: a theoretical analysis. *J. Colloid Interface Sci.* **2004**, *276*, 47−52.
(294) Liu, Y.; Shen, L. From Langmuir kinetics to first- and second-order rate equations for adsorption. *Langmuir* **2008**, *24*, 11625−11630.
(295) Marczewski, A. W. Analysis of kinetic Langmuir model. Part I: Integrated kinetic Langmuir equation (IKL): a new complete analytical solution of the Langmuir rate equation. *Langmuir* **2010**, *26*, 15229−15238.
(296) Doumas, B. T. Standards for total serum protein assays−a collaborative study. *Clin. Chem.* **1975**, *21*, 1159−1166.
(297) Masson, J.-F.; Battaglia, T. M.; Khairallah, P.; Beaudoin, S.; Booksh, K. S. Quantitative measurement of cardiac markers in undiluted serum. *Anal. Chem.* **2007**, *79*, 612−619.
(298) Granqvist, N.; Hanning, A.; Eng, L.; Tuppurainen, J.; Viitala, T. Label-enhanced surface plasmon resonance: a new concept for improved performance in optical biosensor analysis. *Sensors* **2013**, *13*, 15348−15363.
(299) Dickinson, E. Mixed biopolymers at interfaces: Competitive adsorption and multilayer structures. *Food Hydrocolloids* **2011**, *25*, 1966−1983.
(300) Limousin, G.; Gaudet, J.-P.; Charlet, L.; Szenknect, S.; Barthès, V.; Krimissa, M. Sorption isotherms: A review on physical bases, modeling and measurement. *Appl. Geochem.* **2007**, *22*, 249−275.
(301) Yang, Y. J.; Lee, C. H.; Koo, Y. M. Separation of amino acids by simulated moving bed using competitive Langmuir isotherm. *Biotechnol. Bioprocess Eng.* **2004**, *9*, 331.
(302) Bastidas, D. M.; Gómez, R. R.; Cano, E. The isotherm slope. A criterion for studying the adsorption mechanism of benzotriazole on copper in sulphuric acid. *Rev. Metal.* **2005**, *41*, 98−106.
(303) Chen, C. Evaluation of equilibrium sorption isotherm equations. *Open Chem. Eng. J.* **2013**, *7*, 24−44.
(304) Stefan, M. I.; Le Novère, N. Cooperative binding. *PLoS Comput. Biol.* **2013**, *9*, No. e1003106.
(305) Whitty, A. Cooperativity and biological complexity. *Nat. Chem. Biol.* **2008**, *4*, 435−439.
(306) Mattiasson, B.; Ye, L. *Molecularly imprinted polymers in Biotechnology*; Springer International Publishing, 2015; Vol. *150*; pp 1−231.
(307) Konkoli, Z. Safe uses of Hill's model: an exact comparison with the Adair-Klotz model. *Theor. Biol. Med. Modell.* **2011**, *8*, 10.
(308) Hofmeyr, J. H.; Cornish-Bowden, A. The reversible Hill equation: how to incorporate cooperative enzymes into metabolic models. *Bioinformatics* **1997**, *13*, 377−385.
(309) Klotz, I. M. The application of the law of mass action to binding by proteins; interactions with calcium. *Arch. Biochem.* **1946**, *9*, 109−117.
(310) Adair, G. S.; Bock, V.; Field, H. The hemoglobin system: VI. The oxygen dissociation curve of hemoglobin. *J. Biol. Chem.* **1925**, *63*, 529−545.
(311) Borwankar, R. P.; Wasan, D. T. The kinetics of adsorption of surface active agents at gas-liquid surfaces. *Chem. Eng. Sci.* **1983**, *38*, 1637−1649.
(312) Chun, J. H.; Ra, K. H.; Kim, N. Y. Qualitative analysis of the Frumkin adsorption isotherm of the over-potentially deposited hydrogen at the poly-Ni/KOH aqueous electrolyte interface using the phase-shift method. *J. Electrochem. Soc.* **2002**, *149*, E325−E330.
(313) Volkova-Gugeshashvili, M. I.; Volkov, A. G.; Markin, V. S. Adsorption at liquid interfaces: The generalized Frumkin isotherm and interfacial structure. *Russ. J. Electrochem.* **2006**, *42*, 1073−1078.
(314) Rajendran, P. *Plasmonic nanoparticles with tailored attinebility for direct oligonucleotide sensing - optimization and application*. Ph.D. thesis, ETH Zurich, 2015.
(315) Rényi, A. Car parking problem. *Sel. Trans. Math. Stat. Prob* **1963**, *4*, 205.
(316) Flory, P. J. Intramolecular reaction between neighboring substituents of vinyl polymers. *J. Am. Chem. Soc.* **1939**, *61*, 1518−1521.
(317) Evans, J. W. Random and cooperative sequential adsorption. *Rev. Mod. Phys.* **1993**, *65*, 1281−1329.
(318) Talbot, J.; Tarjus, G.; Van Tassel, P. R.; Viot, P. From car parking to protein adsorption: an overview of sequential adsorption processes. *Colloids Surf., A* **2000**, *165*, 287−324.
(319) Onoda, G. Y.; Liniger, E. G. Experimental determination of the random-parking limit in two dimensions. *Phys. Rev. A: At., Mol., Opt. Phys.* **1986**, *33*, 715−716.
(320) Wojtaszczyk, P.; Schaaf, P.; Senger, B.; Zembala, M.; Voegel, J. C. Statistical properties of surfaces covered by large spheres. *J. Chem. Phys.* **1993**, *99*, 7198−7208.
(321) Adamczyk, Z.; Siwek, B.; Zembala, M.; Belouschek, P. Kinetics of localized adsorption of colloid particles. *Adv. Colloid Interface Sci.* **1994**, *48*, 151−280.
(322) Lavalle, P.; Schaaf, P.; Ostafin, M.; Voegel, J. C.; Senger, B. Extended random sequential adsorption model of irreversible deposition processes: from simulations to experiments. *Proc. Natl. Acad. Sci. U. S. A.* **1999**, *96*, 11100−11105.
(323) Feder, J.; Giaever, I. Adsorption of ferritin. *J. Colloid Interface Sci.* **1980**, *78*, 144−154.
(324) Ramsden, J. J. Experimental methods for investigating protein adsorption kinetics at surfaces. *Q. Rev. Biophys.* **1994**, *27*, 41−105.
(325) Senger, B.; Schaaf, P.; Voegel, J. C.; Johner, A.; Schmitt, A.; Talbot, J. Influence of bulk diffusion on the adsorption of hard spheres on a flat surface. *J. Chem. Phys.* **1992**, *97*, 3813−3820.
(326) Norde, W.; Favier, J. P. Structure of adsorbed and desorbed proteins. *Colloids Surf.* **1992**, *64*, 87−93.
(327) Boyer, D.; Talbot, J.; Tarjus, G.; Van Tassel, P.; Viot, P. Exactly solvable models of irreversible adsorption with particle spreading. *Phys. Rev. E: Stat. Phys., Plasmas, Fluids, Relat. Interdiscip. Top.* **1994**, *49*, 5525−5534.
(328) Elaissari, A.; Pefferkorn, E. Polyelectrolyte adsorption at solid/liquid interfaces: A simple model for the structural relaxation and excluded area effects. *J. Colloid Interface Sci.* **1991**, *143*, 85−91.
(329) Szöllősi, G. J.; Derényi, I.; Vörös, J. Reversible mesoscopic model of protein adsorption: From equilibrium to dynamics. *Phys. A* **2004**, *343*, 359−375.
(330) Norde, W.; MacRitchie, F.; Nowicka, G.; Lyklema, J. Protein adsorption at solid-liquid interfaces: Reversibility and conformation aspects. *J. Colloid Interface Sci.* **1986**, *112*, 447−456.
(331) Norde, W. Adsorption of proteins from solution at the solid-liquid interface. *Adv. Colloid Interface Sci.* **1986**, *25*, 267−340.
(332) Buijs, J.; Norde, W.; Lichtenbelt, J. W. T. Changes in the secondary structure of adsorbed IgG and F (ab ') 2 studied by FTIR spectroscopy. *Langmuir* **1996**, *12*, 1605−1613.
(333) Wertz, C. F.; Santore, M. M. Adsorption and relaxation kinetics of albumin and fibrinogen on hydrophobic surfaces: single-species and competitive behavior. *Langmuir* **1999**, *15*, 8884−8894.
(334) Wertz, C. F.; Santore, M. M. Effect of surface hydrophobicity on adsorption and relaxation kinetics of albumin and fibrinogen: single-species and competitive behavior. *Langmuir* **2001**, *17*, 3006−3016.

https://doi.org/10.1021/acs.chemrev.1c00044
Chem. Rev. 2021, 121, 8095−8160

(335) Rabe, M.; Verdes, D.; Rankl, M.; Artus, G. R. J.; Seeger, S. A comprehensive study of concepts and phenomena of the nonspecific adsorption of beta-lactoglobulin. *ChemPhysChem* **2007**, *8*, 862−872.
(336) Van Tassel, P. R.; Viot, P.; Tarjus, G. A kinetic model of partially reversible protein adsorption. *J. Chem. Phys.* **1997**, *106*, 761−770.
(337) Van Tassel, P. R. Statistical mechanical modeling of protein adsorption. *Materialwiss. Werkstofftech.* **2003**, *34*, 1129−1132.
(338) Ball, V.; Schaaf, P.; Voegel, J.-C. *Biopolymers at Interfaces*; CRC Press, 2003; pp 453−484.
(339) Hirsh, S. L.; McKenzie, D. R.; Nosworthy, N. J.; Denman, J. A.; Sezerman, O. U.; Bilek, M. M. M. The Vroman effect: competitive protein exchange with dynamic multilayer protein aggregates. *Colloids Surf., B* **2013**, *103*, 395−404.
(340) Dermutz, H.; Grüter, R. R.; Truong, A. M.; Demkó, L.; Vörös, J.; Zambelli, T. Local polymer replacement for neuron patterning and in situ neurite guidance. *Langmuir* **2014**, *30*, 7037−7046.
(341) Lundström, I. Models of protein adsorption on solid surfaces. *Surfactants, Adsorption, Surface Spectroscopy and Disperse Systems* **1985**, *70*, 76−82.
(342) Vroman, L.; Adams, A. Findings with the recording ellipsometer suggesting rapid exchange of specific plasma proteins at liquid/solid interfaces. *Surf. Sci.* **1969**, *16*, 438−446.
(343) Horbett, T. A. Mass action effects on competitive adsorption of fibrinogen from hemoglobin solutions and from plasma. *Thromb. Haemostasis* **1984**, *51*, 174−181.
(344) Wertz, C. F.; Santore, M. M. Fibrinogen adsorption on hydrophilic and hydrophobic surfaces: geometrical and energetic aspects of interfacial relaxations. *Langmuir* **2002**, *18*, 706−715.
(345) Rabe, M.; Verdes, D.; Seeger, S. Understanding protein adsorption phenomena at solid surfaces. *Adv. Colloid Interface Sci.* **2011**, *162*, 87−106.
(346) Pasche, S.; De Paul, S. M.; Vörös, J.; Spencer, N. D.; Textor, M. Poly(l-lysine)-graft-poly(ethylene glycol) assembled monolayers on niobium oxide surfaces: a quantitative study of the influence of polymer interfacial architecture on resistance to protein adsorption by ToF-SIMS and in situ OWLS. *Langmuir* **2003**, *19*, 9216−9225.
(347) Timney, B. L.; Tetenbaum-Novatt, J.; Agate, D. S.; Williams, R.; Zhang, W.; Chait, B. T.; Rout, M. P. Simple kinetic relationships and nonspecific competition govern nuclear import rates in vivo. *J. Cell Biol.* **2006**, *175*, 579−593.
(348) Eddowes, M. J. Direct immunochemical sensing: basic chemical principles and fundamental limitations. *Biosensors* **1987**, *3*, 1−15.
(349) Schuck, P. Reliable determination of binding affinity and kinetics using surface plasmon resonance biosensors. *Curr. Opin. Biotechnol.* **1997**, *8*, 498−502.
(350) Schuck, P.; Boyd, L. F.; Andersen, P. S. Measuring protein interactions by optical biosensors. *Curr. Protoc. Protein Sci.* **1999**, *17*, DOI: 10.1002/0471140864.ps2002s17.
(351) Karlsson, R.; Katsamba, P. S.; Nordin, H.; Pol, E.; Myszka, D. G. Analyzing a kinetic titration series using affinity biosensors. *Anal. Biochem.* **2006**, *349*, 136−147.
(352) Myszka, D. G.; Morton, T. A.; Doyle, M. L.; Chaiken, I. M. Kinetic analysis of a protein antigen-antibody interaction limited by mass transport on an optical biosensor. *Biophys. Chem.* **1997**, *64*, 127−137.
(353) O'Shannessy, D. J.; Brigham-Burke, M.; Soneson, K. K.; Hensley, P.; Brooks, I. Determination of rate and equilibrium binding constants for macromolecular interactions using surface plasmon resonance: use of nonlinear least squares analysis methods. *Anal. Biochem.* **1993**, *212*, 457−468.
(354) Kenausis, G. L.; Vörös, J.; Elbert, D. L.; Huang, N.; Hofer, R.; Ruiz-Taylor, L.; Textor, M.; Hubbell, J. A.; Spencer, N. D. Poly(l-lysine)-g-poly(ethylene glycol) layers on metal oxide surfaces: attachment mechanism and effects of polymer architecture on resistance to protein adsorption. *J. Phys. Chem. B* **2000**, *104*, 3298−3309.
(355) Huang, N.-P.; Michel, R.; Voros, J.; Textor, M.; Hofer, R.; Rossi, A.; Elbert, D. L.; Hubbell, J. A.; Spencer, N. D. Poly(l-lysine)-g-poly(ethylene glycol) layers on metal oxide surfaces: surface-analytical characterization and resistance to serum and fibrinogen adsorption. *Langmuir* **2001**, *17*, 489−498.
(356) Lowe, S.; O'Brien-Simpson, N. M.; Connal, L. A. Antibiofouling polymer interfaces: poly(ethylene glycol) and other promising candidates. *Polym. Chem.* **2015**, *6*, 198−212.
(357) Ulman, A. Formation and structure of self-assembled monolayers. *Chem. Rev.* **1996**, *96*, 1533−1554.
(358) O'Shannessy, D. J.; Winzor, D. J. Interpretation of deviations from pseudo-first-order kinetic behavior in the characterization of ligand binding by biosensor technology. *Anal. Biochem.* **1996**, *236*, 275−283.
(359) Schuck, P.; Minton, A. P. Analysis of mass transport-limited binding kinetics in evanescent wave biosensors. *Anal. Biochem.* **1996**, *240*, 262−272.
(360) Fisher, R. J.; Fivash, M.; Casas-Finet, J.; Erickson, J. W.; Kondoh, A.; Bladen, S. V.; Fisher, C.; Watson, D. K.; Papas, T. Real-time DNA binding measurements of the ETS1 recombinant oncoproteins reveal significant kinetic differences between the p42 and p51 isoforms. *Protein Sci.* **1994**, *3*, 257−266.
(361) Yarmush, M. L.; Patankar, D. B.; Yarmush, D. M. An analysis of transport resistances in the operation of BIAcore™; implications for kinetic studies of biospecific interactions. *Mol. Immunol.* **1996**, *33*, 1203−1214.
(362) Katsamba, P. S.; et al. Kinetic analysis of a high-affinity antibody/antigen interaction performed by multiple Biacore users. *Anal. Biochem.* **2006**, *352*, 208−221.
(363) Lipschultz, C. A.; Li, Y.; Smith-Gill, S. Experimental design for analysis of complex kinetics using surface plasmon resonance. *Methods* **2000**, *20*, 310−318.
(364) Schaaf, P.; Voegel, J.-C.; Senger, B. From random sequential adsorption to ballistic deposition: a general view of irreversible deposition processes. *J. Phys. Chem. B* **2000**, *104*, 2204−2214.
(365) Schaaf, P.; Talbot, J. Surface exclusion effects in adsorption processes. *J. Chem. Phys.* **1989**, *91*, 4401−4409.
(366) Glaser, R. W.; Hausdorf, G. Binding kinetics of an antibody against HIV p24 core protein measured with real-time biomolecular interaction analysis suggest a slow conformational change in antigen p24. *J. Immunol. Methods* **1996**, *189*, 1−14.
(367) Liu, C.; Huang, D.; Yang, T.; Cremer, P. S. Simultaneous detection of multiple proteins that bind to the identical ligand in supported lipid bilayers. *Anal. Chem.* **2015**, *87*, 7163−7170.
(368) Wild, D.; Kodak, E. Elsevier, 2013.
(369) Saviranta, P.; Okon, R.; Brinker, A.; Warashina, M.; Eppinger, J.; Geierstanger, B. H. Evaluating sandwich immunoassays in microarray format in terms of the ambient analyte regime. *Clin. Chem.* **2004**, *50*, 1907−1920.
(370) Chang, L.; Rissin, D. M.; Fournier, D. R.; Piech, T.; Patel, P. P.; Wilson, D. H.; Duffy, D. C. Single molecule enzyme-linked immunosorbent assays: theoretical considerations. *J. Immunol. Methods* **2012**, *378*, 102−115.
(371) Ekins, R.; Chu, F.; Biggart, E. Development of microspot multi-analyte ratiometric immunoassay using dual fluorescent-labelled antibodies. *Anal. Chim. Acta* **1989**, *227*, 73−96.
(372) Tanno, A. *Resolving the challenges of hand-held electrochemical biosensing*. Ph.D. thesis, ETH Zurich, 2018.
(373) Ekins, R. Measurement of free hormones in blood. *Endocr. Rev.* **1990**, *11*, 5−46.
(374) Chiu, M. L.; Lawi, W.; Snyder, S. T.; Wong, P. K.; Liao, J. C.; Gau, V. Matrix effects - a challenge toward automation of molecular analysis. *JALA* **2010**, *15*, 233−242.
(375) Krotzky, A. J.; Zeeh, B. Immunoassays for residue analysis of agrochemicals: Proposed guidelines for precision, standardization and quality control. *Pure Appl. Chem.* **1995**, *67*, 2065−2088.
(376) Yoshida, H.; Imafuku, Y.; Nagai, T. Matrix effects in clinical immunoassays and the effect of preheating and cooling analytical samples. *Clin. Chem. Lab. Med.* **2004**, *42*, 51−56.
(377) Adams, J. Bound to work: the free hormone hypothesis revisited. *Cell* **2005**, *122*, 647−9.

(378) Laurent, M. R.; et al. Sex hormone-binding globulin regulation of androgen bioactivity in vivo: Validation of the free hormone hypothesis. *Sci. Rep.* **2016**, *6*, 1−12.
(379) Midgley, J. E. M.; Ekins, R. The free thyroid hormone hypothesis and measurement of free hormones. *Clin. Chem.* **1993**, *39*, 1342−1344.
(380) Stenberg, M.; Stiblert, L.; Nygren, H. External diffusion in solid-phase immunoassays. *J. Theor. Biol.* **1986**, *120*, 129−140.
(381) Hansen, R.; Bruus, H.; Callisen, T. H.; Hassager, O. Transient convection, diffusion, and adsorption in surface-based biosensors. *Langmuir* **2012**, *28*, 7557−7563.
(382) de Mol, N. J.; Fischer, M. J. *Handbook of Surface Plasmon Resonance*; 2008; pp 123−172.
(383) Crank, J. *The Mathematics of Diffusion*; 1975.
(384) Ward, A. F. H.; Tordai, L. Time-dependence of boundary tensions of solutions I. the role of diffusion in time-effects. *J. Chem. Phys.* **1946**, *14*, 453−461.
(385) Nygren, H.; Werthen, M.; Stenberg, M. Kinetics of antibody binding to solid-phase-immobilised antigen. Effect of diffusion rate limitation and steric interaction. *J. Immunol. Methods* **1987**, *101*, 63−71.
(386) Ober, R. J.; Ward, E. S. The influence of signal noise on the accuracy of kinetic constants measured by surface plasmon resonance experiments. *Anal. Biochem.* **1999**, *273*, 49−59.
(387) Myszka, D. G.; Arulanantham, P. R.; Sana, T.; Wu, Z.; Morton, T. A.; Ciardelli, T. L. Kinetic analysis of ligand binding to interleukin-2 receptor complexes created on an optical biosensor surface. *Protein Sci.* **1996**, *5*, 2468−2478.
(388) Saftics, A.; Kurunczi, S.; Peter, B.; Szekacs, I.; Ramsden, J. J.; Horvath, R. Data evaluation for surface-sensitive label-free methods to obtain real-time kinetic and structural information of thin films: A practical review with related software packages. *Adv. Colloid Interface Sci.* **2021**, 102431.
(389) Rissin, D. M.; Wilson, D. H.; Duffy, D. C. *The Immunoassay Handbook*; 2013; pp 223−242.
(390) Wild, D. *The immunoassay handbook: theory and applications of ligand binding, ELISA and related techniques*; Newnes, 2013.
(391) Armbruster, D. A.; Pry, T. Limit of blank, limit of detection and limit of quantitation. *Clin. Biochem. Rev.* **2008**, *29* (Suppl 1), S49−52.
(392) Mehrotra, P. Biosensors and their applications - A review. *J. Oral Biol. Craniofac Res.* **2016**, *6*, 153−159.
(393) Frank, S. A. *Specificity and cross-reactivity*; Princeton University Press, 2002.
(394) Baker, M. Reproducibility crisis: blame it on the antibodies. *Nature* **2015**, *521*, 274−276.
(395) Hudson, M. E.; Pozdnyakova, I.; Haines, K.; Mor, G.; Snyder, M. Identification of differentially expressed proteins in ovarian cancer using high-density protein microarrays. *Proc. Natl. Acad. Sci. U. S. A.* **2007**, *104*, 17494−17499.
(396) Haab, B. B.; Dunham, M. J.; Brown, P. O. Protein microarrays for highly parallel detection and quantitation of specific proteins and antibodies in complex solutions. *Genome Biol.* **2001**, *2*, RESEARCH0004.
(397) Uhlén, M.; et al. Proteomics. Tissue-based map of the human proteome. *Science* **2015**, *347*, 1260419.
(398) Schwenk, J. M.; Igel, U.; Neiman, M.; Langen, H.; Becker, C.; Bjartell, A.; Ponten, F.; Wiklund, F.; Grönberg, H.; Nilsson, P.; Uhlen, M. Toward next generation plasma profiling via heat-induced epitope retrieval and array-based assays. *Mol. Cell. Proteomics* **2010**, *9*, 2497−2507.
(399) Zichi, D.; Eaton, B.; Singer, B.; Gold, L. Proteomics and diagnostics: let's get specific, again. *Curr. Opin. Chem. Biol.* **2008**, *12*, 78−85.
(400) Anderson, N. L.; Anderson, N. G. The human plasma proteome: history, character, and diagnostic prospects. *Mol. Cell. Proteomics* **2002**, *1*, 845−867.
(401) Brody, E. N.; Gold, L.; Lawn, R. M.; Walker, J. J.; Zichi, D. High-content affinity-based proteomics: unlocking protein biomarker discovery. *Expert Rev. Mol. Diagn.* **2010**, *10*, 1013−1022.
(402) Rifai, N.; Gillette, M. A.; Carr, S. A. Protein biomarker discovery and validation: the long and uncertain path to clinical utility. *Nat. Biotechnol.* **2006**, *24*, 971−983.
(403) Gold, L.; et al. Aptamer-based multiplexed proteomic technology for biomarker discovery. *PLoS One* **2010**, *5*, No. e15004.
(404) Gibbs, J.; Kennebunk, M. E. Effective blocking procedures. ELISA Technical Bulletin. Kennebunk, ME: Corning Incorporated Life Sciences, 2001; pp 1−6.
(405) Tate, J.; Ward, G. Interferences in immunoassay. *Clin. Biochem. Rev.* **2004**, *25*, 105−120.
(406) Vogt, R. F., Jr; Phillips, D. L.; Henderson, L. O.; Whitfield, W.; Spierto, F. W. Quantitative differences among various proteins as blocking agents for ELISA microtiter plates. *J. Immunol. Methods* **1987**, *101*, 43−50.
(407) Kenna, J. G.; Major, G. N.; Williams, R. S. Methods for reducing non-specific antibody binding in enzyme-linked immunosorbent assays. *J. Immunol. Methods* **1985**, *85*, 409−419.
(408) Nakamura, R.; Muguruma, H.; Ikebukuro, K.; Sasaki, S.; Nagata, R.; Karube, I.; Pedersen, H. A plasma-polymerized film for surface plasmon resonance immunosensing. *Anal. Chem.* **1997**, *69*, 4649−4652.
(409) Chapman, R. G.; Ostuni, E.; Takayama, S.; Holmlin, R. E.; Yan, L.; Whitesides, G. M. Surveying for surfaces that resist the adsorption of proteins. *J. Am. Chem. Soc.* **2000**, *122*, 8303−8304.
(410) Prime, K. L.; Whitesides, G. M. Self-assembled organic monolayers: model systems for studying adsorption of proteins at surfaces. *Science* **1991**, *252*, 1164−1167.
(411) Piehler, J.; Brecht, A.; Valiokas, R.; Liedberg, B.; Gauglitz, G. A high-density poly(ethylene glycol) polymer brush for immobilization on glass-type surfaces. *Biosens. Bioelectron.* **2000**, *15*, 473−481.
(412) Vaisocherová, H.; Brynda, E.; Homola, J. Functionalizable low-fouling coatings for label-free biosensing in complex biological media: advances and applications. *Anal. Bioanal. Chem.* **2015**, *407*, 3927−3953.
(413) Poirier, G. E. *Mechanism of formation of Au vacancy islands in alkanethiol monolayers on Au(111)*. 1997.
(414) Knobler, C. M.; Desai, R. C. Phase transitions in monolayers. *Annu. Rev. Phys. Chem.* **1992**, *43*, 207−236.
(415) Baggerman, J.; Smulders, M. M. J.; Zuilhof, H. Romantic surfaces: a systematic overview of stable, biospecific, and antifouling zwitterionic surfaces. *Langmuir* **2019**, *35*, 1072−1084.
(416) Zolotarjova, N.; Martosella, J.; Nicol, G.; Bailey, J.; Boyes, B. E.; Barrett, W. C. Differences among techniques for high-abundant protein depletion. *Proteomics* **2005**, *5*, 3304−3313.
(417) Wilson, R. Sensitivity and specificity: twin goals of proteomics assays. Can they be combined? *Expert Rev. Proteomics* **2013**, *10*, 135−149.
(418) Whiteaker, J. R.; Zhao, L.; Frisch, C.; Ylera, F.; Harth, S.; Knappik, A.; Paulovich, A. G. High-affinity recombinant antibody fragments (Fabs) can be applied in peptide enrichment immuno-MRM assays. *J. Proteome Res.* **2014**, *13*, 2187−2196.
(419) Davies, C. *The Immunoassay Handbook*; Elsevier, 2013; pp 29−59.
(420) Pieper, R.; Su, Q.; Gatlin, C. L.; Huang, S.-T.; Anderson, N. L.; Steiner, S. Multi-component immunoaffinity subtraction chromatography: an innovative step towards a comprehensive survey of the human plasma proteome. *Proteomics* **2003**, *3*, 422−432.
(421) Zhou, M.; Lucas, D. A.; Chan, K. C.; Issaq, H. J.; Petricoin, E. F., 3rd; Liotta, L. A.; Veenstra, T. D.; Conrads, T. P. An investigation into the human serum "interactome. *Electrophoresis* **2004**, *25*, 1289−1298.
(422) Polaskova, V.; Kapur, A.; Khan, A.; Molloy, M. P.; Baker, M. S. High-abundance protein depletion: Comparison of methods for human plasma biomarker discovery. *Electrophoresis* **2010**, *31*, 471−482.
(423) Ahmed, N.; Barker, G.; Oliva, K.; Garfin, D.; Talmadge, K.; Georgiou, H.; Quinn, M.; Rice, G. An approach to remove albumin for the proteomic analysis of low abundance biomarkers in human serum. *Proteomics* **2003**, *3*, 1980−1987.
(424) Boschetti, E.; Righetti, P. G. The ProteoMiner in the proteomic arena: a non-depleting tool for discovering low-abundance species. *J. Proteomics* **2008**, *71*, 255−264.

https://doi.org/10.1021/acs.chemrev.1c00044
Chem. Rev. 2021, 121, 8095−8160

(425) Qian, W.-J.; Kaleta, D. T.; Petritis, B. O.; Jiang, H.; Liu, T.; Zhang, X.; Mottaz, H. M.; Varnum, S. M.; Camp, D. G., 2nd; Huang, L.; Fang, X.; Zhang, W.-W.; Smith, R. D. Enhanced detection of low abundance human plasma proteins using a tandem IgY12-SuperMix immunoaffinity separation strategy. *Mol. Cell. Proteomics* **2008**, *7*, 1963−1973.
(426) Moritz, R. L.; Ji, H.; Schütz, F.; Connolly, L. M.; Kapp, E. A.; Speed, T. P.; Simpson, R. J. A proteome strategy for fractionating proteins and peptides using continuous free-flow electrophoresis coupled off-line to reversed-phase high-performance liquid chromatography. *Anal. Chem.* **2004**, *76*, 4811−4824.
(427) Li, X.; Gong, Y.; Wang, Y.; Wu, S.; Cai, Y.; He, P.; Lu, Z.; Ying, W.; Zhang, Y.; Jiao, L.; He, H.; Zhang, Z.; He, F.; Zhao, X.; Qian, X. *Exploring the Human Plasma Proteome*; Wiley-VCH Verlag GmbH & Co. KGaA, 2006; pp 221−247.
(428) Yocum, A. K.; Yu, K.; Oe, T.; Blair, I. A. Effect of immunoaffinity depletion of human serum during proteomic investigations. *J. Proteome Res.* **2005**, *4*, 1722−1731.
(429) Barnea, E.; Sorkin, R.; Ziv, T.; Beer, I.; Admon, A. Evaluation of prefractionation methods as a preparatory step for multidimensional based chromatography of serum proteins. *Proteomics* **2005**, *5*, 3367−3375.
(430) Landry, J. P.; Ke, Y.; Yu, G.-L.; Zhu, X. D. Measuring affinity constants of 1450 monoclonal antibodies to peptide targets with a microarray-based label-free assay platform. *J. Immunol. Methods* **2015**, *417*, 86−96.
(431) Ruigrok, V. J. B.; Levisson, M.; Eppink, M. H. M.; Smidt, H.; van der Oost, J. Alternative affinity tools: more attractive than antibodies? *Biochem. J.* **2011**, *436*, 1−13.
(432) Adachi, T.; Nakamura, Y. Aptamers: a review of their chemical properties and modifications for therapeutic application. *Molecules* **2019**, *24*, 4229.
(433) Tuerk, C.; Gold, L. Systematic evolution of ligands by exponential enrichment: RNA ligands to bacteriophage T4 DNA polymerase. *Science* **1990**, *249*, 505−510.
(434) Ellington, A. D.; Szostak, J. W. In vitro selection of RNA molecules that bind specific ligands. *Nature* **1990**, *346*, 818−822.
(435) Gold, L.; Janjic, N.; Jarvis, T.; Schneider, D.; Walker, J. J.; Wilcox, S. K.; Zichi, D. Aptamers and the RNA world, past and present. *Cold Spring Harbor Perspect. Biol.* **2012**, *4*, a003582.
(436) Binz, H. K.; Amstutz, P.; Plückthun, A. Engineering novel binding proteins from nonimmunoglobulin domains. *Nat. Biotechnol.* **2005**, *23*, 1257−1268.
(437) Yang, K.-A.; Barbu, M.; Halim, M.; Pallavi, P.; Kim, B.; Kolpashchikov, D. M.; Pecic, S.; Taylor, S.; Worgall, T. S.; Stojanovic, M. N. Recognition and sensing of low-epitope targets via ternary complexes with oligonucleotides and synthetic receptors. *Nat. Chem.* **2014**, *6*, 1003−1008.
(438) Yang, K.-A.; Pei, R.; Stojanovic, M. N. In vitro selection and amplification protocols for isolation of aptameric sensors for small molecules. *Methods* **2016**, *106*, 58−65.
(439) Hopfield, J. J.; Yamane, T.; Yue, V.; Coutts, S. M. Direct experimental evidence for kinetic proofreading in amino acylation of tRNAIle. *Proc. Natl. Acad. Sci. U. S. A.* **1976**, *73*, 1164−1168.
(440) Gold, L.; Walker, J. J.; Wilcox, S. K.; Williams, S. Advances in human proteomics at high scale with the SOMAscan proteomics platform. *New Biotechnol.* **2012**, *29*, 543−549.
(441) Binz, H. K.; Stumpp, M. T.; Forrer, P.; Amstutz, P.; Plückthun, A. Designing repeat proteins: well-expressed, soluble and stable proteins from combinatorial libraries of consensus ankyrin repeat proteins. *J. Mol. Biol.* **2003**, *332*, 489−503.
(442) Silverman, J.; et al. Multivalent avimer proteins evolved by exon shuffling of a family of human receptor domains. *Nat. Biotechnol.* **2005**, *23*, 1556−1561.
(443) Tiede, C.; et al. Affimer proteins are versatile and renewable affinity reagents. *eLife* **2017**, *6*, DOI: 10.7554/eLife.24903.
(444) Löfblom, J.; Feldwisch, J.; Tolmachev, V.; Carlsson, J.; Ståhl, S.; Frejd, F. Y. Affibody molecules: engineered proteins for therapeutic, diagnostic and biotechnological applications. *FEBS Lett.* **2010**, *584*, 2670−2680.
(445) Skerra, A. Alternative binding proteins: anticalins - harnessing the structural plasticity of the lipocalin ligand pocket to engineer novel binding activities. *FEBS J.* **2008**, *275*, 2677−2683.
(446) Lipovšek, D. Adnectins: engineered target-binding protein therapeutics. *Protein Eng., Des. Sel.* **2011**, *24*, 3−9.
(447) Gebauer, M.; Skerra, A. Engineered protein scaffolds as next-generation antibody therapeutics. *Curr. Opin. Chem. Biol.* **2009**, *13*, 245−255.
(448) Wetzel, S. K.; Settanni, G.; Kenig, M.; Binz, H. K.; Plückthun, A. Folding and unfolding mechanism of highly stable full-consensus ankyrin repeat proteins. *J. Mol. Biol.* **2008**, *376*, 241−257.
(449) Stumpp, M. T.; Binz, H. K.; Amstutz, P. DARPins: a new generation of protein therapeutics. *Drug Discovery Today* **2008**, *13*, 695−701.
(450) Škrlec, K.; Štrukelj, B.; Berlec, A. Non-immunoglobulin scaffolds: a focus on their targets. *Trends Biotechnol.* **2015**, *33*, 408−418.
(451) Solá, R. J.; Griebenow, K. Glycosylation of therapeutic proteins: an effective strategy to optimize efficacy. *BioDrugs* **2010**, *24*, 9−21.
(452) Gupta, S. K.; Shukla, P. Glycosylation control technologies for recombinant therapeutic proteins. *Appl. Microbiol. Biotechnol.* **2018**, *102*, 10457−10468.
(453) Khvorova, A.; Watts, J. K. The chemical evolution of oligonucleotide therapies of clinical utility. *Nat. Biotechnol.* **2017**, *35*, 238−248.
(454) Lostalé-Seijo, I.; Montenegro, J. Synthetic materials at the forefront of gene delivery. *Nature Reviews Chemistry* **2018**, *2*, 258−277.
(455) Crowther, J. R. The ELISA guidebook. *Methods Mol. Biol.* **2000**, *149* (III−IV), 1−413.
(456) Moy, V. T.; Florin, E. L.; Gaub, H. E. Intermolecular forces and energies between ligands and receptors. *Science* **1994**, *266*, 257−259.
(457) Lee, G. U.; Kidwell, D. A.; Colton, R. J. Sensing discrete streptavidin-biotin interactions with atomic force microscopy. *Langmuir* **1994**, *10*, 354−357.
(458) Florin, E. L.; Moy, V. T.; Gaub, H. E. Adhesion forces between individual ligand-receptor pairs. *Science* **1994**, *264*, 415−417.
(459) Merkel, R.; Nassoy, P.; Leung, A.; Ritchie, K.; Evans, E. Energy landscapes of receptor-ligand bonds explored with dynamic force spectroscopy. *Nature* **1999**, *397*, 50−53.
(460) Albrecht, C.; Blank, K.; Lalic-Multhaler, M.; Hirler, S.; Mai, T.; Gilbert, I.; Schiffmann, S.; Bayer, T.; Clausen-Schaumann, H.; Gaub, H. E. DNA: a programmable force sensor. *Science* **2003**, *301*, 367−370.
(461) Rief, M.; Clausen-Schaumann, H.; Gaub, H. E. Sequence-dependent mechanics of single DNA molecules. *Nat. Struct. Biol.* **1999**, *6*, 346−349.
(462) Albrecht, C. H.; Hauke, C.-S.; Gaub, H. E. Differential analysis of biomolecular rupture forces. *J. Phys.: Condens. Matter* **2006**, *18*, S581−S599.
(463) Blank, K.; Lankenau, A.; Mai, T.; Schiffmann, S.; Gilbert, I.; Hirler, S.; Albrecht, C.; Benoit, M.; Gaub, H. E.; Clausen-Schaumann, H. Double-chip protein arrays: force-based multiplex sandwich immunoassays with increased specificity. *Anal. Bioanal. Chem.* **2004**, *379*, 974−981.
(464) Janshoff, A.; Neitzert, M.; Oberdörfer, Y.; et al. Force spectroscopy of molecular systems—single molecule spectroscopy of polymers and biomolecules. *Angew. Chem., Int. Ed.* **2000**, *39*, 3212.
(465) Rief, M.; Spudich, J. A.; Smith, D. A.; Simmons, R. M. *Single-molecule biomechanics with optical methods*; 1999.
(466) Rohr, T. E. *Magnetically assisted binding assays using magnetically labeled binding members*; 1995.
(467) Lee, G. U. *Force discrimination assay*; 2001.
(468) Baselt, D. R.; Lee, G. U.; Natesan, M.; Metzger, S. W.; Sheehan, P. E.; Colton, R. J. A biosensor based on magnetoresistance technology. *Biosens. Bioelectron.* **1998**, *13*, 731−739.
(469) Lee, G. U.; Metzger, S.; Natesan, M.; Yanavich, C.; Dufrêne, Y. F. Implementation of force differentiation in the immunoassay. *Anal. Biochem.* **2000**, *287*, 261−271.
(470) Rife, J. C.; Whitman, L. J. *Fluidic force discrimination*; 2010.

(471) Chang, K.-C.; Hammer, D. A. Influence of direction and type of applied force on the detachment of macromolecularly-bound particles from surfaces. *Langmuir* **1996**, *12*, 2271−2282.
(472) Tekin, H. C.; Cornaglia, M.; Gijs, M. A. M. Attomolar protein detection using a magnetic bead surface coverage assay. *Lab Chip* **2013**, *13*, 1053−1059.
(473) Shiddiky, M. J. A.; Vaidyanathan, R.; Rauf, S.; Tay, Z.; Trau, M. Molecular nanoshearing: an innovative approach to shear off molecules with AC-induced nanoscopic fluid flow. *Sci. Rep.* **2015**, *4*, 3716.
(474) Wang, Y.; Vaidyanathan, R.; Shiddiky, M. J. A.; Trau, M. Enabling rapid and specific surface-enhanced Raman scattering immunoassay using nanoscaled surface shear forces. *ACS Nano* **2015**, *9*, 6354−6362.
(475) Springer, T.; Bockova, M.; Homola, J. Label-free biosensing in complex media: a referencing approach. *Anal. Chem.* **2013**, *85*, 5637−5640.
(476) Nice, E. C.; Catimel, B. Instrumental biosensors: new perspectives for the analysis of biomolecular interactions. *BioEssays* **1999**, *21*, 339−352.
(477) Sjoelander, S.; Urbaniczky, C. Integrated fluid handling system for biomolecular interaction analysis. *Anal. Chem.* **1991**, *63*, 2338−2345.
(478) Nenninger, G. G.; Clendenning, J. B.; Furlong, C. E.; Yee, S. S. Reference-compensated biosensing using a dual-channel surface plasmon resonance sensor system based on a planar lightpipe configuration. *Sens. Actuators, B* **1998**, *51*, 38−45.
(479) Zhang, H. Q.; Boussaad, S.; Tao, N. J. High-performance differential surface plasmon resonance sensor using quadrant cell photodetector. *Rev. Sci. Instrum.* **2003**, *74*, 150−153.
(480) Harvey, A. H.; Gallagher, J. S.; Sengers, J. Revised formulation for the refractive index of water and steam as a function of wavelength, temperature and density. *J. Phys. Chem. Ref. Data* **1998**, *27*, 761.
(481) Nizamov, S.; Mirsky, V. M. Self-referencing SPR-biosensors based on penetration difference of evanescent waves. *Biosens. Bioelectron.* **2011**, *28*, 263−269.
(482) O'Brien, M. J., II; Brueck, S. R. J.; Perez-Luna, V. H.; Tender, L. M.; Lopez, G. P. SPR biosensors: simultaneously removing thermal and bulk- composition effects. *Biosens. Bioelectron.* **1999**, *14*, 145−154.
(483) Boecker, D.; Zybin, A.; Niemax, K.; Grunwald, C.; Mirsky, V. M. Noise reduction by multiple referencing in surface plasmon resonance imaging. *Rev. Sci. Instrum.* **2008**, *79*, 023110.
(484) Cunningham, B. T.; Zhang, M.; Zhuo, Y.; Kwon, L.; Race, C. Recent advances in biosensing with photonic crystal surfaces: a review. *IEEE Sens. J.* **2016**, *16*, 3349−3366.
(485) Özdemir, Ş. K.; Zhu, J.; Yang, X.; Peng, B.; Yilmaz, H.; He, L.; Monifi, F.; Huang, S. H.; Long, G. L.; Yang, L. Highly sensitive detection of nanoparticles with a self-referenced and self-heterodyned whispering-gallery Raman microlaser. *Proc. Natl. Acad. Sci. U. S. A.* **2014**, *111*, E3836−44.
(486) Stamm, C.; Dangel, R.; Lukosz, W. Biosensing with the integrated-optical difference interferometer: dual-wavelength operation. *Opt. Commun.* **1998**, *153*, 347−359.
(487) Kehl, F.; Follonier, S. Self-referenced waveguide grating sensor. *Opt. Lett.* **2016**, *41*, 1447−1450.
(488) Li, M.; Wu, X.; Liu, L.; Fan, X.; Xu, L. Self-referencing optofluidic ring resonator sensor for highly sensitive biomolecular detection. *Anal. Chem.* **2013**, *85*, 9328−9332.
(489) Fan, X.; White, I. M.; Shopova, S. I.; Zhu, H.; Suter, J. D.; Sun, Y. Sensitive optical biosensors for unlabeled targets: A review. *Anal. Chim. Acta* **2008**, *620*, 8−26.
(490) Karlsson, R.; Ståhlberg, R. Surface plasmon resonance detection and multispot sensing for direct monitoring of interactions involving low-molecular-weight analytes and for determination of low affinities. *Anal. Biochem.* **1995**, *228*, 274−280.
(491) Kozma, P.; Hámori, A.; Kurunczi, S.; Cottier, K.; Horvath, R. Grating coupled optical waveguide interferometer for label-free biosensing. *Sens. Actuators, B* **2011**, *155*, 446−450.
(492) Patko, D.; Cottier, K.; Hamori, A.; Horvath, R. Single beam grating coupled interferometry: high resolution miniaturized label-free sensor for plate based parallel screening. *Opt. Express* **2012**, *20*, 23162−23173.
(493) Frutiger, A.; Fattinger, C.; Vörös, J. Ultra-stable molecular sensors by sub-micron referencing and why they should be interrogated by optical diffraction—Part I. The concept of a spatial affinity lock-in amplifier. *Sensors* **2021**, *21*, 469.
(494) Eng, L.; Nygren-Babol, L.; Hanning, A. Label-enhanced surface plasmon resonance applied to label-free interaction analysis of small molecules and fragments. *Anal. Biochem.* **2016**, *510*, 79−87.
(495) Burdett, R. *Handbook of Measuring System Design*; John Wiley & Sons, Ltd, 2005.
(496) West, B. J.; Shlesinger, M. The noise in natural phenomena. *Am. Sci.* **1990**, *78*, 40−45.
(497) Michels, W. C.; Curtis, N. L. A pentode lock-in amplifier of high frequency selectivity. *Rev. Sci. Instrum.* **1941**, *12*, 444−447.
(498) Stutt, C. A. *Low-frequency spectrum of lock-in amplifiers*; 1949.
(499) Patou, F.; Dimaki, M.; Kjærgaard, C.; Madsen, J.; Svendsen, W. E. System-level sensitivity analysis of SiNW-bioFET-based biosensing using lock-in amplification. *IEEE Sens. J.* **2017**, *17*, 6295−6311.
(500) Frutiger, A.; Gatterdam, K.; Blickenstorfer, Y.; Reichmuth, A. M.; Fattinger, C.; Vörös, J. Ultra stable molecular sensors by submicron referencing and why they should be interrogated by optical diffraction—Part II. Experimental demonstration. *Sensors* **2021**, *21*, 9.
(501) Gatterdam, V.; Frutiger, A.; Stengele, K.-P.; Heindl, D.; Lübbers, T.; Vörös, J.; Fattinger, C. Focal molography is a new method for the in situ analysis of molecular interactions in biological samples. *Nat. Nanotechnol.* **2017**, *12*, 1089.
(502) Avella-Oliver, M.; Carrascosa, J.; Puchades, R.; Maquieira, Á. Diffractive protein gratings as optically active transducers for high-throughput label-free immunosensing. *Anal. Chem.* **2017**, *89*, 9002−9008.
(503) Cleverley, S.; Chen, I.; Houle, J.-F. Label-free and amplified quantitation of proteins in complex mixtures using diffractive optics technology. *J. Chromatogr. B: Anal. Technol. Biomed. Life Sci.* **2010**, *878*, 264−270.
(504) Vallée-Bélisle, A.; Plaxco, K. W. Structure-switching biosensors: inspired by Nature. *Curr. Opin. Struct. Biol.* **2010**, *20*, 518−526.
(505) Cornell, B. a.; Braach-Maksvytis, V. L.; King, L. G.; Osman, P. D.; Raguse, B.; Wieczorek, L.; Pace, R. J. A biosensor that uses ion-channel switches. *Nature* **1997**, *387*, 580−583.
(506) Woodhouse, G.; King, L.; Wieczorek, L.; Osman, P.; Cornell, B. The ion channel switch biosensor. *J. Mol. Recognit.* **1999**, *12*, 328−334.
(507) Burns, C. J.; Braach-Maksvytis, V.; King, L. G.; Osman, P. D. J.; Pace, R. J.; Raguse, B.; Wieczorek, L.; Cornell, B. A. AMBRI biosensor: stabilizing artificial membranes and receptor attachment. *Proc. SPIE* **1999**, *'99*, 17−24.
(508) Palmer, A. E.; Tsien, R. Y. Measuring calcium signaling using genetically targetable fluorescent indicators. *Nat. Protoc.* **2006**, *1*, 1057−1065.
(509) Swensen, J. S.; Xiao, Y.; Ferguson, B. S.; Lubin, A. A.; Lai, R. Y.; Heeger, A. J.; Plaxco, K. W.; Soh, H. T. Continuous, real-time monitoring of cocaine in undiluted blood serum via a microfluidic, electrochemical aptamer-based sensor. *J. Am. Chem. Soc.* **2009**, *131*, 4262−4266.
(510) Miranti, C. K.; Brugge, J. S. Sensing the environment: a historical perspective on integrin signal transduction. *Nat. Cell Biol.* **2002**, *4*, E83−90.
(511) Coppolino, M. G.; Dedhar, S. Bi-directional signal transduction by integrin receptors. *Int. J. Biochem. Cell Biol.* **2000**, *32*, 171−188.
(512) Berton, G.; Lowell, C. A. Integrin signalling in neutrophils and macrophages. *Cell. Signalling* **1999**, *11*, 621−635.
(513) Campbell, D. J.; Kim, C. H.; Butcher, E. C. Chemokines in the systemic organization of immunity. *Immunol. Rev.* **2003**, *195*, 58−71.
(514) Tang, L.; Jennings, T. A.; Eaton, J. W. Mast cells mediate acute inflammatory responses to implanted biomaterials. *Proc. Natl. Acad. Sci. U. S. A.* **1998**, *95*, 8841−8846.
(515) Garcia, A. J.; Boettiger, D. Integrin−fibronectin interactions at the cell-material interface: initial integrin binding and signaling. *Biomaterials* **1999**, *20*, 2427−2433.

https://doi.org/10.1021/acs.chemrev.1c00044
Chem. Rev. 2021, 121, 8095−8160

(516) Allen, L. T.; Tosetto, M.; Miller, I. S.; O'Connor, D. P.; Penney, S. C.; Lynch, I.; Keenan, A. K.; Pennington, S. R.; Dawson, K. A.; Gallagher, W. M. Surface-induced changes in protein adsorption and implications for cellular phenotypic responses to surface interaction. *Biomaterials* **2006**, *27*, 3096−3108.
(517) Gretzer, C.; Emanuelsson, L.; Liljensten, E.; Thomsen, P. The inflammatory cell influx and cytokines changes during transition from acute inflammation to fibrous repair around implanted materials. *J. Biomater. Sci., Polym. Ed.* **2006**, *17*, 669−687.
(518) Jones, J. A.; Dadsetan, M.; Collier, T. O.; Ebert, M.; Stokes, K. S.; Ward, R. S.; Hiltner, P. A.; Anderson, J. M. Macrophage behavior on surface-modified polyurethanes. *J. Biomater. Sci., Polym. Ed.* **2004**, *15*, 567−584.
(519) Brodbeck, W. G.; Shive, M. S.; Colton, E.; Nakayama, Y.; Matsuda, T.; Anderson, J. M. Influence of biomaterial surface chemistry on the apoptosis of adherent cells. *J. Biomed. Mater. Res.* **2001**, *55*, 661−668.
(520) Damsky, C. H.; Ilić, D. Integrin signaling: it's where the action is. *Curr. Opin. Cell Biol.* **2002**, *14*, 594−602.
(521) Charo, I. F.; Taubman, M. B. Chemokines in the pathogenesis of vascular disease. *Circ. Res.* **2004**, *95*, 858−866.
(522) Baker, B. R.; Lai, R. Y.; Wood, M. S.; Doctor, E. H.; Heeger, A. J.; Plaxco, K. W. An electronic, aptamer-based small-molecule sensor for the rapid, label-free detection of cocaine in adulterated samples and biological fluids. *J. Am. Chem. Soc.* **2006**, *128*, 3138−3139.
(523) Ferguson, B. S.; Hoggarth, D. A.; Maliniak, D.; Ploense, K.; White, R. J.; Woodward, N.; Hsieh, K.; Bonham, A. J.; Eisenstein, M.; Kippin, T. E.; Plaxco, K. W.; Soh, H. T. Real-time, aptamer-based tracking of circulating therapeutic agents in living animals. *Sci. Transl. Med.* **2013**, *5*, 213ra165.
(524) Nakatsuka, N.; Yang, K.-A.; Abendroth, J. M.; Cheung, K. M.; Xu, X.; Yang, H.; Zhao, C.; Zhu, B.; Rim, Y. S.; Yang, Y.; Weiss, P. S.; Stojanović, M. N.; Andrews, A. M. Aptamer-field-effect transistors overcome Debye length limitations for small-molecule sensing. *Science* **2018**, *362*, 319−324.
(525) Kim, J.; Rim, Y. S.; Chen, H.; Cao, H. H.; Nakatsuka, N.; Hinton, H. L.; Zhao, C.; Andrews, A. M.; Yang, Y.; Weiss, P. S. Fabrication of high-performance ultrathin In2O3 film field-effect transistors and biosensors using chemical lift-off lithography. *ACS Nano* **2015**, *9*, 4572−4582.
(526) Cheung, K. M.; Yang, K.-A.; Nakatsuka, N.; Zhao, C.; Ye, M.; Jung, M. E.; Yang, H.; Weiss, P. S.; Stojanović, M. N.; Andrews, A. M. Phenylalanine Monitoring via Aptamer-Field-Effect Transistor Sensors. *ACS Sens* **2019**, *4*, 3308−3317.
(527) Nakatsuka, N.; Abendroth, J. M.; Yang, K.-A.; Andrews, A. M. Divalent Cation Dependence Enhances Dopamine Aptamer Biosensing. *ACS Appl. Mater. Interfaces* **2021**, *13*, 9425−9435
(528) Yang, K.-A.; Pei, R.; Stefanovic, D.; Stojanovic, M. N. Optimizing cross-reactivity with evolutionary search for sensors. *J. Am. Chem. Soc.* **2012**, *134*, 1642−1647.
(529) Yang, K.-A.; Chun, H.; Zhang, Y.; Pecic, S.; Nakatsuka, N.; Andrews, A. M.; Worgall, T. S.; Stojanovic, M. N. High-affinity nucleic-acid-based receptors for steroids. *ACS Chem. Biol.* **2017**, *12*, 3103−3112.
(530) Nakatsuka, N.; Cao, H. H.; Deshayes, S.; Melkonian, A. L.; Kasko, A. M.; Weiss, P. S.; Andrews, A. M. Aptamer recognition of multiplexed small-molecule-functionalized substrates. *ACS Appl. Mater. Interfaces* **2018**, *10*, 23490−23500.
(531) Nakatsuka, N.; Faillétaz, A.; Eggemann, D.; Forró, C.; Voros, J.; Momotenko, D. Aptamer conformational change enables serotonin biosensing with nanopipettes. *Anal. Chem.* **2021**, *93*, 4033−4041.
(532) Nakatsuka, N.; Heard, K. J.; Faillétaz, A.; Momotenko, D.; Vörös, J.; Gage, F. H.; Vadodaria, K. C. Sensing serotonin secreted from human serotonergic neurons using aptamer-modified nanopipettes. *Mol. Psychiatry* **2021**, 1−11.
(533) Braha, O.; Gu, L. Q.; Zhou, L.; Lu, X.; Cheley, S.; Bayley, H. Simultaneous stochastic sensing of divalent metal ions. *Nat. Biotechnol.* **2000**, *18*, 1005−1007.
(534) Dekker, C. Solid-state nanopores. *Nat. Nanotechnol.* **2007**, *2*, 209−215.
(535) Song, L.; Hobaugh, M. R.; Shustak, C.; Cheley, S.; Bayley, H.; Gouaux, J. E. Structure of staphylococcal alpha-hemolysin, a heptameric transmembrane pore. *Science* **1996**, *274*, 1859−1866.
(536) Braha, O.; Walker, B.; Cheley, S.; Kasianowicz, J. J.; Song, L.; Gouaux, J. E.; Bayley, H. Designed protein pores as components for biosensors. *Chem. Biol.* **1997**, *4*, 497−505.
(537) Bayley, H.; Cremer, P. S. Stochastic sensors inspired by biology. *Nature* **2001**, *413*, 226−230.
(538) Howorka, S.; Siwy, Z. Nanopore analytics: sensing of single molecules. *Chem. Soc. Rev.* **2009**, *38*, 2360−2384.
(539) Gunnarsson, A.; Jönsson, P.; Marie, R.; Tegenfeldt, J. O.; Höök, F. Single-molecule detection and mismatch discrimination of unlabeled DNA targets. *Nano Lett.* **2008**, *8*, 183−188.
(540) Church, G.; Deamer, D. W.; Branton, D.; Baldarelli, R.; Kasianowicz, J. *Characterization of individual polymer molecules based on monomer-interface interactions*. US Patent 5795782.
(541) Branton, D.; et al. The potential and challenges of nanopore sequencing. *Nat. Biotechnol.* **2008**, *26*, 1146−1153.
(542) Madampage, C. A.; Andrievskaia, O.; Lee, J. S. Nanopore detection of antibody prion interactions. *Anal. Biochem.* **2010**, *396*, 36−41.
(543) Madampage, C.; Tavassoly, O.; Christensen, C.; Kumari, M.; Lee, J. S. Nanopore analysis: an emerging technique for studying the folding and misfolding of proteins. *Prion* **2012**, *6*, 116−123.
(544) Shim, J. W.; Tan, Q.; Gu, L.-Q. Single-molecule detection of folding and unfolding of the G-quadruplex aptamer in a nanopore nanocavity. *Nucleic Acids Res.* **2009**, *37*, 972−982.
(545) Wang, S.; Haque, F.; Rychahou, P. G.; Evers, B. M.; Guo, P. Engineered nanopore of phi29 dna-packaging motor for real-time detection of single colon cancer specific antibody in serum. *ACS Nano* **2013**, *7*, 9814−9822.
(546) Fologea, D.; Gershow, M.; Ledden, B.; McNabb, D. S.; Golovchenko, J. A.; Li, J. Detecting single stranded DNA with a solid state nanopore. *Nano Lett.* **2005**, *5*, 1905−1909.
(547) Wei, R.; Gatterdam, V.; Wieneke, R.; Tampé, R.; Rant, U. Stochastic sensing of proteins with receptor-modified solid-state nanopores. *Nat. Nanotechnol.* **2012**, *7*, 257−263.
(548) Bayley, H.; Cremer, P. S. Stochastic sensors inspired by biology. *Nature* **2001**, *413*, 226−230.
(549) Kono, N.; Arakawa, K. Nanopore sequencing: review of potential applications in functional genomics. *Dev., Growth Differ.* **2019**, *61*, 316−326.
(550) Quick, J.; Quinlan, A. R.; Loman, N. J. A reference bacterial genome dataset generated on the MinION^{TM} portable single-molecule nanopore sequencer. *GigaScience* **2014**, *3*, 22.
(551) Laver, T.; Harrison, J.; O'Neill, P. A.; Moore, K.; Farbos, A.; Paszkiewicz, K.; Studholme, D. J. Assessing the performance of the Oxford Nanopore Technologies MinION. *Biomol Detect Quantif* **2015**, *3*, 1−8.
(552) Rotem, D.; Jayasinghe, L.; Salichou, M.; Bayley, H. Protein detection by nanopores equipped with aptamers. *J. Am. Chem. Soc.* **2012**, *134*, 2781−2787.
(553) Gu, L. Q.; Braha, O.; Conlan, S.; Cheley, S.; Bayley, H. Stochastic sensing of organic analytes by a pore-forming protein containing a molecular adapter. *Nature* **1999**, *398*, 686−690.
(554) Bayley, H.; Braha, O.; Gu, L.-Q. Stochastic sensing with protein pores. *Adv. Mater.* **2000**, *12*, 139−142.
(555) Wanunu, M. Nanopores: A journey towards DNA sequencing. *Phys. Life Rev.* **2012**, *9*, 125−158.
(556) de la Escosura-Muñiz, A.; Merkoçi, A. Nanochannels preparation and application in biosensing. *ACS Nano* **2012**, *6*, 7556−7583.
(557) Movileanu, L.; Howorka, S.; Braha, O.; Bayley, H. Detecting protein analytes that modulate transmembrane movement of a polymer chain within a single protein pore. *Nat. Biotechnol.* **2000**, *18*, 1091−1095.

https://doi.org/10.1021/acs.chemrev.1c00044
Chem. Rev. 2021, 121, 8095−8160

(558) Cai, S.; Sze, J. Y. Y.; Ivanov, A. P.; Edel, J. B. Small molecule electro-optical binding assay using nanopores. *Nat. Commun.* **2019**, *10*, 1797.
(559) Clarke, J.; Wu, H.-C.; Jayasinghe, L.; Patel, A.; Reid, S.; Bayley, H. Continuous base identification for single-molecule nanopore DNA sequencing. *Nat. Nanotechnol.* **2009**, *4*, 265−270.
(560) Rozevsky, Y.; Gilboa, T.; van Kooten, X. F.; Kobelt, D.; Huttner, D.; Stein, U.; Meller, A. Quantification of mRNA expression using single-molecule nanopore sensing. *ACS Nano* **2020**, *14*, 13964−13974.
(561) Aramesh, M.; Forró, C.; Dorwling-Carter, L.; Lüchtefeld, I.; Schlotter, T.; Ihle, S. J.; Shorubalko, I.; Hosseini, V.; Momotenko, D.; Zambelli, T.; et al. Localized detection of ions and biomolecules with a force-controlled scanning nanopore microscope. *Nat. Nanotechnol.* **2019**, *14*, 791−798.
(562) Gunnarsson, A.; Jönsson, P.; Marie, R.; Tegenfeldt, J. O.; Höök, F. Single-molecule detection and mismatch discrimination of unlabeled DNA targets. *Nano Lett.* **2008**, *8*, 183−188.
(563) Gunnarsson, A.; Jönsson, P.; Zhdanov, V. P.; Höök, F. Kinetic and thermodynamic characterization of single-mismatch discrimination using single-molecule imaging. *Nucleic Acids Res.* **2009**, *37*, No. e99.
(564) Rissin, D. M.; Kan, C. W.; Campbell, T. G.; Howes, S. C.; Fournier, D. R.; Song, L.; Piech, T.; Patel, P. P.; Chang, L.; Rivnak, A. J.; Ferrell, E. P.; Randall, J. D.; Provuncher, G. K.; Walt, D. R.; Duffy, D. C. Single-molecule enzyme-linked immunosorbent assay detects serum proteins at subfemtomolar concentrations. *Nat. Biotechnol.* **2010**, *28*, 595−599.
(565) Patra, J. K.; Das, G.; Fraceto, L. F.; Campos, E. V. R.; Rodriguez-Torres, M. D. P.; Acosta-Torres, L. S.; Diaz-Torres, L. A.; Grillo, R.; Swamy, M. K.; Sharma, S.; Habtemariam, S.; Shin, H.-S. Nano based drug delivery systems: recent developments and future prospects. *J. Nanobiotechnol.* **2018**, *16*, 71.
(566) Li, J.; Mooney, D. J. Designing hydrogels for controlled drug delivery. *Nat. Rev. Mater.* **2016**, *1*, DOI: 10.1038/natrevmats.2016.71.
(567) Rwei, A. Y.; Wang, W.; Kohane, D. S. Photoresponsive nanoparticles for drug delivery. *Nano Today* **2015**, *10*, 451−467.
(568) Fenton, O. S.; Olafson, K. N.; Pillai, P. S.; Mitchell, M. J.; Langer, R. Advances in biomaterials for drug delivery. *Adv. Mater.* **2018**, No. e1705328.
(569) Kowalski, P. S.; Bhattacharya, C.; Afewerki, S.; Langer, R. Smart biomaterials: recent advances and future directions. *ACS Biomater. Sci. Eng.* **2018**, *4*, 3809−3817.
(570) Blanco, E.; Shen, H.; Ferrari, M. Principles of nanoparticle design for overcoming biological barriers to drug delivery. *Nat. Biotechnol.* **2015**, *33*, 941−951.
(571) Ahmad, Z.; Shah, A.; Siddiq, M.; Kraatz, H.-B. Polymeric micelles as drug delivery vehicles. *RSC Adv.* **2014**, *4*, 17028−17038.
(572) Nag, O. K.; Awasthi, V. Surface engineering of liposomes for stealth behavior. *Pharmaceutics* **2013**, *5*, 542−569.
(573) Caracciolo, G. Liposome-protein corona in a physiological environment: challenges and opportunities for targeted delivery of nanomedicines. *Nanomedicine* **2015**, *11*, 543−557.
(574) Allen, T. M.; Cullis, P. R. Liposomal drug delivery systems: from concept to clinical applications. *Adv. Drug Delivery Rev.* **2013**, *65*, 36−48.
(575) Yan, X.; Scherphof, G. L.; Kamps, J. a. a. M. Liposome opsonization. *J. Liposome Res.* **2005**, *15*, 109−139.
(576) Moghimi, S. M.; Hunter, A. C.; Murray, J. C. Long-circulating and target-specific nanoparticles: theory to practice. *Pharmacol. Rev.* **2001**, *53*, 283−318.
(577) Docter, D.; Westmeier, D.; Markiewicz, M.; Stolte, S.; Knauer, S. K.; Stauber, R. H. The nanoparticle biomolecule corona: lessons learned − challenge accepted? *Chem. Soc. Rev.* **2015**, *44*, 6094−6121.
(578) Walkey, C. D.; Chan, W. C. W. Understanding and controlling the interaction of nanomaterials with proteins in a physiological environment. *Chem. Soc. Rev.* **2012**, *41*, 2780−2799.
(579) Schöttler, S.; Becker, G.; Winzen, S.; Steinbach, T.; Mohr, K.; Landfester, K.; Mailänder, V.; Wurm, F. R. Protein adsorption is required for stealth effect of poly(ethylene glycol)- and poly-(phosphoester)-coated nanocarriers. *Nat. Nanotechnol.* **2016**, *11*, 372−377.
(580) Barrán-Berdón, A. L.; Pozzi, D.; Caracciolo, G.; Capriotti, A. L.; Caruso, G.; Cavaliere, C.; Riccioli, A.; Palchetti, S.; Laganà, A. Time evolution of nanoparticle−protein corona in human plasma: relevance for targeted drug delivery. *Langmuir* **2013**, *29*, 6485−6494.
(581) Aggarwal, P.; Hall, J. B.; McLeland, C. B.; Dobrovolskaia, M. A.; McNeil, S. E. Nanoparticle interaction with plasma proteins as it relates to particle biodistribution, biocompatibility and therapeutic efficacy. *Adv. Drug Delivery Rev.* **2009**, *61*, 428−437.
(582) Moghimi, S. M.; Patel, H. M. Serum-mediated recognition of liposomes by phagocytic cells of the reticuloendothelial system − the concept of tissue specificity. *Adv. Drug Delivery Rev.* **1998**, *32*, 45−60.
(583) Johnstone, S. A.; Masin, D.; Mayer, L.; Bally, M. B. Surface-associated serum proteins inhibit the uptake of phosphatidylserine and poly(ethylene glycol) liposomes by mouse macrophages. *Biochim. Biophys. Acta, Biomembr.* **2001**, *1513*, 25−37.
(584) Nakatsuka, N.; Hasani-Sadrabadi, M. M.; Cheung, K. M.; Young, T. D.; Bahlakeh, G.; Moshaverinia, A.; Weiss, P. S.; Andrews, A. M. Polyserotonin nanoparticles as multifunctional materials for biomedical applications. *ACS Nano* **2018**, *12*, 4761−4774.
(585) Kelly, P. M.; Åberg, C.; Polo, E.; O'Connell, A.; Cookman, J.; Fallon, J.; Krpetić, Ž.; Dawson, K. a. Mapping protein binding sites on the biomolecular corona of nanoparticles. *Nat. Nanotechnol.* **2015**, *10*, 1−8.
(586) Clements, A. M.; Botella, P.; Landry, C. C. Spatial mapping of protein adsorption on mesoporous silica nanoparticles by stochastic optical reconstruction microscopy. *J. Am. Chem. Soc.* **2017**, *139*, 3978−3981.
(587) Zhang, Y.; Wu, J. L. Y.; Lazarovits, J.; Chan, W. C. W. An analysis of the binding function and structural organization of the protein corona. *J. Am. Chem. Soc.* **2020**, *142*, 8827.
(588) Müller, M.; Vörös, J.; Csúcs, G.; Walter, E.; Danuser, G.; Merkle, H. P.; Spencer, N. D.; Textor, M. Surface modification of PLGA microspheres. *J. Biomed. Mater. Res., Part A* **2003**, *66*, 55−61.
(589) Patel, H. M. Serum opsonins and liposomes: their interaction and opsonophagocytosis. *Crit. Rev. Ther. Drug Carrier Syst.* **1992**, *9*, 39−90.
(590) Vonarbourg, A.; Passirani, C.; Saulnier, P.; Benoit, J.-P. Parameters influencing the stealthiness of colloidal drug delivery systems. *Biomaterials* **2006**, *27*, 4356−4373.
(591) Ishida, T.; Harashima, H.; Kiwada, H. Liposome clearance. *Biosci. Rep.* **2002**, *22*, 197−224.
(592) Mima, Y.; Hashimoto, Y.; Shimizu, T.; Kiwada, H.; Ishida, T. Anti-PEG IgM is a major contributor to the accelerated blood clearance of polyethylene glycol-conjugated protein. *Mol. Pharmaceutics* **2015**, *12*, 2429−2435.
(593) Salmaso, S.; Caliceti, P. Stealth properties to improve therapeutic efficacy of drug nanocarriers. *J. Drug Delivery* **2013**, *2013*, 374251−374252.
(594) Kim, H. R.; Andrieux, K.; Delomenie, C.; Chacun, H.; Appel, M.; Desmaële, D.; Taran, F.; Georgin, D.; Couvreur, P.; Taverna, M. Analysis of plasma protein adsorption onto PEGylated nanoparticles by complementary methods: 2-DE, CE and Protein Lab-on-chip system. *Electrophoresis* **2007**, *28*, 2252−2261.
(595) Gref, R.; Lück, M.; Quellec, P.; Marchand, M.; Dellacherie, E.; Harnisch, S.; Blunk, T.; Müller, R. H. Stealth' corona-core nanoparticles surface modified by polyethylene glycol (PEG): influences of the corona (PEG chain length and surface density) and of the core composition on phagocytic uptake and plasma protein adsorption. *Colloids Surf., B* **2000**, *18*, 301−313.
(596) Moghimi, S. M.; Hunter, A. C.; Andresen, T. L. Factors controlling nanoparticle pharmacokinetics: an integrated analysis and perspective. *Annu. Rev. Pharmacol. Toxicol.* **2012**, *52*, 481−503.
(597) Juliano, R. L.; Stamp, D. The effect of particle size and charge on the clearance rates of liposomes and liposome encapsulated drugs. *Biochem. Biophys. Res. Commun.* **1975**, *63*, 651−658.

(598) Alexis, F.; Pridgen, E.; Molnar, L. K.; Farokhzad, O. C. Factors affecting the clearance and biodistribution of polymeric nanoparticles. *Mol. Pharmaceutics* **2008**, *5*, 505−515.
(599) Walkey, C. D.; Olsen, J. B.; Guo, H.; Emili, A.; Chan, W. C. W. Nanoparticle size and surface chemistry determine serum protein adsorption and macrophage uptake. *J. Am. Chem. Soc.* **2012**, *134*, 2139−2147.
(600) Furumoto, K.; Yokoe, J. I.; Ogawara, K. I.; Amano, S.; Takaguchi, M.; Higaki, K.; Kai, T.; Kimura, T. Effect of coupling of albumin onto surface of PEG liposome on its in vivo disposition. *Int. J. Pharm.* **2007**, *329*, 110−116.
(601) Vert, M.; Domurado, D. Poly(ethylene glycol): protein-repulsive or albumin-compatible? *J. Biomater. Sci., Polym. Ed.* **2000**, *11*, 1307−1317.
(602) Knop, K.; Hoogenboom, R.; Fischer, D.; Schubert, U. S. Poly(ethylene glycol) in drug delivery: pros and cons as well as potential alternatives. *Angew. Chem., Int. Ed.* **2010**, *49*, 6288−6308.
(603) Hamad, I.; Hunter, A. C.; Szebeni, J.; Moghimi, S. M. Poly(ethylene glycol)s generate complement activation products in human serum through increased alternative pathway turnover and a MASP-2-dependent process. *Mol. Immunol.* **2008**, *46*, 225−232.
(604) Rodriguez, P. L.; Harada, T.; Christian, D. A.; Pantano, D. A.; Tsai, R. K.; Discher, D. E. Minimal "Self" peptides that inhibit phagocytic clearance and enhance delivery of nanoparticles. *Science* **2013**, *339*, 971−975.
(605) Hu, C.-M. J.; Zhang, L.; Aryal, S.; Cheung, C.; Fang, R. H.; Zhang, L. Erythrocyte membrane-camouflaged polymeric nanoparticles as a biomimetic delivery platform. *Proc. Natl. Acad. Sci. U. S. A.* **2011**, *108*, 10980−10985.
(606) Parodi, A.; Quattrocchi, N.; van de Ven, A. L.; Chiappini, C.; Evangelopoulos, M.; Martinez, J. O.; Brown, B. S.; Khaled, S. Z.; Yazdi, I. K.; Enzo, M. V.; Isenhart, L.; Ferrari, M.; Tasciotti, E. Synthetic nanoparticles functionalized with biomimetic leukocyte membranes possess cell-like functions. *Nat. Nanotechnol.* **2013**, *8*, 61−68.
(607) Poot, A.; Beugeling, T.; van Aken, W. G.; Bantjes, A. Detection of surface-adsorbed (1ipo)proteins by means of a two-step enzyme-immunoassay: A study on the Vroman effect. *J. Biomed. Mater. Res.* **1990**, *24*, 1021−1036.
(608) Vroman, L.; Adams, A. L. Peculiar behavior of blood at solid interfaces. *J. Polym. Sci., Part C: Polym. Symp.* **1971**, *34*, 159−165.
(609) Vroman, L.; Adams, A. L.; Fischer, G. C.; Munoz, P. C. Interaction of high molecular weight kininogen, factor XII, and fibrinogen in plasma at interfaces. *Blood* **1980**, *55*, 156−159.
(610) Gristina, A. G. Biomaterial-centered infection: microbial adhesion versus tissue integration. *Science* **1987**, *237*, 1588−1595.
(611) Busscher, H. J.; van der Mei, H. C.; Subbiahdoss, G.; Jutte, P. C.; van den Dungen, J. J.; Zaat, S. A.; Schultz, M. J.; Grainger, D. W. Biomaterial-associated infection: locating the finish line in the race for the surface. *Sci. Transl. Med.* **2012**, *4*, 153rv10−153rv11.
(612) Spitzfaden, C.; Grant, R. P.; Mardon, H. J.; Campbell, I. D. Module−module interactions in the cell binding region of fibronectin: stability, flexibility and specificity. *J. Mol. Biol.* **1997**, *265*, 565−579.
(613) García, A. J. Get a grip: integrins in cell−biomaterial interactions. *Biomaterials* **2005**, *26*, 7525−7529.
(614) Maddikeri, R. R.; Tosatti, S.; Schuler, M.; Chessari, S.; Textor, M.; Richards, R. G.; Harris, L. G. Reduced medical infection related bacterial strains adhesion on bioactive RGD modified titanium surfaces: a first step toward cell selective surfaces. *J. Biomed. Mater. Res., Part A* **2008**, *84*, 425−435.
(615) Boudou, T.; Crouzier, T.; Ren, K.; Blin, G.; Picart, C. Multiple functionalities of polyelectrolyte multilayer films: new biomedical applications. *Adv. Mater.* **2010**, *22*, 441−467.
(616) Choudhury, R. R.; Gohil, J. M.; Mohanty, S.; Nayak, S. K. Antifouling, fouling release and antimicrobial materials for surface modification of reverse osmosis and nanofiltration membranes. *J. Mater. Chem. A* **2018**, *6*, 313−333.
(617) Banerjee, I.; Pangule, R. C.; Kane, R. S. Antifouling coatings: recent developments in the design of surfaces that prevent fouling by proteins, bacteria, and marine organisms. *Adv. Mater.* **2011**, *23*, 690−718.
(618) Wu, S.; Liu, X.; Yeung, K. W. K.; Liu, C.; Yang, X. Biomimetic porous scaffolds for bone tissue engineering. *Mater. Sci. Eng., R* **2014**, *80*, 1−36.
(619) Su, Y.; Luo, C.; Zhang, Z.; Hermawan, H.; Zhu, D.; Huang, J.; Liang, Y.; Li, G.; Ren, L. Bioinspired surface functionalization of metallic biomaterials. *J. Mech. Behav. Biomed. Mater.* **2018**, *77*, 90−105.
(620) Tiller, J. C.; Liao, C. J.; Lewis, K.; Klibanov, A. M. Designing surfaces that kill bacteria on contact. *Proc. Natl. Acad. Sci. U. S. A.* **2001**, *98*, 5981−5985.
(621) Kaur, R.; Liu, S. *Antibacterial surface design − Contact kill*; 2016.
(622) Shukla, A.; Fleming, K. E.; Chuang, H. F.; Chau, T. M.; Loose, C. R.; Stephanopoulos, G. N.; Hammond, P. T. Controlling the release of peptide antimicrobial agents from surfaces. *Biomaterials* **2010**, *31*, 2348−2357.
(623) Wisniewski, N.; Reichert, M. Methods for reducing biosensor membrane biofouling. *Colloids Surf., B* **2000**, *18*, 197−219.
(624) Tang, L.; Thevenot, P.; Hu, W. Surface chemistry influences implant biocompatibility. *Curr. Top. Med. Chem.* **2008**, *8*, 270−280.
(625) Gray, M.; Meehan, J.; Ward, C.; Langdon, S. P.; Kunkler, I. H.; Murray, A.; Argyle, D. Implantable biosensors and their contribution to the future of precision medicine. *Vet. J.* **2018**, *239*, 21−29.
(626) Onuki, Y.; Bhardwaj, U.; Papadimitrakopoulos, F.; Burgess, D. J. A review of the biocompatibility of implantable devices: current challenges to overcome foreign body response. *J. Diabetes Sci. Technol.* **2008**, *2*, 1003−1015.
(627) Clark, L. C., Jr; Lyons, C. Electrode systems for continuous monitoring in cardiovascular surgery. *Ann. N. Y. Acad. Sci.* **1962**, *102*, 29−45.
(628) Wang, J. Glucose biosensors: 40 years of advances and challenges. *Electroanalysis* **2001**, *13*, 983.
(629) American Diabetes Association, Standards of medical care in diabetes-2015 abridged for primary care providers. *Clin. Diabetes* **2015**, *33*, 97−111.
(630) Wickramasinghe, Y.; Yang, Y.; Spencer, S. A. Current problems and potential techniques in in vivo glucose monitoring. *J. Fluoresc.* **2004**, *14*, 513−520.
(631) Kovatchev, B.; Tamborlane, W. V.; Cefalu, W. T.; Cobelli, C. The artificial pancreas in 2016: a digital treatment ecosystem for diabetes. *Diabetes Care* **2016**, *39*, 1123−1126.
(632) Klonoff, D. C. The benefits of implanted glucose sensors. *J. Diabetes Sci. Technol.* **2007**, *1*, 797−800.
(633) Yoo, E.-H.; Lee, S.-Y. Glucose biosensors: an overview of use in clinical practice. *Sensors* **2010**, *10*, 4558−4576.
(634) Shibata, H.; Heo, Y. J.; Okitsu, T.; Matsunaga, Y.; Kawanishi, T.; Takeuchi, S. Injectable hydrogel microbeads for fluorescence-based in vivo continuous glucose monitoring. *Proc. Natl. Acad. Sci. U. S. A.* **2010**, *107*, 17894−17898.
(635) Unruh, R. M.; Roberts, J. R.; Nichols, S. P.; Gamsey, S.; Wisniewski, N. A.; McShane, M. J. Preclinical evaluation of poly (hema-co-acrylamide) hydrogels encapsulating glucose oxidase and palladium benzoporphyrin as fully implantable glucose sensors. *J. Diabetes Sci. Technol.* **2015**, *9*, 985−992.
(636) Heo, Y. J.; Shibata, H.; Okitsu, T.; Kawanishi, T.; Takeuchi, S. Long-term in vivo glucose monitoring using fluorescent hydrogel fibers. *Proc. Natl. Acad. Sci. U. S. A.* **2011**, *108*, 13399−13403.
(637) Scholten, K.; Meng, E. A review of implantable biosensors for closed-loop glucose control and other drug delivery applications. *Int. J. Pharm.* **2018**, *544*, 319−334.
(638) Mortellaro, M.; DeHennis, A. Performance characterization of an abiotic and fluorescent-based continuous glucose monitoring system in patients with type 1 diabetes. *Biosens. Bioelectron.* **2014**, *61*, 227−231.

https://doi.org/10.1021/acs.chemrev.1c00044
Chem. Rev. 2021, 121, 8095−8160